

SiC-deposited ceramic membranes for treatment of oil-in-water emulsions

Chen, M.

DOI

[10.4233/uuid:e00f2539-c0b9-49a4-a20f-8a4d0e68cba7](https://doi.org/10.4233/uuid:e00f2539-c0b9-49a4-a20f-8a4d0e68cba7)

Publication date

2023

Document Version

Final published version

Citation (APA)

Chen, M. (2023). *SiC-deposited ceramic membranes for treatment of oil-in-water emulsions*. [Dissertation (TU Delft), Delft University of Technology]. <https://doi.org/10.4233/uuid:e00f2539-c0b9-49a4-a20f-8a4d0e68cba7>

Important note

To cite this publication, please use the final published version (if applicable). Please check the document version above.

Copyright

Other than for strictly personal use, it is not permitted to download, forward or distribute the text or part of it, without the consent of the author(s) and/or copyright holder(s), unless the work is under an open content license such as Creative Commons.

Takedown policy

Please contact us and provide details if you believe this document breaches copyrights. We will remove access to the work immediately and investigate your claim.

SiC-deposited ceramic membranes for treatment of oil-in-water emulsions

Dissertation

for the purpose of obtaining the degree of doctor
at Delft University of Technology
by the authority of the Rector Magnificus prof.dr.ir. T.H.J.J. van der Hagen
chair of the Board for Doctorates
to be defended publicly on
Tuesday 4 July 2023 at 10:00 o'clock

by

Mingliang CHEN

Master of Engineering in Environmental Engineering, University of Chinese
Academy of Sciences, China

Born in Anqing, China

This dissertation has been approved by the promotor.

Composition of the doctoral committee:

Rector Magnificus,	chairperson
Prof.dr.ir. L.C. Rietveld	Delft University of Technology, promotor
Dr.ir. S.G.J. Heijman	Delft University of Technology, promotor

Independent members:

Prof.dr.ir. Ruud van Ommen	Delft University of Technology
Prof.dr. Yingchao Dong	Dalian University of Technology, China
Prof.dr.ir. Jules B. van Lier	Delft University of Technology
Dr.ir. Mieke W.J. Luiten-Olieman	University of Twente
Dr. Melike Begum Tanis-Kanbur	Technical University of Denmark, Denmark

This research presented in this thesis was performed at the Sanitary Engineering Section, Department of Watermanagement, Faculty of Civil Engineering, Delft University of Technology, The Netherlands. This research was funded by the China Scholarship Council, and also partially supported by the Lamminga Fund.



Cover by: Mingliang CHEN

Copyright © 2023 by Mingliang CHEN

Printed by: proefschrift-ai.nl

ISBN: 978-94-6384-461-1

An electronic version of this dissertation is available at <https://repository.tudelft.nl/>

Contents

Chapter 1	Introduction	5
Chapter 2	Ceramic membrane filtration for oily wastewater treatment: basics, membrane fouling and fouling control	11
Chapter 3	State-of-the-art ceramic membranes for oily wastewater treatment: Modification and application	47
Chapter 4	Highly permeable silicon carbide-alumina ultrafiltration membranes for oil-in-water filtration produced with low-pressure chemical vapor deposition	75
Chapter 5	Evaluation of fouling by oil-in-water emulsion at constant flux and constant transmembrane pressure: Implications for modification of ceramic membranes	99
Chapter 6	Oil-in-water emulsion separation: Fouling of alumina membranes with and without a silicon carbide deposition in constant flux filtration mode	127
Chapter 7	Conclusion and outlook	161
	References	167
	Summary	201
	Acknowledgements	205
	Curriculum vitae	207
	List of Publications	208

Chapter 1 |

Introduction

1.1. Oily wastewater

Oily wastewater is mainly produced in industries such as metal finishing, petroleum refining, food processing, and oil and gas production. Due to the large generated volumes, negative impacts on the aquatic environment, and potential threats to human health, these streams are becoming one of the major environmental concerns (Coca et al., 2011; Jiménez et al., 2018). Oil in oily wastewater can be classified into three categories, namely free, dispersed, and emulsified oils. Free and dispersed oils have a relatively large droplet size ($> 20 \mu\text{m}$), and can easily be removed by conventional treatment technologies, such as (electro-) coagulation/flocculation, gravity settling, flotation, and centrifugation (Gupta et al., 2017; Padaki et al., 2015; Saththasivam et al., 2016). However, it is much more difficult to remove emulsified oils from oily wastewater, because the small sized particles ($< 20 \mu\text{m}$) are highly stable, due to the used surfactants, considerably increasing the repulsive charge between oil droplets with a high zeta potential (Dickhout et al., 2017; Tummons et al., 2020). Therefore, when dealing with oil-in-water (O/W) emulsions, conventional technologies are not effective to meet the increasingly stringent discharge standards (Adham et al., 2018; Padaki et al., 2015).

The composition and characteristics (e.g., pH) of oily wastewater varies considerably in various industries. It was found that the content of organic carbon of oily wastewater is typically high in food and drinking industry, while the oil content is relatively low in metal processing industry (Tanudjaja et al., 2019). Produced water, as a by-product of oil and gas extraction processes, is considered as the largest stream of oily wastewater in the world. Due to the high volume-to-product ratio (up to 3), the annual global volume of produced water in 2020 has been estimated to be as high as 54 billion cubic meters (Adham et al., 2018; Munirasu et al., 2016). Besides oil, other complex constituents are commonly observed in produced water, which either come from the subsurface of the extraction wells or the chemicals added in the extraction processes (Chang et al., 2019; Wenzlick and Siefert, 2020). Therefore, the composition and characteristics of produced water are site-specific, making it challenging to deal with and reuse these wastewater streams.

1.2. Membrane based treatment of oily wastewater

Microfiltration (MF) and ultrafiltration (UF) have been widely studied to handle O/W emulsions, because of their distinct advantages over conventional methods, such as high flux, steady and good permeate quality, and small footprint (Chen et al., 2016a; Ebrahimi et al., 2010; Hua et al., 2007). The high mechanical, thermal and chemical stability of ceramic membranes make these membranes particularly suitable for industrial wastewater treatment, such as oily wastewater. While the one-time manufacturing cost of ceramic membranes is higher than that of polymeric membranes, they can be a more cost-effective option for water treatment applications due to longer membrane lifespan and better performance. Compared to polymeric membranes, ceramic membranes have a

Chapter 1

narrower pore size distribution, a higher porosity, and higher hydrophilicity (Dong et al., 2019; Wang et al., 2022b; Wu et al., 2022; Zhang et al., 2019). Therefore, better (reversible and irreversible) fouling control in water treatment has been observed than when polymeric membranes are used (Hofs et al., 2011; Nagasawa et al., 2020). Furthermore, ceramic membranes can potentially be cleaned with harsh chemicals and backwashed at high pressures for enhanced performance recovery, which could guarantee a longer service life (> 15 years) (Gu et al., 2021; Lee et al., 2015).

The commercially available ceramic membranes, used in oily wastewater treatment, are alumina (Al_2O_3), titania (TiO_2), zirconia (ZrO_2) and silicon carbide (SiC) (Asif and Zhang, 2021). The relative properties of these membranes vary. As shown in Figure 1.1, Al_2O_3 membranes are cheaper than other ceramic membranes, but they have the lowest permeability with a less hydrophilic surface, leading to a higher fouling potential. TiO_2 and ZrO_2 membranes have a higher permeability and a more hydrophilic surface than that of the Al_2O_3 membrane, thus improved fouling control has been observed in water treatment. SiC membranes have the highest permeability and they own a super-hydrophilic (static water contact angle below 5°) and (negatively) charged surface, creating a low fouling property (Hofs et al., 2011; Xu et al., 2020).

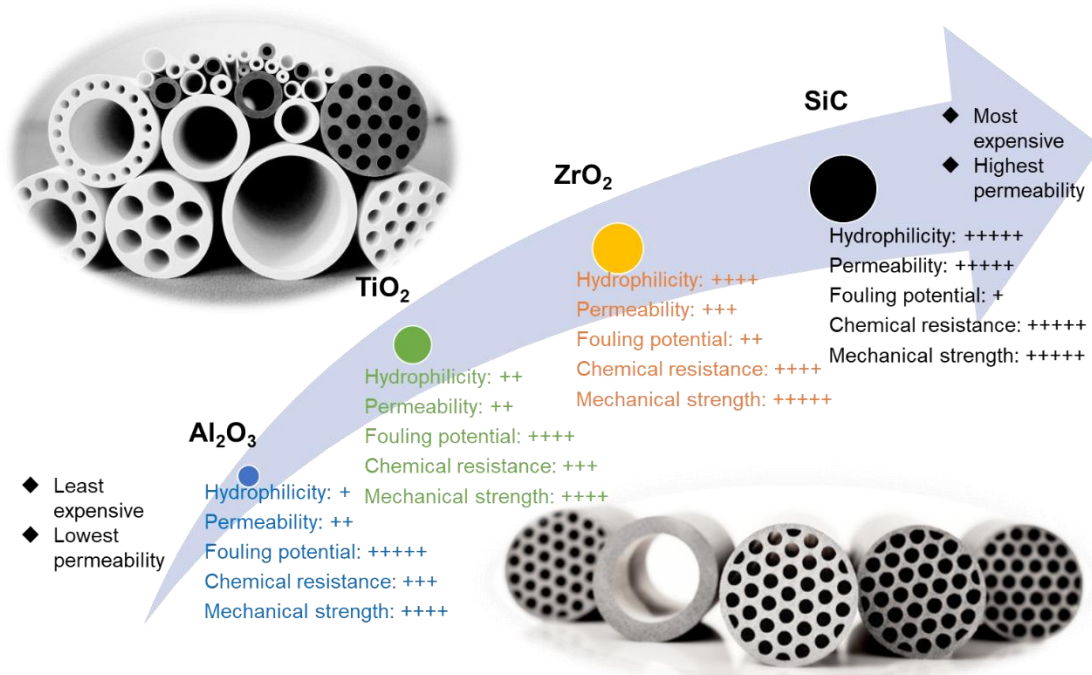


Figure 1.1. Relative properties of commonly used ceramic membranes for water treatment (Asif and Zhang, 2021). The inserted pictures represent the tubular ceramic membranes developed at Fraunhofer IKTS, Germany (top left) and at Liqtech, Denmark (right bottom).

1.3. Thesis research framework

1.3.1. Problem statement

SiC membranes exhibit a low fouling potential, thus being promising for O/W emulsions treatment. However, SiC membranes are normally prepared at high sintering temperatures, up to 2000 °C in an inert atmosphere, making them more expensive than the traditional ceramic membranes (Fraga et al., 2017b; Hotza et al., 2020).

The objective of this thesis was, therefore, to potentially reduce the fabrication cost of commercial SiC membranes by preparing SiC membranes at lower temperatures and using cheaper supports (e.g., Al₂O₃).

Novel SiC-deposited Al₂O₃ membranes were prepared by low pressure chemical vapor deposition (LPCVD) at a temperature of 750 °C. Although commercial SiC membranes are considered to have a low fouling characteristic, fouling properties of these newly developed SiC-deposited ceramic membranes could be affected by, e.g., the surface properties of the membranes (and the support), characteristics of feed and operational conditions, and was thus subject of study, as schematically shown in Figure 1.2.

In addition, the performance of the newly developed SiC-deposited membranes in O/W emulsions treatment could be related to:

- the deposition parameters of LPCVD. The properties of the ceramic membranes such as pore size, porosity, surface morphology, and water permeance are affected by the deposition parameters (e.g., deposition time, temperature). The deposition of the SiC layer on the Al₂O₃ membrane surface may make the membrane more fouling resistant, but the loss of water permeance should also be considered.
- filtration mode and operational parameters. Constant pressure filtration and constant flux filtration are generally used to evaluate membrane fouling in literature. The comparison of these two filtration modes is rarely made, especially when membrane modification and treatment of O/W emulsions are involved. In addition, operational parameters such as transmembrane pressure (TMP) and permeate flux can have an impact on membrane fouling.
- the characteristics of O/W emulsions. The complexity and variation in composition of O/W emulsions make membrane fouling difficult to control. The role of each component of O/W emulsions should be studied to provide a better understanding on membrane fouling.

Understanding these above mentioned factors and mechanisms could then lead to feasible application of the novel SiC-deposited Al₂O₃ membranes for the treatment of O/W emulsions.

■ Chapter 1

1.3.2. Research questions

To achieve the main objective, extensive literature reviews were performed (Chapters 2 and 3) and the following three, specific research questions were formulated:

- (1) What is the impact of the various deposition parameters on the properties (e.g., morphology, pore sizes and water permeance) of the SiC deposited Al_2O_3 membranes? (Chapter 4)
- (2) Among the two types of filtration modes (constant pressure and constant flux filtration), which one is the most suitable to assess the performance of the SiC deposited Al_2O_3 membranes before and after deposition? (Chapter 5)
- (3) What is the effect of filtration parameters (e.g., permeate flux) on SiC deposited Al_2O_3 membrane fouling? and what is the role of quality (e.g., surfactant concentration, pH, salinity and divalent ions) of the O/W emulsions in membrane fouling? (Chapter 6)

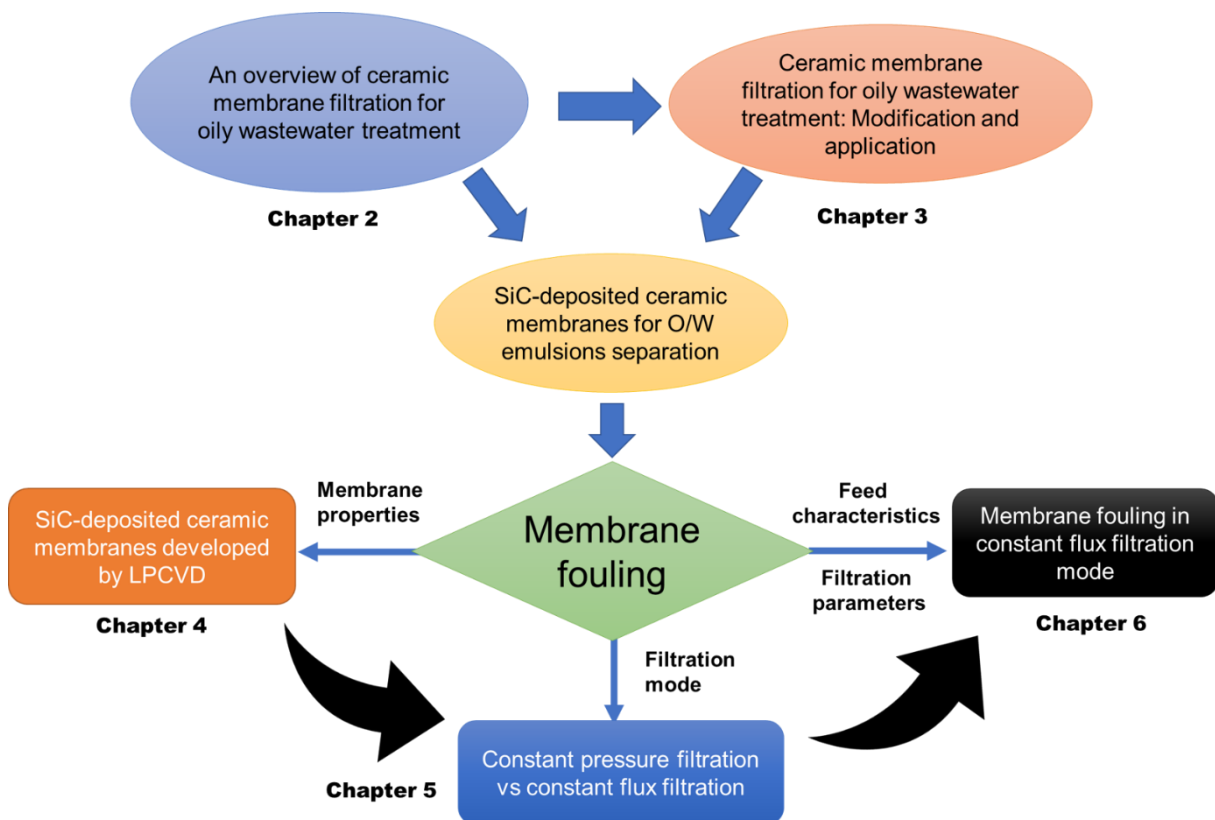


Figure 1.2. Schematic overview of the main chapters of this thesis.

1.3.3. Outline of the thesis

In this thesis, novel SiC-deposited Al_2O_3 membranes were developed and tested for O/W emulsions treatment, aiming at a better understanding of the effect of surface properties of the membranes, characteristics of feed, and operational conditions on membrane fouling and potential upscaling of this technology.

■ Chapter 1

Chapter 2 consists of a literature review on ceramic membrane filtration for oily wastewater treatment. An overview of different types of ceramic membranes and their performance in oily wastewater treatment was presented. In addition, the factors that affect membrane fouling and related fouling control strategies were discussed.

Among the various strategies used for membrane fouling control in oily wastewater treatment, membrane modification is the most studied. In **Chapter 3** the advantages and disadvantages of different methods used for ceramic membrane modification were compared, aiming for improved filtration performance in oily wastewater treatment. In addition, the performance of these modified membranes in terms of oil rejection, permeate flux and fouling was assessed.

A novel SiC-deposited Al₂O₃ membrane was developed by LPCVD and in **Chapter 4** the effect of the deposition time on the properties of the membranes was systematically studied via various characterization methods. The antifouling performance of the deposited membranes was tested with an O/W emulsion.

In **Chapter 5** the membrane performance before and after deposition at constant pressure filtration and constant flux filtration conditions were respectively compared. The threshold flux of the membranes with varying deposition times was first determined. In constant flux filtration, membrane fouling was studied below and above the threshold flux, respectively. The membrane performance was further tested at the same driving force and the same initial flux, respectively during constant pressure filtration experiments.

Each component in oily wastewater may play a role in membrane fouling. In addition, membrane surface hydrophilicity and charge are considered to be vital on membrane fouling. Therefore, the effects of emulsion chemistry (surfactant concentration, pH, salinity and Ca²⁺) and operation parameters (permeate flux and filtration time) were comparatively evaluated for the Al₂O₃ membranes with and without a SiC deposition in constant flux filtration mode in **Chapter 6**.

Finally, conclusions and recommendations for future research are presented in **Chapter 7**.

Chapter 2 |

Ceramic membrane filtration for oily wastewater treatment: basics, membrane fouling and fouling control

This chapter is based on:

Chen, M., Heijman, S. G., & Rietveld, L. C. (2023). Ceramic membrane filtration for oily wastewater treatment: basics, membrane fouling and fouling control. To be submitted for publication.

Abstract

Oily wastewater is produced in various industries, such as food and beverage production, metal processing, and oil and gas extraction. It has an adverse impact on the environment and ecosystems if directly discharged. However, after proper treatment, the water can be reused for other purposes. Membrane technology has been found to be effective to remove oil droplets from oil-in-water emulsions in comparison to traditional methods. Ceramic membrane filtration is assumed to be more effective than filtration by polymeric membranes. It has a lower fouling tendency and higher recoverability. Another advantage of ceramic membranes lies in their higher mechanical, chemical and thermal stability, permitting more aggressive chemical cleaning. Membrane fouling, however, is still one of the major challenges in oily wastewater treatment. In this review, we first discuss the properties of oily wastewater and ceramic membranes (materials and type) for oily wastewater treatment. Secondly, the factors that affect ceramic membrane fouling by oil droplets are presented. Finally, we discuss the strategies that have been used to control ceramic membrane fouling during the filtration process and opportunities for improved fouling control are identified. We concluded that membrane fouling is strongly related to the characteristics of oily wastewater (e.g., oil concentration, pH, salinity, surfactant type and concentration, and temperature), membrane properties (e.g., surface hydrophilicity, charge and roughness) and operational parameters (e.g., cross-flow velocity, TMP and permeate flux). By using pretreatment, membrane fouling can be reduced. Backpulsing/backwashing is effective to maintain a long-term operation. Chemical cleaning is effective to restore the performance of the ceramic membranes with an accumulation of irreversible fouling. In addition, membrane modification could be applied to enhance permeate flux, fouling resistance and oil rejection of ceramic membranes.

2.1. Introduction

Due to the rapid industrial growth, vast amounts of oily wastewater are produced by a wide range of industries, such as oil and gas, petrochemical, food, textile, leather and metal finishing (Coca et al., 2011; Fakhru'l-Razi et al., 2009; Kajitvichyanukul et al., 2011). Oily wastewater, especially produced water, generated from oil and gas wells, contains a high level of pollutants. It may cause a series of problems if directly discharged into the aquatic environment (Salahi et al., 2013). Therefore, these oil/water mixtures should be treated to meet the stringent discharge regulations and reduce the environmental impacts (Kumar et al., 2015). Furthermore, the explosive growth of world population and economy has resulted in greater demands for clean freshwater and, therefore recycling industrial oily wastewater should also be considered (Pendergast and Hoek, 2011).

Oily wastewater can be classified into three types, i.e., free, dispersed and emulsified oils, by considering the droplet size. Free oil has a droplet size greater than 150 μm with a lower specific gravity than water and can thus easily be removed by traditional techniques like flotation. Dispersed oil, with oil droplet sizes ranging from 25 μm to 150 μm , is more stable than free oil and will only coalesce by an external force induced e.g., by centrifugal processes (Zhu et al., 2017). Oily wastewater with a droplet size of less than 20 μm , is classified as emulsified oil (Kajitvichyanukul et al., 2011; Lin et al., 2019). Emulsified oils are usually stabilized by surfactants and are, therefore, resistant to coalescence to form larger oil droplets (Kajitvichyanukul et al., 2011). This makes them difficult to be removed from wastewater. Various technologies have been used to separate oily wastewater based on the oil droplet size (Yu et al., 2017). These include coagulation and flocculation, gravitational settling, dissolved air flotation, hydrocyclone, and adsorption. However, when dealing with stable oil-in-water (O/W) emulsions, the above-mentioned methods have difficulties, i.e., too low separation efficiency to meet reinjection and reuse purposes (Janknecht et al., 2004). Moreover, the traditional methods have high capital and operational costs and require a large operation space (Fakhru'l-Razi et al., 2009; Padaki et al., 2015; Saththasivam et al., 2016). The advantages and disadvantages of the commonly used methods for oily wastewater treatment have been compared in Table 2.1.

■ Chapter 2

Table 2.1 Comparison of oily wastewater treatment methods (Fakhru'l-Razi et al., 2009; Saththasivam et al., 2016).

Methods	Principle	Advantages	Disadvantages
Coagulation/flocculation	Break the emulsion and promote droplet coalescence via chemical additives	Enhanced oil coalescence and aggregation, increase the removal of solids and organic compounds	Not effective for dissolved oil removal, a large volume of sludge is produced
Gravitational settling	Separation of free oil (> 150 μm) based on the specific gravity of oil droplets	No energy requirement, cheaper, effective for large oil droplets and suspended particles removal	Not suitable for stable emulsion and dissolved oil removal
Dissolved air flotation	Oil droplets attach to the dissolved air bubbles and float to the surface	Suitable for the removal smaller particles and oil droplets > 20 μm	Difficult to remove dissolved oil, not cost effective to produce large amount of air that are smaller than oil droplets
Hydrocyclone	Free oil separation under centrifugal force	Compact modules, higher efficiency for smaller oil droplets	Fouling and clogging, energy requirement, not effective to remove stable oil emulsion
Adsorption	Retain contaminants by porous adsorbent	Compact modules, high quality effluent, cheaper	High retention time, generated chemical waste related to the regeneration of adsorbent
Polymeric membrane	Remove particles, colloids and oil droplets (< 20 μm) based on size exclusion	High quality permeate, small footprint, little chemical requirement	Membrane fouling, susceptible to degradation at temperatures higher than 50 °C, sensitive to chemical cleaning
Ceramic membrane	Remove particles, colloids and oil droplets (< 20 μm) based on size exclusion	High quality permeate, small footprint, little chemical requirement, high chemical, thermal and mechanical stability	Membrane fouling, Higher cost than polymeric membranes, brittleness, defects

■ Chapter 2

Membrane separation is one of the most promising methods for oily wastewater treatment, especially O/W emulsions (Obaid et al., 2017; Tanudjaja et al., 2019). The separation of oily wastewater by membranes has several advantages, including a high oil removal efficacy, no chemical addition, and a more compact design, compared to traditional technologies (Padaki et al., 2015). The high mechanical, thermal and chemical stability of ceramic membranes make these membranes particularly suitable for industrial wastewater treatment, such as oily wastewater (Hyun and Kim, 1997). The initial manufacturing cost of ceramic membranes is higher compared to their polymeric counterparts. However, the performance of ceramic membranes in water and wastewater treatment, including extended lifespan and reduced maintenance requirements, can offset the overall water production cost (Gu et al., 2021). Besides, because of the hydrophilic surface, the high porosity and the narrow pore size distribution, ceramic membranes are considered to have a higher permeate flux and lower membrane fouling (Goh and Ismail, 2018; K. Shams Ashaghi, 2007; Li et al., 2020). Moreover, they are known as materials with good tolerance to high oil content and other foulants in the feed. After fouling, the membranes can be cleaned in-place (CIP) with more aggressive chemicals at a higher temperature (Asif and Zhang, 2021; Jarvis et al., 2022; Tomczak and Gryta, 2020), while, polymeric membranes normally suffer from degradation when the temperature is higher than 50 °C (Saththasivam et al., 2016). A schematic review of the advantages of ceramic membranes for water treatment over polymeric counterparts can be found in a recent review (Li et al., 2020). As a result, ceramic membranes have been widely studied in oily wastewater treatment. As shown in Figure 2.1, the number of publications about ceramic membranes for oily wastewater treatment, as well as the number of citations of papers per year, increased considerably, from 20 and 733 to 101 and 3866 respectively, between the years 2012 and 2020.

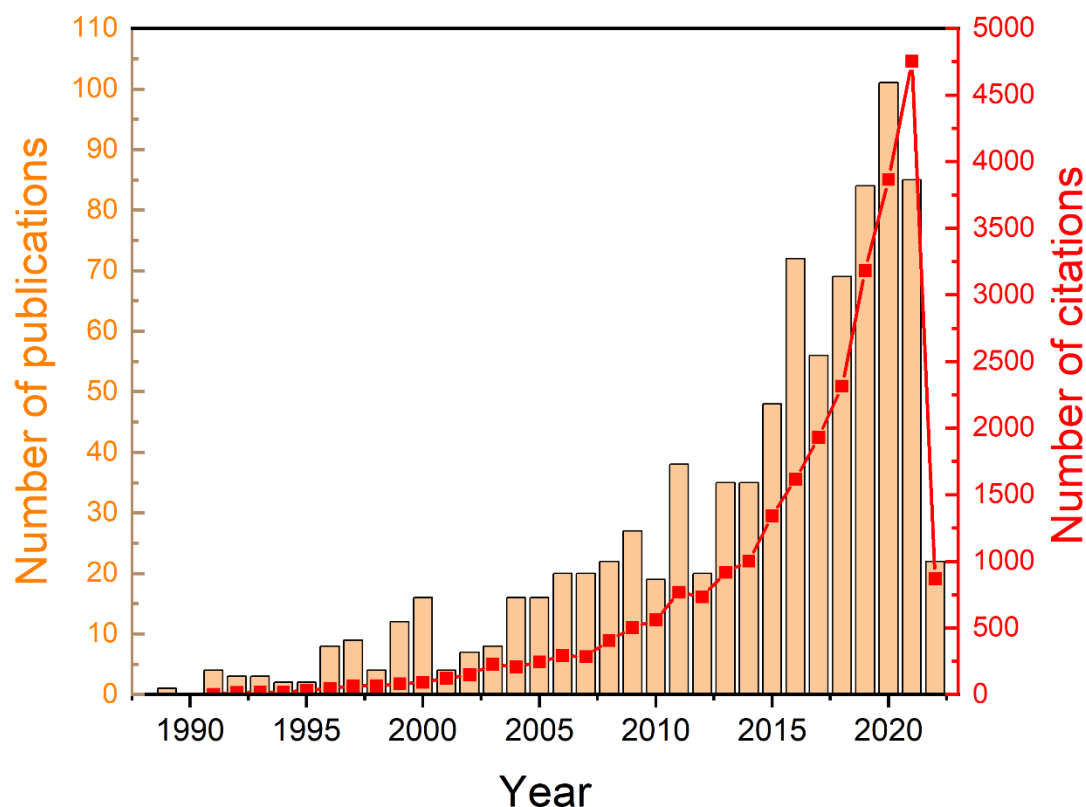


Figure 2.1. Numbers of publications and citations on the topic of ceramic membranes for oily wastewater treatment from 1989 to 2022. The data were extracted from Web of Science in March 2022, with the keywords of “ceramic membrane AND (oily wastewater OR oil-in-water emulsion OR produced water)”.

The membranes, however, suffer from fouling problems during the filtration process, in which a layer of oil droplets, suspended particles and other components of wastewater is formed on the membrane surface and/or membrane pores are plugged or blocked by small oil droplets and particles (Rezazazemi et al., 2018). Membrane fouling causes a decrease in permeance, resulting in a lower flux or higher operating pressures (Lu et al., 2016a). As a consequence, it is important to control membrane fouling effectively during the filtration process (Ebrahimi et al., 2017). Reducing membrane fouling can lead to a decrease in operating costs and thus to a potential increase in ceramic membrane applications on the oily wastewater treatment market.

In their previous work, Dickhout et al. (2017) explored the interaction between the membrane and produced water emulsion from a colloidal perspective. Huang et al. (2018) conducted a review of antifouling membranes for oily wastewater treatment, focusing on the interplay between wetting and membrane fouling. More recently, Tanudjaja et al. (2019) provided an overview of various aspects related to the practical applications of membrane filtration for oily wastewater treatment. However, to date, no review papers

■ Chapter 2

have specifically addressed fouling of ceramic membrane filtration in the treatment of oily wastewater. In order to achieve a comprehensive understanding of ceramic membrane fouling by oily wastewater, in this review, we first introduce the composition of oily wastewater and then the ceramic membranes (materials and type) for oily wastewater filtration. Afterwards, the factors affecting ceramic membrane fouling during oily wastewater separation are discussed from the aspects of feed characteristics, membrane properties, and operational parameters. Finally, the commonly used strategies (pretreatment, backpulsing/backwashing, chemical cleaning and membrane modification) for fouling control of ceramic membrane filtered by oily wastewater are reviewed and opportunities for improved fouling control are identified.

2.2. Ceramic membrane filtration for oily wastewater treatment

2.2.1. Composition of oily wastewater

Oily wastewater mainly contains oil and grease and some other contaminants, such as suspended particles, dissolved organic substances, chemical additives (e.g., surfactants), and inorganic substances (e.g., heavy metals, and salts) (Lee and Neff, 2011). However, the composition of oily wastewater varies considerably in various industries. A high content of organic carbon is commonly observed in the food and drinking industry, while the oil content in metal processing industry is very low (Tanudjaja et al., 2019).

Produced water during oil and gas extraction is the largest stream of oily wastewater in the world with a global estimated 3:1 volume-to-product ratio, adding up to an estimated annual global volume of 54 billion cubic meters in 2020 (Adham et al., 2018; Munirasu et al., 2016). To prevent operational problems and improve oil recovery, surfactants and other chemical additives are commonly used in the oil and gas industry (Dickhout et al., 2017; Jiménez et al., 2018). Produced water also contains other constituents from the subsurface (Abadi et al., 2011). The physical and chemical properties of the produced water vary considerably, depending on the geographic location, operational conditions and age of the oil and gas fields. For example, salinity and hardness level, mainly composed of Cl^- , Na^+ , Ca^{2+} and Mg^{2+} , vary from 0 to 300000 mg L^{-1} (Jiménez et al., 2018). The total organic carbon (TOC) concentration is normally in a range of 500-1000 mg L^{-1} (Adham et al., 2018). Typically, the total dissolved solids (TDS), and major ions (e.g., Cl^- , Na^+ , Ca^{2+} , Ba^{2+} , Mg^{2+} and Sr^{2+}) increase with well lifetime, while alkalinity, pH and TOC decrease with time (Chang et al., 2019). In addition, a high water to oil production ratio is often found in many aging oil wells (Wenzlick and Siefert, 2020).

2.2.2. Materials used to produce ceramic membranes

The ceramic membranes widely used in oily wastewater treatment are alumina (Al_2O_3), zirconia (ZrO_2), titania (TiO_2), silicon carbide (SiC) and low-cost ceramic membranes (e.g., mullite, and kaolin) (Figure 2.2A). Al_2O_3 and ZrO_2 membranes were first used for oily

■ Chapter 2

wastewater treatment due to their commercial availability on the market (Bhave and Fleming, 1988; Chen et al., 1991) (Figure 2.2A). Membrane filtration with an Al_2O_3 membrane was considered as the best available technology among the treatments of oilfield brines by the US EPA in 1992 (Zaidi et al., 1992). Compared with Al_2O_3 membrane, ZrO_2 membrane has a higher and more stable flux in addition to be less susceptible to fouling (Koltuniewicz and Field, 1996; Wang et al., 2000; Yang et al., 1998). The higher hydrophilic and negatively charged surface of ZrO_2 membrane leads to the weak attachment of oil droplets. Therefore, higher fluxes and lower fouling have been observed (Wang et al., 2000; Wang et al., 2022b).

Afterwards, zeolite ceramic membranes were synthesized by in situ crystallization on the inner surface of tubular α -alumina substrates for oily wastewater treatment (Li et al., 2008; Liu et al., 2008). It was found that the zeolite layer can improve the fouling resistance of the membrane due to the enhanced surface hydrophilicity. In addition, the nano-channel pathways along the zeolite pores favour the transport of water molecules (Anis et al., 2021; Cui et al., 2008).

In the present decade (since 2009), TiO_2 and SiC membranes have been developed for the separation of oily wastewater (Figure 2.2A). Zhang et al. (2009) first studied the TiO_2 -doped Al_2O_3 composite membrane with an average pore size of $0.2 \mu\text{m}$ for oily wastewater filtration, a higher and more stable permeate flux was observed for the Al_2O_3 - TiO_2 composite membrane than that of Al_2O_3 membrane. Ebrahimi et al. (2009) used TiO_2 membrane for oil-field produced water filtration with an oil rejection of up to 99%.

Compared with the Al_2O_3 , ZrO_2 , and TiO_2 membranes, SiC membranes have been considered to have a higher mechanical strength, chemical resistance and a lower thermal expansion coefficient (Ciora et al., 2004; König et al., 2014; Shi et al., 2006). Furthermore, SiC membranes have a lower irreversible fouling and higher permeate flux than polymeric membranes and traditional ceramic membranes (Chen et al., 2022; Chen et al., 2020b; Eray et al., 2021; Hofs et al., 2011). As a result, SiC membranes have been demonstrated for pilot and full-scale produced water treatment (Pedenaud et al., 2011; Prado-Rubio et al., 2012). More recently, silicon nitride (Si_3N_4) ceramic membranes were developed and studied for O/W separation. The membrane with a pore size of $0.68 \mu\text{m}$ was found to have a high oil rejection (95%) and permeate flux ($390 \text{ L m}^{-2} \text{ h}^{-1}$ (LMH)) at a transmembrane pressure (TMP) of 1 bar in an alkaline environment (Abadikhah et al., 2018; Li et al., 2018).

One of the major limitations for industrial application of the ceramic membranes is their higher costs than their polymeric counterparts, because of the utilization of expensive inorganic precursors (Al_2O_3 , ZrO_2 , TiO_2 , Si_3N_4 and SiC), smaller surface area per module and high sintering temperatures, associated with high energy consumption (Nandi et al., 2009). For example, commercial SiC ceramic membranes are usually sintered at a temperature up to $2000 \text{ }^\circ\text{C}$ in an argon atmosphere (Das et al., 2020a). Therefore, clay-based or clay-bonded and solid-state waste-based low-cost ceramic membranes have been developed for the separation of O/W emulsion in the last decade (Figure 2.2A)

Chapter 2

(Abbasi et al., 2010a; Abbasi et al., 2010b; Chen et al., 2020c; Das et al., 2020b; Eom et al., 2014; Mohammadi et al., 2004; Nandi et al., 2010; Song et al., 2006; Wu et al., 2022). These low-cost ceramic membranes are usually prepared with e.g., kaolin, quartz, mullite, feldspar, bauxite and coal fly ash, at a temperature below 1500 °C (Chen et al., 2016a; Zou et al., 2019a; Zou et al., 2019b; Zou et al., 2019c). As shown in Figure 2.3, the performance of the low-cost ceramic membranes is comparable with traditional commercial ceramic membranes in terms of permeate flux and oil rejection (Kumar et al., 2015; Mestre et al., 2019; Zhu et al., 2016; Zhu et al., 2019). However, the chemical stability of these membranes may be lower due to the existence of impurity and higher porosity in the membrane matrix, thus leading to a shorter lifetime (Singh et al., 2020). Therefore, they are mainly studied with synthetic O/W emulsions at a lab-scale; no pilot or full-scale applications have been demonstrated yet.

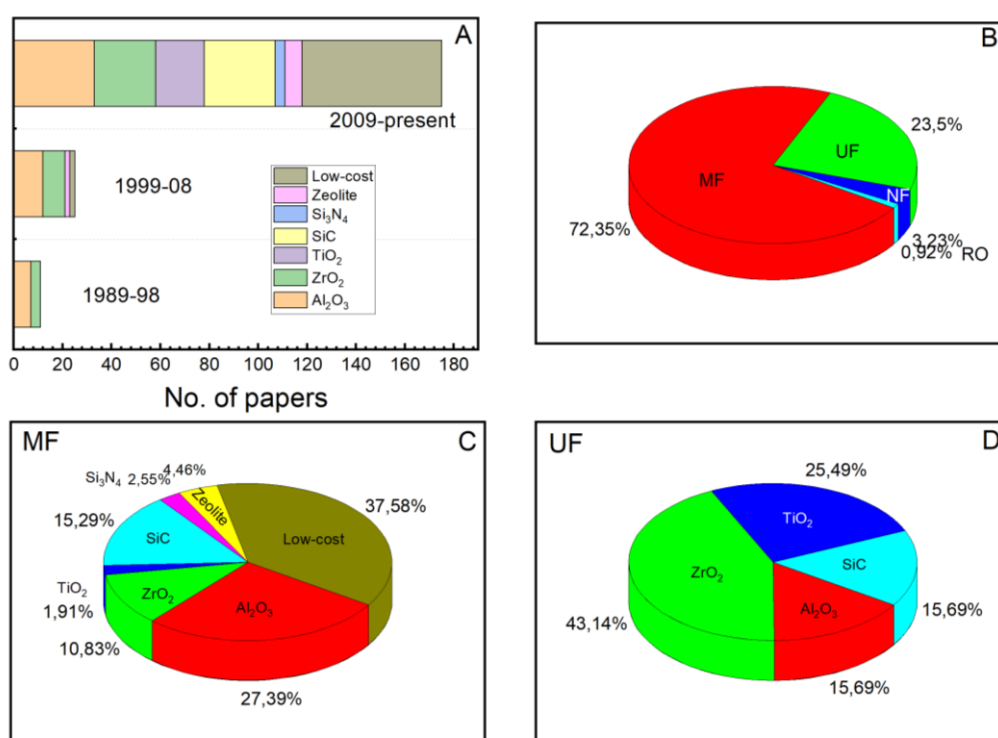


Figure 2.2. (A) Numbers of papers of different ceramic membranes in three divided decades (updated in September 2021), (B) percentage of each type of ceramic membranes, (C) percentage of different ceramic MF membrane materials, and (D) percentage of different ceramic UF membrane materials for oily wastewater or produced water treatment. Note that some papers report on several ceramic materials or types in each, so the number of ceramic membrane materials and types rather than the number of papers is presented here.

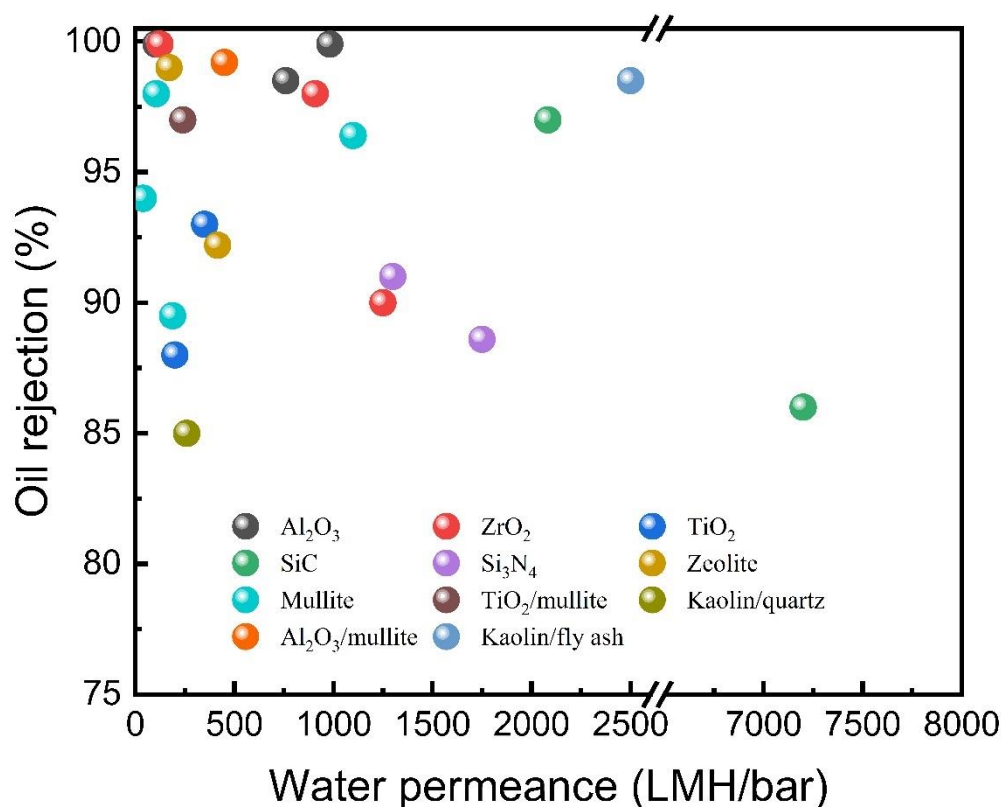


Figure 2.3. Relationship of oil rejection and initial water permeance of traditional ceramic membranes and low-cost ceramic membranes. Here we chose 22 samples from literature (Table S1, supplementary information) to have a general performance comparison of traditional ceramic membranes with low-cost ceramic membranes.

2.2.3. Type of ceramic membranes used for oily wastewater filtration

The type of ceramic membranes used for oily wastewater treatment include microfiltration (MF), ultrafiltration (UF), nanofiltration (NF) and zeolite reverse osmosis (RO) (Figure 2.2B). Ceramic MF and UF membranes are the most (> 95%) studied ones for oily wastewater treatment among the four types of membranes (Figure 2.2B). In MF, Al₂O₃, SiC and low-cost ceramic membranes are the top three membranes studied in literature (Figure 2.2C), while in UF, also ZrO₂, and TiO₂ membranes are used, where ZrO₂ membrane accounts for the highest percentage (Figure 2.2D). TiO₂ and zeolite are respectively used as ceramic NF and RO membranes for produced water treatment (Liu et al., 2008; Motta Cabrera et al., 2021).

Table 2.2 lists the configuration of the commercial ceramic membranes used for oily wastewater treatment as reported in literature. Considering the high fouling potential and variable composition of oily wastewater, tubular ceramic MF and UF are the most used because they have a higher fouling resistance and are ease to clean (Mueller et al., 1997;

■ Chapter 2

Wang et al., 2000). For model O/W emulsions and refineries, these membranes have shown a high oil rejection (> 98%) (Zsirai et al., 2016). Although a lower flux has been found at a higher oil concentration in the feed, the rejection of the membrane has not been compromised. For real oily wastewater, like produced water, MF or UF treatment alone is not sufficient (Chang et al., 2019; Munirasu et al., 2016). For example, despite having a much higher permeate flux than other ceramic membranes, the oil rejection of SiC MF membrane is only 73-86 % for produced water treatment (Zsirai et al., 2016), and the TiO₂ UF only reaches a maximum rejection of 88% (Zsirai et al., 2016). Unlike the model O/W emulsions, oil droplet size distribution could be much wider in real oily wastewater. The presence of small oil droplets enables them to pass through the membrane easily. Additionally, the salinity of real oily wastewater, such as produced water, is very high, compromising the effectiveness of the membrane's surface charge in oil rejection.

Given that low rejection is commonly observed by ceramic MF/UF for real oily wastewater, especially produced water, NF and RO should then be considered as a post-treatment step. Because the temperature of produced water could be as high as 85 °C, ceramic membranes are more suitable to use than polymeric membranes, since they would encounter degradation issues at these high temperatures (Atallah et al., 2019b). Ceramic NF and zeolite RO membranes are relatively new technologies (Fakhru'l-Razi et al., 2009; Voigt et al., 2019). Ebrahimi et al. (2009) reported the use of commercial NF membranes, preceded by either MF or UF for the treatment of model (synthetic) and real produced water. The ceramic membrane systems showed up to 99% oil removal, but severe flux reduction of NF membranes was observed during real produced water filtration. In another study, a total oil removal of up to 99.5% was also obtained using ceramic UF followed by ceramic NF as a final treatment of oilfield produced water (Ebrahimi et al., 2010). Besides the high oil rejection, ceramic NF also exhibited high TOC (75-90%) rejection and 100% total suspended solids (TSS) rejection. Furthermore, most divalent cations and anions (e.g., Ba²⁺, Ca²⁺, Mg²⁺ and SO₄²⁻) can be efficiently removed from produced water (Motta Cabrera et al., 2021). Zeolite RO ceramic membranes are normally synthesized at lab-scale. Because of the uniform sub-nanometer- or nanometer-scale pores of zeolites, these membranes could be used to reject dissolved organic pollutants and salts from produced water (Liu et al., 2008).

■ Chapter 2

Table 2.2 Comparison of commercial ceramic membrane filtration in the treatment of oily wastewater.

Membrane			Feed condition					Performance			Refs
Material	Pore size (μm)	Configuration	Oil type	d_{oil} (μm)	C_f (mg L^{-1})	CFV (m s^{-1})	TMP (bar)	Initial flux (LMH/bar)	Final flux (LMH/bar)	R^d (%)	
$\alpha\text{-Al}_2\text{O}_3$	0.2	Tubular	Crude oil	1-10	250	0.24	0.69	760	61	98.5	(Mueller et al., 1997)
$\alpha\text{-Al}_2\text{O}_3$	0.8	Tubular	Crude oil	1-10	250	0.24	0.69	982	48	99.9	(Mueller et al., 1997)
$\alpha\text{-Al}_2\text{O}_3$	0.1-0.2	Tubular	Rolling emulsion	10-20	10000	3-5	1-2	54	~	99.8	(Wang et al., 2000)
ZrO_2	0.1-0.2	Tubular	Rolling emulsion	10-20	10000	3-5	1-2	125	62.5	99.9	(Wang et al., 2000)
$\alpha\text{-Al}_2\text{O}_3$	0.05	Tubular	Synthetic oily wastewater	~	500	1.68	2	~	85	98	(Hua et al., 2007)
ZrO_2	0.2	~	Refinery oil	~	6000	2.56	1.1	218	109	99.4	(Zhong et al., 2003)
$\alpha\text{-Al}_2\text{O}_3$	0.2	Tubular	Refinery oil	~	26	2.25	1.25	350	260	84.6	(Abadi et al., 2011)
ZrO_2	0.1	Tubular	Produced water	1-100	100	2	2	908	87.5	98	(Weschenfelder et al., 2015a)

■ Chapter 2

ZrO ₂	0.1	Tubular	Produced water	~	25±2	3	1.5	700	200	88	(Weschenfelder et al., 2015b)
TiO ₂	50kDa	Triangular	Produced water	~	20-57	2	0.4	200-250	100	71-88	(Zsirai et al., 2016)
TiO ₂	2	Triangular	Produced water	~	30-84	2	0.4	350-600	300	80-93	(Zsirai et al., 2016)
TiO ₂	0.05	Tubular	Produced water	~	565	0.6-1.3	1	70	5	99	(Ebrahimi et al., 2009)
SiC	0.04	Tubular	Olive mill wastewater	~	275	2	67 ^b	2083	347	97	(Fraga et al., 2017a)
SiC	0.04	Tubular	Produced water	~	20-57	2	0.4	1500-1900	500	61-85	(Zsirai et al., 2016)
SiC	0.5	Tubular	Produced water	~	38-57	2	0.4	7200-8400	2500	73-86	(Zsirai et al., 2016)
NF ^a -TiO ₂	1000Da	Tubular	Produced water	~	565	~	1	20	20	99.53	(Ebrahimi et al., 2010)

C_f-oil concentration in the feed, CFV-cross-flow velocity, d_{oil}-oil droplet size, R_d-oil rejection, ~ not mentioned, a-UF pretreatment, b-constant flux, LMH.

2.3. Ceramic membrane fouling in oily wastewater treatment

Membrane fouling, causing a decreased permeate flux and increased operating costs, is one of the primary challenges influencing the long-term operation of membranes (Dickhout et al., 2017; Miller et al., 2017; Padaki et al., 2015). As shown in Figure 2.4, the type of fouling depends on feed composition (foulant component, pH, ionic strength, and temperature), membrane structural and physicochemical properties (pore size, hydrophilicity/hydrophobicity, surface charge and roughness), and operational conditions (TMP, permeate flux, and cross-flow velocity). The factors that affect the ceramic membrane's fouling in oily wastewater treatment are further discussed in this section.

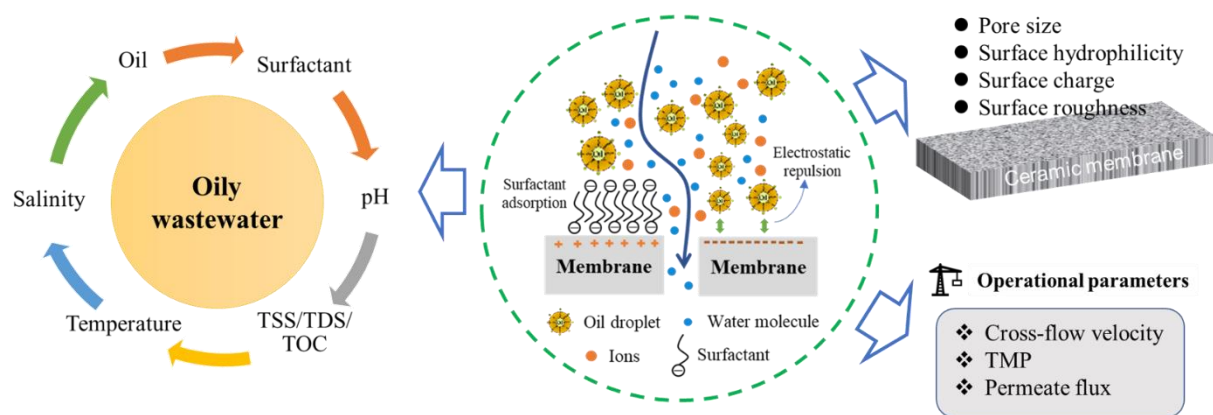


Figure 2.4. Schematic diagram of the three main factors on ceramic membrane fouling during oily wastewater treatment.

2.3.1. Effect of oily wastewater characteristics on membrane fouling

Membrane fouling is strongly affected by the characteristics of oily wastewater such as oil concentration, pH, ionic strength, surfactant type and concentration, and temperature (Chen et al., 2022; Nagasawa et al., 2020). With an increase in oil concentration in the feed, a larger permeate flux decline and higher oil rejection are normally observed as a thicker oil layer is formed over the membrane surface that is difficult to be removed by hydraulic cleaning (Hua et al., 2007; Kumar et al., 2015; Mohammadi et al., 2004; Suresh et al., 2016). In the cross-flow microfiltration of oily wastewater using an $\alpha\text{-Al}_2\text{O}_3$ membrane, Hua et al. (2007) observed that the TOC removal efficiencies increased from 95.8% to 98% with an increase in oil concentration from 250 to 1000 mg/L. Kumar et al. (2015) also found a larger flux decline in the microfiltration of synthetic oily wastewater when oil concentration increased from 50 to 200 mg/L. At the highest oil concentration (200 mg/L), oil rejection reached 99.64%. The type of oil can affect the droplet behaviour near a membrane surface. Oils with a higher viscosity are not easily removed by cross-flow and are thus more likely to attach on the membrane surface (Tummons et al., 2020).

■ Chapter 2

The effect of pH on oil emulsion depends on the surfactants used for emulsion preparation. For instance, the properties (zeta potential and droplet size) of the O/W emulsion, stabilized by dioctyl sulfosuccinate sodium salt and Span 80, respectively, have not been affected by pH, based on studies by Lobo et al. (2006) and Zhang et al. (2009). The effect of solution pH on membrane fouling is mainly caused by the electrostatic interactions between the charged membrane surface and the charged oil droplets (Zhang et al., 2009). A higher stable permeate flux and higher oil rejection has been found at higher pH due to the stronger electrostatic repulsion between the oil droplets and membrane surface (Abadikhah et al., 2018). In addition, Hua et al. (2007) observed a higher negative charge of oil droplets at a higher pH. In that case, the higher permeate flux of the Al₂O₃ membrane was the result of a more “open” cake layer at high pH, due to the inter-droplet interaction.

Ceramic membrane filtration is frequently used for high temperature oil emulsion separation due to its high thermal stability. At higher temperatures the permeate flux of ceramic membranes increase, because of the decrease of the viscosity of water (Abadi et al., 2011; Chang et al., 2014; Mohammadi et al., 2004; Zhu et al., 2019). However, membrane fouling can also be higher as oil droplets can deform to some degree and block the membrane pores due to lower viscosities of the oil at a higher temperature (Chang et al., 2014; Mohammadi et al., 2004).

Salts, commonly present in produced water, are known to affect both the characteristics of oil droplets and the interaction at the interface of oil and membrane and, thereby, membrane fouling (Tanudjaja et al., 2017). A higher concentration of salts in the feed leads to more fouling and lower rejection, due to the effect of compressed electrical double layer and reduced oil-water interfacial tension (Hua et al., 2007; Virga et al., 2020; Zhang et al., 2013). The charge and shape of the oil droplets are also affected by the salts (Weschenfelder et al., 2019). Abbasi et al. (2010a), e.g., found that the permeate flux of ceramic membrane decreases with an increase in the salt concentration from 25 to 200 g/L. However, Weschenfelder et al. (2019) found that the presence of salts can improve permeate flux when the membrane and oil emulsion have opposite charges.

Oil emulsions are normally stabilized by surfactants and, therefore, the type and concentration of the present surfactant are important in determining the interaction between oil droplets and membrane. A higher permeate flux has been observed when ZrO₂ membranes were used to separate an anionic (glycolic acid ethoxylate oleyl ether) surfactant-stabilized emulsion, while a lower permeate flux was observed for a cationic (hexadecyl trimethyl ammonium bromide) surfactant-stabilized emulsion. This difference in flux can be attributed to the effects of electrostatic repulsion and electrostatic attraction between the membrane surface and droplets (Matos et al., 2016). However, an opposite conclusion was drawn by Lu et al. (2015b) who found that irreversible membrane fouling could be alleviated during ultrafiltration of O/W emulsions with an TiO₂ ceramic membrane oppositely charged to the stabilization surfactant, due to synergetic steric hindrance and demulsification. It was speculated that

■ Chapter 2

the electrostatic attraction of positively charged surfactants on the negatively charged membrane surface and pores form a surfactant barrier which prevents oil droplets' penetration. In addition, due to less positively charged surfactants in the solution, small oil droplets become unstable and tend to coalesce into larger droplets, which are more likely to be rejected by the membrane. In a recent study, Chen et al. (2022) found that increase in surfactant concentration (below the critical micelle concentration (CMC)) may then enhance the interaction between oil and membrane, and thereby improve membrane performance. With an increase in anionic surfactant concentration, the irreversible fouling of both positively charged and negatively charged ceramic membranes was reduced. The primary reason for fouling alleviation on the positively charged membrane surface was attributed to the adsorption of surfactant. On the other hand, the reduction in fouling on the negatively charged membrane was attributed to the enhanced electrostatic repulsion between the membrane and oil droplets. Irrespective of the type of surfactants, a decline of permeate flux has been observed for SiC UF when the concentration of surfactant increases (above the CMC) (Shi et al., 2019). Matos et al. (2016) found that the permeate flux of ZrO₂/TiO₂ UF (50 kDa) membrane decreased with the concentration of cationic surfactant stabilized emulsions. For emulsions stabilized by nonionic surfactant, the membrane only showed a decrease of permeate flux when the concentration of surfactant was above the CMC. The permeate flux of the membrane was enhanced for emulsions stabilized by anionic surfactants with a concentration below the CMC. Another effect of increasing surfactant concentration is the lower oil-water interfacial tension, which means that the oil droplets are more deformable and thus easier squeeze through the membrane pores. For example, a transition from high to low oil rejection was observed for three types (anionic, cationic and nonionic) of surfactant-stabilized emulsions filtered by SiC MF membrane with increased surfactant concentration (Virga et al., 2020).

Unlike synthetic O/W emulsions, the real oily wastewater (e.g., produced water) contain many other components such as suspended particles, dissolved organic compounds and solids, which may accelerate membrane fouling. For example, Tomczak and Gryta (2020) observed a larger decrease of permeate flux when applying ultrafiltration to real oily wastewater than that of synthetic O/W emulsion made from the same oil. The interaction of oil emulsions with suspended particles could thus be a major reason for causing ceramic membrane fouling. Abdalla et al. (2019) also studied the effect of suspended inorganic particles on the microfiltration of oil emulsion. Compared with the emulsion alone, the addition of suspended solids (bentonite) in the oil emulsion resulted in a permeance decrease of 3.5-5 times. In contrast, Tomczak and Gryta (2020) found that pre-filtration adversely affect membrane fouling during ultrafiltration of oily wastewater. Without pre-filtration, the suspended particles could form a cake layer on the membrane surface, preventing the occurrence of internal fouling and leading to a higher stable permeate flux. In addition, the particulate matter present in produced wastewater is more likely aggregated due to the high salinity of the solution. Membrane fouling becomes more

■ Chapter 2

serious when the aggregates break into smaller particles at elevated shear force, leading to intermediate pore blocking (He and Vidic, 2016). Polymeric additives used to enhance oil recovery via increasing the viscosity of water injected into the reservoirs can also have a negative effect on membrane fouling. Weschenfelder et al. (2021) found that the flux decline of ZrO₂ membranes reached 84% in 40 min operation for feed prepared with 0.1 g L⁻¹ polymer and 100 g L⁻¹ NaCl. The flux reduction was still high (83% decline) even for a feed prepared with only 1 g L⁻¹ polymer. The saturated dissolved solids could form crystalline particles (e.g., CaCO₃ and BaSO₄) in the bulk of oily wastewater and then deposit on the membrane surface, even though it can be alleviated by adjusting the pH of the feed (Simonič, 2019). The gradual buildup of the precipitates on the membrane surface would result in a decline in permeate flux (Loganathan et al., 2015). Characterization of flux and permeate quality during oily wastewater treatment is generally used to monitor the performance degradation of the membrane due to fouling. However, it cannot provide further information on membrane fouling due to the effect of interactions of different components in produced water and their interactions with the membranes. Therefore, detailed characterizations of the autopsied membranes would provide valuable insights into the fouling processes in ceramic membranes. Thibault et al. (2017) proposed a possible fouling formation sequence in ceramic ultrafiltration of produced water, based on the so-called micro-characterizations such as backscattered electron (BSE) imaging and wavelength-dispersive (WDS) X-ray maps (Figure 2.5). Firstly, the local surface linear defects, arising from the sol-gel synthesis of the selective layer, are responsible for fouling initialization. These defect areas can act as nucleation sites, favouring the precipitation of saturated species (e.g., Mg(OH)₂, SiO₂, and BaSO₄). Following this initial inorganic precipitation, oil compounds may then preferentially adsorb on the precipitates or co-precipitation of dissolved organic matter and silica may occur. Eventually, the filtration performance was decreased, and the operating life of the ceramic membrane was shortened. In addition, reaction with anatase in the selective layer was observed during the crystallization of BaSO₄, suggesting that other types of ceramic membranes should be considered when dealing with produced water with high levels of dissolved Ba.

Chapter 2

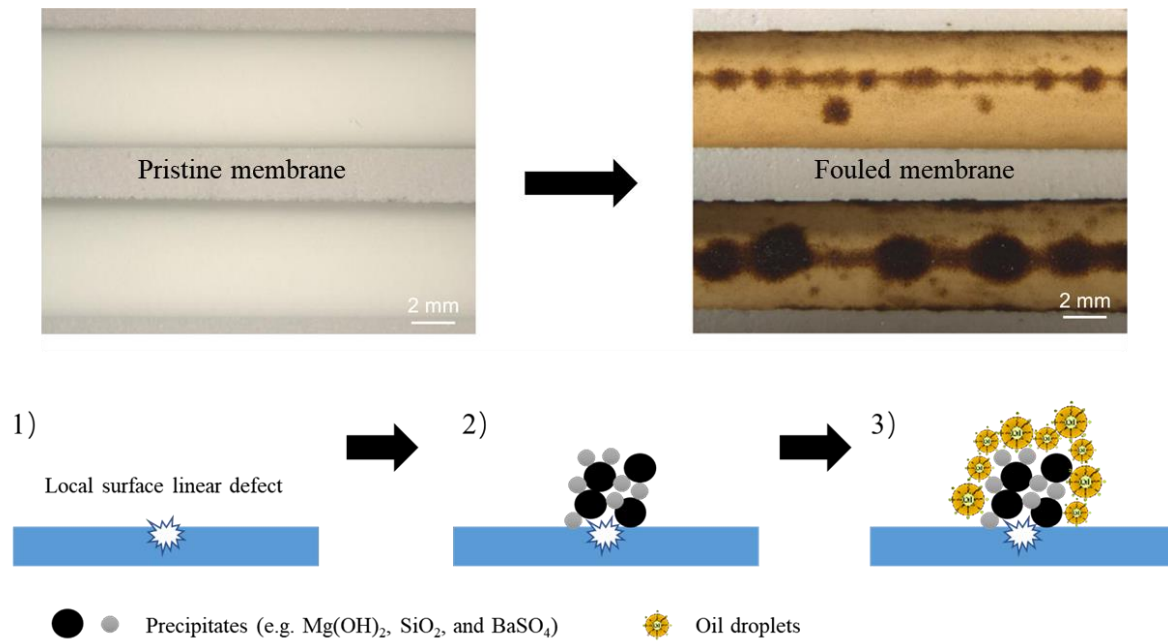


Figure 2.5. Possible sequence of fouling formation on the ceramic membrane surface for ultrafiltration of produced water (Thibault et al., 2017). The surface linear defects are the possible reason leading to the initialization and propagation of fouling on membrane surface.

In order to gain a better insight on the fouling mechanism of oil on the membrane surface, many other non-invasive techniques have been developed to visualize membrane fouling process. One such technique, known as direct observation through membrane (DOTM), involves using a microscope equipped with a video camera. Tummons et al. (2016) reported using DOTM to reveal the fouling behaviour of sodium dodecyl sulfate (SDS) stabilized O/W emulsions on the surface of an anodic alumina Anopore membrane ($0.2 \mu m$). The study found that membrane fouling by oil droplets occurred in three distinct stages: (1) droplets attachment and clustering, (2) droplet deformation, (3) droplet coalescence. In addition, electrical impedance spectroscopy (EIS), ultrasonic time-domain reflectometry (UTDR) and optical coherence tomography (OCT) have been shown to provide valuable information on fouling process of droplets on membrane surfaces (Tanudjaja et al., 2019; Tummons et al., 2020). However, these techniques are still limited in their applications either due to the requirement of a special membrane module or the low image resolution of the equipment.

2.3.2. Effect of membrane properties on membrane fouling

Membrane pore size

The rejection mechanism of MF and UF membranes is mainly based on the size-sieving effect. A smaller pore size gives a better rejection as well as less irreversible fouling (Ghidossi et al., 2009). Oil droplets larger than the membrane pore size may accumulate on the membrane surface blocking the pores and eventually forming a deposition or cake

■ Chapter 2

layer. A complete pore blocking is easier formed on a membrane surface with smaller pore sizes, leading to serious fouling and higher oil rejection (Huang et al., 2018a; Nagasawa et al., 2020). However, oil droplets are deformable, and they can squeeze through the membrane when TMP is higher than critical pressure (more discussion in section 2.3.3). Therefore, irreversible fouling can still occur even if the membrane pore size is smaller than the oil droplets (Nagasawa et al., 2020). Ebrahimi et al. (2010) observed a lower decline of the flux of the membranes with a pore size of 0.1 μm and 20 kDa compared to a membrane with a pore size of 0.2 μm . Whereas, Jiang et al. (2013) found that an MF ceramic membrane with a larger pore size can mitigate fouling for the treatment of flowback water from a shale gas well.

Membrane surface hydrophilicity

Hydrophilicity is one of the most important surface properties of the filter medium (Chang et al., 2010a; Zhou et al., 2010), since the affinity between foulants and the membrane surface under water is important for membrane fouling. A hydrophilic surface could effectively prevent the deposition or adsorption of the hydrophobic oil droplets from the emulsions (Dickhout et al., 2017) and thus improve the membrane permeate flux (Chang et al., 2014; Lu et al., 2016b; Srijaroonrat et al., 1999). Ceramic membranes are normally prepared with metal oxides and all of them are hydrophilic because of the surface hydroxyls, making them, in principle, suitable for oily wastewater treatment (Lu et al., 2016a). In addition, the surface hydrophilicity of the ceramic membranes was found to be related to the open porosity of the membranes. A higher hydrophilic surface was observed for membranes with a higher open porosity, leading to lower fouling due to smaller adhesion force of oil droplets (Jiang et al., 2022). However, an explanation for this phenomenon was not found. Among the ceramic membranes, SiC membranes show superhydrophilic properties with a static water contact angle below 5° , resulting in a high water permeance and low fouling potential for O/W separation (Jiang et al., 2020; Xu et al., 2020).

Membrane surface charge

Membrane surface charge becomes increasingly important when charged foulants are present in the feed (Tang et al., 2011). Electrostatic interaction will dominate the membrane fouling at low salinity in the feed water. However, with a high concentration of salts presented, the charge effect will be weakened due to the compression of the electrical double layer (He and Vidic, 2016; Zhang et al., 2009). In addition, the membrane surface charge is strongly dependent on iso-electric point (IEP) of the membrane materials and the pH of the solution. Oil droplets in produced water are usually negatively charged, also due to the addition of anionic surfactants to improve oil recovery. Therefore, the selection of a membrane with the same surface charge to oil droplets can mitigate membrane fouling. This becomes more important when the membrane pore sizes are comparable to that of the oil droplets (Nagasawa et al., 2020). SiC membranes have the

■ Chapter 2

lowest IEP (pH 2.6) among ceramic membranes, making them thus more suitable for oily wastewater treatment with a low salt concentration or ionic strength (Hofs et al., 2011; Skibinski et al., 2016). Zsirai et al. (2016) compared performance of SiC and TiO₂ membranes in a pilot-scale study of produced water filtration and the results suggested that the SiC MF membranes had the highest fouling propensity among the ceramic membranes. This was explained by the following two reasons: firstly, the high salinity of the produced water screened the electrostatic interaction between SiC membrane and oil droplets. Secondly, all membranes were filtered at the same pressure, a higher fouling propensity could happen in SiC MF as the initial flux was more than 10 times higher than that of other ceramic membranes.

Membrane surface roughness

The effect of surface roughness on membrane fouling is under debate. In some studies, increased surface roughness was found to increase membrane fouling due to the enhanced interaction between oil droplets and the rougher membrane surface (Rana and Matsuura, 2010; Zhong et al., 2013). However, a decreased fouling tendency was observed for (super)hydrophilic membranes with a rough surface (hierarchical structure) than the one with a smooth surface. The proposed mechanism is that water can be trapped in the micro-/nanoscale structure and in this way, reducing the contact area of the membrane to which oil-droplets can attach (Dickhout et al., 2017; Huang et al., 2018b).

2.3.3. Effect of operational parameters on membrane fouling

Cross-flow velocity

Membrane separation can be operated in either a dead-end or cross-flow mode. The use of cross-flow filtration with turbulent flow can effectively reduce membrane fouling by sweeping away the deposited pollutants on the membrane surface, permitting longer filtration cycles. Turbulent flow is easier to be obtained in membrane feed channels with a wider diameter at lower crossflow velocities compared to capillary membranes. At a very high crossflow velocity, turbulent flow can also be achieved in capillary membranes (e.g., 0.7 mm inner diameter) while leading to high energy consumption (Table 2.3). Also, a higher permeate flux can be observed at higher cross-flow velocities due to stronger turbulence formed on the membrane surface. For oily wastewater separation, the operation with ceramic membranes in the cross-flow mode is increasing (Zsirai et al., 2016). However, with increasing cross-flow velocity, the shape of oil droplets is strongly deformed and the flocs are prone to breakup on the membrane surface or in the cross-flow pump due to the high shear forces. In these cases, the oil droplet and particles can pass or block the membrane pores, leading to more severe fouling and/or low rejection (Darvishzadeh and Priezjev, 2012; He and Vidic, 2016).

■ Chapter 2

Table 2.3 Correlation of feed channel diameter and crossflow velocity to achieve turbulent flow in membrane filtration.

Feed channel diameter	Crossflow velocity	Flow type	Energy consumption
Small	High	Turbulent	High
Big	Small	Turbulent	Low

Permeate flux

So far, few papers have paid attention to the effect of permeate flux on ceramic membrane fouling for oily wastewater treatment. Fraga et al. (2017a) assessed a SiC membrane for the treatment of olive mill wastewater at constant flux filtration. A flux of 67 LMH was decided for the test as the lowest TMP increase was observed. Loganathan et al. (2015) found that the optimal permeate flux range is 125-130 LMH for ultrafiltration of oily wastewater in a pilot study. In this flux range, stable and sustained operations were achieved. However, several authors have studied the effect of permeate flux on polymeric membrane-based oily wastewater treatment (He et al., 2017a; He et al., 2017b; Kasemset et al., 2016; Kirschner et al., 2017; Kirschner et al., 2019; Miller et al., 2014a; Miller et al., 2014b). In most studies, the results indicate that TMP increases gradually and then approaches a steady state if the flux is below the threshold flux (He et al., 2017a; He et al., 2016; Miller et al., 2014b). However, a three-stage fouling is developed when the flux is above threshold flux (Figure 2.6). In stage 1, a gradual increase of TMP has been observed followed by a sharp TMP jump (stage 2). Finally, the TMP enters a pseudo-steady state region. Below the threshold flux, modest increase in fouling resistance was observed for both constant flux and constant pressure filtration conditions, while above the threshold flux, fouling was more severe in the constant flux system (Miller et al., 2014a). Fux and Ramon (2017) have found that during operation at low flux, the oil droplets are spherical, being easily removed by cross-flow cleaning, while a high flux would lead to droplets' deformation and irreversible deposition on the membrane surface or in the membrane pores.

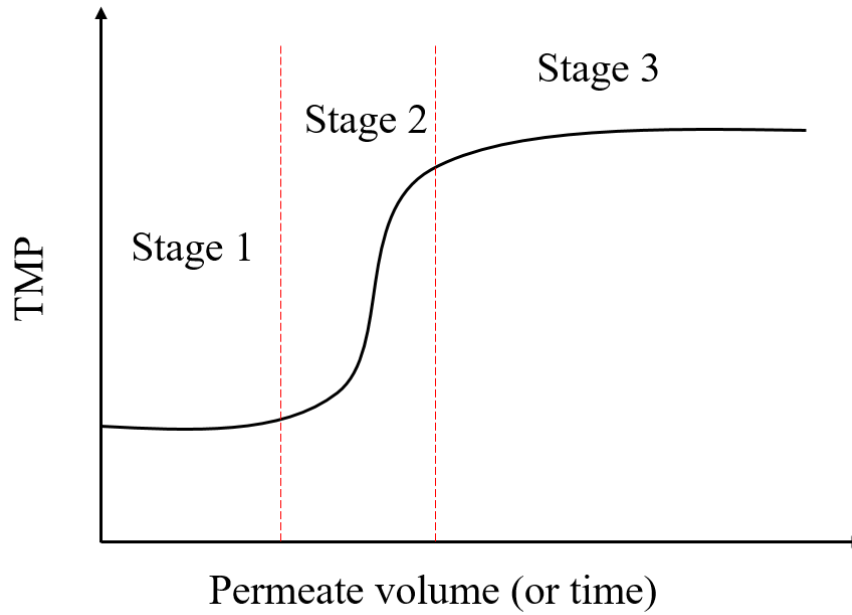


Figure 2.6. Fouling develops in three stages in constant flux cross-flow filtration with flux above the threshold flux (He et al., 2017b).

Operational pressure

During the filtration of O/W emulsions by a membrane, the rejection of solutes could be different from the rigid particulate as the shape of oil droplets varies, depending on the applied pressure. Therefore, oil droplets can coalesce or break into smaller ones, entering or penetrating the membrane pores that are narrower than the average size of oil droplets (Faibish and Cohen, 2001a; He et al., 2017b). A model was put forward by Nazzal and Wiesner (1996) to describe the TMP required for a droplet to deform and permeate the membrane (critical pressure). The model was later corrected by Cumming et al., (2000) and validated by Darvishzadeh and Priezjev (2012). The critical pressure, P_{crit} can be described as:

$$P_{crit} = \frac{2\sigma \cos \theta}{r_p} \sqrt[3]{1 - \frac{2 + 3 \cos \theta - \cos^3 \theta}{4(r_d/r_p)^3 \cos^3 \theta - (2 - 3 \sin \theta + \sin^3 \theta)}} \quad (1)$$

Where σ is the interfacial tension of the oil phase and aqueous phase, r_d is the oil droplet size, r_p is the diameter of membrane pores, θ is the contact angle of oil and membrane.

Table 2.4 summarizes the critical pressures for ceramic membranes in oily wastewater treatment. As can be seen, the critical pressures are usually located in the range of 1-3 bars for MF and UF ceramic membranes. Higher critical pressures are observed for larger oil droplets filtered by membranes with the same or similar pore sizes. In addition, membranes with smaller pore sizes have been found to have a higher critical pressure for rejecting oil droplets with comparable sizes. When TMP is higher than the critical

■ Chapter 2

pressure, a lower oil rejection but a higher permeate flux can be observed (Nagasawa et al., 2020). Furthermore, when the nominal pore size of membranes was similar, the membrane with a larger pore size distribution was found to have a lower oil rejection as oil droplets can pass through some larger pores of the membrane (Shirzadi et al., 2022).

Table 2.4 Critical pressures for O/W wastewater based ceramic MF/UF membranes in different studies.

Pore size (μm)	Membrane	Critical pressure (bar)	Method	Mean droplet size (μm)	Refs
0.05	$\alpha\text{-Al}_2\text{O}_3$	2	Experiments	0.45	(Hua et al., 2007)
0.2	ZrO_2	1.55	Experiments	---	(Zhong et al., 2003)
0.2	$\alpha\text{-Al}_2\text{O}_3$	1.25	Experiments	3	(Abadi et al., 2011)
0.2	$\text{TiO}_2\text{-Al}_2\text{O}_3$	2.4	Experiments	6	(Chang et al., 2014)
0.68	Si_3N_4	1	Experiments	0.68	(Abadikhah et al., 2018)
0.15	---	1	Analytic	0.9	(Darvishzadeh and Priezjev, 2012)
0.5	$\alpha\text{-Al}_2\text{O}_3/\text{ZrO}_2$	2.8	Analytic	11	(Srijaroonrat et al., 1999)

--- not reported

2.4. Fouling control of ceramic membrane for oily wastewater filtration

Membrane fouling is gradually formed during the oily wastewater filtration process. A cake layer (reversible fouling) can be formed on the membrane surface when the oil droplet size is larger than the pore size of membrane and can be removed by regular backpulsing/backwashing. Internal clogging may occur when the particles are smaller than the membrane pore size which further reduces the pore volume, thus resulting in constriction of pore flow (irreversible fouling) (Kim et al., 1997; Silalahi et al., 2009). Chemical cleaning is widely used to recover the membrane performance after accumulation of irreversible fouling. In Figure 2.7, we can see that the commonly used methods for fouling control of ceramic membranes in oily wastewater treatment include:

pretreatment, backpulsing/backwashing, and chemical (acid and/or base) cleaning (Shams Ashaghi et al., 2007). In addition, membrane modification can be an effective way to alleviate membrane fouling.

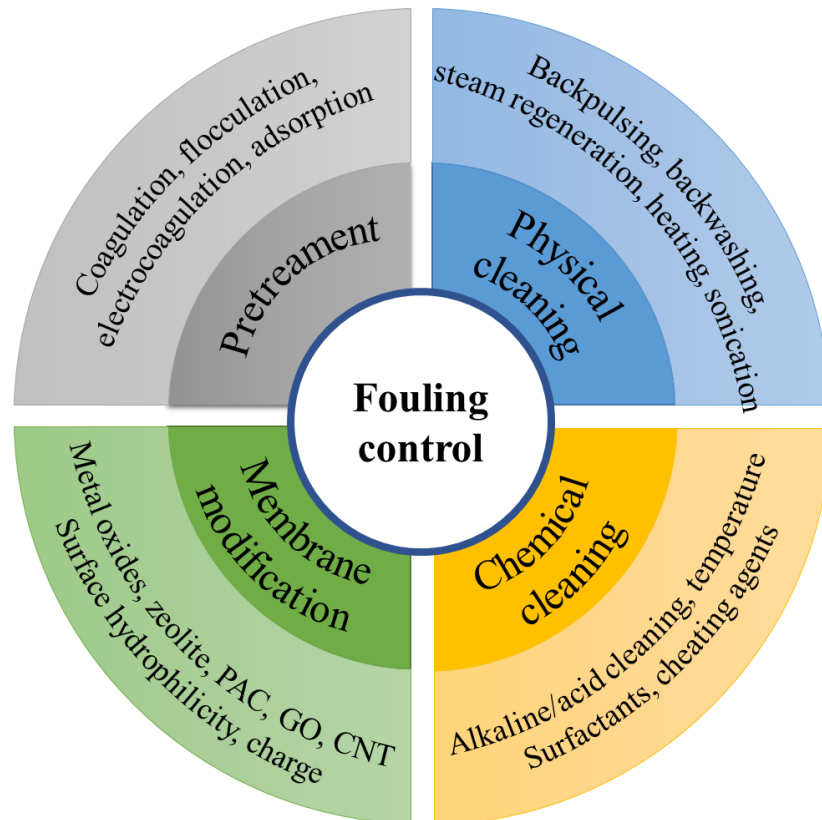


Figure 2.7. Fouling control of ceramic membranes for oily wastewater treatment. The strategies include pretreatment, physical cleaning, chemical cleaning and membrane modification.

2.4.1. Pretreatment

Pretreatment to enhance oily wastewater treatment efficacy by ceramic membranes include coagulation/flocculation (Abbasi et al., 2012; Zhong et al., 2003), electrocoagulation (Changmai et al., 2019) and adsorption (Rasouli et al., 2017b). Aluminum and iron salts are commonly used for coagulation and the concentration of coagulant is important to increase membrane flux and oil rejection (Abbasi et al., 2012; Rasouli et al., 2017a). Flocculants can also be used to decrease membrane fouling and improve permeate quality. Zhong et al. (2003) compared five types of flocculants (inorganic and polymeric) for the pretreatment of refinery wastewater. The most effective flocculant was 3530S (a derivative of polyacrylamide). Changmai et al. (2019) utilized electrocoagulation-microfiltration for the treatment of oily wastewater. The concentration of oil and grease could considerably be reduced in 20 min and then ceramic membranes were used to remove the flocs. Due to the increase in the size of oil droplets after coagulation/flocculation as well as the formation of large flocs on the membrane

■ Chapter 2

surface, a highly porous cake layer and low attractive energy between the cake layer and the membrane surface was formed and the extent of pore plugging was decreased (Zhong et al., 2003). However, when the flocculant is overdosed, sludge flocs could be formed and could block the membrane pores and thus increase membrane mass transfer resistance (Abbasi et al., 2012).

Oily wastewater treatment can also be enhanced by a hybrid adsorption-membrane filtration process. A combination of powdered activated carbon (PAC) with membrane filtration is generally used (Abbasi et al., 2011; Rasouli et al., 2017b; Yang et al., 2011a). Abbasi et al. (2011) studied the effect of the concentration of PAC on the performance of ceramic membranes. Permeate flux of the membranes increased at a low concentration of PAC loading (200-400 ppm), while a decrease of permeate flux of the membranes was observed at high PAC concentrations due to the deposition of PAC particles on the membrane surface. Yang et al. (2011a) also used PAC (100 ppm) as an additive in the microfiltration-PAC system for emulsion filtration. Membrane fouling was effectively mitigated due to the mechanical scouring effect of PAC particles. Other adsorbents such as zeolite can also be used in the pretreatment step to reduce membrane fouling (Rasouli et al., 2017b).

2.4.2. Backpulsing/backwashing

In Table 2.5, an overview is given of the performance of ceramic MF/UF membranes with and without backpulsing/backwashing for oily wastewater treatment. Backpulsing is done at a shorter duration (the time backwashing is applied) and higher frequency (time between backwashing) as compared to backwashing. During the long-term filtration, backpulsing/backwashing has a positive effect on MF/UF membrane filtration performance, which is normally conducted at 1-4 bar (Ebrahimi et al., 2010; Zsirai et al., 2016). It can remove the surface deposits and unblock the pores. In addition, backpulsing/backwashing would allow a higher average flux, requiring a lower membrane surface area and, as a consequence, resulting in more compact systems with reduced footprints (Weschenfelder et al., 2015b). The frequency and duration of backwashing can be adjusted to achieve an improved recovery (Jepsen et al., 2018). Weschenfelder et al. (2015a) found that a higher effective permeate flux was obtained at a higher backwashing frequency. In addition, a combination of backpulsing and backwashing led to the highest effective permeate flux. Zsirai et al. (2018) also observed that a higher flux can be sustained via the application of backpulsing during the cleaning-in-place process. Furthermore, backwashing can be enhanced (so called ECB) with chemicals such as NaOH and acid to extend the timespan between chemical cleaning (so called CIP) being required for produced water treatment (Loganathan et al., 2015).

■ Chapter 2

Table 2.5 Backpulsing/backwashing performance of ceramic membranes for oily wastewater treatment.

Feed	Membrane	Pore size (μm)	Backpulsing/backwashing conditions	Results	Refs
Dilute oil-in-water suspension	$\alpha\text{-Al}_2\text{O}_3$	0.2/0.8	$P = 1.4 \text{ bar}$, $t_b = 0.2, 0.5 \text{ s}$, $f = 0.01\text{-}0.1 \text{ Hz}$	The permeate flux was increased up to 25 times with backpulsing.	(Ramirez and Davis, 1998)
Unstable secondary emulsion	ZrO_2	0.1	$P = 3 \text{ bar}$, $t_b = 0.7 \text{ s}$, $t_i = 1 \text{ min}$	Steady state flux was increased from 450 to 1000 LMH after backpulsing	(Srijaroonrat et al., 1999)
Oil/water emulsion	ZrO_2	0.1	$P = 4 \text{ bar}$, $t_b = 0.2, 0.5, 1 \text{ s}$	The permeate flux with backpulsing was 3-fold higher than that without backpulsing	(Cakl et al., 2000)
Olive mill wastewater	SiC	0.04	$P = 3 \text{ bar}$, $t_b = 0.8 \text{ s}$, $t_i = 10 \text{ min}$	By backpulsing, the final TMP was reduced from 0.53 to 0.48 bar after 24h filtration at a constant flux of 67 LMH	(Fraga et al., 2017a)
Real and synthetic produced water	$\alpha\text{-Al}_2\text{O}_3$	0.1/0.2/0.5	$P = 2 \text{ bar}$, $t_b = 1 \text{ min}$, $t_i = 30 \text{ min}/60 \text{ min}$	A 22% and 30% improvement of permeate effective flux could be achieved when backwashing was applied every 60 and 30 min respectively	(Weschenfelder et al., 2015a)
Refinery wastewater	$\alpha\text{-Al}_2\text{O}_3$	0.2	$P = 2 \text{ bar}$, $t_b = 15 \text{ s}$, $t_i = 280 \text{ s}$	The periodic backwashing of ceramic membrane can maintain its performance in a long-term operation	(Abadi et al., 2011)
Oilfield produced water	ZrO_2	0.1	$P = 2 \text{ bar}$, $t_b = 30 \text{ s}$, $t_i = 40 \text{ min}$	The flux increased 35% immediately after the first backwashing	(Weschenfelder et al., 2015b)

P-backpulsing/backwashing pressure, t_b -backpulsing/backwashing duration, t_i -backpulsing/backwashing interval, f-backpulsing/backwashing frequency ($f = 1/t_i$).

2.4.3. Chemical cleaning

Although the decline of permeate flux can be prevented by using a periodic backpulsing/backwashing process, it is necessary to use chemical cleaning when the loss of permeate flux reaches 50-60% (Abadi et al., 2011). In Table 2.6, the chemical cleaning efficacy of different methods have been compared for oily wastewater treatment by ceramic membranes. As can be observed, the cleaning efficacy is affected by many factors, e.g., membrane properties, oily wastewater characteristics, cleaning chemicals, cleaning temperature, pressure, and duration. Usually, ceramic membranes can be easily cleaned after fouling by a synthetic oil emulsion. Zhu et al. (2016) used 0.1% NaOH aqueous solution to backflush the soybean oil fouled TiO₂-mullite ceramic membrane, and found that over 96% of the original flux can be recovered after the first generation cycle. Abadikhah et al. (2019) tested SiO₂ nanoparticles modified Si₃N₄ ceramic hollow fiber membrane with gasoline prepared emulsion, the membrane recovery was up to 92% by soaking the fouled membrane in HCl (0.5 M) and NaOH (0.5 M) aqueous solutions for 15 min, respectively. However, the membrane cleaning efficacy is much lower when challenged with the combined emulsion/suspension than with emulsion alone. It was found that the residual permeance of the ZrO₂ membrane is 16-fold lower after fouling by a combined emulsion/bentonite suspension based on six short runs with a standard chemical cleaning between each run (Abdalla et al., 2019). Due to the complex composition of real oily wastewater, such as produced water, the flux recovery of ceramic membrane is, in general, lower than for model O/W emulsion (Table 2.6).

The membrane properties such as pore size can affect the cleaning efficacy too. Silalahi and Leiknes (2009) compared the flux recovery of Al₂O₃ ceramic membrane with a nominal pore sizes of 0.1, 0.2 and 0.5 μm, respectively, for crude oil emulsion filtration. Membranes with a smaller pore size had a higher flux recovery in almost all cleaning combinations as oil droplets are mainly present on the surface of the membrane. Similar results have also been reported by other authors (Ebrahimi et al., 2010; Ghidossi et al., 2009). When challenged with produced water, membranes with a pore size of 0.1 μm had a flux recovery of 61%, whereas the cleaning efficacy was only 33% for the membranes with a pore size of 0.2 μm (Ebrahimi et al., 2010). Ghidossi et al. (2009) found that chemical washing could not regenerate the ZrO₂-TiO₂ membrane with a pore size of 0.1 μm for oily wastewater treatment due to internal fouling. A 300-kDa membrane was observed to have a high permeance recovery after chemical cleaning. From these studies, a membrane with smaller pore sizes seemed to be more suitable for oily wastewater treatment to obtain a higher flux recovery with chemical cleaning. In addition, membrane surface hydrophilicity and surface charge can also affect the flux recovery of ceramic membranes. A higher flux recovery is normally observed for membranes with a more hydrophilic surface (Lu et al., 2016a).

Alkaline and acid solutions are widely used for ceramic membrane cleaning due to its chemical stability (Kayvani Fard et al., 2018b; Li et al., 2020). Alkaline solutions can

■ Chapter 2

remove the organic compounds from the membrane surface, while inorganic compounds (e.g. scaling materials) can be effectively removed by acid solutions (Porcelli and Judd, 2010). To improve the cleaning efficacy, a combination of the two solutions is commonly utilized. For produced water applications, the most effective cleaning cycle is alkaline solution cleaning followed by an acid rinse (Chen et al., 1991). Weschenfelder et al. (2015b) studied the cleaning efficacy of ZrO₂ membranes after filtration with produced water. The flux recovery of the membrane was only 40% after hot water rinsing, but could be increased up to 58% after alkaline cleaning and to 86% of the original flux after subsequent acid cleaning. By optimizing the chemical cleaning protocol, Fraga et al. (2017a) found that the flux of SiC membrane can be recovered to 100% after hot water rinsing, acid/alkaline and alkaline/acid cleaning after filtering olive mill wastewaters. Simonič (2019) also reported that the best strategy to fully restore the ceramic UF membrane performance was, firstly, using alkaline solution ASG (PRU 06–03, Gütling, Germany) at 40 °C for 1 h at 1bar. Then the membrane was flushed with distilled water. Afterwards, the membrane was cleaned with HCl (pH = 3) for 30 min followed by final flushing with water.

In addition, the cleaning efficacy of the ceramic membrane can be further improved with chemicals at a higher temperature. Silalahi and Leiknes (2009) found that after filtering with crude oil emulsion, the permeance recovery of Al₂O₃ membranes can reach 91% when cleaned at 45 °C with alkaline and acid solutions. A higher permeance recovery (99%) was observed when cleaned at 80 °C. Fraga et al. (2017a) also compared the chemical cleaning efficacy at room temperature and 60 °C. The membrane could only be recovered to 23% permeance when cleaned at room temperature, while the permeance was totally restored after cleaning at 60 °C. Complete recovery of membrane performance after fouling by real oily wastewater was also achieved by 1–3 wt% NaOH and H₃PO₄ solutions at 50 °C (Tomczak and Gryta, 2020).

Other chemicals such as surfactants (e.g., SDS) and chelating agents (e.g., ethylene diamine tetra acetic acid (EDTA)) have also been used for ceramic membrane cleaning. Surfactants can detach the oil from the membrane surface due to reduced oil-water surface intension. Chelating agents are expected to form complexes with oil droplets and separate them from the membrane surface (Garmsiri et al., 2017). Garmsiri et al. (2017) compared the cleaning efficacy of SDS with three other chemicals (H₂SO₄, NaOH and EDTA), and, with concentration of 10 mM, it was found to be the best cleaning agents to recover ceramic membrane performance after filtration of a simulated O/W emulsion.

Since ceramic membranes are resistant to oxidation, oxidants, such as sodium hypochlorite (NaClO), ozone (O₃) and hydrogen peroxide (H₂O₂), are widely used to remove organic and biological foulants on the membrane surface and/or in the pores through oxidation and/or disinfection (Porcelli and Judd, 2010; Wang et al., 2014). However, these oxidants are not commonly used to clean the ceramic membranes after

■ Chapter 2

fouling by oil droplets because they are found to be ineffective to degrade the oil droplets (Chang et al., 2001).

2.4.4. Other cleaning methods

To minimize the chemical waste after chemical cleaning, other cleaning methods have been explored. As an alternative to chemical cleaning, Atallah et al. (2019a) applied a steam regeneration technique to recover the performance of ceramic membranes in the filtration of produced water at 80-85 °C. It was found that the permeate flux recovery of the membrane was only 50% with backflushing only, but it could be increased even up to 200% with the injection of steam directly into the feed channels in conjunction with backflushing. This high flux recovery was attributed to a sudden change in the viscosity of the constituents in the cake layer. The viscosity of the filter cake was reduced for the duration of the steam exposure time, leading to more effective release from the membrane surface. After steam regeneration, the membrane still maintained a high temperature, leading to the reduction of feed viscosity and flux recovery of over 100%.

Heat treatment can also be used for the recovery of ceramic membrane performance via heating it in an oven. Abadikhah et al. (2018) restored 99% of the flux of emulsion fouled Si_3N_4 membranes after heating at 400 °C for 1h, while Chen et al. (2019) recovered the membrane performance up to 100% after oil fouling at 600 °C for 2h.

To enhance the ZrO_2 ceramic membrane separation process, an ultrasonic field was applied by Shu et al. (2007) in the treatment of O/W emulsion wastewater. The flux recovery ratio of the membrane was around 40% with water cleaning under sonication, but it could be increased to 70% combining with the use of chemical agents.

As observed in Table 2.6, the cleaning efficacy of ceramic membranes is related to the scale of the filtration experiment too. A higher permeance recovery has been found at bench scale than at pilot scale. This efficacy difference is caused by flow paths and uniform distribution of cleaning solution, which is more effective on a membrane surface with smaller module sizes (Weschenfelder et al., 2015a).

■ Chapter 2

Table 2.6 Cleaning of ceramic membranes by various methods for oily wastewater treatment.

Oily water source	Membrane	Pore size (μm)	Scale	Cleaning methods	Operation condition (Tem, Time, TMP)	Permeance recovery (%)	Refs
Crude oil	$\alpha\text{-Al}_2\text{O}_3$	0.1	b	1%v- Derquim (pH 9.8) + 1%v-Ultrasil 73 (pH 2.65)	80 °C, 0.85 \pm 0.1 bar	98	(Silalahi and Leiknes, 2009)
Crude oil	$\alpha\text{-Al}_2\text{O}_3$	0.1	b	1%v-Ultrasil 73 (pH 2.65) + 1%v-Derquim (pH 9.8)	80 °C, 0.85 \pm 0.1 bar	99	(Silalahi and Leiknes, 2009)
Crude oil	$\alpha\text{-Al}_2\text{O}_3$	0.1	b	1%v-Surfactron CD50 (pH 2.25) + 1%v-Derquim (pH 9.8)	45 °C, 0.85 \pm 0.1 bar	91	(Silalahi and Leiknes, 2009)
Crude oil	$\alpha\text{-Al}_2\text{O}_3$	0.2	b	1%v-Ultrasil 73 (pH 2.65) + 1%v-Derquim (pH 9.8)	80 °C, 0.85 \pm 0.1 bar	90	(Silalahi and Leiknes, 2009)
Crude oil	$\alpha\text{-Al}_2\text{O}_3$	0.5	b	1%v-Ultrasil 73 (pH 2.65) + 1%v-Derquim (pH 9.8)	80 °C, 0.85 \pm 0.1 bar	60	(Silalahi and Leiknes, 2009)
Soybean oil	mullite	1.02	b	0.1% NaOH	Room temperature	65	(Zhu et al., 2016)
Soybean oil	TiO ₂ -mullite	0.11	b	0.1% NaOH	Room temperature	96	(Zhu et al., 2016)
Rolling emulsion	ZrO ₂	0.1-0.2	p	1% NaOH + 1% citric acid	70 °C	78	(Wang et al., 2000)
Produced water	TiO ₂	1000 Da	b	lye solutions (1% (w/ w) NaOH solution, Ultrasil P3-14, Ultrasil P3-10)	30 to 60 min	41	(Ebrahimi et al., 2010)
Gasoline emulsion	Si ₃ N ₄	0.68	b	Heating at 400 °C	1 h	99	(Abadikhah et al., 2018)

■ Chapter 2

Produced water	ZrO ₂	0.1	b	Alkaline solution (1000 mg/L NaOH +100 mg/L NaClO) + acid solution (8 mg/L citric acid + 8 mg/L glycolic acid)	70 °C, recirculated 15 min	95	(Weschenfelder et al., 2015a)
Produced water	ZrO ₂	0.1	p	Alkaline solution (1000 mg/L NaOH +100 mg/L NaClO) + acid solution (8 mg/L citric acid + 8 mg/L glycolic acid)	70 °C, recirculated 15 min	83	(Weschenfelder et al., 2015a)
Produced water	SiC	0.04	p	6% NaOH + 6% citric acid	30 min, 0.55-0.6 bar	50	(Zsirai et al., 2018)
Olive mill wastewater	SiC	0.04	p	4% NaOH + 2% citric acid	25 °C	23	(Fraga et al., 2017a)
Olive mill wastewater	SiC	0.04	p	4% NaOH + 2% citric acid	60 °C	100	(Fraga et al., 2017a)
Produced water	ZrO ₂	0.1	b	Hot water rinsing	50 °C, 10 min, 0.5 bar	40	(Weschenfelder et al., 2015b)
Produced water	ZrO ₂	0.1	b	Hot water rinsing + KOH (10 mL/L) /alkylbenzene sulphonate (7 mL/L)	50 °C, 10 min + 40 °C, 30 min, 0.5 bar	58	(Weschenfelder et al., 2015b)
Produced water	ZrO ₂	0.1	b	Hot water rinsing + KOH (10 mL/L) /alkylbenzene sulphonate (7 mL/L) + Citric acid (8 mL/L)/glycolic acid (8 mL/L)	50 °C, 10min + 40 °C, 30min + 60 °C, 30 min, 0.5 bar	86	(Weschenfelder et al., 2015b)
Real oil emulsion	α-Al ₂ O ₃ -ZrO ₂	0.05	b	Water flushing + alkaline solution, ASG (PRU 06-03, Gütling, Germany) + HCl (pH = 3)	40 °C (alkaline cleaning), 1h, 1 bar	99.9	(Simonič, 2019)
Oily wastewater	~	8 kDa	p	Water flushing + 3% NaOH + 3% H ₃ PO ₄	50 °C, 1h + 50 °C, 1h	100	(Tomczak and Gryta, 2020)
Oil sand wastewater	TiO ₂	0.1	p	Citric acid (pH = 2.5) + NaOH (pH = 13)	~	100	(Loganathan et al., 2015)

b-bench scale, p-pilot scale, ~-not mentioned, Tem-temperature.

2.4.5. Membrane modification

In the filtration of O/W emulsions, the interaction between oil droplets and membrane surface is vital for membrane fouling. Reducing oil droplets adhesion on the membrane surface and/or in the pores can be achieved by precoating a thin layer of nano-materials (Anantharaman et al., 2020) or by changing surface properties such as charge, roughness and hydrophilicity (Dickhout et al., 2017). Thus, surface modification of ceramic membranes can make the membranes less susceptible to fouling (Shams Ashaghi et al., 2007).

Improving surface hydrophilicity and enabling a higher surface negative charge are two of the mostly used strategies for ceramic membrane modification (Chen et al., 2021). To improve surface hydrophilicity, nano-sized metal oxides such as TiO₂, ZrO₂, γ -Al₂O₃, Fe₂O₃ and SiO₂ have been used to enhance permeate flux and oil rejection in addition to the fouling alleviation of ceramic membranes (Chang et al., 2010b; Chang et al., 2014; Chen et al., 2016b; Lu et al., 2016b; Zhou et al., 2010). Besides, zeolites, PAC and graphene oxide have also been used to improve the separation efficacy of ceramic membranes during oil separation (Cui et al., 2008; Hu et al., 2015; Kayvani Fard et al., 2018a). Since oil droplets are stabilized with charged surfactants, electrostatic interaction between membrane surface and oil droplets is important for membrane fouling too. To reduce membrane fouling, Zhang et al. (2009) doped TiO₂ in Al₂O₃ powder to prepare a composite microfiltration ceramic membrane. The doping not only improved membrane surface hydrophilicity, but also shifted the isoelectric point of the membrane towards lower pH, increasing the negative charge. In addition, Chen et al. (2020b) found that the fouling resistance of Al₂O₃ membrane can be improved after deposition with a thin layer of SiC for O/W emulsion separation. The deposited SiC layer increased the negative charge of the membrane and, in this way, enhanced the electrostatic repulsion between the membrane surface and oil droplets. Furthermore, some organic polymers can also be used for ceramic membrane modification. For example, Chen et al. (2020a) grafted highly flexible polydimethylsiloxane (PDMS) brushes onto membranes. The grafting layer improved the permeate flux and fouling resistance during the separation of highly viscous O/W emulsions.

Despite that membrane fouling can be reduced after modification, there are still some challenges in relation to the modified membranes. For example, the durability and thermal stability of the coated nanoparticles or grafted polymers on the membrane surface may be a problem for practical applications. The nanostructure and properties of the coated layer could be damaged during frequent chemical or physical cleaning. In addition, the permeance of the membrane is generally lower after modification due to additional resistance of the layer formed after modification, leading to lower water production in constant pressure filtration. Furthermore, the modified layer may be effective to oil fouling, but cannot always address the fouling caused by other components

(e.g. particulate fraction, dissolved organic matter and solids) in produced water (Miller et al., 2014b).

2.5. Conclusion and future outlook

As one of the most promising technologies for oily wastewater separation, ceramic membranes have a better permeate quality, fewer chemicals addition, a longer service life and a reduced footprint compared to conventional methods. In terms of the type of ceramic membranes, MF and UF membranes are the most frequently used. They have shown a high oil removal efficacy for most of the oily wastewaters except for the produced water. Ceramic NF should be considered to improve oil, dissolved organics and salt rejection in produced water treatment. Developing low-cost ceramic membranes with clay or solid-state wastes has also been studied to reduce the costs of traditional ceramic membranes, long-term investigations of these membranes for oily wastewater treatment should be studied as a proof-of-concept.

Membrane fouling is one of the largest challenges for oily wastewater treatment. The selection of proper membranes can alleviate membrane fouling. Ceramic membranes with a higher surface hydrophilicity and charge, such as SiC membranes, are considered to have less fouling. However, there is not a consistent conclusion about the effect of membrane pores on fouling. To prevent the formation of complete pore blocking, applying the membranes with a larger pore size may mitigate the fouling. However, internal fouling is also easier to be formed in membranes with a larger pore size, leading to less permeate flux recovery. To achieve better oil filtration performance, the pore size, surface hydrophilicity and charge of the ceramic membranes should therefore be optimized together. As fouling can be initiated and accelerated by surface defects of the selective layer, the integrity of ceramic membranes should be maintained via careful control of the parameters of the membrane fabrication process.

Crossflow filtration with ceramic membranes for oily wastewater treatment has been preferred, as oil accumulation on the membrane surface can be suppressed with shear forces. More attention should be paid to the research on the permeate flux effect on ceramic membrane fouling as, in practical applications, constant flux filtration is preferred, but is rarely studied for oily wastewater treatment. If constant pressure filtration is applied, TMP should be below the critical pressure to prevent the penetration of oil droplets into the pores.

Pretreatment, backpulsing/backwashing and chemical cleaning are effective to reduce the fouling, recovering the permeance and extend the lifetime of the ceramic membranes. Pretreatment including coagulation/flocculation, electrocoagulation and adsorption can increase the membrane permeate flux, but overdosing may have an adverse effect. Backpulsing/backwashing has been recommended to maintain a long filtration run, but it's not effective to remove irreversible fouling. Chemical cleaning is necessary when the

■ Chapter 2

accumulation of irreversible fouling is high. To fully recover the ceramic membrane performance after the treatment of real oily wastewater, a combination of the use of chemical agents (base and acid) at high temperatures should be considered. In addition, steam regeneration, ultrasonic and heating could be effective for the regeneration of ceramic membrane and to minimize the waste production caused by chemical cleaning.

Membrane modification could improve ceramic membrane performance (higher permeate flux and oil rejection) and mitigate membrane fouling during the separation process. However, few studies have been focused on the stability of the coated layer in cleaning operation, which is commonly applied in practical applications. Therefore, the durability of nanoparticles and the long-term stability of the modified membranes is still to be studied.

Acknowledgement

Mingliang Chen acknowledges the China Scholarship Council for his PhD scholarship under the State Scholarship Fund (No. 201704910894). We would like to thank Nadia van Pelt for her help on language and grammar issues of the manuscript.

■ Chapter 2

Supplementary information

Table S2.1 Oil rejection and initial water permeance of traditional ceramic membranes and low-cost ceramic membranes.

Membranes	Water permeance (LMH/bar)	Oil rejection (%)	Refs
Al ₂ O ₃	982	99.9	(Mueller et al., 1997)
Al ₂ O ₃	760	98.5	(Mueller et al., 1997)
Al ₂ O ₃	105	99.9	(Yang et al., 1998)
ZrO ₂	1250	90	(Zou et al., 2021)
ZrO ₂	125	99.9	(Wang et al., 2000)
ZrO ₂	130	99.8	(Yang et al., 1998)
ZrO ₂	908	98	(Weschenfelder et al., 2015a)
TiO ₂	200	88	(Zsirai et al., 2016)
TiO ₂	350	93	(Zsirai et al., 2016)
SiC	7200	86	(Zsirai et al., 2016)
SiC	2083	97	(Fraga et al., 2017b)
Si ₃ N ₄	1750	88.6	(Li et al., 2018)
Si ₃ N ₄	1300	91	(Abadikhah et al., 2018)
Zeolite	170	99	(Cui et al., 2008)
Zeolite	415	92.2	(Barbosa et al., 2018)
Mullite	40	94	(Abbasi et al., 2010a)
Mullite	188	89.5	(Chen et al., 2016a)
Mullite	106	98	(Chen et al., 2016a)
Mullite	1100	96.4	(Rashad et al., 2021)
Mullite/TiO ₂	240	97	(Zhu et al., 2016)

■ Chapter 2

Kaolin/quartz	260	85	(Vasanth et al., 2011)
Fly ash/ Al_2O_3	450	99.2	(Zou et al., 2019b)
Kaolin/fly ash	2500	98.5	(Zou et al., 2021)

Chapter 3 |

State-of-the-art ceramic membranes for oily wastewater treatment: Modification and application

This chapter is based on:

Chen, M., Heijman, S. G., & Rietveld, L. C. (2021). State-of-the-art ceramic membranes for oily wastewater treatment: Modification and application. Membranes, 11(11), 888 (Editor's choice).

Abstract

Membrane filtration is considered one of the most promising methods for oily wastewater treatment. Because of the hydrophilic surface, ceramic membranes show less fouling compared with their polymeric counterparts. Membrane fouling, however, is an inevitable phenomenon in the filtration process, leading to higher energy consumption and a shorter lifetime of the membrane. It is therefore important to improve the fouling resistance of the ceramic membranes in oily wastewater treatment. In this review, we first focus on the various methods used for ceramic membrane modification, aiming for application in oily wastewater. Then the performance of the modified ceramic membranes is discussed and compared. We found that, besides the traditional sol-gel and dip-coating methods, atomic layer deposition is promising for ceramic membrane modification in terms of the control of layer thickness, and pore size tuning. Enhanced surface hydrophilicity and surface charge are two of the most used strategies to improve the performance of ceramic membranes for oily wastewater treatment. Nano-sized metal oxides such as TiO_2 , ZrO_2 and Fe_2O_3 and graphene oxide are considered to be the potential candidates for ceramic membrane modification for flux enhancement and fouling alleviation. The passive antifouling ceramic membranes, e.g., photocatalytic and electrified ceramic membranes, have shown some potential in fouling control, oil rejection and flux enhancement, but have their limitations.

3.1. Introduction

Water scarcity is a worldwide problem that threatens the sustainable development of society (Mekonnen and Hoekstra, 2016; Werber et al., 2016). The consumption of water by the industry sector is continuously rising in the last decades (Willet et al., 2019). In the meantime, large amounts of wastewater are produced in various industrial processes, leading to the pollution of the aquatic environment and thus threatening human health (Lefebvre and Moletta, 2006; Yang and Li, 2017). One of the typical examples is oily wastewater, which is produced by several industries, such as food and beverage, and textile production, metal finishing, and oil & gas extraction (Chen et al., 2020c; Chen et al., 2016a; Ibrahim et al., 2009; Zhu et al., 2016). The largest stream of oily wastewater in the world is produced during the oil & gas extraction process (produced water). It is estimated that the annual global volume of produced water reached 54 billion cubic meters in 2020 (Adham et al., 2018; Munirasu et al., 2016). To deal with oily wastewater, various treatment technologies have been developed, including flotation, coagulation & flocculation, gravitational settling, hydrocyclone, and adsorption (Coca et al., 2011; Duraisamy et al., 2013; Gupta et al., 2017). However, most of the above technologies are limited by the use of large volumes of chemical agents, the need for a large installation space, and a low separation efficacy for small oil droplets. It is therefore important to develop a robust, energy-efficient and low-cost technology for sustainable oily wastewater treatment (Padaki et al., 2015).

Membrane separation is considered as one of the most promising methods for oily wastewater treatment, especially for oil/water (O/W) emulsion separation with an oil droplets size smaller than 20 μm (Lin et al., 2019; Zhu et al., 2017). Compared with traditional methods, membrane separation has a higher oil removal efficacy, a more compact design and a smaller footprint. The high mechanical, chemical and thermal stability of ceramic membranes makes them particularly suitable for oily wastewater treatment (Abadi et al., 2011; Motta Cabrera et al., 2021; Zou et al., 2019a; Zou et al., 2019b; Zou et al., 2019c). It is assumed that ceramic membranes have a narrow pore size distribution, high porosity and hydrophilicity. Therefore, lower fouling is commonly observed in ceramic membranes compared to their polymeric counterparts (Hofs et al., 2011). Membrane fouling, however, is an inevitable phenomenon during the separation process. For oily wastewater treatment, large oil droplets may accumulate on the membrane surface causing cake layer formation. The membrane pore size can also be blocked or plugged by small droplets, leading to internal clogging. For both cases, the membrane performance deteriorates. This can be expressed by the reduction of water permeation flux, increase in transmembrane pressure (TMP) and increase in energy consumption (Zhang et al., 2016a). To control membrane fouling, backpulsing/backwashing can be applied periodically to remove reversible fouling (Cakl et al., 2000; Gao et al., 2020). When the performance of the membrane decreases by 50-60%, chemical cleaning is needed to remove irreversible fouling and to restore the membrane performance (Abadi et al., 2011). However, the robustness of the membrane

may decrease after frequent chemical cleaning, which has been found to be a challenge for ceramic nanofiltration (NF) membranes (Kramer et al., 2019). When membrane cleaning is not effective anymore, the membrane has to be replaced (Tummons et al., 2020).

In order to solve the membrane fouling problem fundamentally, the most common strategy is to construct fouling-resistant membrane surfaces via membrane modification (Anantharaman et al., 2020; Miller et al., 2017; Rezakazemi et al., 2018). In addition, pre-coating of a protective layer on the membrane surface is found to be effective for fouling alleviation (Anantharaman et al., 2020; Lu et al., 2016b; Zhao et al., 2005), but this is not covered in this review. Membrane modification is achieved by changing the surface physicochemical properties of the membrane to alleviate the interaction between the oil droplets and membrane surfaces (Gu et al., 2021; Li et al., 2020). It is assumed that surface hydrophilicity, charge and roughness are the three main factors affecting membrane fouling (Miller et al., 2017). A smooth surface is considered to be beneficial for fouling alleviation (Vrijenhoek et al., 2001). Membranes with a higher hydrophilic surface are supposed to have a lower propensity for adhesion to the hydrophobic oil droplets and are observed to have lower fouling (Chang et al., 2014; Zhou et al., 2010). For O/W emulsions stabilized by surfactants, the surface charge of the membranes becomes important for feeds with a low salinity (Dickhout et al., 2017). The membrane surface can then be modified to enhance the electrostatic repulsion between oil droplets and membrane surface (Chen et al., 2020b). In this way, oil droplets are less prone to be adsorbed on the surface or inside the pores. More recently, ceramic membranes coupled with photocatalysts (e.g., TiO_2) or Fenton catalysts (e.g., Fe_2O_3) have been developed to degrade the organic pollutants deposited on the surface via the strong radicals (e.g., $\cdot\text{OH}$) produced by the catalyst (Golshenas et al., 2020; Park et al., 2012). To alleviate membrane fouling, electrically active materials can also be incorporated into the matrix of ceramic membranes or coated on the membrane surface (Geng and Chen, 2016). With the assistance of external electricity, the organic pollutants can then be degraded by electro-oxidation or oxidized by the strong oxidizing intermediates. Other new ceramic membranes such as piezoelectric ceramic membranes have also been developed to alleviate the fouling by oil droplets via the in-situ generated ultrasound to suppress the accumulation of oil droplets on the membrane surfaces (Mao et al., 2020; Mao et al., 2019).

In this review, we first present the various methods, currently used, for ceramic membrane modification, the advantages and disadvantages of these methods are then discussed and compared. Afterwards, the current status, mechanism and performance on the state-of-the-art anti-fouling ceramic membranes for the treatment of oily wastewater are presented. Finally, potential opportunities and challenges of using modified ceramic membranes for oily wastewater treatment are highlighted.

3.2. Modification methods of ceramic membranes

Ceramic membranes are mostly composed of metal oxides and manufactured by high-temperature sintering. In principle, they are considered to be hydrophilic due to the presence of hydroxyl (-OH) groups on the membrane surface. However, the -OH groups density of the membrane is reduced after high-temperature calcination (Chang et al., 2010b). Surface modification of ceramic membranes can make the membranes less susceptible to fouling (Miller et al., 2017). In 1898, Martin and Cherry (1898) reported the modification of ceramic Pasteur-Chamerland water filters for the first time with gelation or silicic acid. Nowadays many more ceramic membranes modification techniques exist, such as sol-gel (De Lange et al., 1995), dip-coating (Xia et al., 2000), doping/blending (Zhang et al., 2009), grafting (Wei and Li, 2009), hydrothermal synthesis (Suresh et al., 2016), chemical vapor deposition (CVD) (Ha et al., 1996), and atomic layer deposition (ALD) (Li et al., 2012).

3.2.1. Sol-gel

The most commonly used strategy for ceramic membrane modification is the sol-gel process that is appropriate for making thin and porous layers with controllable porosity on a wide range of substrates (Duan et al., 2022; He et al., 2022; Lu et al., 1997). This method provides membranes with relatively thin top layers and it has widely been used for industrial ceramic membranes production (Nair et al., 1997). Basically, there are two kinds of sol-gel techniques: polymerization of molecule units (PMU) and destabilization of colloidal solutions (DCS). The PMU process is controlled by the hydrolysis of alkoxides and polycondensation followed by ageing and drying in the ambient atmosphere. The DCS process uses peptization of inorganic salts or hydrous metal oxides with an electrolyte and then these colloidal solutions are destabilized and gelation is obtained (Amin et al., 2016; Hench and West, 1990). The precursor sol can either be deposited on the membrane support to form a top layer (e.g., by dip-coating or spin coating) or cast into a suitable container with the desired shape to obtain the membrane (Guizard, 1996). To prevent the formation of defects and pinholes in membranes, the preparation should be done in a dust-free environment. In addition, partial gelation in the sol should be avoided (Guizard, 1996). Due to the particle aggregation at the sol stage in the DCS route, the PMU route has been considered to be more suitable for ceramic NF membrane fabrication (Cai et al., 2015). The modification of ceramic membranes via the sol-gel method aims for narrowing membrane pore sizes and endowing a lower fouling surface (Duan et al., 2022; Wang et al., 2022a). Bayat et al. (2016) prepared a γ -alumina ultrafiltration (UF) membrane on an α -alumina substrate by the sol-gel technique for separation of oil from real oily wastewater. The γ -alumina separation layer had an average pore size of 20.3 nm and exhibited a high permeate flux 112.7 L·m⁻²·h (LMH) and an oil rejection of 84% at a TMP of 5 bar. The low oil rejection was possibly due to the penetration of small oil droplets of feed at a relatively high temperature (35 °C).

3.2.2. Dip-coating

The dip-coating technique, offering the advantages of flexibility and ease of operation, is also frequently used for ceramic membrane modification (Xia et al., 2000). Dip-coating can be used for the coatings of sols or suspensions of submicrometer powders (Bonekamp, 1996). A dry substrate is dipped into a ceramic powder suspension or sol and then withdrawn from it, enabling the membrane surface to absorb a layer of suspension or sol due to the capillary forces. Once the layer comes into contact with the atmosphere it will rapidly dry and then a controlled calcination process follows (Barati et al., 2020). Generally, the coating thickness by a dip-coating process is in the range of 100 nm–100 μm (Bonekamp, 1996). Yang et al. (1998) fabricated an asymmetric $\text{ZrO}_2/\alpha\text{-Al}_2\text{O}_3$ composite membrane with zirconia fine powder suspensions at concentrations of 5-20%. The zirconia top layer had a thickness of 20 μm and an average pore size of 0.2 μm . The performance of the prepared $\text{ZrO}_2/\alpha\text{-Al}_2\text{O}_3$ composite membrane was compared with three commercial alumina membranes for separating O/W emulsions and the results indicated that the zirconia membrane had the highest stable permeate flux and same oil rejection as $\gamma\text{-Al}_2\text{O}_3$ membrane despite its higher mean pore size.

3.2.3. Surface grafting

Surface grafting is achieved by the combination of polymer chains onto a solid surface via a chemical reaction process, forming a strong covalent bond between the polymer brushes and the surface (Faibish and Cohen, 2001a; Rezakazemi et al., 2018). Therefore, the grafting layer has long-term chemical stability. The precursors for grafting are mostly polymers such as fluoroalkylsilanes (FAS) (Krajewski et al., 2006), poly(vinylpyrrolidone) (PVP) (Faibish and Cohen, 2001b), polyethylene oxide (PEO) (Atallah et al., 2019b) and poly(vinylacetate) (PVAc) (Jou et al., 1999). To initialize the grafting, membrane surfaces may be pretreated by chemicals, UV-irradiation, plasma or enzymes (Nady et al., 2011). Depending on the kind of grafting polymers, the specific properties of the membrane can be changed from superhydrophilic to superhydrophobic, which would widen the possible application ranges of the membranes. Hydrophilic ceramic membranes, with high mechanical strength, and a high chemical and oxidant tolerance, are modified by surface grafting mainly to make them hydrophobic or superhydrophobic for membrane distillation applications (Hendren et al., 2009). However, it can also be used for ceramic membrane modification to improve its anti-fouling abilities for oily wastewater treatment. A novel fouling-resistant zirconia-based UF membrane was modified by Faibish and Cohen (2001a) via free-radical graft polymerization of PVP chains onto the membrane surface. The membrane was evaluated for the filtration of microemulsions with oil droplets size of 18-66 nm. Due to the effective decrease in membrane pore size by grafted PVP chains, the modified membrane demonstrated higher oil rejection compared to the pristine ceramic membrane. In addition, the modified membrane exhibited lower irreversible fouling as a result of the effective masking of $-\text{OH}$ surface groups by PVP chains to reduce the association of solution species with the membrane surface.

3.2.4. Blending or doping

Another membrane modification method is the blending or doping of inorganic nano-sized particles into the membrane matrix (Jin et al., 2023; Monash and Pugazhenthii, 2011; Zhang et al., 2009). In this method, the nanoparticles are physically mixed with membrane precursors and then sintered at optimized temperatures via solid-state reactions. This method has also widely been applied to the fabrication of composite organic/inorganic membranes, and numerous types of inorganic materials, such as titanium dioxide (TiO_2) (Tetteh et al., 2021), silicon dioxide (SiO_2) (Yao et al., 2022), zeolites (Zhang et al., 2021) and carbon nanotubes (Kim et al., 2012), have been incorporated into organic polymers for the production of NF/reverse osmosis (RO) membranes. Doping/blending can also enrich the surface functionality of ceramic membranes. Liu et al. (2018) doped SiO_2 nanoparticles into the alumina matrix and increased the hydrophilicity of the membrane, resulting in a 20.5 % and 6 % enhancement in water flux and oil rejection.

3.2.5. Hydrothermal method

Hydrothermal synthesis has widely been used for inorganic materials and zeolite membrane preparation (Huang and Yang, 2007; Xu et al., 2004; Yang and Park, 2019). In a typical hydrothermal reaction, an aqueous mixture of precursors is heated in an autoclave at temperatures of 80–230 °C for several hours or up to days (Yeo et al., 2013). For membrane modification, the membrane support is firstly immersed in the solution with a mixture of precursors, then the autoclave is placed in an oven for the hydrothermal process. Afterwards, the membranes are washed, dried and calcined. This method offers several advantages such as low cost, simple set-up and high yield (Senapati and Maiti, 2020). Therefore, several researchers have modified ceramic membranes via the hydrothermal process to improve their oil separation efficacy. Suresh et al. (2016) prepared TiO_2 and $\gamma\text{-Al}_2\text{O}_3$ composite membranes via a hydrothermal method, and due to the enhanced surface hydrophilicity, both membranes showed a higher permeate flux, while maintaining similar oil rejection for oil emulsion filtration. Paimen et al. (2020) also deposited $\alpha\text{-Fe}_2\text{O}_3$ on the Al_2O_3 hollow fibre support via the hydrothermal route. The deposited $\alpha\text{-Fe}_2\text{O}_3$ layer improved the permeate flux of the membrane due to the increase in surface hydrophilicity. To remove dissolved organics in produced water, Liu et al. (2008) prepared $\alpha\text{-Al}_2\text{O}_3$ supported RO zeolite membranes by hydrothermal synthesis. The uniform sub-nanometer- or nanometer-scale pores of zeolite favoured the passage of water over organic pollutants. Therefore, the membrane obtained a high organic rejection but gave low permeance.

3.2.6. Chemical vapour deposition

With the CVD method the pore structure and pore size are optimized to improve the selectivity of ceramic membranes. Via the reaction of one or several gas phase precursors inside or around the substrate pores, a thin film is deposited on the porous substrate at a

temperature between 400 and 1000 °C (Mavukkandy et al., 2020). The CVD method is easier to use than the traditional sol-gel and dip-coating methods, because it does not need a repeated coating process (Khatib and Oyama, 2013). CVD is a scalable technology, when empirical conditions for preparing good quality membranes (e.g., silica membranes) have been identified (Pedersen, 2016). Currently, most studies about ceramic membranes modification by the CVD process have focused on the tailoring of membrane pore size for applications in gas separation (Zhang et al., 2016b), fuel cells (Meng et al., 2007), and catalyst membrane reactors (Nomura et al., 2006). However, the application of CVD to fabricate high-performance ceramic membranes for water treatment, especially for O/W separation, has also been reported in the literature: silica (Zhang et al., 2017), silicon carbide (SiC) (Chen et al., 2020b) and carbon nanotubes (Chen et al., 2012) have been studied as a coating layer for ceramic membrane modification by means of CVD to increase oil rejection and/or improve membrane fouling resistance.

3.2.7. Atomic layer deposition

ALD is a new technique for thin film deposition which is suitable for depositing uniform and conformal films on complex three-dimensional supports at a much lower temperature (from room temperature to 300 °C) than CVD (Kukli et al., 2016). This method was first developed in the semiconductor industry for the miniaturization of semiconductor devices (George, 2010) and then it was used for other applications such as membrane modification (Li et al., 2011). Compared with other deposition techniques such as CVD, molecular beam epitaxy (MBE), and evaporation, ALD can precisely control the thickness of the film at the Ångstrom or monolayer level with a high quality (pin-hole free films) (Leskelä and Ritala, 2003). With this technique, two or more precursors are made to react with one another cyclically. Normally one reaction cycle involves four different steps: 1) exposure of the first reactant A, 2) purging of the reaction chamber to remove unreacted precursors and by-products, 3) exposure of the second reactant B, 4) further purging to remove unreacted precursors and by-products. Depending on the required film thickness, the reaction can be repeated on the substrate surface, based on the growth cycle.

Li et al. (2012) modified ceramic membranes with Al₂O₃ layers by the ALD deposition route. The membrane pore size decreased with the increasing ALD cycles and thus the pure water flux suffered from a decline. However, the retention to bovine serum albumin increased from 2.9% to 97.1%. Shang et al. (2017) prepared a tight ceramic NF membrane by depositing a TiO₂ layer via the ALD technique. After modification, the membrane maintained higher water permeance than commercial, tight polymer NF membranes and sol-gel-made tight ceramic NF membranes. Tight ceramic NF membranes are promising in O/W separation, especially for produced water, as they can remove micro-oil droplets, dissolved organics and multivalent ions at the same time. However, until now ALD has only been used for modification of polymeric membranes (Yang et al., 2018b), and stainless steel meshes (Kang et al., 2020) to improve their oil separation performance. To

date, studies about ceramic membranes modified by ALD for O/W separation have not been carried out yet.

3.2.8. Comparison of the different ceramic membrane modification methods

An overall comparison of the different ceramic membrane modification methods is presented in Table 3.1. All these modification methods have been found to be effective to improve ceramic membrane performance for oily wastewater treatment. However, these methods have their advantages and disadvantages in various aspects. Firstly, the layer thickness should be an important criterion to evaluate a modification method considering the trade-off between the membrane permeance and selectivity (Park et al., 2017). Sol-gel coating gives a thinner layer (50 nm-4 μm) than the dip-coating method, and thus it can be used for the preparation of ceramic NF membranes. Surface grafting aims to form polymeric chains on the membrane surface, and the layer thickness depends on the chain length of the used polymers and grafting time. Doping/blending is a physical mixing of the membrane precursors and nanoparticles, which would only change the surface functionality of ceramic membranes with a minor effect on membrane pore sizes. Zeolite RO membranes prepared by the hydrothermal method generally have a thick top layer, enabling a high rejection to organic molecules but giving low permeance (Liu et al., 2008). Compared with the traditional ceramic membrane modification methods, CVD and ALD can obtain a relatively thin film on substrates. Especially, the ALD can achieve a thin layer with atomic layer thickness, with the potential to control membrane pore sizes at the nanoscale.

Secondly, the antifouling ability of ceramic membranes depends on the physicochemical properties (e.g., hydrophilicity and iso-electric point (IEP)) of the coated materials. In this regard, the materials that can be used for modification is another criterion when selecting the methods. Sol-gel is used for the coating of some common metal oxides such as $\gamma\text{-Al}_2\text{O}_3$, ZrO_2 , TiO_2 , or their mixtures (Cai et al., 2015). However, dip-coating can be extended for almost all types of inorganic materials due to its high flexibility. Surface grafting is mainly used for the silanation of ceramic membranes to create a hydrophobic surface for membrane distillation. Doping/blending is also suitable for most inorganic materials if the doping materials can withstand a high sintering temperature as the membrane while maintaining their physicochemical properties. Hydrothermal synthesis is mainly used for the preparation of zeolite membranes. Metal oxides can also be synthesized on the membrane surface by this method, but is rarely described in literature. CVD has widely been used for the deposition of inorganic and organic thin films. For ceramic membrane modification, SiO_2 , SiC and CNT are used for O/W separation. Similar to CVD, ALD is also used for the deposition of organic and inorganic layers on the membrane support. Therefore, CVD and ALD are supposed to be more effective than traditional sol-gel and dip-coating methods for modifications of ceramic membranes.

Lastly, the scalability and overall costs should be considered. Sol-gel and dip-coating are mature techniques for the fabrication of commercial ceramic membranes. However,

■ Chapter 3

defects can be formed in the selective layer which may affect membrane performance (Thibault et al., 2017). In addition, doping/blending is a versatile and cost-effective way to modify ceramic membranes in just one step, which can save the preparation costs of the membrane while enabling the surface functionality, but is only suitable for MF/UF. The long synthesis time and low permeance of the resulting membranes prepared by hydrothermal methods are problematic and, therefore, this method does not seem appropriate for membrane modification for oily wastewater treatment. CVD has been scaled up for ceramic membrane preparations mainly for gas separation (Khatib and Oyama, 2013). The number of ceramic membranes prepared via the CVD for the water treatment field is still low possibly due to its high cost, compared with the traditional sol-gel and dip-coating methods. ALD is considered as one of the most promising methods to fine tune membrane surface properties and pore structures. However, the upscaling and the high costs of ALD is currently limiting its wide applications in the membrane field (Li et al., 2021), but the continuous improvement and development of ALD reactors would make it feasible in the coming future.

■ Chapter 3

Table 3.1 Comparison of various ceramic membrane modification methods for oily wastewater treatment.

Modification method	Layer thickness	Membrane type	Layer material	Temperature (°C)	TRL	Advantages	Disadvantages	Ref.
Sol-gel	50 nm – 4 μm	UF, NF	γ-Al ₂ O ₃ , ZrO ₂ , TiO ₂ , TiO ₂ -ZrO ₂	350-600	9	-narrow pore size distribution -relatively controllable composition -easy scale up	-defect formation -thick layers -particle agglomeration	(Bayat et al., 2016; Cai et al., 2015; Das and Maiti, 2009; Lee et al., 2020; Qiu et al., 2017; Tsuru et al., 2001; Vacassy et al., 1997)
Dip-coating	100 nm – 100 μm	MF, UF, NF	Most inorganic materials	800-1000	9	-high flexibility -excellent homogeneity	-susceptible to defect -multiple coating and baking steps -thick layers	(Mavukkandy et al., 2020; Yang et al., 1998)
Surface grafting	~	MF, UF, NF	Polymeric monomers	Room temperature	4	-controllable introduction of graft chains -simple and cheap -long-term chemical stability	-need initiation -mainly for hydrophobisation of ceramic membrane	(Nady et al., 2011)

■ Chapter 3

Doping/blending	~	MF, UF	Most inorganic materials	Same temperature as the membrane	9	-simplicity -cost effective -reproducibility	-large pore size	(Monash and Pugazhenth, 2011; Zhang et al., 2009)
Hydrothermal synthesis	1 – 10 μm	MF, RO	Zeolite, TiO ₂ , γ-Al ₂ O ₃ , Fe ₂ O ₃	80-230	4	-low synthesis temperature -low cost	-limited materials -long synthesis time -thick layer	(Cui et al., 2008; Liu et al., 2008; Paiman et al., 2020; Yeo et al., 2013)
CVD	4 nm – 10 μm	MF, UF, NF	Organic and inorganic materials	400- 1000	6	-high coating uniformity -few defects and scalable	-high deposition temperature -high cost	(Mavukkandy et al., 2020)
ALD	Monolayer to few nanometers	MF, UF, NF	Organic, inorganic and metallic materials	Room temperature to 300	4	-conformal and uniform layers -pin-hole free films -ultrathin layers -low deposition temperature	-low throughput -high cost -scale up limitation	(Lee et al., 2020; Mavukkandy et al., 2020; Weber et al., 2019)

TRL - Technology Readiness Levels

3.3. Performance of antifouling ceramic membranes for oily wastewater treatment

Membrane fouling is inevitable despite that ceramic membranes are proven to be less fouled by oil droplets compared with their polymeric counterparts (Murić et al., 2014). Membrane characteristics including membrane pore size, surface charge, roughness, and hydrophobicity/hydrophilicity have an effect on membrane fouling (Zhang et al., 2015). To improve the fouling resistance of ceramic membranes for oily wastewater treatment, various strategies and materials have been developed for ceramic membrane modification. Besides oil droplets, membrane fouling can also be affected by other components (e.g., surfactants, salinity, and particles) in oily wastewater (He and Vidic, 2016; Lu et al., 2015a). Therefore, the modification should be tailored based on the characteristics of oily wastewater to achieve a better filtration performance. The foulants such as surfactants in oily wastewater were found to improve the flux of membranes (Trinh et al., 2019), but not part of this work. In this section, the modified ceramic membranes studied for oily wastewater treatment are discussed and compared.

Here, the ceramic membranes are further classified into active and passive antifouling membranes based on the antifouling mechanism (Figure 3.1). The active antifouling ceramic membranes mean that the fouling can be reduced or mitigated by coating a hydrophilic and/or charged layer on membrane surfaces, while the passive antifouling ceramic membranes normally need the assistance of chemicals (e.g., H₂O₂) or external energy (e.g., electricity, UV) to achieve their antifouling ability. Therefore, these two types of antifouling ceramic membranes are discussed separately.

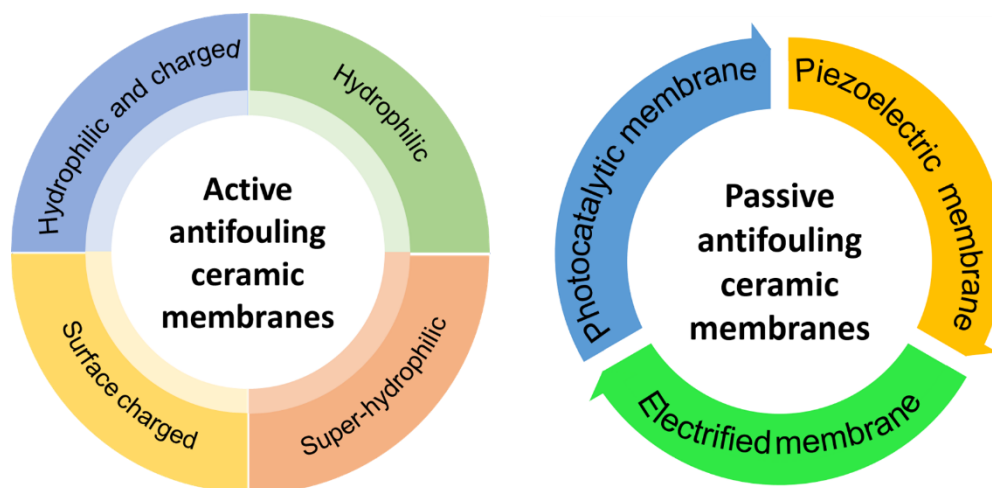


Figure 3.1. Active and passive antifouling ceramic membranes for oily wastewater treatment.

3.3.1. Active antifouling ceramic membranes

Hydrophilic ceramic membrane

Due to the formation of a water molecule layer on the surface to prevent the contact with pollutants from the solution, a hydrophilic surface (water contact angle < 90°) is

considered to be less prone to be fouled by organic compounds and microorganisms. As a result, improving surface hydrophilicity of ceramic membranes is one of the main routes to alleviate membrane fouling due to the increased affinity of the surface for water over oil (Zhu et al., 2013). Nano-scale TiO_2 , ZrO_2 , Fe_2O_3 , $\gamma\text{-Al}_2\text{O}_3$ and SiO_2 have been used to enhance the hydrophilicity of commercial ceramic membranes. Zhou et al. (2010) used nano-sized ZrO_2 to modify commercial Al_2O_3 membranes. The result showed that the steady flux kept 88% of the initial flux and oil rejection was higher than 97.8%, because the coating made the membrane more hydrophilic with a water contact angle of 20° on the ZrO_2 coating. Chang et al. (2014) also developed an Al_2O_3 supported TiO_2 membrane with a water contact angle of 8° , which was much lower than that of the pristine membrane. The results indicated that the ceramic membrane modified by a mixture of 2 mol/L $\text{Ti}(\text{SO}_4)_2$ and 1 mol/L urea had the highest flux. In addition, TiO_2 coating caused a higher oil rejection and lower fouling of the membrane due to a lower attraction force of the hydrophilic coating to oil droplets. In order to overcome the low flux of ceramic membranes for produced water treatment, Marzouk et al. (2021) modified commercial ceramic TiO_2 membranes with SiO_2 nanoparticles by dip-coating. Due to the improved surface hydrophilicity, the flux and total organic carbon rejection of the membranes were improved considerably at 0.5 wt% SiO_2 loading.

Other metal oxides such as Fe_2O_3 , MnO_2 , CuO and CeO_2 have also been studied to prepare a more hydrophilic ceramic membrane. Lu et al. (2016a) studied the effects of the various metal oxides (i.e., TiO_2 , Fe_2O_3 , MnO_2 , CuO , and CeO_2) as a filtration layer on a ZrO_2 membrane for O/W emulsion separation. Even though the surface charge of these metal oxides varies, the irreversible fouling is mainly determined by the hydrophilic character of filtration-layer metal oxides (Lu et al., 2016a). Highly hydrophilic Fe_2O_3 is regarded as a potential filtration-layer material for MF/UF ceramic membrane modification for O/W emulsion treatment.

Besides metal oxides, other materials, such as zeolite and activated carbon (AC), have also been used for ceramic membranes modification to improve their surface hydrophilicity. Cui et al. (2008) synthesized zeolite-NaA/ Al_2O_3 MF membranes by an in situ hydrothermal method for the separation of O/W emulsion. The pore size of NaA/ Al_2O_3 MF membrane decreased from 2.1 μm to 1.2 μm , leading to a higher oil rejection than that of the original support. Meanwhile, the modified membrane consistently kept a higher permeate flux. This was explained by the following two reasons. Firstly, water can be transported through both inter-particle membrane pores and intra-particle zeolite pores, which enhances the permeate flux of the membranes. Secondly, the hydrophilic nature of zeolite prevents the adsorption of oil that may result in membrane fouling. To increase the permeate flux and create lower fouling of the alumina membrane, a hybrid $\text{Al}_2\text{O}_3/\text{AC}$ membrane was developed by mixing alumina powder and powdered activated carbon (PAC) sintered at 1150°C under vacuum. The incorporation of PAC into the Al_2O_3 matrix created a more hydrophilic surface (Kayvani Fard et al., 2018a).

■ Chapter 3

Due to the functional groups such as carboxyl, epoxy, and hydroxyl groups in graphene oxide (GO), a GO modified membrane is highly hydrophilic in water (Hu et al., 2015; Lee et al., 2013; Lou et al., 2014). Hu et al. (2015) prepared GO membranes on a commercial Al_2O_3 support and compared the performance of membranes before and after modification for filtration of O/W emulsion. The flux of the GO membrane was about 27.8% higher than that of the unmodified membrane at the same pressure and lower oil content in the permeate was observed.

Superhydrophilic ceramic membrane

A superhydrophilic (water contact angle $< 5^\circ$) and underwater superoleophobic (oil contact angle $> 150^\circ$) membrane surface is proven to be more effective to mitigate membrane fouling by hydrophobic oil droplets (Chen et al., 2016b). It is known that the fish scales can be protected from oil contamination in water and it was found that these surfaces have a superhydrophilic and underwater superoleophobic property (de Leon and Advincula, 2014; Liu et al., 2009). Learning from these studies, many new materials with the same characteristics have been developed via surface engineering to broaden their applications in various fields. The hydrophilicity of a solid surface is governed by its surface free energy (chemical composition) and surface morphology (hierarchical structure) (Zhu et al., 2014). Thus, to achieve a superhydrophilic property, a surface with hierarchical macro/nanostructures and hydrophilic chemical components is necessary (Wei et al., 2018). A membrane surface with such properties has also been developed and studied for O/W separation, where water tends to permeate through the membrane while oil is repelled (Ge et al., 2018; Shi et al., 2016; Wu et al., 2018; Zhang et al., 2018b).

Chen et al. (2016b) developed an all-inorganic ceramic membrane with superhydrophilic and underwater superoleophobic properties via dip-coating of silica nanoparticles. The results showed that the membrane displayed a higher anti-fouling ability with high oil rejection ($> 99.95\%$). In addition, the membrane was considered to have a longer service life and stronger anti-fouling ability than general polymeric membranes and traditional ceramic membranes. A superhydrophilic and underwater superoleophobic $\text{TiO}_2/\text{Al}_2\text{O}_3$ composite membrane was designed by Zhang et al. (2018a), where a closely aligned TiO_2 nanorod array was prepared on the ceramic membrane surface. Due to the superhydrophilicity and narrower pore sizes of the membrane, an ultra-low oil adhesion force (0.084 mN) was achieved and 99.1% oils could be rejected by the membrane. Furthermore, the membrane maintained a high-water flux of 41.8 LMH under gravity.

Hydrophilic organic polymers with reactive groups are also used to prepare superhydrophilic and underwater superoleophobic ceramic membranes. Maguire-Boyle et al. (2017) created a superhydrophilic surface on alumina ceramic MF membranes with cysteic acid ($\text{HO}_2\text{CCH}(\text{NH}_2)\text{CH}_2\text{SO}_3\text{H}$) by chemical functionalization. The TMP was much lower for the modified membrane to obtain the same flux than that of the unmodified one.

Chapter 3

Surface charged ceramic membrane

Electrostatic interactions are also important for membrane rejection and fouling as it affects the interactions between solutes and membranes (Dickhout et al., 2017). It has been reported that for the rejection of oil droplets the effect of electrostatic repulsion in a membrane is more important than steric hindrance of the pore size for low ionic strength emulsions (Dickhout et al., 2017; Tian et al., 2020). The surface charge of ceramic membranes is highly dependent on the pH and iso-electric point (IEP) of the ceramic materials (Lobo et al., 2006). If the pH is above the IEP of the ceramic materials, the membrane surface charge will be negative, while the membrane surface is positively charged when the pH is below the IEP (Atallah et al., 2017). Consequently, for an anionic surfactant stabilized oil emulsion, repulsive and attractive forces exist between the oil droplets and membrane surface when pH is respectively above and below IEP (schematically shown in Figure 3.2). The IEP of common ceramic materials in water at 25 °C are given in Table 3.2 below.

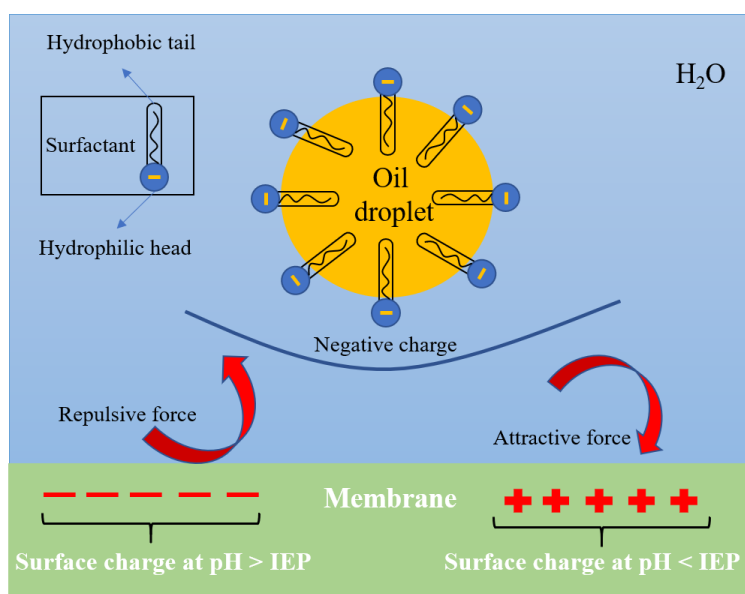


Figure 3.2. Interaction between the oil droplets stabilized by anionic surfactant and the membrane at various pH values.

Table 3.2 The IEP of common ceramic materials in the water at 25 °C (Abadikhah et al., 2018; Atallah et al., 2017; Keramati et al., 2016; Skibinski et al., 2016).

Ceramic materials	$\alpha\text{-Al}_2\text{O}_3$	TiO_2	ZrO_2	SiO_2	SiC	Si_3N_4
IEP	8-9	3.9-8.2	4-6	1.8-2.7	2.6	3.3

Most metal oxides have an IEP below 7, which means that the membranes prepared by these metal oxides have a negative charge at neutral pH. Lobo et al. (2006) studied, amongst others, the influence of pH on the UF of an O/W emulsion from a metal industry. The active layer of the inorganic membrane consisted of $\text{TiO}_2/\text{ZrO}_2$. Basic pHs enhanced membrane permeate flux, while at low pH values ($\text{pH} \leq 4$), the membrane surface became positively charged and anionic surfactants adsorbed on the membrane surface, causing flux decline and surfactant monomers permeation through the membrane.

Although the IEP of SiO_2 is below 3, the stability of amorphous SiO_2 in water is problematic, which limits its applications in water treatment (Aghaeinejad-Meybodi and Ghasemzadeh, 2017; Tsuru et al., 2001). Nevertheless, crystal SiO_2 , like cristobalite and quartz, is found to be stable in water. Al-Harbi et al. (2017) prepared silica-based cross-flow membranes with silica sand and glass waste as precursors for the treatment of oily wastewater. A cristobalite layer was obtained by controlled surface crystallization on the quartz surface. Although both quartz and cristobalite have a negative surface charge for pH higher than 2, the zeta potential value of the cristobalite (e.g., -42 mV at pH 6) was nearly twice lower than that of the quartz (e.g., -21 mV at pH 6) and thus a higher repulsion existed between oil droplets (negatively charged) and the membrane surface. After filtration of oily wastewater, only the filters with a cristobalite layer had a high filtration capacity with a good recovery after backwashing.

SiC and Si_3N_4 materials also have a very low IEP (close to SiO_2) and high chemical stability. Xu et al. (2020) compared the performance of alumina and SiC hollow fibre membranes for MF of O/W emulsion, the results indicated that the SiC membrane had a smaller pore size, but gave a higher flux due to a higher hydrophilic surface. In addition, a better anti-fouling ability was observed for the SiC membrane owing to electrostatic repulsion to oil. The application of asymmetric Si_3N_4 hollow fibre membrane for MF of O/W emulsion was studied by Abadikhah et al. (2018). The stable normalized permeate flux of the membrane increased from 0.2 to 0.34 when the pH of the feed emulsion increased from 2 to 12, due to the increased negative charge of Si_3N_4 .

Hydrophilic and surface charged ceramic membranes

Both the surface charge and hydrophilicity of the membranes can be tailored during modification, depending on the used materials. To improve the permeate flux, Zhang et al. (2009) doped TiO_2 powder to mix with Al_2O_3 powder to prepare a composite $\text{TiO}_2\text{-Al}_2\text{O}_3$ ceramic membrane. The doping improved the membrane hydrophilicity and shifted the isoelectric point towards a lower pH. A higher and more stable flux was thus observed for the $\text{TiO}_2\text{-Al}_2\text{O}_3$ composite membrane than that of the Al_2O_3 membrane for separation of sodium dodecyl sulfate (SDS) stabilized O/W emulsion. SiC was also doped with Al_2O_3 powder to prepare an $\text{Al}_2\text{O}_3\text{-SiC}$ porous ceramic composite tube by extrusion. It was found that the negative surface charge and hydrophilicity of the membrane became stronger after SiC doping, and thus the SiC doped membrane demonstrated a higher permeate flux combined with a better fouling resistance (Jiao et al., 2019). More recently, Chen et al.

■ Chapter 3

(2020b) prepared a low fouling silicon carbide-alumina UF membrane for oily wastewater filtration by low-pressure chemical vapour deposition (LPCVD). The membrane had a better fouling resistance compared with the pristine alumina membrane due to a combination of improved surface hydrophilicity and negative charge. However, amphoteric bitumen in produced water can have both positive and negative surface charges. In this case, the attraction of these foulants to the ceramic membrane surface should be prevented. Atallah et al. (2019b) modified the γ -Al₂O₃ and TiO₂ ceramic membranes with polyethylene oxide (PEO) functional organosilanes for produced water treatment. The membrane became more hydrophilic but charge-neutral. In this way, the interaction of the amphoteric bitumen in produced water with negatively charged ceramic membrane surfaces was suppressed. After modification, the membranes had a higher permeate flux as well as a higher flux recovery upon backflushing.

Challenges of active antifouling ceramic membranes

The active antifouling ceramic membranes can slow down the membrane fouling process by minimizing the interactions between the foulants and membranes. However, an additional mass transfer resistance is usually introduced due to either an increase of membrane top layer thickness or a decrease of membrane pore sizes (Gu et al., 2021). The decrease of membrane pore size can improve membrane selectivity and potentially prevent the occurrence of internal fouling, while a reduction of pure water permeance is commonly observed for the membranes after modifications (Gu et al., 2021). To overcome this trade-off, a thin layer of highly hydrophilic polymers or nano-sized metal oxides is preferred to be used for ceramic membrane modifications to avoid the loss of water flux (Geise et al., 2010). In this regard, a high mechanical and chemical stability of the coated layer should be guaranteed to extend their lifetime (Geise et al., 2010). In addition, confined surface deposition (deposition mainly on the membrane surface) was found to be effective to improve ceramic membrane fouling resistance with a minor effect on water permeance (Gu et al., 2020).

Furthermore, the surface roughness is affected during modification. The increase of surface roughness can increase water flux due to a larger effective filtration area, but may lead to a higher fouling potential (Gu et al., 2021). However, regularly surface-patterned ceramic membranes, inducing turbulence of fluid on the membrane surface, are considered to increase both the flux and fouling resistance simultaneously (Tsai et al., 2019). These ceramic membranes prepared via the 3D printing technique is promising for wastewater treatment (Lyu et al., 2020), which may be an option for oily wastewater treatment.

■ Chapter 3

3.3.2. Passive antifouling ceramic membranes

Photocatalytic ceramic membrane

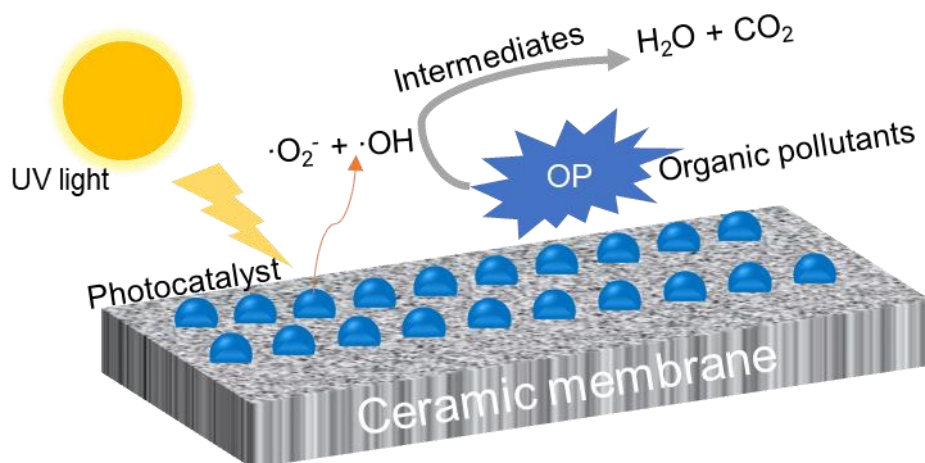


Figure 3.3. Schematic diagram depicting mechanisms that organic pollutants degradation on the photocatalytic ceramic membrane surface.

Photodegradation of organic compounds present in water and wastewaters with the application of a photocatalyst has been widely studied in literature (Mozia, 2010). The most suitable photocatalysts are typically made of some polycrystalline semiconductor solids such as TiO_2 , ZnO , $SrTiO_3$, RuO_2 , and CdS . In particular, crystal TiO_2 (anatase) has widely been used because of its low costs and high photostability (Molinari et al., 2001). The mechanism of the photocatalytic ceramic membrane to degrade organic pollutants can be explained with the schematic diagram shown in Figure 3.3. When the photocatalyst is irradiated by light (Ultraviolet (UV) or Visible), pairs of electrons and holes are excited, due to the adsorption of photons in the material. Then the photo-generated electrons can produce active radicals like $\cdot O_2^-$ and $\cdot OH$ by reacting with O_2 and H_2O , respectively (Kumar and Chowdhury, 2020). Those active species decompose organic pollutants to intermediates, CO_2 , H_2O and mineral salts due to the oxidizing and reducing power (Sakka, 2013).

The performance of photocatalytic mesoporous alumina membranes was tested by Azmi et al. (2019) for oil emulsion separation. The photocatalyst (copper-doped ceria) was deposited on the alumina support by a sol-gel method. Under UV irradiation, an increase in the permeance, from 36 to 1422 LMH, was observed in the separation of 1000 ppm oil emulsion. The dosage of photocatalyst on the membrane surface is quite crucial as a too low dosage of photocatalyst leads to a lower photodegradation performance, while a high dosage may cause pore blockage of the membrane. In order to address this issue, Alias et al. (2019) developed a photocatalytic nanofiber-coated (graphitic carbon nitride ($g-C_3N_4$)) ceramic membrane via electrospinning to prevent pore blockage by the photocatalysts. With the assistance of UV irradiation, a permeate flux of 640 LMH and an oil rejection of 99% were found for 180 min cross-flow oily wastewater filtration at 2 bar. Even after

■ Chapter 3

three cycles of 180 min filtration, the membrane could still maintain a permeate flux of 577 LMH and an oil rejection of 97%.

One of the main challenges of the photocatalytic ceramic membrane is how to illuminate the membrane surface with UV light once the membrane surface is covered with pollutants. Therefore, most studies use a flat membrane at a laboratory scale. For a single tubular membrane, the photocatalyst can be deposited on the permeate side (support layer) to be able to be illuminated by UV light (Starr et al., 2016). For both cases, a light transmission material (e.g., quartz) needs to be used as membrane housing. In addition, the possibility of catalyst deactivation and loss during long-term filtration is problematic. The full-scale application of monolithic shaped ceramic membranes coupled with a photocatalyst is therefore still not practically feasible (Nyamutswa et al., 2020).

Piezoelectric ceramic membrane

The concept of piezoelectric porous membranes for oily wastewater treatment is relatively new. These membranes can control membrane fouling by applying an alternating voltage on both sides of the membrane to generate in situ vibration from within the membrane, realizing the self-cleaning ability (Mao et al., 2019). In addition, the investment and operation costs of this membrane are supposed to be lower as compared with the traditional membrane combined with physical and chemical cleaning (Mao et al., 2020). A schematic diagram to show the membrane module incorporating the piezoelectric membrane and its anti-fouling performance is presented in Figure 3.4. The anti-fouling performance can be ascribed to vibrations and cavitation generated by the ultrasound, which prevent cake-layer formation and pollutant accumulation (Mao et al., 2018).

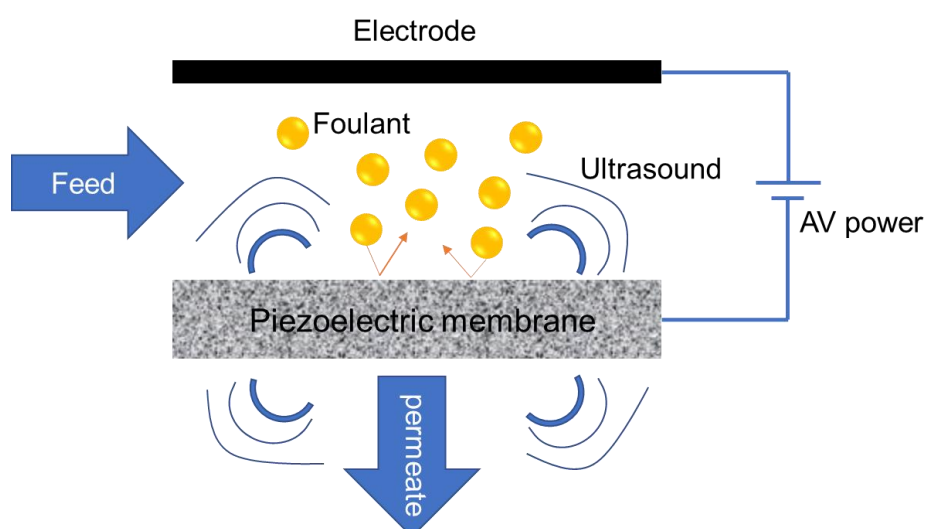


Figure 3.4. Schematic of the self-cleaning mechanism of the piezoelectric membrane. The membrane can create in-situ ultrasound to remove the pollutants deposited on the surface.

The first application of piezoelectric ceramic membranes for O/W emulsion separation was studied by Mao et al. (2018). Lead zirconate titanate (PZT) was used to prepare a

porous ceramic membrane because of its high piezoelectric and stable porous properties. The membrane possessed the strongest vibration with an alternating voltage signal at 190 kHz and preserved a maximum steady flux of approximately 71% of its initial value. A positive correlation with the alternate voltage amplitude and the stationary relative flux was observed for the membrane. For the studied oil concentrations (200 to 5000 ppm), the membrane with pulsed voltage always had a higher normalized stable permeance than the one without voltage applied. In addition, oil rejection by this membrane could be higher than 95%. In a following study by the same group, an Al₂O₃ MF membrane was prepared by dip-coating of the α -Al₂O₃ dispersion on the PZT ceramic substrate. The membrane had a water permeance of 220 LMH/bar with an average pore size of 100 nm. With in-situ ultrasound generation during the filtration process, the stable permeate flux of the membrane improved by 48% as compared with the situation without ultrasound generation (Mao et al., 2020). In addition, an oil rejection higher than 99.5% was observed, which was higher than that of the piezoelectric membrane in the previous study (Mao et al., 2018).

Electrochemically enhanced ceramic membrane

Electrochemically enhanced filtration is also a new technology for membrane fouling mitigation (Fan et al., 2015). Unlike the piezoelectric membrane, the fouling mitigation of electrochemically enhanced ceramic membranes is realized via either charge inversion or electrochemical oxidation. Most foulants are charged in the wastewaters and O/W emulsion is one of the examples. To better show this filtration process, a schematic diagram is presented in Figure 3.5. By applying an electric field, charged particles are moved away from the membrane surface with the same charge as to the particles. In this way, the foulants such as charged oil droplets could be prevented from forming a fouling layer on the membrane surface. Alternatively, a positive charge can be applied on the conductive membrane to induce the electrosorption of negatively charged substances to improve their rejection. Afterwards, the desorption of the negatively charged substances is achieved by changing the potential periodically (Mantel et al., 2021). In addition, electrochemical reactions at the membrane surface usually occur in the electrically-assisted filtration process for electrified membranes. As a result, organic matter in the feed can be removed via the electro-oxidation process or oxidized by strong oxidizing intermediates such as $\cdot\text{OH}$, $\text{HO}_2\cdot$ and H_2O_2 produced via directly oxidizing water molecules with the membrane as an anode. In this way, the organic fouling layer on the membrane surface or in the pores can be decomposed into intermediates, CO_2 and H_2O , therefore, the membrane performance can be recovered (Yang et al., 2011b).

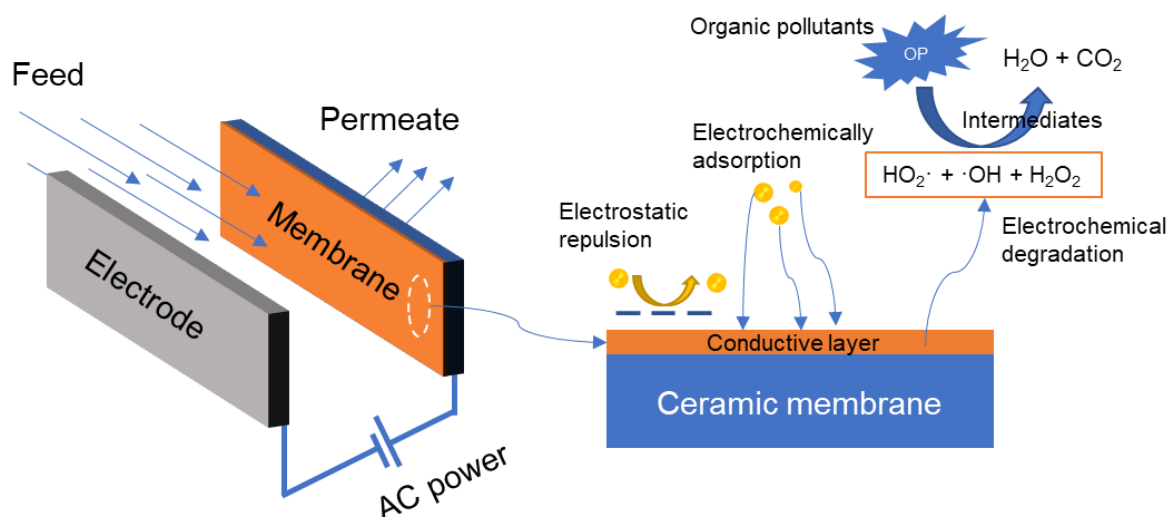


Figure 3.5. Schematic diagram of the electrochemically assisted membrane filtration process.

Geng and Chen (2016) studied the anti-fouling performance of tubular Al_2O_3 ceramic membrane after coating a layer of Magnéli Ti_4O_7 coupled with external electricity. The results showed that the permeate flux and oil rejection of the modified membrane were considerably improved when the electric field was applied. Moreover, the modified membranes could maintain 91.8% of their initial specific permeate flux under the applied potential of 40 V during 1 h operation. Due to the higher permeate flux and less pumping energy, the total energy consumption of electrically assisted filtration of oily wastewater decreased by 58% as compared with the pristine membrane in terms of $\text{kWh}\cdot\text{m}^{-3}$ permeate, even though additional DC power supply was provided. Yang et al (2015) deposited a layer of 1D IrO_2 nanorods on an Al_2O_3 ceramic membrane via a dip-coating and thermal decomposition method. Due to the effect of electrochemical reactions and electrophoresis during the filtration process, the modified membrane showed a slower decline rate of permeate flux and fouling could also be minimized. In addition to flux enhancement, an increase in organic matter rejection was also achieved due to the electrochemical reactions. However, the electrophoresis effect was found to be more effective than the electrochemical effect, not only for membrane fouling control, but also for membrane cleaning.

Despite that the electrified (piezoelectric and electrochemically enhanced) ceramic membrane shows promising results in fouling control and oil rejection, this technology still faces some challenges. Firstly, the materials used to fabricate the membrane need either a high electrical conductivity or a piezoelectric property. Secondly, it is quite difficult to effectively incorporate the electrified ceramic membranes and counter electrodes into a standard membrane module. In addition, at a larger system scale, to ensure a sufficiently high charge density across the membrane surface, higher potentials would be required to achieve a good filtration performance. However, this needs more corrosion resistant counter electrodes and leads to a higher energy consumption (Zhu and Jassby, 2019).

3.3.3. Comparison of the performance of antifouling ceramic membranes for oily wastewater treatment

In Table 3.3, novel ceramic membranes and ceramic membranes modified with different materials and methods are compared for oily wastewater treatment. Because the feed characteristics and operational parameters are varied in literature, the performance of the membranes could have been influenced. Therefore, we only give a general impression on the performance of the modified ceramic membranes for oily wastewater treatment.

Considering permeate flux, oil rejection and fouling resistance, modification can effectively improve ceramic membrane performance. In terms of flux enhancement, the coating with nano-sized metal oxides (γ - Al_2O_3 , TiO_2 , ZrO_2 and Fe_2O_3) is effective in increasing the permeate flux of α - Al_2O_3 membranes due to the enhanced surface hydrophilicity (Chang et al., 2010b; Chang et al., 2014; Zhou et al., 2010). In addition, the permeate flux of e.g., α - Al_2O_3 membranes could be further enhanced by GO coating. As a 2D coating material, GO has an atomic thickness with a hydrophilic property, making it a potential building block for membrane modification with a “water favoured” surface (Huang et al., 2015). Catalytic ceramic membranes (photocatalytic and electrified membranes) have a relatively higher flux than the modified membranes with only improved surface hydrophilicity. The organic matter can be degraded by the radicals excited by the catalyst, thereby suppressing the deposition of oil droplets on the membrane surface.

Because O/W emulsion normally has a droplet size distribution in the range of 1-10 μm (Chang et al., 2014; Hu et al., 2015), a high oil rejection has been found for most of the ceramic MF/UF membranes. As oil droplets are deformable, their shape and sizes can be changed depending on the operational parameters, thereby affecting the rejection (Abadikhah et al., 2018). The GO, Ti_4O_7 and g- C_3N_4 modified α - Al_2O_3 membranes are observed to have both a high oil rejection and a high permeate flux. Although the carbon nanotube (CNT) modified ceramic membrane have a very high rejection of oil droplets from the emulsion, it gives the lowest permeance, compared with the membrane modification with other materials.

TiO_2 , ZrO_2 and Fe_2O_3 modified ceramic membranes have shown the lowest fouling among the nano-sized metal oxides. These metal oxides can both improve surface hydrophilicity and create a lower negative charged surface. Therefore, oil droplets are repelled from the membrane surface. GO modified ceramic membrane has a higher flux decline than metal oxides modified membranes, possibly due to its higher flux and longer filtration time. Membranes with a high initial flux are more prone to pore blocking and constriction (Zhu et al., 2017). The passive antifouling ceramic membranes, such as photocatalytic, electrified membranes, are all found to be effective for fouling alleviation. The oil droplets can be prevented from depositing on these membrane surfaces via charge inversion or degradation by radicals or in situ generated ultrasound.

■ Chapter 3

Table 3.3. Comparison of the performance of antifouling ceramic membranes for oily wastewater treatment.

Membrane	Configuration	Method	Function	Pore size (μm)	C_f (mg/L)	NF_i (LMH/bar)	NF_s (LMH/bar)	R_d (%)	FD (%)	FT (min)	Refs
$\text{Fe}_2\text{O}_3/\text{ZrO}_2$	Disc, D = 47 mm	Pulsed-laser deposition	Hydrophilic	50 kDa	Crude oil, 100	~	~	95 _{COD}	12	30	(Lu et al., 2016b)
$\gamma\text{-Al}_2\text{O}_3/\alpha\text{-Al}_2\text{O}_3$	Tubular (7-channels), OD = 31 mm	Dip-coating	Hydrophilic/charge	0.14	Engine oil, 1000	450	315	98.5	30	60	(Chang et al., 2010b)
$\text{ZrO}_2/\alpha\text{-Al}_2\text{O}_3$	Tubular (7-channels), ID = 6 mm, OD = 31 mm	Dip-coating	Hydrophilic/charge	0.2	Engine oil, 1000	316	276	97.8	12.6	100	(Zhou et al., 2010)
$\text{TiO}_2/\alpha\text{-Al}_2\text{O}_3$	Tubular (19-channels), OD = 31 mm	Dip-coating	Hydrophilic/charge	0.2	Hydraulic oil, 4000	244	213	99.75	12.5	120	(Chang et al., 2014)
$\text{GO}/\text{Al}_2\text{O}_3$	Tubular (19-channels), ID = 3 mm, OD = 31 mm	Vacuum filtration	Hydrophilic	0.2	Machine oil, 1000	950	728	98.7	23.3	140	(Hu et al., 2015)

Chapter 3

NaA/Al ₂ O ₃	Tubular, ID = 10 mm, OD = 13 mm	Hydrothermal synthesis	Hydrophilic	1.2	Lubricant oil, 1000	109	60	99.5	45	50	(Cui et al., 2008)
TiO ₂ /Al ₂ O ₃	Disc	PVD + Hydrothermal reaction	Super-hydrophilic	0.98	Toluene, 1/30 mL	287	~	93	~	~	(Zhang et al., 2018a)
SiO ₂ /ceramic mixture	Disc	Sol-gel	Super-hydrophilic	~2	Oilfield water	~	~	99.95	~	~	(Chen et al., 2016b)
TiO ₂ -doped α-Al ₂ O ₃	Tubular, ID = 10 mm, OD = 12 mm	Doping + sintering	Negative charge	0.2	Soybean oil, 5000	705	605	~	14	120	(Zhang et al., 2009)
CNT/YSZ	Disc, D = 26 mm	CVD	Increase rejection	0.7	Blue oil based ink, 210	36	26	100	28.6	550	(Chen et al., 2012)
IrO ₂ /Al ₂ O ₃	~	Dip-coating	Electrified degradation	< 1	Peanut oil, 200	414	331	96.3 _{COD}	20	160	(Yang et al., 2015)
Ti ₄ O ₇ /Al ₂ O ₃	Tubular, ID = 8 mm, OD = 14 mm	Dip-coating	Electrified degradation	0.2	Peanut oil, 200	1018	914	97.9 _{COD}	9.2	60	(Geng and Chen, 2016)

■ Chapter 3

CuO/CeO ₂ /Al ₂ O ₃	Hollow fiber	Sol-gel	Photocatalytic degradation	0.05	1000	1815	1422	92	22	240	(Azmi et al., 2019)
g-C ₃ N ₄ /Al ₂ O ₃	Hollow fiber	Electro-spinning	Photocatalytic degradation	0.25	Crude oil, 1000	816	640	99 _{TOC}	21	180	(Alias et al., 2019)
PZT	Disc, D = 30 mm	~	Generated ultrasound	0.3	Soybean oil, 500	86	73.1	95.3 _{TOC}	15	180	(Mao et al., 2018)
Al ₂ O ₃ /PZT	Disc, D = 30 mm	Dip-coating	Generated ultrasound	0.1	Soybean oil, 200	230	185	99.5 _{TOC}	20	120	(Mao et al., 2020)

D – diameter of disc, ID – inner diameter of tube, OD – outer diameter of tube, C_f – oil concentration in the feed, NF_i – normalized initial flux, NF_s – normalized stable flux, R^d – oil rejection, FD – flux decline percentage, FT – filtration time, ~ not reported, a – permeate volume (mL).

3.4. Concluding remarks

Ceramic membranes are promising for oily wastewater treatment with a high oil removal efficacy, compact design and a small footprint. However, membrane fouling consistently restricts process efficacy. In this review, we have compared various methods that are used for ceramic membrane modification, which have been applied for oily wastewater treatment, as well as the performance of these ceramic membranes in terms of permeate flux, oil rejection and fouling resistance. The following conclusions can be drawn:

- Although sol-gel and dip-coating are the most frequently used methods for ceramic membranes modification, the emerging modification method ALD has shown great potential on the control of layer thickness and pore size distribution of the ceramic membranes.
- Nano-sized metal oxides have mostly been used as material for ceramic membrane modification for oily wastewater treatment. Among them, TiO_2 , ZrO_2 and Fe_2O_3 are considered the most promising ones to improve ceramic membrane performance, increasing surface hydrophilicity and/or surface charge of membranes. In addition, the GO modified ceramic membranes can improve permeate flux, oil rejection and fouling resistance at the same time. However, the scalability of these anti-fouling ceramic membranes is still challenging.
- To control the fouling problems by oil droplets, also passive antifouling ceramic membranes have been developed, including photocatalytic, piezoelectric and electrochemically enhanced, modified ceramic membranes. However, the performance of these membranes is only tested in a controlled environment for a short time, making it difficult to upscale, and the appropriate materials used to prepare these membranes are expensive.

Acknowledgement

Mingliang Chen acknowledges the China Scholarship Council for his PhD scholarship under the State Scholarship Fund (No. 201704910894).

Chapter 4 |

Highly permeable silicon carbide-alumina ultrafiltration membranes for oil-in-water filtration produced with low-pressure chemical vapor deposition

This chapter is based on:

Chen, M., Shang, R., Sberna, P. M., Luiten-Olieman, M. W., Rietveld, L. C., & Heijman, S. G. (2020). Highly permeable silicon carbide-alumina ultrafiltration membranes for oil-in-water filtration produced with low-pressure chemical vapor deposition. Separation and Purification Technology, 253, 117496.

Abstract

Silicon carbide (SiC) ceramic membranes are of particular significance for wastewater treatment due to their mechanical strength, chemical stability, and antifouling ability. Currently, the membranes are prepared by SiC-particle sintering at a high temperature. The production suffers from long production time and high costs. In this paper, we demonstrated a more economical way to produce SiC ultrafiltration membranes based on low-pressure chemical vapor deposition (LPCVD). SiC was deposited in the pores of alumina microfiltration supports using two precursors (SiH_2Cl_2 and $\text{C}_2\text{H}_2/\text{H}_2$) at a relatively low temperature of 750 °C. Different deposition times varying from 0 to 150 min were used to tune membrane pore size. The pure water permeance of the membranes only decreased from 350 $\text{L m}^{-2} \text{h}^{-1} \text{bar}^{-1}$ to 157 $\text{L m}^{-2} \text{h}^{-1} \text{bar}^{-1}$ when the deposition time was increased from 0 to 120 min due to the narrowing of membrane pore size from 71 to 47 nm. Increasing the deposition time from 120 to 150 min mainly resulted in the formation of a thin, dense layer on top of the support instead of in the pores. Oil-in-water emulsion separation experiments illustrated that both the reversible and irreversible fouling of the SiC deposited UF membrane was considerably lower as compared to the pristine alumina support. The unique feature that pore sizes decrease linearly as a function of SiC deposition time creates opportunities to produce low-fouling SiC membranes with tuned pore sizes on relatively cheap support.

4.1. Introduction

In recent years, ceramic membranes, especially microfiltration (MF) and ultrafiltration (UF), have been used for drinking water production and wastewater treatment (Chen et al., 2020c; Kayvani Fard et al., 2018b). The mechanical, chemical, and thermal stability of ceramic membranes favours their durable applications in high temperature and corrosive environments where polymeric membranes may not be applicable (Chen et al., 2017; Chen et al., 2016a). In addition, ceramic membranes can be chemically cleaned under extreme conditions, after severe fouling, to recover their performance. This can also extend their service lifetime in industrial applications (He and Vidic, 2016).

Among the ceramic membranes, SiC membranes have been extensively studied for high-temperature and high-pressure gas-phase reactive separations, due to their combination of properties such as hardness, chemical resistance, low thermal expansion coefficient and high thermal shock resistance (Dabir et al., 2017; Kim et al., 2017). The use of SiC membranes in water purification has been reported as well (Fraga et al., 2017a; He and Vidic, 2016; Hofs et al., 2011; Skibinski et al., 2016; Zsirai et al., 2016). It has been observed that the SiC MF membranes have high water permeance (de Wit et al., 2015; Eom et al., 2012; Facciotti et al., 2014) and are suitable for long-term applications in slightly oxidative environments such as swimming pool water (Skibinski et al., 2016). Moreover, due to surface characteristics that consist of a combination of super-hydrophilicity and a highly negative charge, SiC membranes exhibit lower reversible and irreversible fouling for surface water and, especially, produced water treatment, when compared with other ceramic and polymeric membranes (He and Vidic, 2016; Hofs et al., 2011).

Pure SiC membranes have been synthesized with various methods such as liquid phase sintering and sintering at low-pressures (Deng et al., 2014). However, to form strong covalent Si-C bonds, a high sintering temperature up to 2000 °C in an argon atmosphere and the addition of sintering aids such as Al₂O₃ (Das et al., 2018; Zhou et al., 2011) and templates (Eom and Kim, 2008) are usually necessary for the production of SiC membranes (Fraga et al., 2017b; Wei et al., 2017). As a result, the SiC membrane production is quite costly. It is challenging to prepare thin SiC layers in the range of ultrafiltration (pores 2 – 100 nm) or even nanofiltration (pores 1 – 2 nm) by solid particle sintering, giving rise to limited use of SiC membranes in the water treatment field (König et al., 2014).

■ Chapter 4

Thus, an alternative processing route to prepare SiC UF membranes at reduced temperatures would be required. Up to now, there are mainly two other approaches employed, mostly for SiC gas separation: chemical vapor deposition (CVD) /chemical vapor infiltration (CVI), and pyrolysis of pre-ceramic polymer precursors (Ciora et al., 2004; Elyassi et al., 2007; Lee and Tsai, 1998; Sea et al., 1998). In CVD/CVI, macroporous α -alumina or SiC membranes are usually used as the supports for the deposition of a thick layer of SiC with one or two precursors at 700-800 °C, followed by a calcination process at 1000 °C in Ar (Lee and Tsai, 1998; Sea et al., 1998). Ciora et al. (2004) first reported the preparation of nanoporous hydrogen-selective SiC membranes on γ -Al₂O₃ tubular supports by using CVD with the two precursors triisopropylsilane (TPS) and 1,3-disilabutane (DSB). Despite both precursors can produce nanoporous membranes, a high-temperature post-treatment was necessary to improve the H₂ permeance and H₂/H₂O selectivity. In the second approach, a dip-coating technique through the pyrolysis of allyl-hydridopolycarbosilane (AHPCS) has also been developed by Ciora et al. (2004). Membranes prepared by polycarbosilane (PCS) pyrolysis at 600 °C gave satisfactory H₂ permeance despite a relatively low H₂/N₂ selectivity. However, due to the film shrinkage during the conversion of the polymer precursors to SiC, this method had to be repeated several times to obtain a defect-free film (Colombo et al., 2010; König et al., 2014). Although it is thus feasible with both reported methods to prepare SiC nanoporous membranes at lower temperatures, the prepared membranes usually have a thick SiC layer, which negatively affects the water permeance and, therefore, they are predominately limited for the purpose of gas-separation applications. More recently, König et al. (König et al., 2014) developed UF SiC membranes on macroporous SiC supports by coating a suspension of α -SiC powder and AHPCS in n-hexane or n-hexane/n-tetradecane. The prepared membranes showed a defect-free mesoporous surface, but still, quite low water permeance (0.05–0.06 L m⁻² h⁻¹ bar⁻¹) was observed.

It thus remains a challenge to produce SiC UF membranes at low temperatures with high water permeance, especially for oil-in-water emulsion separation, which is usually affected by severe fouling problems when using other ceramic and polymeric membranes (Fraga et al., 2017b). Recent studies have shown that the fabrication of ultrathin SiC membranes by means of low-pressure chemical vapor deposition (LPCVD) is a promising platform for cell culturing (Nguyen et al., 2017). To the best of our knowledge, the fabrication of SiC UF membranes via LPCVD has not been realized yet. Therefore, in this work, LPCVD was used to deposit a thin layer of SiC in the pores

■ Chapter 4

of commercial ceramic alumina membranes with the objective to use them for oil-in-water emulsion filtration with reduced membrane fouling.

4.2. Materials and methods

4.2.1. Materials

Commercial tubular ceramic membranes (CoorsTek, the Netherlands) with an inner diameter of 7 mm and an outer diameter of 10 mm were used as support for LPCVD deposition. These membranes are composed of a selective layer of α -alumina with a pore size of 100 nm (specification of the manufacturer) on macroporous α -alumina support. The membranes have an average pure water flux of $382 \text{ Lm}^{-2}\text{h}^{-1}\text{bar}^{-1}$, as given by the manufacturer. However, great variations in actual permeance were observed during the tests (20 tubes). Therefore, only the membranes with similar permeance, being around $350 \text{ Lm}^{-2}\text{h}^{-1}\text{bar}^{-1}$, were chosen for the LPCVD deposition.

4.2.2. Low-pressure chemical vapor deposition

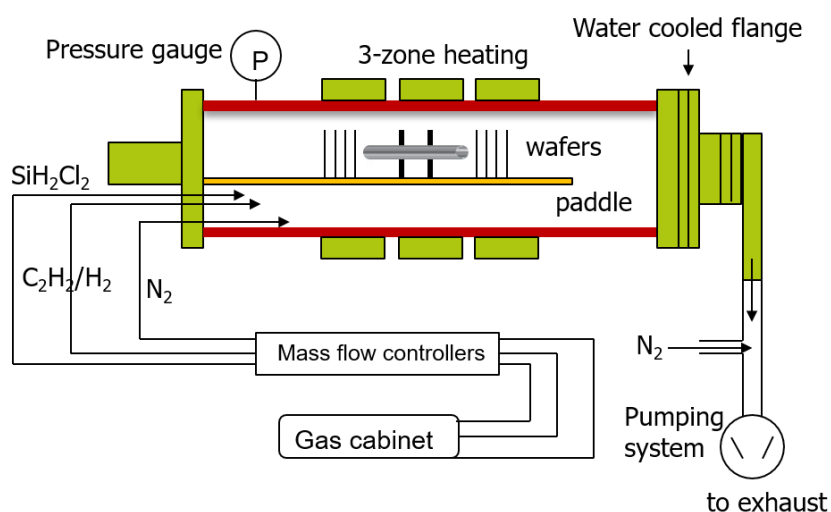


Figure 4.1. Schematic of the LPCVD system used for the membrane deposition of SiC layers.

The membrane tubes were cut into 15 cm long segments to fit the LPCVD chamber. The SiC layer was deposited onto the support, both on the inner and outer surface, in a hot-wall LPCVD furnace (Tempress Systems BV, the Netherlands), as shown in Figure 4.1. Dichlorosilane (SiH_2Cl_2) and acetylene (C_2H_2), diluted at 5% in hydrogen (H_2), were used as precursors, respectively. The purging gas, employed in the system, was ultrapure nitrogen (N_2), obtained from a liquid nitrogen source. In the reactor,

■ Chapter 4

the support membranes were placed in the center of the chamber with their long-axis parallel to the precursors' flow direction.

The deposition parameters, temperature, and pressure were selected based on the study of Morana et al. (2013) on wafers, to obtain a thin and continuous amorphous SiC layer on the membrane surface. Therefore, the depositions were performed at a temperature of 750 °C and pressure of 80 Pa. In addition, a gas flow ratio (SiH₂Cl₂ to C₂H₂) of 3 with a total gas flow of 500 sccm was chosen, while the deposition time was varied between 0 and 150 min to tune layer thickness and membrane pore size. In order to simplify the sample names, all samples are labeled as Dx, where x represents the deposition time (x = 0, 60, 90, 120, and 150 min).

During the deposition, silicon wafers with a diameter of 100 mm and a thickness of 525 (±25) μm were placed next to the membranes to monitor the deposited layer thickness. The layer thickness was later determined by an ellipsometer (M-2000UI, J.A.Woollam Co. Inc., USA), based on the change of the light polarization principle (Shang et al., 2017). Additionally, the growth rate of the SiC layer, obtained through linear regression between layer thickness and the deposition time, was used to estimate the rate of pore size change of the membrane.

4.2.3. Membrane characterization

The morphology of the pristine alumina and LPCVD modified SiC membranes were observed by scanning electron microscopy (SEM, FEI Nova NanoSEM 450, USA). The Si/Al intensity ratios of the samples were determined using energy dispersive X-ray (EDX) analyzer (Ametek EDAX^{TSL}) at 10 kV accelerating voltage, which is coupled in an SEM-EDX system. Prior to observation, membrane samples were sputtered with a thin layer of gold to increase sample conductivity, which is necessary to obtain a clear image. The average pore size and pore size distribution of the membranes were measured by capillary flow porometry (Porolux 500, IBFT GmbH, Germany). FC43 (Benelux Scientific B.V., the Netherlands) was used as the wetting agent for porometry measurements, and the flow and feed pressure were recorded in time. The pore size and pore size distribution were then calculated using the Young-Laplace equation (Shang et al., 2015):

$$D = \frac{4\gamma \cdot \cos\theta \cdot SF}{P} \quad (1)$$

■ Chapter 4

where D is the pore diameter of the membrane (m), γ is the surface tension of the wetting liquid (N/m), θ is the contact angle of the liquid on the membrane surface (0°), P is the used pressure (bar), and SF is the shape factor ($SF = 1$).

The water flux of the membrane before and after deposition was examined, filtering demineralized water at a constant transmembrane pressure (TMP) of 1.5 bar. Membrane fluxes and the water temperature were monitored every 30 s. In order to compare the membrane water permeance, all membrane permeance were corrected to the equivalent at 20°C using the following equation (2) (Shang et al., 2017):

$$L_{p,20^\circ\text{C}} = \frac{J \cdot e^{-0.0239 \cdot (T-20)}}{\Delta P} \quad (2)$$

where $L_{p,20^\circ\text{C}}$ is the permeance at 20°C ($\text{L m}^{-2} \text{h}^{-1} \text{bar}^{-1}$), J is the measured membrane flux ($\text{L m}^{-2} \text{h}^{-1}$), ΔP is the measured TMP (bar), T is the temperature of water ($^\circ\text{C}$).

4.2.4. Oil-in-water emulsion preparation

To ensure that all oil-in-water emulsions had the same characteristics during all experiments, a stock emulsion was prepared, which was then diluted to the desired oil concentration. The stock emulsion was prepared by mixing 3 mL mineral oil (330760, Sigma-Aldrich) and 0.6 g sodium dodecyl sulphate (SDS) (Sigma-Aldrich) with 2 L of demineralized water. We chose mineral oil to prepare the emulsion because its properties are very similar to those of crude oil. This stock emulsion was continuously stirred with a magnetic stirrer (L23, LABINCO, the Netherlands) at a speed of 1500 rpm for 24 h and then ultrasonicated (521, Branson, US) for 2 h until it appeared milky white. The emulsion did not segregate for 3 days, indicating good stability and homogeneity. Afterward, the emulsion was diluted to 6 L with a concentration of 400 mg L^{-1} for the filtration experiments. The used oil concentration was in the normal range typically observed in oily wastewater (Ahmad et al., 2018). The emulsion has a pH of around 5.6 measured by a pH sensor (inoLab™ Multi 9420 - WTW). The oil droplet size distribution was analyzed with a particle size analyzer (Bluewave, Microtrac, USA), and the average oil droplet size of the emulsion was $2 \mu\text{m}$ (Figure S4.1, supplementary information).

4.2.5. Constant flux crossflow fouling experiments with backwash

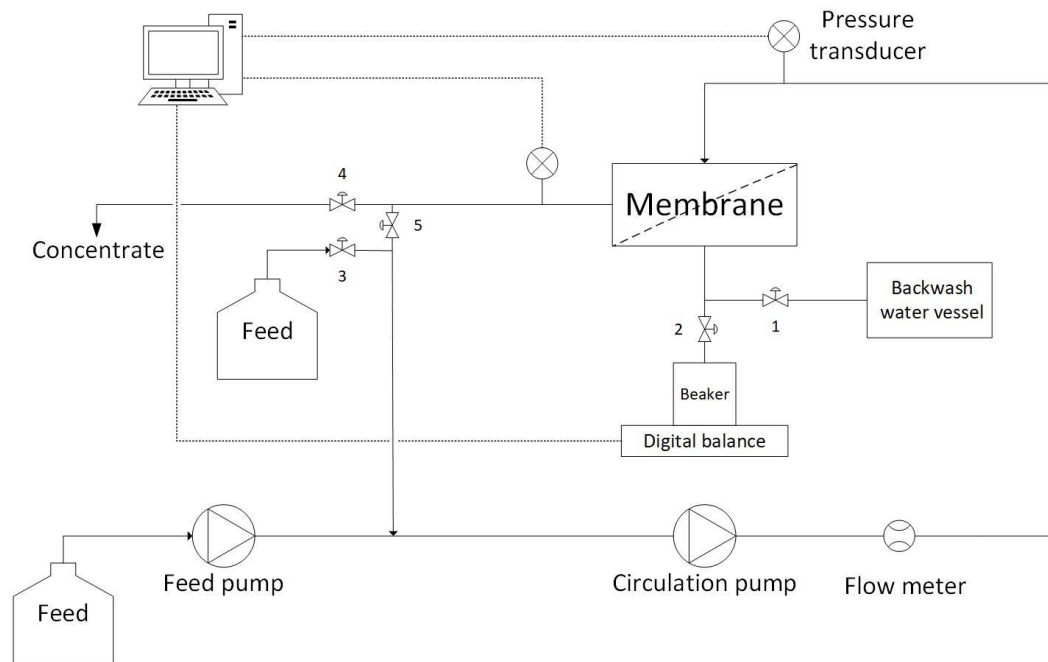


Figure 4.2. Schematic view of the filtration set-up. During the experiment, the feed pump was always at a flow of 0.3 L/h, the effective filtration area of the membrane is 0.003 m² and the membrane had a constant flux of 100 L m⁻² h⁻¹. The function of each numbered valve was explained in supplementary information (Table S4.1).

The membrane filtration set-up with backwash was designed for constant flux experiments (Figure 4.2). The system contained a feed pump (DDA12-10, Grundfos, Denmark) to dose the emulsion into the circulation loop and to control the permeate flux, and a circulation pump (VerderGear, Verder B.V., the Netherlands) to provide a fixed crossflow velocity of 0.44 m/s, monitored by a flow meter (YF-S402, Zhongjiang energy-efficient electronics co., Ltd., China). A backwashing vessel, filled with demineralized water, was connected to a compressed air system, and a fixed pressure of 3 bar was set for backwashing. Two high-precision pressure transducers (GS4200-USB, ESI, UK) were installed on the two sides of the membrane module to monitor the pressure variations. Since the pressure of the permeate stream was equal to atmospherical, the pressure exhibited by the pressure transducers was TMP. A digital balance (KERN EWJ 600, Germany) was used to measure the permeate flux in case there was a difference with the feed pump flow. During the experiments, the pressure, temperature and flow were continuously logged at a time interval of 30 s.

■ Chapter 4

The pristine (D0) and modified (D120) membranes were tested separately with the above mentioned constant flux filtration set-up to compare the membrane fouling resistance before and after deposition. A new membrane was used for each test. The oil-in-water emulsion was used as a model foulant in this study. All filtration experiments were done at room temperature (22 °C) and carried out in duplicate. Prior to each filtration experiment, the membranes were immersed in demineralized water overnight to wet all the pores. The set-up was thoroughly flushed with demineralized water to remove residual chemicals and air in the system. Afterward, the initial permeance of each membrane was determined with demineralized water at a constant flux of 100 L m⁻² h⁻¹ for 10 min. Each fouling experiment consisted of 7 cycles, and each cycle was composed of three phases in the following order: 1) Filtration of oil-in-water emulsion at a constant flux of 100 L m⁻² h⁻¹ for 18 min, 2) Backwashing the membrane module with demineralized water at a fixed pressure of 3 bar for 30 s to remove the hydraulically reversible fouling, 3) Forward flush with feed for 15 s at a crossflow velocity of 0.44 m/s. The purpose of the forward flush is to purge the membrane module to remove the backwash remaining liquids and replace the solution in the loop with the fresh feed. The explanation to choose a constant flux of 100 L m⁻² h⁻¹, filtration time of 18 min and a crossflow velocity of 0.44 m/s is given in the supporting information (Figure S4.2 and Figure S4.3). The filtration-backwash-forward flush phase is shown in Table S4.1.

During the constant flux filtration experiment, the TMP increases in time due to membrane fouling by oil droplets. In order to better compare the membrane performance before and after deposition, the TMP and permeance (P) of the membranes during filtration were normalized to the initial TMP₀ and P₀, which were measured by filtering demineralized water.

The membrane resistance was calculated based on the resistance-in-series model (Huang et al., 2017; Xing et al., 2019), as shown in Eq. (3):

$$R_t = \frac{TMP}{\mu J} = R_m + R_r + R_{ir} \quad (3)$$

where J is the membrane flux (m/s), TMP is the applied trans-membrane pressure (Pa), μ is the viscosity of the permeate (Pa·s), R_t (m⁻¹) represents the total resistance, which is consist of intrinsic membrane resistance (R_m), hydraulically reversible resistance (R_r), and irreversible unphysical removable resistance (R_{ir}). R_m was determined through the filtration of demineralized water and R_t was measured

■ Chapter 4

according to the final filtration pressure of wastewater. The fouled membrane was backwashed with demineralized water under a pressure of 3 bar and then R_r was measured. The R_{ir} was calculated from $R_t - R_r - R_m$.

4.3. Results and discussion

4.3.1. Thickness and growth kinetics of SiC layers on a silicon wafer

The growth rate of the SiC layer in the pores of the porous ceramic membrane could not be measured directly. To have an indication of the growth rate, silicon wafers were used as substrates to measure the SiC layer thickness with ellipsometry. The results (Figure 4.3) show a linear relationship between the deposition time and SiC layer thickness. The growth rate is determined from the slope of the linear regression and is 0.3 nm/min.

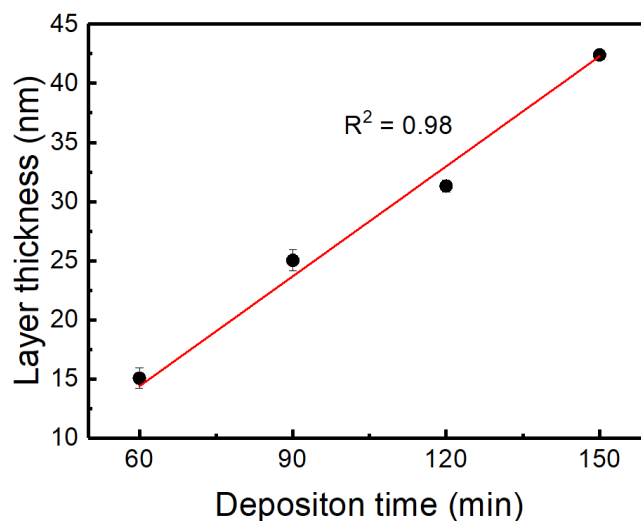


Figure 4.3. Correlation between the thickness of the deposited SiC layer and deposition time onto a silicon wafer.

Wang and Tsai (2000) also studied the SiC deposition with LPCVD at 750 °C and observed a growth rate of 0.87 nm/min, which is higher than the one we found, probably due to the higher pressure in the reaction system they used. The growth rate we found was also much lower than that of plasma-enhanced chemical vapor deposition (PECVD), though deposited at much lower temperatures (200-400 °C) (Iliescu et al., 2008a; Iliescu et al., 2008b). However, a lower growth rate could lead to better control of the film thickness on the target substrates, which is especially

■ Chapter 4

important for membrane modification, where uniform deposition into pores is of importance (Lee and Tsai, 1998).

4.3.2. Morphological evolution of membranes under various deposition times

The cross-section structure of the pristine membrane was analyzed using a scanning electron microscope. The separation layer of the membranes had a thickness of around 25 μm as clearly observed in Figure 4.4, but variations from 21 to 25 μm were found for the various samples (Figure S4.4).

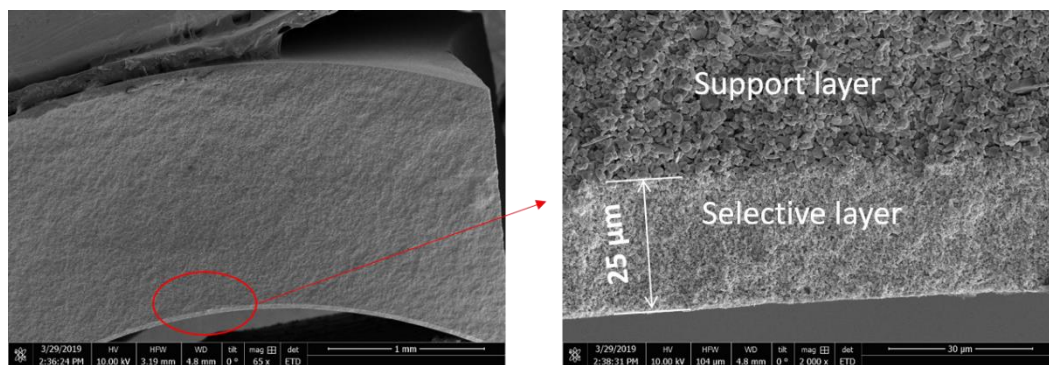


Figure 4.4. SEM images of the cross-section of the pristine alumina membrane.

In Figure 4.5, SiC deposited tubes with various deposition times and one pristine alumina tube are depicted, showing a change of color from white to brown and black after increasing SiC deposition time. Black is a typical color for a SiC membrane, indicating that the alumina membrane samples were deposited with a homogeneous layer of SiC after around 90 min. Also the inside of the tubes, deposition time 90 min or longer, were examined after breaking, and display uniform colored black surface as well. The inside of the deposited tube's wall, though, was white, indicating that the deposition penetrated only a small part of the alumina tube's wall (see lower right in Figure 4.5).

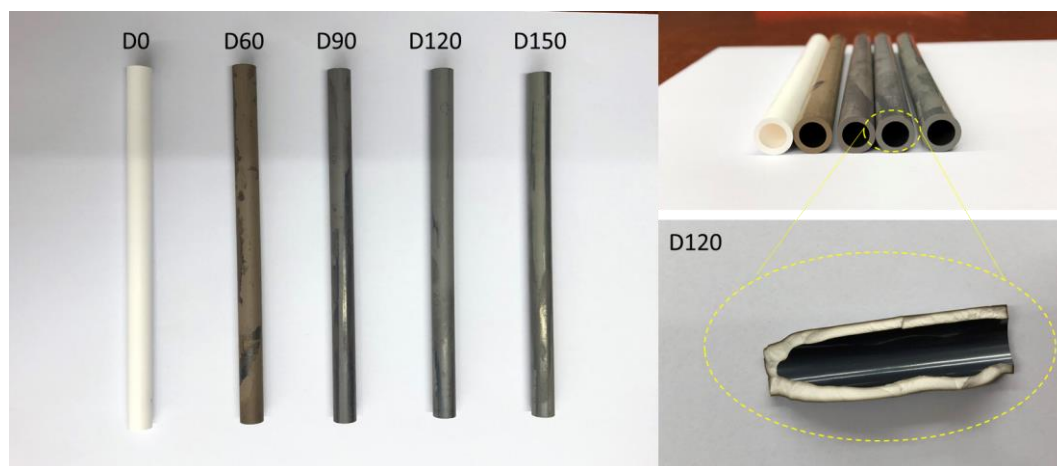


Figure 4.5. Photos of the pristine membrane and LPCVD-deposited membranes.

The surface morphologies of the pristine and deposited alumina membranes were further investigated by SEM observations. In Figure 4.6, surface SEM images of the pristine ceramic membrane and SiC deposited ceramic membranes (different deposition times) are shown. The images demonstrate that no continuous SiC layer is deposited on top of the support membrane's surface but the SiC is mainly deposited in the pores. It also shows that prolongation of the deposition time, from 60 to 150 min, results in a considerable decrease in pore size.

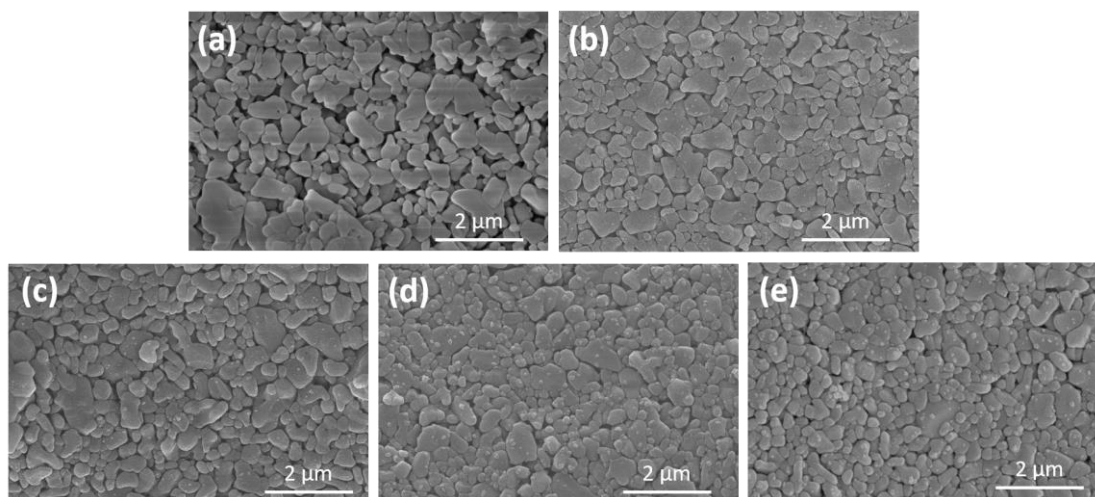


Figure 4.6. Surface SEM images of (a) the pristine ceramic membrane (D0), and SiC-modified ceramic membranes with increasing deposition times: (b) D60, (c) D90, (d) D120, (e) D150.

In addition, longer deposition times allow the precursors, dichlorosilane and acetylene, to diffuse more in-depth into the support. To study the effect of the penetration of the precursors on the membrane's morphology, cross-sectional SEM pictures of the membranes were made. From Figure 4.7C it can be observed that after

■ Chapter 4

90 min a SiC layer started to be formed on top of the top layer, while after 150 min, it appeared to cover the entire top layer.

SEM-EDS line scans were made to provide elemental identification of the SiC deposition in the pores. The results are depicted in Figure 4.7F, showing the Si/Al intensity ratios of the different SiC deposited membranes as a function of the distance from the membrane surface. In the first 90 min the gas diffuses around 10 μm into the top layer of the support and after 120 min SiC was deposited in the pores of the entire support's top layer. It looks like there is less infiltration after 150 min as compared to 120 min. This could be caused by a variation in the thickness of the top layer. Figure S4.4 shows that the supports' top layer varied between 21-25 μm so it means that after 120 min SiC is already deposited in the pores of the entire top layer. In the initial period of LPCVD deposition (0-120 min), the pores among particles were large enough to allow rapid and unlimited diffusion of precursors into the pores, and sufficient adsorption and reaction happened on the particle surface. With further increase of the deposition time, the diffusion of the precursors into the pores would be restricted due to the narrowing pore mouth. Thus, the deposition rate of SiC layer inside the pores reduced after 120 min. As a result, deposition mainly happened on the top surface and resulted in the addition of a new, dense thin film. Similar profiles have been observed by Dendooven et al. (2010) and Gordon et al. (2003). Overall, these above-mentioned discussions revealed that the LPCVD is an effective conformal deposition technique over complex three-dimensional structures like the tubular membranes used in our work.

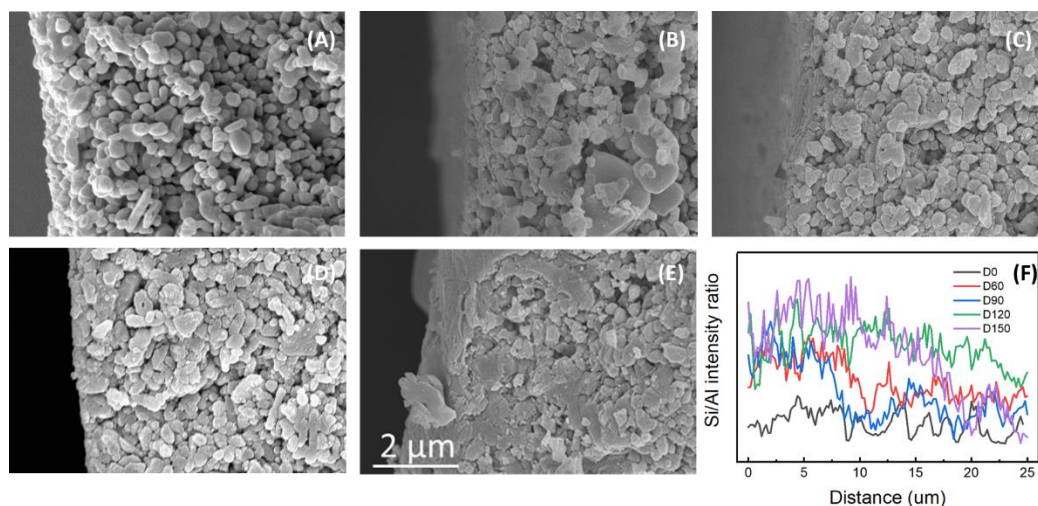


Figure 4.7. The cross-sectional SEM image and of the pristine and LPCVD modified membranes: D0 (A), D60 (B), D90 (C), D120 (D), D150 (E) and corresponding line-scan EDS spectra (F). All images have the same magnification and the scale bar is shown in E.

4.3.3. Effect of LPCVD deposition on pure water flux and membrane pore size

Pure water permeance tests were conducted on both the pristine membranes and the LPCVD modified membranes after different deposition times. The results of the pure water permeance test are displayed in Figure 4.8a. The permeance of the membranes decreased linearly from $350 \text{ Lm}^{-2}\text{h}^{-1}\text{bar}^{-1}$ to $157 \text{ Lm}^{-2}\text{h}^{-1}\text{bar}^{-1}$ when the deposition time was increased from 0 min to 120 min. After 120 min the decline in permeance was lower.

Pore size measurements of the pristine alumina membrane and the LPCVD deposited membranes were performed and the results are shown in Figure 4.8b. The alumina membrane, black line in Figure 4.8b, had a broad pore size distribution, and contained pores between 40-80 nm with an average of 71 nm. Compared to the pristine membrane, the deposited membranes had a narrower pore size distribution and smaller average pore sizes. A substantial decline in pore size was observed with increased deposition time, from 71 nm to 43 nm after 150 min of SiC deposition. Figure 4.8c demonstrates that the pore diameter decline was linear except the pore size measured after 60 min of deposition, where a slight deviation from the line can be observed. The phenomenon of the linear permeance and pore size decline has also been described in previous studies (Lee and Tsai, 1998; Lin and Burggraaf, 1993), where CVD was used to modify the membranes. As the water permeance decreased

with the same slope, we assume that something went wrong during the pore size measurement of the tube with a deposition time of 60 min.

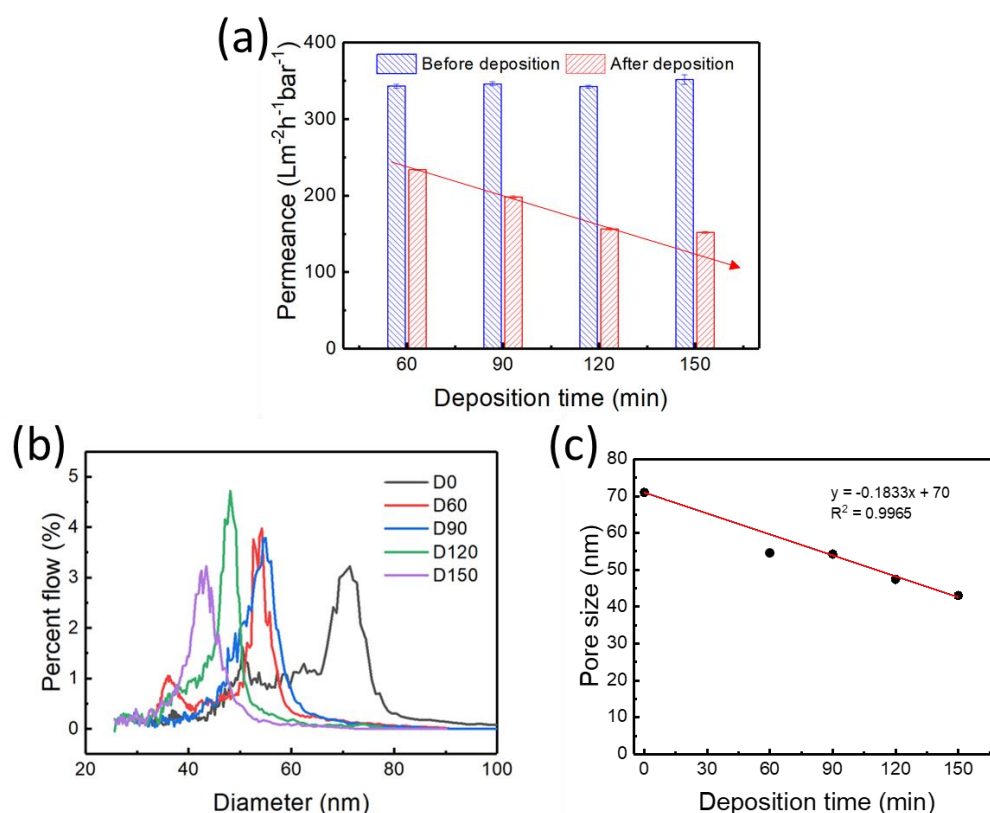


Figure 4.8. (a) Pure water permeance and (b) pore size distribution of pristine membrane and LPCVD modified membranes; (c) linear fit of pore size variations with deposition time (D60 is not included).

4.3.4. Filtration of an oil-in-water emulsion

The SiC deposited membrane with 120 min deposition time (D120) and the pristine alumina membrane (D0) were compared with respect to the filtration of an oil-in-water emulsion. The initial permeance of both membranes for emulsion filtration were close to their pure water permeance, indicating the membranes were not fouled at the initial stage (Figure S4.5). To better compare the membrane performance, we normalized the TMP and permeance. In Figure 4.9a the normalized TMP is visualized as a function of the filtration time, showing a fast increase in the relative TMP of both D0 and D120 during one filtration cycle, indicating that considerable fouling occurred in both membranes. However, the pristine alumina membrane maintained a high TMP increase rate during all filtration cycles. In contrast, a much slower TMP increase was

Chapter 4

observed for the SiC deposited membrane with 120 min deposition time. The final relative TMP of D0 was more than 1.5 times higher than that of D120, suggesting fouling was much less after modification.

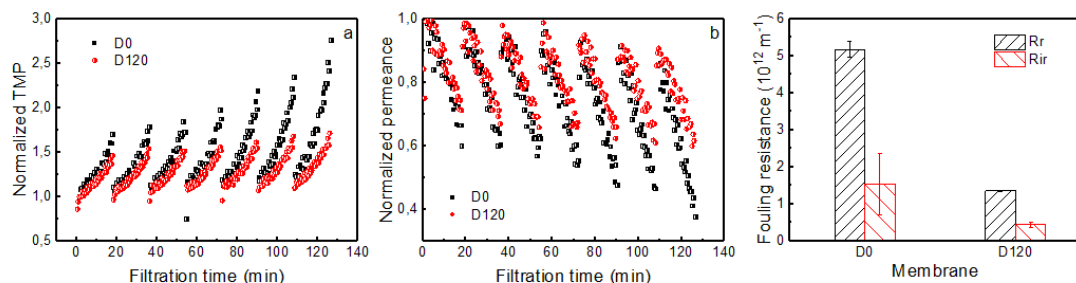


Figure 4.9. (a) Normalized TMP, (b) normalized permeance, and (c) fouling resistance of D0 and D120 for oil-in-water emulsion filtration.

At the end of each cycle, the membranes were hydraulically backwashed with demineralized water before starting the next filtration cycle. It was found that the permeance of both membranes (Figure 4.9b) was only slightly reduced after the first backwashing, indicating the reversible fouling was mainly responsible for the permeance loss. The gradual development of irreversible fouling was observed for both membranes during subsequent filtration cycles. To further reveal the influence of the SiC deposited layer on fouling mitigation, the resistance distribution during the filtration process was analyzed. Figure 4.9c shows the reversible and irreversible fouling resistance for both membranes during the entire filtration process. Both the reversible and irreversible fouling resistance of D120 was smaller than that of D0, indicating that the SiC deposited layer mitigated the membrane fouling during oil-in-water emulsion filtration. Based on the above discussions, it can be concluded that the SiC deposited membrane was less prone to fouling as compared to the pristine membrane for oil-in-water emulsion filtration.

The pore sizes of D0 and D120 are much smaller than the average size of the oil droplets. Therefore, it is assumed that the surface properties of the SiC deposited layer are the most important in avoiding fouling. Previous studies also showed that SiC membranes have a low fouling tendency as compared to other ceramic and polymeric membranes, which is closely related to super hydrophilicity (Hofs et al., 2011) and the low iso-electric point (pH 2.8) of SiC (Skibinski et al., 2016). The pristine alumina membrane has a relatively high iso-electric point which is about 9 (Atallah et al., 2017). The emulsion used in this study had a pH of 5.6, which means that the modified

■ Chapter 4

membrane surface was negatively charged while the pristine membrane had a positive surface charge during the filtration process. The emulsion also had a highly negative charge due to the negative charge of the surfactant (SDS) surrounding the oil droplet (Lin and Rutledge, 2018). Therefore, electrostatic-interaction would be different for the two membranes, and the SiC layer of the modified membrane would protect the membrane from adsorbing or depositing oil droplets not only due to the hydrophilic characteristics of the surface, but also because of electrostatic repulsion forces between the membrane surface and oil droplets. In contrast, electrostatic adhesion could happen on alumina membrane surface due to the opposite charge between membrane surface and oil droplets which would accelerate membrane fouling.

4.4. Conclusion

In this work, tubular SiC UF membranes with pore sizes between 43-55 nm were manufactured on an alumina supporting tube via low-pressure chemical vapor deposition, a straightforward and more economical method to produce SiC UF membranes (see cost analysis in S4.5, supplementary information). Pure water permeance of the modified membranes decreased linearly until a deposition time of 120 min from $350 \text{ Lm}^{-2}\text{h}^{-1}\text{bar}^{-1}$ to $157 \text{ Lm}^{-2}\text{h}^{-1}\text{bar}^{-1}$. Pore size measurements also depict a linear decline in pore size with increasing deposition time (confirmed by SEM images). Deposition times longer than 120 min mainly resulted in the addition of a thin, dense selective layer on top of the support. The developed SiC-deposited UF membranes show a low fouling characteristic and a small permeance loss during oil-in-water emulsion filtration, probably due to a combination of hydrophilic and charge interactions. These findings create opportunities to produce low fouling SiC membranes with tuned pore sizes on relatively cheap support.

■ Chapter 4

Acknowledgements

Mingliang Chen acknowledges the China Scholarship Council for his PhD scholarship under the State Scholarship Fund (No. 201704910894). We appreciate Prof. Louis Winnubst (University of Twente) for the valuable suggestions on the manuscript and thank Dr. B. Morana (Delft University of Technology) for the help on SiC deposition.

Supplementary information

S4.1. Oil droplet size distribution

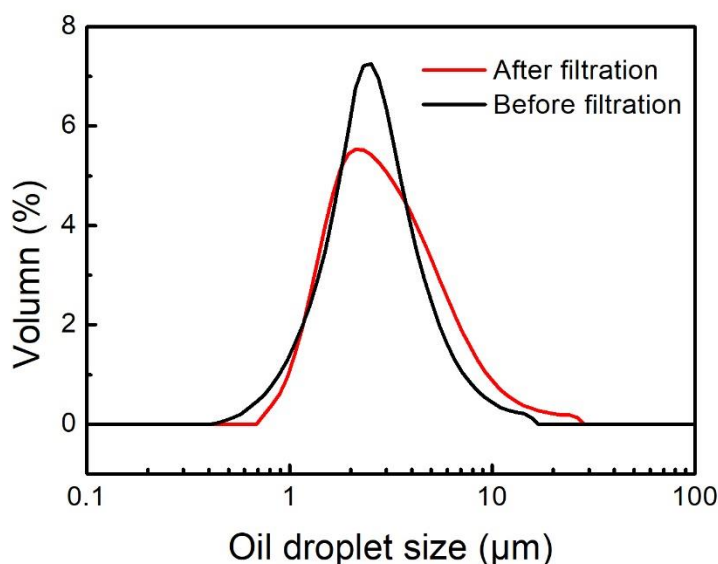


Figure S4.1. Oil droplet size distributions of the emulsions before and after filtration by a membrane.

S4.2. Determine suitable filtration parameters

In this study, the flux of 100 LMH, permeation time 18 min and crossflow velocity 0.44 m/s were chosen based on the following reason. Firstly, we used a pristine alumina membrane to filter the oil emulsion at a constant flux of 80 LMH in dead-end mode (Fig. S2a), serious fouling was observed in 20 min. Due to the rapid increase in transmembrane pressure (TMP), the flux could not be maintained constant. Therefore, we provided a crossflow velocity to diminish membrane fouling. A crossflow velocity of 0.44 m/s could effectively reduce the fouling. The result was illustrated in Fig. S2b, as the TMP of the membrane only increased lightly in 40 min. For the multi-cycle filtration experiment, we wanted to reduce the filtration time of each cycle. Therefore, we increased the permeate flux to 100 LMH, and a higher fouling rate was observed than that at a flux of 80 LMH in 18 min. After 18 min, faster fouling of the membrane occurred, leading to a decrease of the permeate flux (Fig. S3). Therefore, we stopped the filtration experiment at 18 min and backwashed the membrane to recover the membrane performance.

Chapter 4

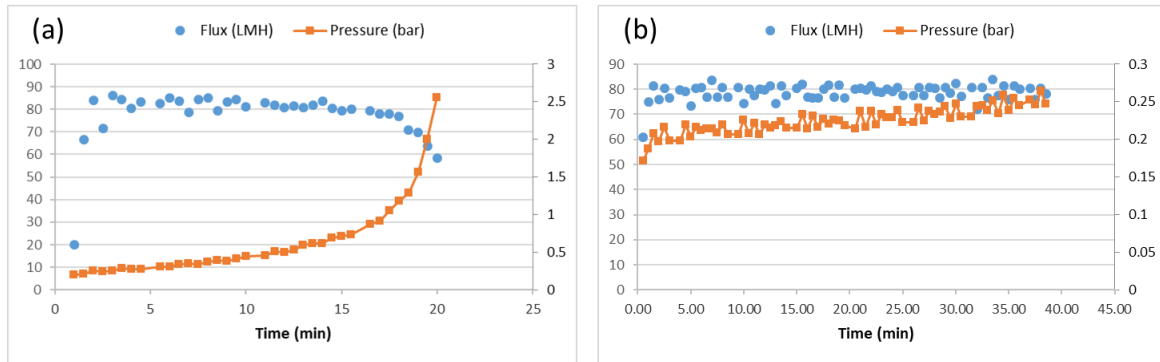


Figure S4.2. Oil-in-water emulsion filtration at a constant flux of 80 LMH by pristine alumina ceramic membrane with (b) and without (a) crossflow velocity. The emulsion had an oil concentration of 400 mg L^{-1} and pH of 5.6. The crossflow velocity was set to 0.44 m/s.

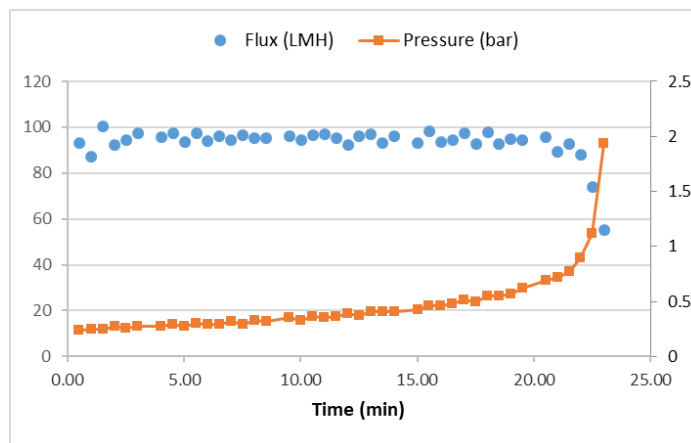


Figure S4.3. Oil-in-water emulsion filtration at a constant flux of 100 LMH by pristine alumina ceramic membrane with a crossflow velocity of 0.44 m/s. The emulsion had an oil concentration of 400 mg L^{-1} and pH of 5.6.

Table S4.1. Operational phases of membrane setup.

Phase	Valve 1	Valve 2	Valve 3	Valve 4	Valve 5	Circulation pump
Filtration	Close	Open	Close	Close	Open	On
Backwash	Open	Close	Close	Open	Open	Off
Forward flush	Close	Open	Open	Open	Close	On

Chapter 4

S4.3. Selective layer thickness of ceramic tubes

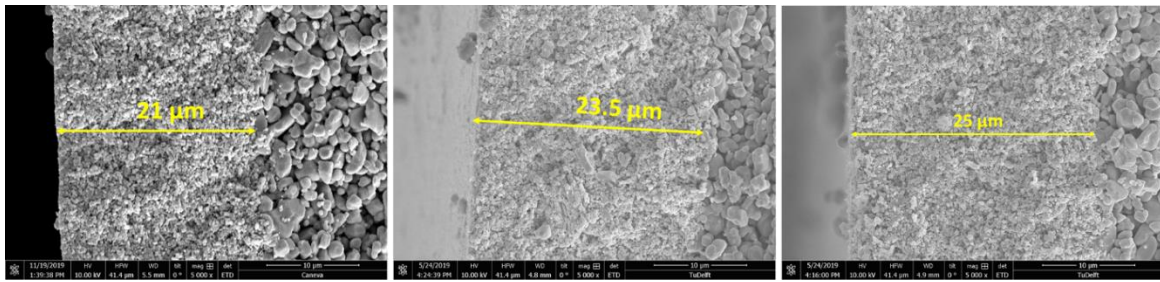


Figure S4.4. Cross-sectional SEM images of three ceramic tubes. The images show that the selective layer thickness varies between 21 and 25 μm for different tubes.

S4.4. Oil-in-water emulsion filtration

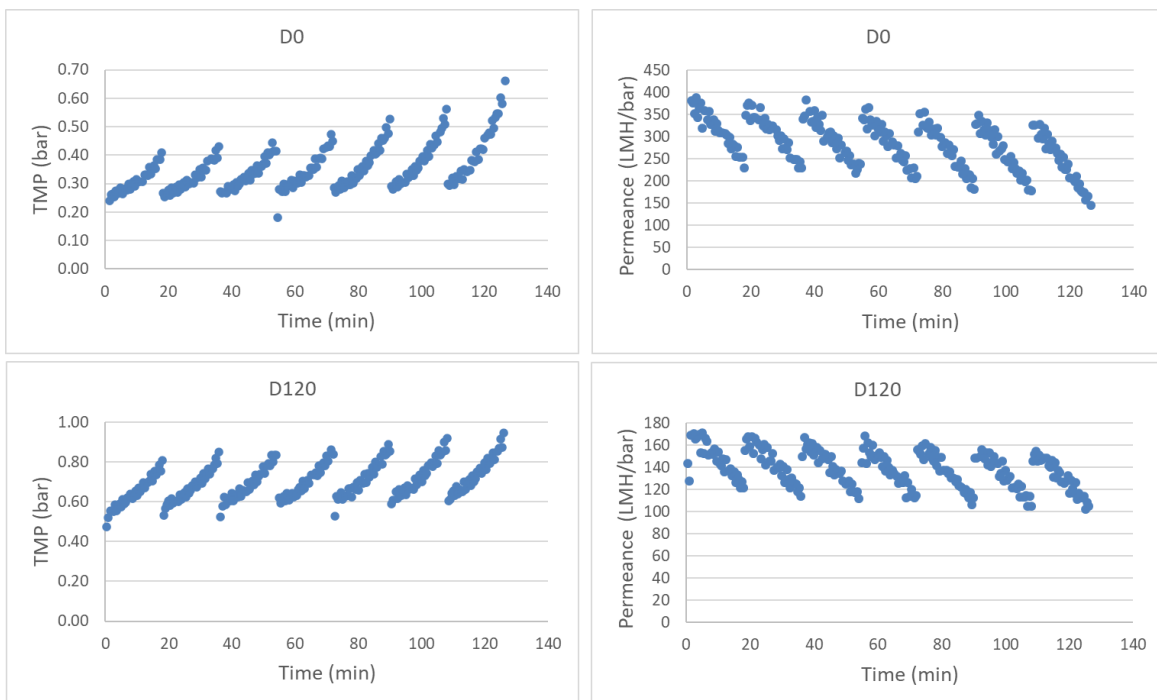


Figure S4.5. Variations of TMP and permeance of D0 and D120 during the filtration of oil-in-water emulsion at a constant flux of 100 LMH. The emulsion had an oil concentration of 400 mg L^{-1} and pH of 5.6.

The variations of transmembrane pressure (TMP) and permeance of D0 and D120 were shown in Fig. S5. The initial TMP of D120 was almost two times higher than that of D0 due to smaller permeance. The oil emulsion permeance of both membranes were close to their pure water permeance. After 7 cycles of filtration, more fouling was observed in D0 even though it had a higher initial permeance.

■ Chapter 4

S4.5. Cost analysis

In this thesis, we compare the costs of SiC-deposited alumina membranes with those of commercial membranes. Due to the confidential nature of the parameters used in the preparation of commercial SiC membranes, we rely on the retail price of commercial membranes as a reference. The costs of SiC-deposited alumina membranes can be categorized into two parts: the cost of alumina supports and the cost of the LPCVD system. For the cost of the LPCVD system, we exclude the one-time furnace cost from our calculations and focus solely on the chemical and energy costs. Table S4.2 provides the dimensions and prices of commercial SiC membranes (Liqtech) as well as alumina membranes (CoorsTek).

Table S4.2. Comparison of commercial SiC and alumina membranes. The prices of the two membranes were based on quotations obtained from the respective companies in 2019.

Membrane	Supplier	Configuration	ID (cm)	OD (cm)	Length (cm)	Price (€)
SiC	Liqtech	Tubular	7	10	25	200
Al ₂ O ₃	CoorsTek	Tubular	7	10	15	65

The cost of commercial SiC membranes is assumed to be equal to the price on the quotation.

Since the membrane with a deposition time of 90 minutes exhibits the best fouling resistance, we select 90 minutes as the duration for calculating the chemical cost. The entire LPCVD process requires additional time for heating and pumping the reaction chamber. Typically, the total time necessary to complete the entire process is approximately 4 hours. Consequently, the cost of the LPCVD process can be determined by considering the chemical cost (refer to Table S4.3) and energy cost (refer to Table S4.4) for a 90-minute deposition.

Table S4.3. Chemical cost of LPCVD (90 minutes)

Precursor	Flow rate (sccm)	Price	Cost (€)
DCS	65	35 €/kg	866.09
C ₂ H ₂	22	50 €/kg	0.12
H ₂	413	2 €/kg	0.17
N ₂	500	1 €/L	45
			911.38

DCS – Dichlorosilane, the price of each precursor was found from Alibaba.com on 25th May, 2023.

■ Chapter 4

Table S4.4. Energy cost of LPCVD (4 h)

Parameter	Value
Power of furnace	5 kW
Power of pump	15 kW
Deposition time	90 min
Total usage time	4 h
Electricity price in the Netherlands	0.62 € /kWh
Total cost	49.6 €

The power of furnace and pump are assumed in the table.

To calculate the ultimate cost of a SiC-deposited alumina membrane, we make the assumption that 30 tubes can be deposited simultaneously in the LPCVD system. This arrangement results in an approximate cost of 97 € per tube, which is less than half the cost of commercial SiC membranes.

Chapter 5 |

Evaluation of fouling by oil-in-water emulsion at constant flux and constant transmembrane pressure: Implications for modification of ceramic membranes

This chapter is based on:

Chen, M., Heijman, S. G., & Rietveld, L. C. (2023). Evaluation of fouling by oil-in-water emulsion at constant flux and constant transmembrane pressure: Implications for modification of ceramic membranes. To be submitted for publication.

Abstract

Membrane modification has been widely used for water purification and wastewater treatment to decrease fouling of ceramic membranes. However, the way fouling experiments are conducted has a strong impact on the evaluation of the fouling resistance of the pristine and modified membranes, which is rarely studied. Therefore, in this study, alumina and SiC-deposited alumina membranes were respectively studied for oil-in-water emulsion filtration using both constant flux and constant transmembrane pressure experiments. The threshold flux of the membranes was first determined by flux-stepping experiments. In a single cycle constant flux filtration experiment, the development of fouling of the membranes was consistent with the results of the threshold flux experiments. However, the fouling character changed when backwash was involved in constant flux experiments and it was also related to the permeate flux. The improved surface hydrophilicity and charge made backwash more effective for the modified membranes, while extensive modification had a negative effect on membrane fouling due to the larger loss in membrane permeance, compared to the permeance of the other membranes. In the constant pressure experiment, the backwash efficacy was only related to the permeance of the membranes, while an effect of surface properties was not observed. Therefore, constant flux filtration experiments with backwash are recommended to be applied to evaluate the performance of the membranes with and without modification, because they not only have a better representation of practical conditions, but also make it easier to observe the effect of surface properties on membrane fouling.

5.1. Introduction

Among the membrane technologies, microfiltration (MF)/ultrafiltration (UF) are widely used for drinking water production (Fiksdal and Leiknes, 2006; Mavrov et al., 1998), wastewater treatment (Hoinkis et al., 2012; Raffin et al., 2013) and pretreatment for high-pressure NF and RO processes (Ordóñez et al., 2011; Pearce, 2008), due to their low energy requirement and small footprint. In addition, MF/UF are also considered to be one of the most effective ways to deal with oil-in-water (O/W) emulsions (Chen et al., 2022; Chen et al., 2021).

The filtration mechanism for MF/UF is mainly based on size exclusion (Miller et al., 2017). During the filtration process, suspended particles, colloids and oil droplets are retained on the membrane surface or in the pores. This leads to the so-called membrane fouling, which could cause a series of negative effects such as a decline of water production or a higher operational pressure due to an increased mass-transfer resistance (Zhang et al., 2016a). As a result, the capital and operational costs increase due to higher energy consumption, requiring chemical cleaning of the fouled membranes and shorter membrane unit's service life. It is therefore important to mitigate membrane fouling during the filtration process.

Various techniques may be used to alleviate membrane fouling. The feed may be pre-treated by dosing additives (e.g., coagulant and flocculant) or oxidants (e.g., permanganate, chlorine) to reduce the amount of foulants that may block the membrane pores (Heng et al., 2008; Lin et al., 2013; Wu et al., 2006). However, this can increase the operational costs due to the need of additional unit operations. Operational parameters, such as cross-flow velocity, permeate flux, and transmembrane pressure (TMP) can be adjusted to reduce foulant build-up on the membrane surface, but it cannot radically solve the fouling problem (Zhang et al., 2016a).

Membrane modification is considered to be one of the most promising methods to reduce membrane fouling (Chen et al., 2021). This is normally achieved by building a fouling resistant surface on the membrane support. Various methods, such as surface coating (Chang et al., 2014), surface grafting (Nady et al., 2011), physical doping/blending (Zhang et al., 2009) and surface deposition (Chen et al., 2022; Chen et al., 2020b), have been adopted to construct such surfaces. The newly constructed surface can change the physicochemical properties of the membrane to minimize the negative interaction between the foulants and membrane surface, thereby decreasing

■ Chapter 5

fouling. This is typically realized via enhancing the surface hydrophilicity and electrostatic interactions between the foulants and membranes in light of the fact that most of the foulants in nature are hydrophobic and charged in the aquatic environment (Rana and Matsuura, 2010).

Nevertheless, it is inevitable that a higher mass-transfer resistance is normally observed for MF/UF membranes after modification, due to either a decrease in membrane pore sizes or an increase in the selective layer thickness of the membrane. Therefore, the permeance of the modified membranes is usually smaller than that of the pristine membranes (Gu et al., 2021).

To effectively evaluate the extent of fouling mitigation for a modified membrane, the fouling rate during filtration and the fouling state after cleaning should be determined. There are two different filtration modes, namely constant TMP filtration and constant flux filtration (Figure 5.1). Constant TMP filtration is more frequently used in a laboratory environment as it is relatively easy to perform. With a fixed TMP, the permeate flux of the membrane declines as it fouls. In contrast, constant flux filtration is preferred in industrial practice to maintain a constant production flow. To maintain the desired permeate flux, the TMP increases over time as the membrane fouls.

As the permeance is different for the modified and pristine membranes, fouling on the membrane surface or in the pores may be affected. As schematically shown in Figure 5.1, due to the smaller permeance, the initial TMP and flux of the modified membrane are, respectively, higher and lower than that of the pristine membrane in constant flux mode and constant TMP mode (Blankert et al., 2021; Miller et al., 2014a). As fouling is affected by the initial states, the higher initial flux through a pristine membrane may lead to more fouling in constant TMP mode (Blankert et al., 2021). Differences in the filtration flux naturally occur for membranes with different permeances, making a fair comparison difficult. In comparison, in constant flux filtration mode, the higher initial TMP of the modified membrane also has a negative effect on fouling, making the comparison beneficial for membranes with a higher permeance (Kouchaki Shalmani et al., 2020).

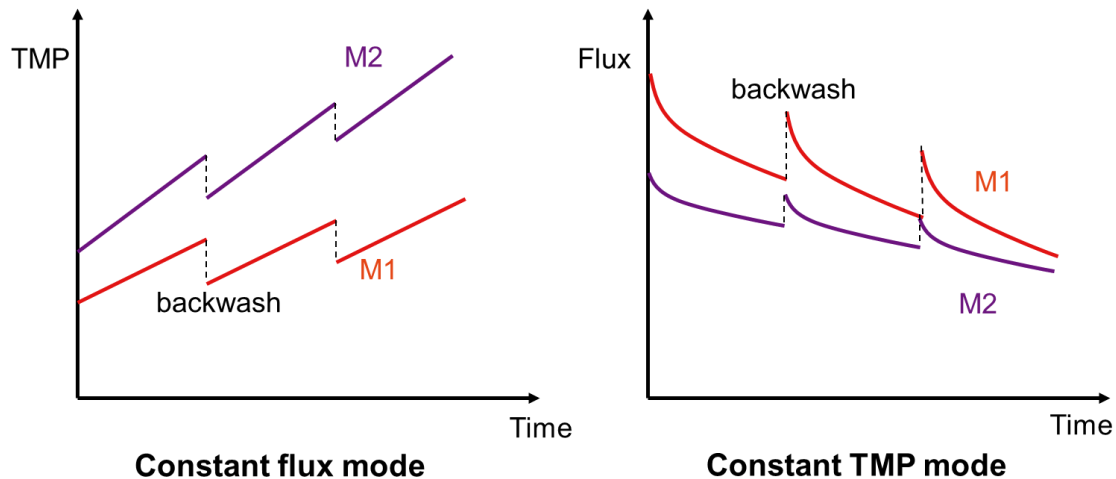


Figure 5.1. Possible filtration profiles of the pristine membrane (M1) and the modified membrane (M2) at constant flux (left) and constant TMP (right) conditions.

Therefore, in both filtration modes, membrane fouling is affected by the variations of initial states of the membranes with different permeance. In a previous study, Miller et al. (2014a) compared the fouling of polymeric membranes at, respectively, constant TMP and constant flux modes for O/W emulsions. Mass-transfer resistance changes during fouling were compared at various fluxes for the two filtration modes. At low fluxes, the fouling resistance and its change were independent of the operational mode. In contrast, the change in fouling resistance was much higher in constant flux filtration than in constant TMP filtration experiments at high flux conditions. Although it was confirmed that membrane fouling could be affected by the filtration modes, the effect of membrane permeance and the irreversible fouling (fouling that cannot be removed by physical or hydraulic cleaning) was not considered. More recently, Blankert et al. (2021) also compared the fouling of membranes with different permeance at the two operational modes. The results showed that a bias may occur for a less-permeable membrane in constant TMP filtration mode due to a lower filtration flux. Hence, constant flux filtration experiments were recommended for fouling evaluation. However, the study only focused on single cycle filtration, without considering the effect of irreversible fouling, while irreversible fouling is considered as the main contributor to high energy consumption and operational costs in full-scale installations (Kimura et al., 2004; Kimura et al., 2014). Therefore, a filtration experiment with multiple cycles may provide more valuable insights for practical applications. In addition, modification can also have an impact on membrane performance due to the newly formed functional layer. The combination of both factors (the decrease of permeance and the potential decrease of fouling by the newly

■ Chapter 5

formed selective layer) will finally determine the performance of a modified membrane.

Due to the rich hydroxyl groups formed on the particle surface, SiC is highly hydrophilic. In addition, SiC has a low iso-electric point (pH = 2-3), leading to a highly negatively charged surface (Skibinski et al., 2016; Xu et al., 2020). These properties may lead to less fouling during filtration of O/W emulsions.

Therefore, in this study, the performance of the more conventional, commercially available alumina (Al_2O_3) ceramic membrane and silicon carbide (SiC)-deposited ceramic membranes were respectively compared in constant flux and constant TMP modes with O/W emulsions. Backwash and multiple filtration cycles were applied to evaluate the irreversible fouling. The SiC-deposited membranes were prepared by low-pressure chemical vapour deposition (LPCVD) to deposit a thin layer of SiC on the Al_2O_3 membrane surface and/or in the pores. Different deposition times were applied to obtain the membranes with varying permeance. In constant flux filtration experiments, the threshold fluxes (defined as the flux at which the rate of fouling rapidly increases) of the membranes were firstly determined and then membrane fouling was evaluated at fluxes below and above the threshold flux. In constant TMP filtration experiments, the fouling of the membranes was studied with equal driving forces at two different TMPs. In addition, a comparison with equal initial fluxes but different driving forces was performed to eliminate the effect of the difference in initial filtration flux.

5.2. Materials and methods

5.2.1. Materials

Mineral oil (330760, Sigma-Aldrich), sodium chloride (NaCl) (99%, Baker Analyzed), and sodium dodecyl sulphate (SDS) (> 99%, Sigma-Aldrich) were used for the preparation of O/W emulsions. Citric acid (99.9%, powder) and NaOH (0.1 M, Merck, Germany) were used for membrane cleaning. All chemicals and solvents were used as received without further purification. Demineralized water (produced by a reverse osmosis filter, a candle filter and a resin vessel), was used to prepare the aqueous solution and to rinse the filtration system and membrane samples.

■ Chapter 5

5.2.2. Ceramic membranes

Commercial single-channel tubular ceramic Al₂O₃ membranes with a pore size of 100 nm were provided by CoorsTek Industry (the Netherlands). The inner and outer diameter, and the length of the tubular membranes are 7 mm, 10 mm, and 150 mm respectively. SiC-deposited membranes were prepared by LPCVD, with Al₂O₃ tubes as support, at Else Kooi Lab, TU Delft. A thin layer of SiC was deposited on the Al₂O₃ tubes using two precursors (SiH₂Cl₂ and C₂H₂/H₂) at a temperature of 750 °C and pressure of 80 Pa. Three different deposition times (60, 90 and 120 min) were chosen to obtain the SiC-deposited membranes with varying permeance. More details on the preparation can be found in Chen et al. (2020b). The deposited SiC membranes are referred to as D60, D90, D120, corresponding to the deposition time of 60, 90 and 120 min. The pristine Al₂O₃ membranes are referred to as D0. The characteristics of the membranes are listed in Table 5.1.

Table 5.1 Characteristics of the Al₂O₃ and SiC-deposited membranes.

Membrane label	Deposition time (min)	Selective layer	Pore size ^a (nm)	Permeance (Lm ⁻² h ⁻¹ bar ⁻¹)
D0	0	α-Al ₂ O ₃	71	350±10
D60	60	SiC	60	250±15
D90	90	SiC	54	200±20
D120	120	SiC	47	150±10

a – the data are from Chen et al. (2022).

5.2.3. Membrane characterization

The surface charge of the membranes was characterized by the zeta potential using an electrokinetic analyser, SurPASS (Anton Paar, Graz, Austria). The instrument measures the streaming potential of the solid surface and then the corresponding zeta potential is automatically calculated using the Helmholtz–Smoluchowski equation (Nagasawa et al., 2020). Potassium chloride (KCl, 1 mM) was used as the electrolyte solution. The samples were measured at the same pH value as the O/W emulsion.

The water contact angles of the Al₂O₃ and SiC-deposited membranes were measured by a contact angle measurement machine (Dataphysics OCA20, Germany). The surface

■ Chapter 5

roughness of the membranes was measured by atomic force microscopy (AFM) (Dimension Icon, Bruker, USA).

5.2.4. Oil-in-water emulsion

O/W emulsions were prepared by mixing mineral oil, SDS and NaCl in demineralized water. To make sure that the feed characteristics were consistent for each experiment, a stock emulsion was prepared with the following steps. First, 0.053g NaCl was added in 0.9 L demineralized water and stirred for 10 min, afterwards, 0.9g SDS was added to the NaCl solution. When SDS was totally dissolved, 4.5 mL mineral oil was added and continuously stirred with a magnetic stirrer (L23, LABINCO, the Netherlands) at a speed of 1500 rpm for 24 h. To improve emulsification and homogenization, the O/W mixture was further treated with an energy-intensive sonifier (Branson 450) at an intensity of 40% for 30 min.

The stock emulsion was diluted 10 times in 1 mM NaCl solution to obtain a final oil concentration of 400 mg L⁻¹, SDS of 100 mg L⁻¹ and NaCl of 1 mM for filtration experiments. Each filtration run was finished on the same day to reduce the effect of oil droplet aggregates or coalescence. The pH and conductivity of the emulsions were 5.6 and 156 μs/cm, as measured by a multi-meter sensor (inoLab™ Multi 9420 - WTW). The emulsion has an oil droplet size distribution in a range 1-10 μm (Fig. S5.1) and zeta potential of -90 mV, which were analyzed with a particle size analyzer (Bluewave, Microtrac, USA) and a Malvern Zetasizer Nano ZS (Malvern Instruments Ltd., UK), respectively.

5.2.5. Fouling experiments with O/W emulsions

Constant flux crossflow fouling experiments

A constant permeate flux crossflow fouling apparatus was used for comparing the fouling of the membranes (Figure 5.2), which has been described in detail in Chen et al. (2020b). The effective filtration area of each membrane module was 0.003 m². The constant permeate flux was controlled by a diaphragm pump (DDA12-10, Grundfos, Denmark) at the feed side. A constant crossflow velocity of 0.44 m s⁻¹ was provided by a circulation pump (VerderGear, Verder B.V., the Netherlands) based on our previous study (Chen et al., 2020b). During the filtration, the concentrate valve was closed and the oil concentration in the closed loop (150 mL) gradually increased with filtration time (e.g., 120 mL permeate was produced in 30 min at a flux of 80 L m⁻² h⁻¹). Because

■ Chapter 5

the pressure at the permeate side was equal to atmospheric, the TMP was thus determined by the average of the inlet and outlet pressures on the two sides of the membrane module, which were monitored by two pressure transducers (GS4200-USB, ESI, UK). The pressures were continuously logged with a time interval of 30 s to the computer. During the filtration, the membrane was fouled and the membrane resistance increased, resulting in an increase in TMP.

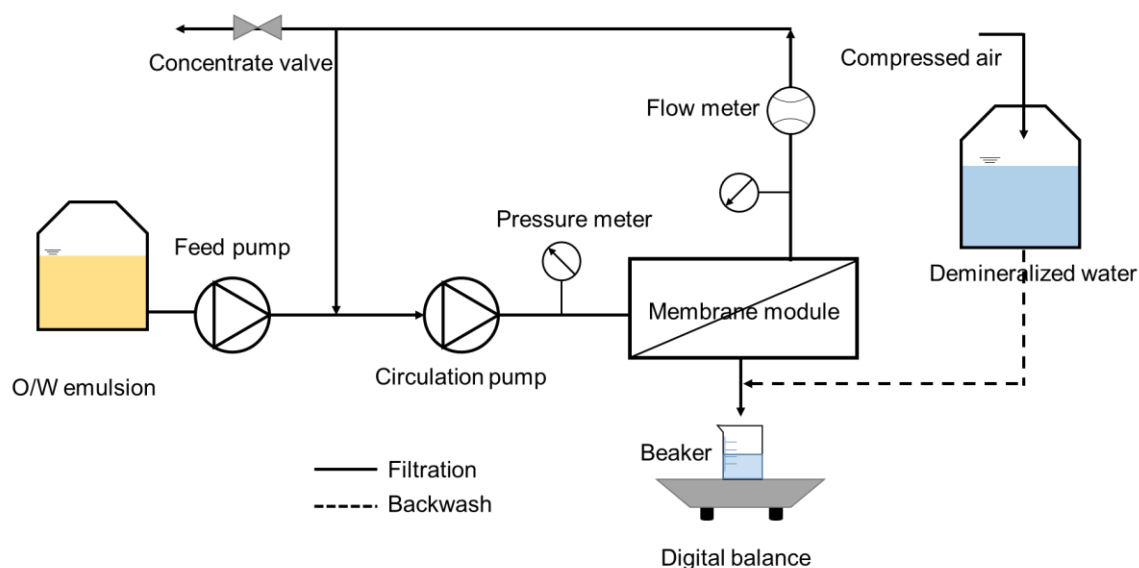


Figure 5.2. Constant flux crossflow filtration setup for O/W emulsion separation integrated with backwash (Chen et al., 2022).

The filtration experiments were conducted at room temperature (22 ± 3 °C). Before each filtration experiment, the system was thoroughly cleaned with demineralized water to remove residual chemicals and air. Afterwards, the membrane was loaded in the membrane module and the water permeance of the membrane was measured, at the same permeate fluxes as used for O/W filtration, with demineralized water. As fouling is closely related to the permeate flux, the threshold flux of all membranes was first determined by the flux stepping experiments as recommended in literature (Kasemset et al., 2016; Kirschner et al., 2017; Miller et al., 2014b). In this protocol, the membrane was initially operated at a low, constant flux ($40 \text{ L m}^{-2} \text{ h}^{-1}$) for 10 min, then the flux was increased with $10 \text{ L m}^{-2} \text{ h}^{-1}$ and the membrane was operated for another 10 min. In this manner, the flux was gradually increased from $40 \text{ L m}^{-2} \text{ h}^{-1}$ to a final flux of $110 \text{ L m}^{-2} \text{ h}^{-1}$, where a rapid fouling was observed. Between each flux step, the membrane was backwashed at 3 bar for 15 s to remove the possible accumulated fouling from the previous flux step. To check if backwash affects the fouling character, the membranes were respectively tested with a single cycle filtration at fluxes below

■ Chapter 5

and above the threshold flux and multiple cycle filtration with backwash, at three permeate fluxes (Table 5.2).

In single cycle filtration, the experiments were extended for a longer period compared with the multiple cycles filtration experiments to differentiate the fouling between membranes. For multiple cycle filtration, the fouling experiment for each membrane consisted of six cycles. Each filtration cycle was composed of three phases: 1) Filtration at a specified flux for a pre-set time (Table 5.2), 2) Backwashing the membrane module with demineralized water at a fixed pressure of 3 bar for 15 s to remove hydraulically reversible fouling, 3) Forward flush with feed emulsion for 15 s to remove the backwash remaining liquids and replace the solution in the loop with the fresh feed.

Table 5.2 Permeate flux and the corresponding filtration time per cycle for constant flux multiple cycles filtration experiments.

Flux ($\text{L m}^{-2} \text{h}^{-1}$)	80	90	100
Time (min)	30	20	18

Constant TMP crossflow fouling experiments

Constant TMP crossflow fouling experiments were performed with a setup shown in Figure 5.3. Unlike the constant flux experiment, only one pump (VerderGear, Verder B.V., the Netherlands) was used to pump the feed solution through the membrane module. The feed flow rate was monitored using a flow meter (Zhongjiangenergy-efficient electronics co., Ltd., China) and a same crossflow velocity (0.44 m s^{-1}) was used as in the constant flux experiment. Two pressure transducers from ESI (GS4200-USB, UK) were used to monitor the pressures on two sides of the membranes. The TMP and crossflow velocity of the system were adjusted by controlling the feed pump and a pressure control valve (FDV30KTZ, KNF) (downstream of the membrane module) simultaneously. In addition, a backwash vessel filled with demineralized water was installed at the permeate side. A fixed pressure of 3 bar was used to remove hydraulic reversible fouling of the membrane for 15 s.

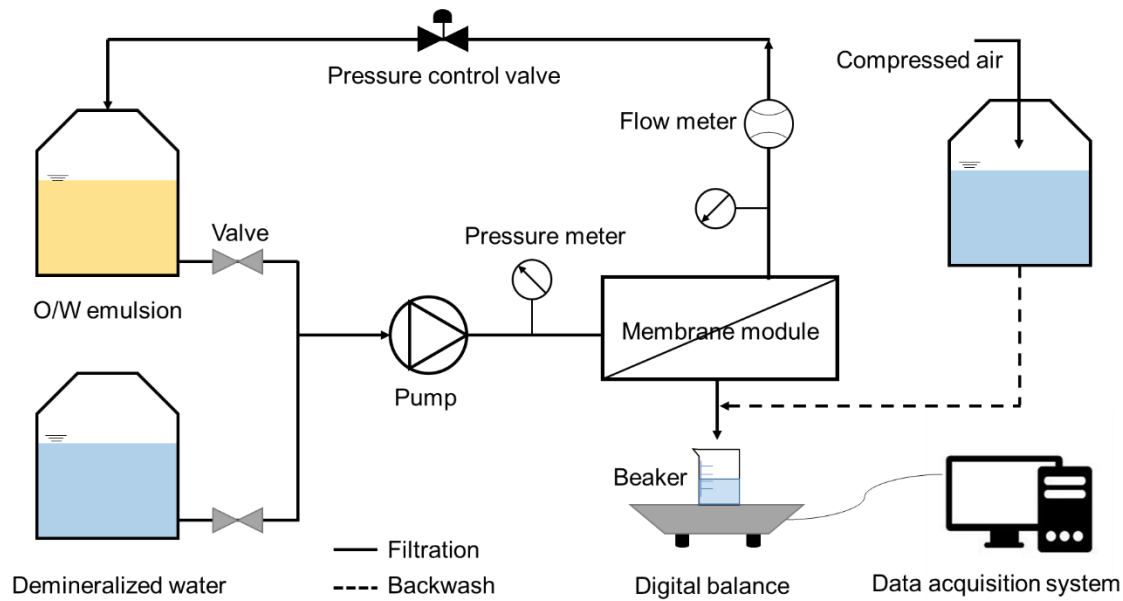


Figure 5.3. Constant TMP crossflow filtration setup for O/W emulsion separation integrated with backwash.

Permeate from the membrane module was collected in a beaker on a digital balance (FZ-3000iWP, A&D company). The change in mass was automatically recorded every 30 s to the computer and therefore the permeate flux of the membrane was calculated by the following Eq. (1):

$$J = \frac{\Delta M}{\rho A \Delta t} \quad (1)$$

Where J is the flux ($\text{Lm}^{-2}\text{h}^{-1}$), ΔM is the mass of permeate during a filtration period of Δt , ρ is the density of permeate and A is the effective filtration area of the membrane (0.003 m^2).

To begin a constant TMP fouling experiment, the membrane was first tested with demineralized water for 10 min to get a stable permeate flux at the setting pressures. Afterwards, the feed line was switched to the O/W emulsion to initialize the fouling experiment.

The fouling experiments in constant TMP mode were executed in two ways. First, all membranes were respectively compared at the same driving forces of 0.5 bar and 1 bar for three cycles. Each cycle lasted 20 min. In this case, the permeate flux was lower for the less permeable membranes. Afterwards, fouling experiments with different driving forces were adopted to obtain similar initial fluxes for all membranes (Table S5.1). These experiments consisted of six cycles with a duration of 20 min each.

■ Chapter 5

5.2.6. Membrane cleaning

The membranes were regenerated after each filtration run with the following method. First, the membranes were cleaned with a base solution by soaking them in a sodium hydroxide solution (0.01M NaOH) for 1 h at 65 °C, followed by three times rinsing with demineralized water. Afterwards, the membranes were soaked in a citric acid solution (0.01M) for another 1 h at 65 °C, as recommended in literature (Fraga et al., 2017a; Zsirai et al., 2018). If the performance of the membranes was not fully recovered after the chemical treatment, the membranes were heated at 200 °C for 2 h in a muffle furnace (Nabertherm Controller P 300, Germany). The membranes were not used until the permeance was recovered to the value of the clean membrane.

5.2.7. Data analysis

Normalized TMP, permeance and flux were employed to make the comparison between the different membranes possible, as variations in the initial pressure and flux existed among the membranes with varying permeance.

5.3. Results and discussion

5.3.1. Threshold flux determination

The results of the flux stepping experiments and the threshold fluxes of all membranes are shown in Fig. S5.2 and S5.3. The threshold fluxes of the membranes were determined with TMP_{avg} values as a function of permeate flux, which is considered as the most accurate method according to the study by Kirschner et al. (2017). The threshold flux of the pristine Al_2O_3 membrane was $94.7 \text{ L m}^{-2} \text{ h}^{-1}$. After a deposition of a SiC layer for 60 min, the threshold flux of D60 decreased to $86 \text{ L m}^{-2} \text{ h}^{-1}$. With a further increase in deposition time to 90 min, the threshold flux of D90 was improved to $95.7 \text{ L m}^{-2} \text{ h}^{-1}$. However, the threshold flux of the membrane (D120) decreased to $85 \text{ L m}^{-2} \text{ h}^{-1}$ when the deposition time was extended to 120 min. Therefore, D90 was considered to be the membrane with highest fouling resistance. In the studies by He et al. (2016), an apparent correlation was found between the threshold flux and foulant zeta potential. This confirms that an enhanced repulsive force between the modified membrane and foulant can increase threshold flux. However, on the other hand, the negative effects caused by surface modification, such as a decrease in membrane pore size and an increase in membrane hydraulic resistance, were considered to decrease threshold flux (Kasemset et al., 2016).

■ Chapter 5

For a short deposition time (60 min), the membrane (D60) was endowed with a slightly negatively charged and more hydrophilic surface (Table S5.1 and Fig. S5.4, supporting information). This may lead to the alleviation of membrane fouling. However, deposition also decreased the membrane pore sizes, resulting in a lower water permeance. Therefore, the membrane had to be operated at a higher pressure to maintain the same flux as the pristine membrane. The electrostatic repulsion in the D60 membrane was apparently not strong enough to compensate for the loss of water permeance, leading to a decrease in threshold flux. When the deposition time was increased to 90 min, a much higher negative charge was observed for D90 as compared with D60. Such a considerable increase in the zeta potential of the membrane would result in a much stronger electrostatic repulsion between the membrane surface and oil droplets. In this case, apparently, the effect of electrostatic repulsion outweighed the loss of water permeance of the membrane, leading to a slightly higher threshold flux than that of the Al₂O₃ membrane. Compared with D90, a further increase in the deposition time of the SiC layer had little effect on enhancing the zeta potential of the membrane (D120). However, the pore size reduction and increase in membrane selective layer thickness made the water permeance of the membrane even smaller, leading to a decrease in the threshold flux again. The decrease in threshold flux, due to extensive surface modification (e.g., higher concentrations of modifying agents or longer deposition time), was also observed in the previous studies (Kasemset et al., 2016; Kirschner et al., 2017). Kasemset et al. (2016) studied the effect of polydopamine (PDA) coating on the threshold flux of hydrophobic polysulfone UF membranes. PDA is a highly hydrophilic materials and it improves the membrane surface hydrophilicity even at low initial concentrations or short coating times. The increased surface hydrophilicity of the membrane made it more resistant to fouling by hydrophobic oil droplets under a given shear force. A higher threshold flux was thus observed. When using high initial PDA concentrations or longer coating times, the threshold flux of the modified membranes decreased due to a substantial loss of water permeance.

From the above results, it was thus concluded that the threshold fluxes of the pristine Al₂O₃ and SiC-deposited ceramic membranes were in the following order: D90 > D0 > D60 ≈ D120.

5.3.2. Fouling comparison at constant flux

Single cycle filtration

Constant flux crossflow single cycle filtration was performed on alumina membrane (D0) and SiC-deposited membranes (D60, D90 and D120) with an O/W emulsion feed to determine the difference in total fouling between membranes. Figure 5.4 presents the normalized TMP evolution as a function of filtration time at 60, 80, 90, and 100 L m⁻² h⁻¹. These fluxes are, respectively, either below or above the threshold flux of the membranes. As shown in Figure 5.4A, at 60 L m⁻² h⁻¹, the normalized TMP of all membranes increased linearly over 1h filtration time at a slow rate. Except for D120, the fouling curves of the other three membranes overlapped, indicating that the fouling rate was similar. Since 60 L m⁻² h⁻¹ is well below the threshold flux, fouling was sufficiently slow so that the samples maintained a relatively stable, long-term operation. Similar results were also reported when using polymeric membranes for filtration O/W emulsion at fluxes below the threshold flux (Kirschner et al., 2017; Miller et al., 2014b).

When the membranes were operated at 80 L m⁻² h⁻¹, a distinct difference was observed as compared with the condition at 60 L m⁻² h⁻¹. All membranes experienced a relatively constant slow increase in TMP in the first 20 min and then the TMP increased rapidly, indicating a substantial increase in fouling rate. Since 80 L m⁻² h⁻¹ was still below the threshold flux, a slow and constant increase of TMP was to be expected (He et al., 2016). However, because the membranes were operated in a closed loop crossflow filtration system, the oil concentration increased with filtration time, probably accelerating the fouling of the membranes (Yang et al., 2019). In addition, it can be expected that pore blockage was the main fouling mechanism during the initial slow, linear TMP increase stage (Ho and Zydney, 2002). To maintain the constant flux over the entire filtration area, the flux through the open pores increased, leading to fouling acceleration (Ognier et al., 2004), in this case, after 20 min.

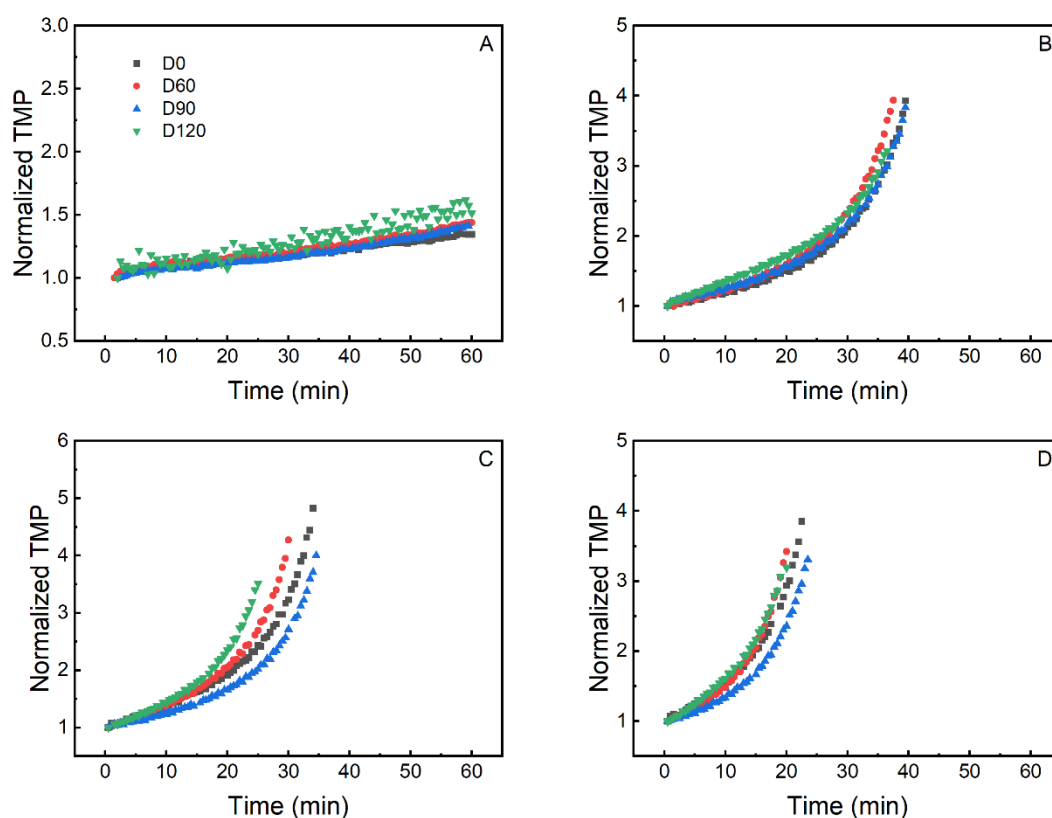


Figure 5.4. Normalized TMP during constant flux fouling of Al_2O_3 and SiC-deposited ceramic membranes with O/W emulsion in single cycle filtration experiments. (A) 60, (B), 80, (C) 90, and (D) $100 \text{ L m}^{-2} \text{ h}^{-1}$.

At $90 \text{ L m}^{-2} \text{ h}^{-1}$, the rapid increase in (normalized) TMP happened earlier for all membranes, as expected (Zhu et al., 2017). In addition, from Figure 5.4C it can be observed that the TMP increase was higher for D60 and D120, since $90 \text{ L m}^{-2} \text{ h}^{-1}$ was above their threshold flux. The lower TMP increase of D90 was attributed to its high threshold flux. At $100 \text{ L m}^{-2} \text{ h}^{-1}$, a similar TMP increase order was observed except that the extent of TMP increase of D60 was close to that of D120. Overall, the order of the extent of the TMP increase of the membranes during single cycle filtration of an O/W emulsion was consistent with their threshold flux values.

Multiple cycles filtration

In Figure 5.5A, the normalized permeance of all membranes at a flux of $80 \text{ L m}^{-2} \text{ h}^{-1}$ was compared. However, it was difficult to discern the difference in the fouling of each membrane due to the overlap of fouling curves. Therefore, the permeance recovery of all membranes after each backwash for emulsion filtration at three different fluxes

■ Chapter 5

was illustrated in Figure 5.5B, C and D. The permeance recovery of all membranes declined as the number of backwash cycle increased, suggesting that the hydraulically irreversible fouling gradually increased. In addition, a higher decrease of permeance recovery after each backwash was observed for all membranes when permeate flux increased. This indicates that the permeate flux not only affected the permeance decline during the filtration cycle, but also had an influence on the backwash efficacy of the membranes.

At $80 \text{ L m}^{-2} \text{ h}^{-1}$ (Figure 5.5B), the permeance recovery of D120 after the first backwash was a little smaller than of the other membranes. However, with more backwash cycles, the permeance recovery of D120 considerably decreased, only reaching 85% after the 5th backwash, while the other three membranes had a high permeance recovery of 95%. During the single cycle filtration experiment, we observed that the fouling of all membranes was similar at the flux of $80 \text{ L m}^{-2} \text{ h}^{-1}$. Therefore, the permeance recovery could be related to the backwash efficacy. Due to the properties of SiC, it was expected that polar interactions between the membrane and oil droplets would be lower. As a result, the attachment of oil droplets to the modified membrane surfaces was less compared to the original alumina membrane. However, although D120 had the most negatively charged surface, the permeance recovery after backwash was poor, compared with other membranes. The D120 membrane exhibits the lowest permeance compared to other membranes, requiring a higher transmembrane pressure (TMP) to achieve an equivalent flux. This elevated TMP can potentially overcome the electrostatic repulsive forces, resulting in increased deformation of droplets on the membrane surface. Additionally, since backwash was conducted at a constant pressure (3 bar), it was probably less effective for less permeable D120 membrane. Then, the remaining foulants could accelerate membrane fouling due to reduced repulsion between the fouled membrane and foulants (Hube et al., 2021).

Therefore, in a multicycle filtration experiment, using the same backwash flux for all membranes can facilitate the comparison of their cleaning efficacy. This is because the backwash flux is the driving force that removes the cake layer from the membranes. However, the permeability of the membranes will affect the cleaning efficacy. By increasing the backwash pressure from D0 to D120, the backwash cleaning will be more effective for the deposited membranes, particularly D120, when the same backwash flux is used.

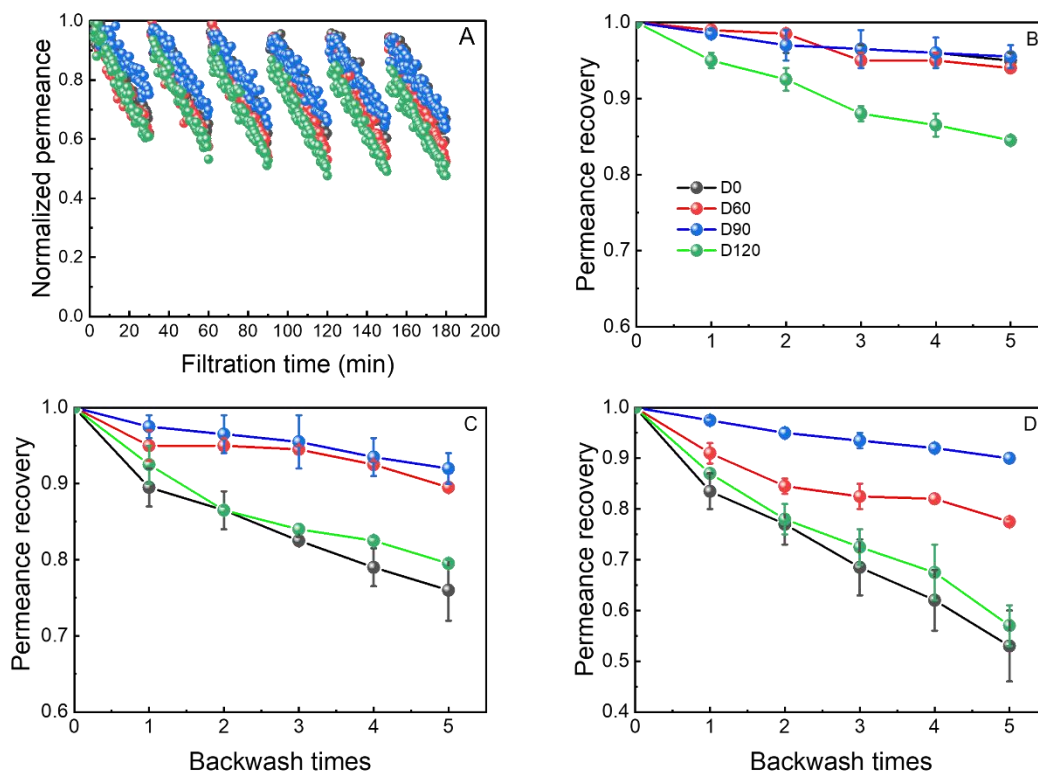


Figure 5.5. Normalized permeance of all membranes after each backwash at a flux of $80 \text{ L m}^{-2} \text{ h}^{-1}$ (A). Permeance recovery after each backwash during constant flux fouling of Al_2O_3 and SiC-deposited ceramic membranes with O/W emulsion at various fluxes. (B) $80 \text{ L m}^{-2} \text{ h}^{-1}$, (C) $90 \text{ L m}^{-2} \text{ h}^{-1}$, and (D) $100 \text{ L m}^{-2} \text{ h}^{-1}$.

As shown in Figure 5.5C, at $90 \text{ L m}^{-2} \text{ h}^{-1}$, the higher permeate flux possibly caused a stronger drag force acting on the oil droplets, which consequently led to more irreversible fouling (Chen et al., 2022). As a result, the permeance recovery of the pristine Al_2O_3 membrane (D0) was the lowest after each backwash due to the lack of electrostatic repulsion between the membrane and oil droplets. In addition, although D60 had a higher permeance than that of D90, its negative surface charge was much lower than that of D90. Therefore, the adsorption of negatively charged oil droplets on D90 was expected to be weaker than that of D60, leading to a higher permeance recovery during backwash (Chang et al., 2017; Chang et al., 2015). Compared with D120, D90 had a higher permeance and a similar negative surface charge. As a result, the permeance recovery of D90 was higher. The higher backwash efficacy of D60 compared to D120 indicates that the effect of permeance outcompeted the influence of enhanced surface charge. According to the study by Vroman et al. (2020), a critical backwash flux exists to reach a high backwash efficacy during ultrafiltration of a bentonite suspension. Above the critical backwash flux, the backwash became

effective. The low backwash efficacy of D120 was probably due to the backwash flux being below the critical backwash flux. For D0, the increase of permeate flux led to a higher drag force pressing the oil droplet toward the membrane and finally resulting in the adherence to the membrane. In addition, oil deformation increased with permeate flux, making it more difficult to be removed by backwash (Fux and Ramon, 2017).

At $100 \text{ L m}^{-2} \text{ h}^{-1}$, the same backwash efficacies were observed as at $90 \text{ L m}^{-2} \text{ h}^{-1}$. The permeance recovery of D90 was much higher than that of the other membranes, indicating that D90 was best resistant against fouling.

Overall, the fouling of the membranes was affected by several factors, i.e., permeate flux and membrane properties, especially when backwash was involved. Without backwash (single cycle filtration), fouling of the membrane was mainly determined by the interactions between the membrane surface and the foulants. With backwash, however, considerable improvement on fouling control was obtained for the mildly modified membranes (D60 and D90). Similar results were reported by Ma et al. (2000; 2001), who found that for filtration of carboxylate modified latex by membranes, fouling was not strongly dependent on the membrane surface chemistry without backpulsing. However, when backflushing was applied, the permeate volume was respectively increased by 10% and decreased by 20% when the modified membrane and particles had like and opposite charges, compared with the unmodified one.

5.3.3. Fouling comparison at constant TMP

Same driving force

The SiC-deposited membranes and Al_2O_3 membrane were compared at two different TMPs (0.5 and 1 bar) for O/W emulsion filtration, as shown in Figure 5.6. At 0.5 bar, a flux decline was observed for D0 and D60 (Figure 5.6A). In comparison, the fluxes of D90 and D120 did not change with the filtration time, indicating that no fouling happened in these membranes. When a constant TMP was applied on membranes, D0 had the highest initial flux, up to $150 \text{ L m}^{-2} \text{ h}^{-1}$. This flux was much higher than the threshold flux of D0, and probably therefore (ir)reversible fouling was observed. The initial flux of D60 was around $100 \text{ L m}^{-2} \text{ h}^{-1}$, which was also higher than the threshold flux of D60. However, unlike the flux of D0, the flux of D60 was almost recovered after backwash, indicating they were mainly hydraulically reversible fouling. The initial fluxes of D90 and D120 were around 70 and $60 \text{ L m}^{-2} \text{ h}^{-1}$, which were well below the

Chapter 5

threshold fluxes of the membranes. As a result, the fouling hardly built up on the membrane surface.

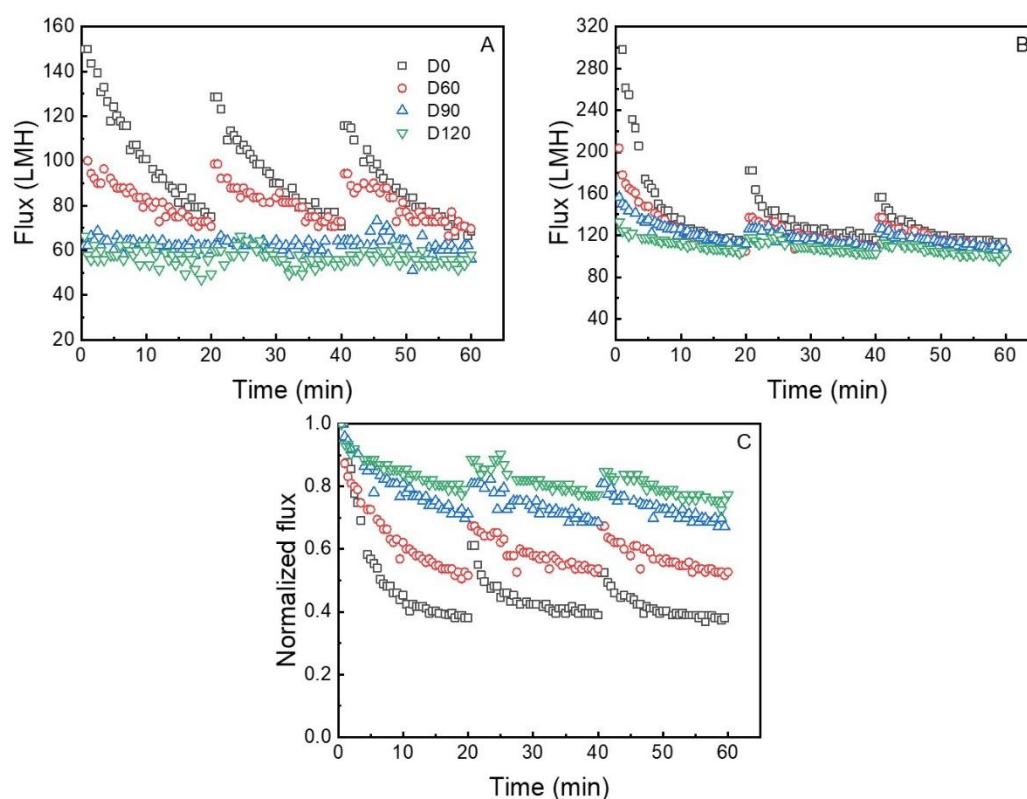


Figure 5.6. Time-dependent variations of permeate flux of Al_2O_3 and SiC-deposited ceramic membranes for O/W emulsion filtration with three cycles. (A) 0.5 bar, (B) 1 bar, (C) normalized flux at 1 bar.

At 1 bar, flux declines of all membranes were observed. The initial fluxes of all membranes were higher than the threshold fluxes of the membranes, as depicted in Figure 5.6B. Due to its higher initial flux, the flux decline of D0 was much higher than the decline of the other three membranes. As the fouling curves of the SiC-deposited ceramic membranes overlapped (Figure 5.6B), the normalized flux was presented in Figure 5.6C, to better illustrate the fouling and flux recovery of the membranes. From Figure 5.6C it can be observed that D120 had the smallest flux decline and the highest flux recovery, followed by D90, D60 and D0. A higher initial flux was likely to lead to a higher drag force acting on oil droplets, making them more firmly attached to the membrane surface (Zhu et al., 2017). In addition, oil deformation is also easier at a higher flux, possibly leading to oil penetration into membrane pores and irreversible fouling (Fux and Ramon, 2017). However, it should be noted that the permeate production was also less for membranes with a lower permeance, when the same

constant TMPs were applied. Therefore, less fouling was observed for the less permeable membranes (Blankert et al., 2021). Comparison at the constant TMPs with a similar initial flux is thus needed to have a better assessment of the membrane fouling.

Equal initial fluxes at constant TMP

Figure 5.7 illustrates the permeance recovery of membranes after each backwash based on equal initial fluxes (Table S5.2) at constant TMP. It appeared that D0 had the highest flux recovery among the membranes, followed by D60, D90 and D120. One possible explanation for this phenomenon was that the initial flux was much higher than the threshold flux for all membranes, leading to similar fouling accumulation in the filtration process. The membrane which had a higher permeance thus got a higher cleaning efficacy due to higher backwash flux. This indicates that the pristine membrane is best against fouling. Apparently, this conclusion leads to an impression that modification is not useful for fouling alleviation, which is contradictory to the fact.

When membranes were compared at similar initial fluxes, higher TMPs were required for the less permeable membranes. Unlike rigid particles, oil droplets are deformable. Oil deformation is expected to be higher at higher pressures (Darvishzadeh and Priezjev, 2012). The deformation of oil droplets on the membrane surface would possibly make them more firmly attached and difficult to remove during backwash. In addition, the backwash efficacy can be lower for the less permeable membranes due to lower backwash flux because a constant backwash pressure was applied during the experiments.

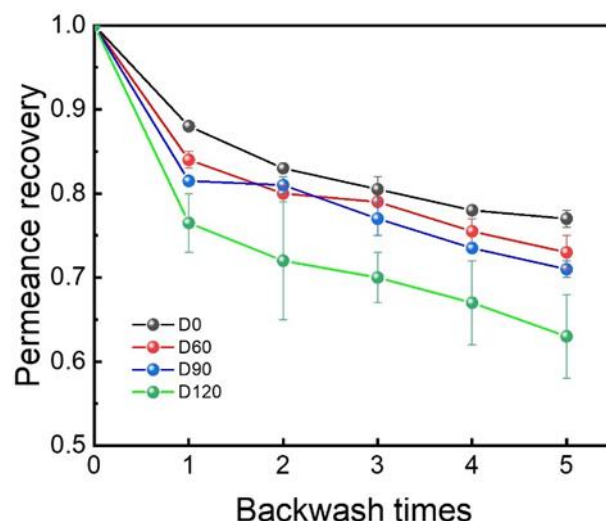


Figure 5.7. Permeance recovery during constant pressure O/W emulsion filtration with Al_2O_3 and SiC-deposited ceramic membranes at similar initial fluxes.

5.3.4. Implications for membrane modification

Membrane modification has been widely used to improve membrane rejection and/or to develop fouling resistant membranes for water treatment, especially for O/W emulsions. In some cases, the trade-off between the membrane selectivity and permeability may be overcome by coating a highly hydrophilic thin layer on the membrane support (Mahmodi et al., 2022; Wang et al., 2013). Still, the decrease in pure water permeance of the modified membrane is a common phenomenon (Chen et al., 2020b; Miller et al., 2014b). To evaluate the fouling resistance, a constant TMP filtration system is generally applied at a laboratory scale. However, the results found in this work suggest that the effect of permeance of the membranes seems to be dominant. The backwash efficacy was only related to the permeance of membranes, while an effect of surface properties was not observed. The improved fouling resistance of the membrane after modification could be attributed to the huge loss in permeance, thereby resulting in a much lower initial flux and fouling when operated at the same driving force as the pristine membrane. However, in constant flux filtration experiments, we found that the loss of water permeance of the membranes after modification may lead to negative effects on fouling resistance even though the surface property of membranes became less prone to the target pollutants. Apparently, these two filtration modes give different conclusions on the performance of the modified ceramic membranes for the O/W emulsions filtration. In constant TMP experiments, the best modified membranes are those with the least permeance, which

are not necessarily the optimal choices in practice. On the contrary, the constant flux experiments clearly reveal the competing effect between the permeance and improved fouling resistance, which also serves as the best simulation for practical filtering of O/W emulsions. In addition, due to the high initial flux of the clean membrane, severe fouling often occurs at the start of the constant TMP experiment. This could be prevented by imposing a lower flux in constant flux filtration (Miller et al., 2014a). Therefore, constant flux filtration experiments with backwash are recommended to be applied to evaluate the performance of the membranes with and without modification for O/W filtration as well as other types of wastewater treatment. As the height of permeate flux can also affect the order of fouling tendency, experiments tested at several permeate fluxes would be preferred.

5.4. Conclusion

The performance of alumina and SiC-deposited ceramic membranes was respectively compared at constant flux and constant TMP filtration modes with O/W emulsions in order to evaluate its practical applicability. The filtration conditions (filtration modes, permeate flux and TMP), membrane properties and the backwash affected the fouling of the membranes. The following conclusions were drawn:

- During single cycle constant flux filtration experiments, it was difficult to make a distinction between the fouling of the membranes when the permeate flux was low (60 and $80 \text{ L m}^{-2} \text{ h}^{-1}$). At higher permeate flux (90 and $100 \text{ L m}^{-2} \text{ h}^{-1}$), the fouling of one of the modified membranes (D90) was lowest, followed by the pristine membrane and the other two modified membranes.
- When backwash was involved in constant flux filtration mode, except for D120, hardly any difference in irreversible fouling was observed at a low flux ($80 \text{ L m}^{-2} \text{ h}^{-1}$). At higher fluxes (90 and $100 \text{ L m}^{-2} \text{ h}^{-1}$), two of the three modified membranes (D90 and D60 respectively) performed better, in terms of irreversible fouling, than the pristine membrane, indicating the importance of incorporating backwash (same flux) in a fouling experiment for good evaluation.
- During the constant TMP filtration experiments, membrane fouling was observed to be only related to the membrane permeance, while an effect of surface properties was not observed.

■ Chapter 5

- Since it also the case in operation of a full scale MF/UF plant, experiments with constant flux filtration with backwash were considered to be the most suitable for irreversible membrane fouling comparison, as compared with constant TMP filtration or experiments without backwash, leading to erratic conclusions.

Acknowledgements

Mingliang Chen acknowledges the China Scholarship Council for his PhD scholarship under the State Scholarship Fund (No. 201704910894). We thank WaterLab at TU Delft for providing the help on the measurement of samples. Bob Siemerink, and Iske Achterhuis from Twente University are acknowledged for the support concerning the zeta potential measurements.

Supplementary information

S5.1. Oil droplet size distribution

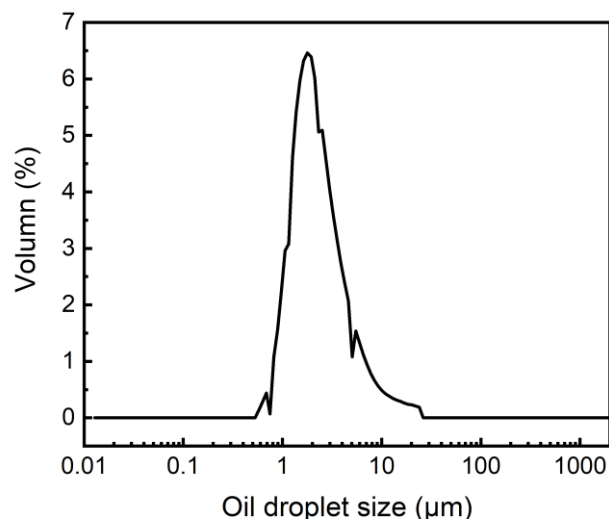


Figure S5.1. Oil droplet size distribution of O/W emulsion. The majority of oil droplets are distributed within the size range of 1-10 μm .

S5.2. Threshold flux

The results of flux stepping experiments of all membranes are shown in Fig. S5.2. At a relatively low flux (40 and 50 $\text{Lm}^{-2}\text{h}^{-1}$), the TMP profiles were almost constant, suggesting the fouling resistance was not increasing with time. With the increase of permeate flux, the TMP slowly increased with time over 10 min constant flux interval. An abrupt increase of TMP with time was observed when the flux was increased up to 90 $\text{Lm}^{-2}\text{h}^{-1}$, indicating an increase in the fouling rate. To determine the threshold flux ($J_{\text{threshold}}$), TMP_{avg} values as a function of permeate flux were plotted, as presented in Fig. S5.3. This method was considered to be the most accurate one according to the study by Kirschner et al. (2017). TMP_{avg} was calculated based on the arithmetic mean of the TMP values recorded during each flux step. From this plot, a linear regression line through the data points below the threshold flux was drawn by requiring a regression coefficient $R^2 \geq 0.99$. Then the other linear regression line was established by drawing the next two or three points after the threshold flux. The flux at the intersection of the two lines was identified as the threshold flux.

The estimated threshold flux of the membranes was given in Fig. S5.3. The threshold flux of the pristine Al_2O_3 membrane was 94.7 $\text{Lm}^{-2}\text{h}^{-1}$. After a deposition of SiC layer for 60 min, the threshold flux of D60 decreased to 86 $\text{Lm}^{-2}\text{h}^{-1}$. With further increase of

Chapter 5

the deposition time to 90 min, the threshold flux of D90 was improved to $95.7 \text{ L m}^{-2} \text{ h}^{-1}$, which is slightly higher than that of the pristine Al_2O_3 membrane. However, the threshold flux of the membrane (D120) decreased to $85 \text{ L m}^{-2} \text{ h}^{-1}$ when the deposition time was extended to 120 min. Therefore, D90 was considered to be the membrane with highest fouling resistance.

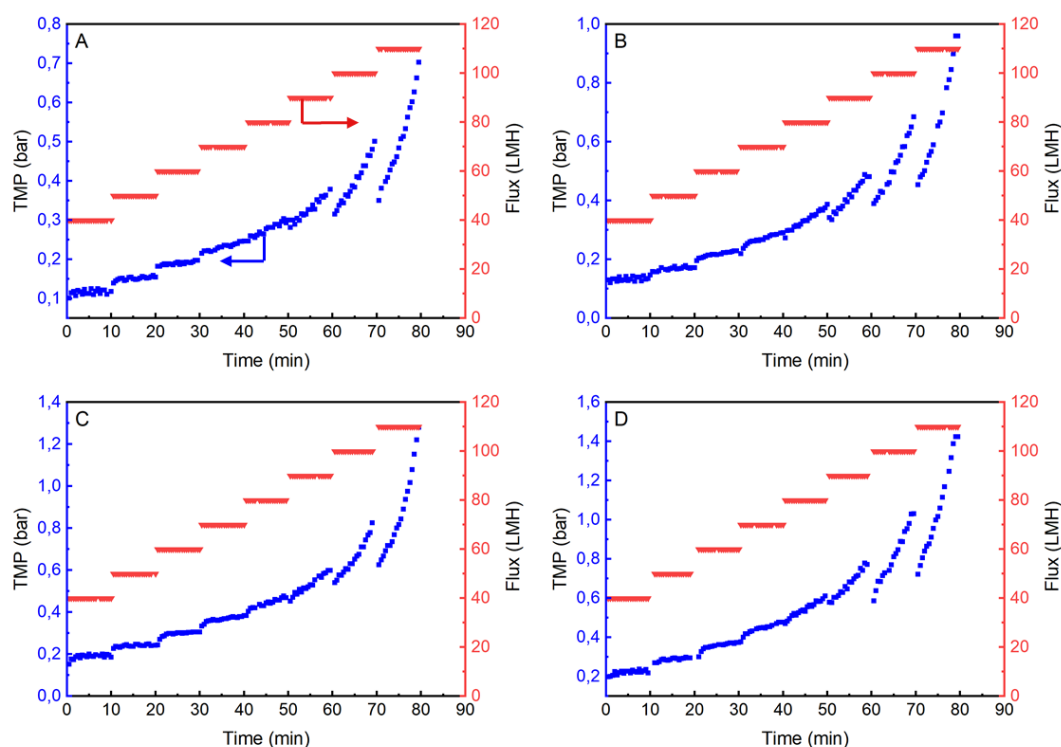


Figure S5.2. Flux stepping experiment with Al_2O_3 and SiC-deposited ceramic membranes. (A) D0, (B) D60, (C) D90, and (D) D120. The flux was gradually increased from 40 to $110 \text{ L m}^{-2} \text{ h}^{-1}$ with an interval of $10 \text{ L m}^{-2} \text{ h}^{-1}$. The filtration time under each flux was 10 min. TMP was recorded during each flux. O/W emulsion was used as the foulant and the crossflow velocity was 0.44 m/s . Between each flux, the membranes were backwashed at 3 bar for 15s to reduce the effect of fouling accumulation from previous flux step.

Chapter 5

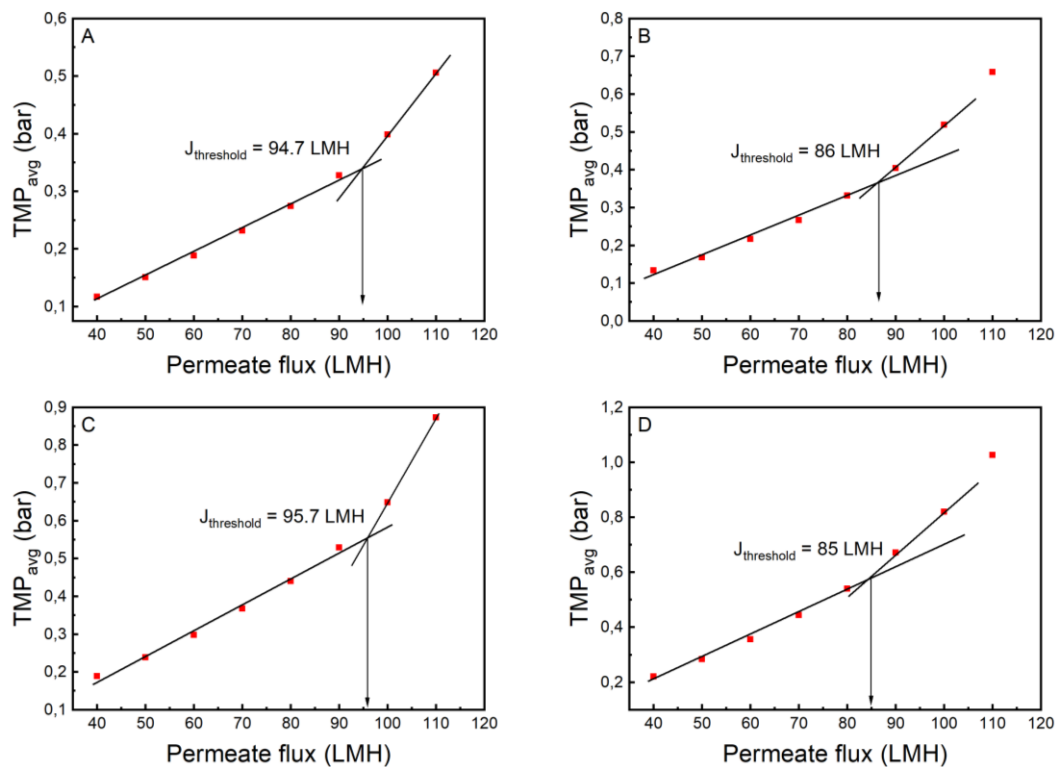


Figure S5.3. Threshold flux determination from flux stepping experiment shown in Fig. 2. (A) D0, (B) D60, (C) D90, and (D) D120. TMP_{avg} was calculated as the arithmetic mean of all TMPs recorded during each flux step. Based upon the slope of the $TMP_{avg}/flux$ relationship, the data were separated into two regions. The intersection of two regression lines was identified as the threshold flux ($J_{threshold}$).

Table S5.1. Same initial flux and corresponding TMP of the membranes in constant TMP experiments.

Membranes	D0	D60	D90	D120
Initial flux (LMH)	175	167	169	167
TMP (bar)	0.49	0.63	0.74	1.1

S5.3. Surface roughness

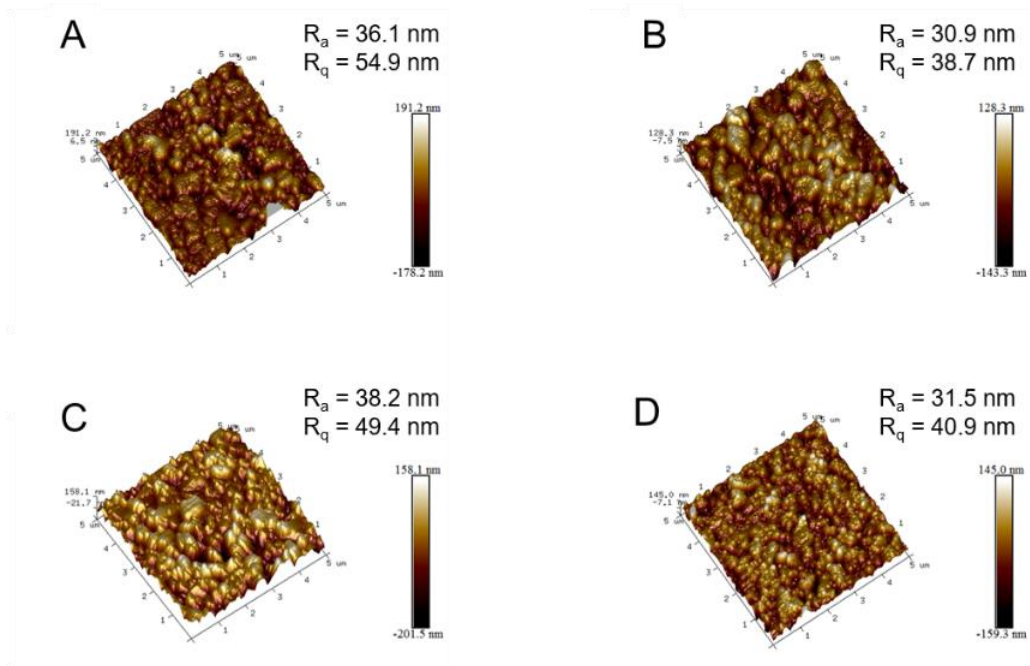


Figure S5.4. AFM micrographs and surface roughness of the alumina membrane and SiC-deposited ceramic membranes, (A) D0, (B) D60, (C) D90, and (D) D120.

■ Chapter 5

S5.4. Water contact angle

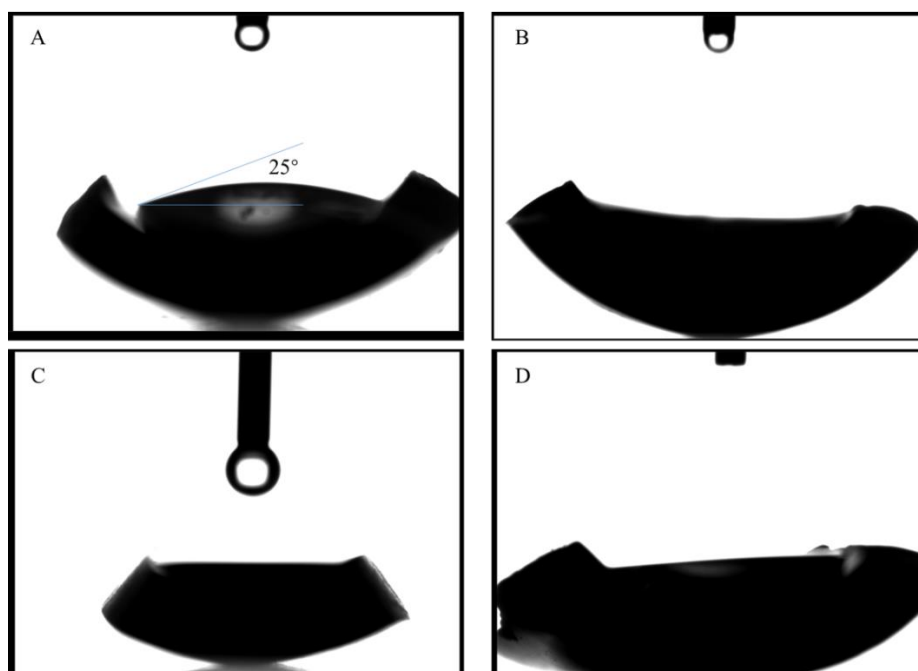


Figure S 5.5. Water contact angle of the alumina membrane and SiC-deposited ceramic membranes, (A) D0, (B) D60, (C) D90, and (D) D120.

S5.5. Zeta potential

Table S5.2. Zeta potential of membranes measured at pH around 5.6

Membranes	D0	D60	D90	D120
Zeta potential (mV)	2.252	-20	-36.47	-38.35

Chapter 6 |

Oil-in-water emulsion separation: Fouling of alumina membranes with and without a silicon carbide deposition in constant flux filtration mode

This chapter is based on:

Chen, M., Heijman, S. G., Luiten-Olieman, M. W., & Rietveld, L. C. (2022). Oil-in-water emulsion separation: Fouling of alumina membranes with and without a silicon carbide deposition in constant flux filtration mode. Water Research, 216, 118267.

Abstract

In this study, the effects of emulsion chemistry (surfactant concentration, pH, salinity and Ca^{2+}) and operation parameters (permeate flux and filtration time) were comparatively evaluated for alumina and silicon carbide (SiC) deposited ceramic membranes, with different physicochemical surface properties. The original membranes were made of 100% alumina, while the same membranes were also deposited with a SiC layer to change the surface charge and hydrophilicity. The SiC-deposited membrane showed a lower reversible and irreversible fouling when permeate flux was below $110 \text{ Lm}^{-2}\text{h}^{-1}$. In addition, it exhibited a higher permeance recovery after physical and chemical cleaning, as compared to the alumina membranes. Increasing sodium dodecyl sulphate (SDS) concentration in the feed decreased the fouling of both membranes, but to a higher extent in the alumina membranes. The fouling of both membranes could be reduced with increasing the pH of the emulsion due to the enhanced electrostatic repulsion between oil droplets and membrane surface. Because of the screening of surface charge in a high salinity solution (100 mM NaCl), only a small difference in irreversible fouling was observed for alumina and SiC-deposited membranes under these conditions. The presence of Ca^{2+} in the emulsion led to high irreversible fouling of both membranes, because of the compression of diffusion double layer and the interactions between Ca^{2+} and SDS. The low fouling tendency and/or high cleaning efficacy of the SiC-deposited membranes indicated their potential for oily wastewater treatment.

6.1. Introduction

Oily wastewater is becoming one of the major environmental concerns due to the large generated volumes, negative impacts on the aquatic environment, and potential threats to human health (Lin and Rutledge, 2018; Lin et al., 2019). Especially, emulsified oils in oil-in-water (O/W) emulsions are difficult to remove from a solution due to their small size ($< 20 \mu\text{m}$), and the high stability caused by the used surfactants, which considerably increase repulsive charge between oil droplets with a high zeta potential (Lu et al., 2016a; Zhu et al., 2016).

Microfiltration (MF) and ultrafiltration (UF) have been widely studied to handle O/W emulsions, because of their distinct advantages over conventional methods, such as high flux, steady and good permeate quality, compact design, and small footprint (Chen et al., 2016a; Ebrahimi et al., 2010; Hua et al., 2007). Ceramic membranes are gaining increasing attention for O/W emulsion separation as they have a narrow pore size distribution, a higher porosity, and higher hydrophilicity than polymeric membranes (Dong et al., 2019; Wang et al., 2022b; Wu et al., 2022; Zhang et al., 2019). Therefore, better (reversible and irreversible) fouling control in water treatment has been observed than when polymeric membranes are used (Hofs et al., 2011; Nagasawa et al., 2020). Furthermore, ceramic membranes can potentially be cleaned with harsh chemicals and backwashed at high pressures, due to the high thermal, mechanical and chemical stability, for enhanced performance recovery, which can guarantee a longer service life (Eray et al., 2021; Nagasawa et al., 2020; Shi et al., 2022).

Still, fouling of the ceramic membranes is one of the major operational problems, as it increases the operational costs of the ceramic membranes during the filtration of O/W emulsions. It is generally acknowledged that membrane fouling is influenced by membrane properties, emulsion characteristics, and operational conditions (Lehman and Liu, 2009; Nagasawa et al., 2020). A hydrophilic membrane surface is supposed to be more permeable to water over hydrophobic oil droplets, thereby decreasing membrane fouling (Dickhout et al., 2017). In O/W emulsions, oil droplets are usually charged, positively or negatively, depending on the type and characteristic of the stabilizing surfactants. Therefore, electrostatic interactions between oil droplets and a charged membrane surface are assumed to play an important role in membrane fouling too. However, contrasting results regarding the role of electrostatic interaction have been reported. For example, in UF of O/W emulsions, stabilized by various types of surfactants, Matos et al. (2016) found that the negatively charged

ZrO₂/TiO₂ ceramic membrane had a higher flux during filtration of an emulsion stabilized with an anionic surfactant. It was concluded that the electrostatic repulsion prevents the formation of a cake layer on the membrane surface and thus reduces the fouling. However, a lower flux was observed when filtering an emulsion stabilized with a cationic surfactant. A similar phenomenon was reported by Zhang et al. (2009), who found that a higher and more stable permeate flux was achieved for MF of an emulsion stabilized with sodium dodecyl sulphate (SDS, anionic), using a negatively charged TiO₂ doped Al₂O₃ membrane. In contrast, Lu et al. (2015b) found that the TiO₂/ZrO₂ ceramic membranes had less irreversible fouling and a higher rejection of dissolved organics when challenged with O/W emulsions stabilized with an oppositely charged surfactant to the membrane. A synergetic steric effect and a demulsification effect were considered as the main reasons for the lower fouling due to the prevention of pore blockage.

Hence, there is no consensus in the currently available literature on whether electrostatic repulsion or electrostatic attraction plays a role in ceramic membrane fouling alleviation. The contradicting results on the effect of electrostatic interaction on membrane fouling may be explained by the differences in the feed characteristics, such as oil droplets size, surfactant concentration, and salinity. In addition, these studies were conducted at a constant pressure filtration mode, where a decline of permeate flux over time was observed. As a result, the observed fouling behaviour is not only caused by the interaction between oil droplets and membrane surface but also due to the changing hydrodynamic environment and solute concentration near the membrane (Miller et al., 2014b). In practice, constant flux MF/UF filtration is preferred since the rate of permeate flow through the membrane's pores is more constant than in fixed TMP studies. The maintained constant hydrodynamic environment near the membrane surface favours the comparison of membrane fouling (Miller et al., 2014a; Miller et al., 2014b).

Therefore, this study is dedicated to a better understanding of the effect of surface charge of ceramic membranes on membrane fouling in constant flux filtration mode of an O/W emulsion stabilized with an anionic surfactant. Backwashing and multiple filtration cycles were performed in order to distinguish between hydraulic reversible and hydraulic irreversible fouling. SDS, a commonly used anionic surfactant, was employed to prepare negatively charged oil droplets. Al₂O₃ ceramic membrane and SiC-deposited ceramic membranes were selected, since both Al₂O₃ and SiC have a hydrophilic surface, but the iso-electric point (IEP) of these two materials is different.

Al₂O₃ usually has a relatively high IEP (8-9), while a low IEP (2-3) has been found for SiC (Xu et al., 2020). Therefore, the surface charge of the two membranes would be opposite in a neutral environment, potentially leading to different fouling mechanisms. In addition, other factors like permeate flux, SDS concentration, pH, salinity, and Ca²⁺ concentration were investigated.

6.2. Materials and methods

6.2.1. Materials

Mineral oil (330760, Sigma-Aldrich), sodium chloride (NaCl) (99%, Baker Analyzed), calcium chloride dehydrate (CaCl₂·2H₂O) (99%, Merck KGaA, Germany) and SDS (> 99%, Sigma-Aldrich) were used for the preparation of the O/W emulsion. HCl (≥ 37%, Honeywell, Fluka™) and NaOH (0.1 M, Merck, Germany) were used for pH adjustment and membrane cleaning. Citric acid (99.9%, powder) was ordered from VWR International. All chemicals and solvents were used as received without further purification. Demineralized water (conductivity < 0.1 μs cm⁻¹), produced at WaterLab, TU Delft (water filtered by a reverse osmosis filter, a candle filter and a resin vessel), was used to prepare the aqueous solution and to rinse the filtration system and membrane samples.

6.2.2. Ceramic membranes

Commercial single-channel tubular ceramic Al₂O₃ membranes with a pore size of 100 nm were provided by CoorsTek Industry (the Netherlands) and commercial flat Al₂O₃ membranes were purchased from Inopor (Germany). The tubular membranes consist of a selective layer and a support layer both with α-Al₂O₃, having an inner diameter of 7 mm, an outer diameter of 10 mm and a length of 150 mm. The flat membranes have a pore size of 100 nm with a diameter of 100 mm and a thickness of 3 mm. The SiC-deposited membranes were prepared by low-pressure chemical vapor deposition (LPCVD), with Al₂O₃ tubes as support, at Else Kooi Lab, TU Delft. The Al₂O₃ tubes were deposited with a thin layer of amorphous SiC using two precursors (SiH₂Cl₂ and C₂H₂/H₂) at a temperature of 750 °C and pressure of 80 Pa (Morana et al., 2013). Three different deposition times (60, 90 and 120 min) were chosen to obtain SiC-deposited membranes with various pore sizes. More details on the preparation can be found in Chen et al. (2020b). The deposited SiC membranes are referred to as D60, D90, D120, corresponding to the deposition time of 60, 90 and 120 min, respectively. The pristine

■ Chapter 6

Al₂O₃ membranes are referred to as D0. The characteristics of the membranes are listed in Table 6.1. The flat disc membrane samples were deposited at the same conditions as used for the tubular ones for zeta potential measurements.

Table 6.1 Characteristics of the Al₂O₃ and SiC-deposited membranes.

Membrane label	Deposition time (min)	Selective layer	Pore size (nm)	Permeance (L m ⁻² h ⁻¹ bar ⁻¹)
D0	0	α-Al ₂ O ₃	71 ^a	350±10
D60	60	SiC	60	270±15
D90	90	SiC	54	220±20
D120	120	SiC	47	177±10

a – the pore size measured with porometry is a little smaller than that (100 nm) provided by supplier.

6.2.3. Membrane characterization

The surface charge of the membranes was characterized by the zeta potential with an electrokinetic analyser, SurPASS (Anton Paar, Graz, Austria). The instrument measures the streaming potential of the solid's surface and then the corresponding zeta potential is automatically calculated using the Helmholtz–Smoluchowski equation (Nagasawa et al., 2020). Potassium chloride (KCl, 5 mM) was used as the electrolyte solution, while the pH was adjusted by HCl (0.1 M) and NaOH (0.1 M). Before the test, the flat membrane discs were cut into a rectangular shape (20 × 10 mm) to match the module. The samples were measured in a range of pH values from 2–10 with a pH difference of 1 using an automated titration unit.

The water contact angle of the Al₂O₃ and SiC-deposited membranes were measured by a contact angle measurement (Dataphysics OCA20, Germany). The morphology of the ceramic membranes was characterized by a field emission scanning electron microscopy (SEM, FEI Nova Nano SEM 450, USA). The pore size distribution of the membranes was determined by capillary flow porometry (Porolux 500, IBFT GmbH, Germany). The surface roughness of the membranes was measured by atomic force microscopy (AFM) (Dimension Icon, Bruker, USA).

6.2.4. Oil-in-water emulsion

The O/W emulsions were prepared by adding 3 mL mineral oil to 2 L of demineralized water in the presence of SDS as the stabilizing agent. First, the emulsion was continuously stirred with a magnetic stirrer (L23, LABINCO, the Netherlands) at a speed of 1500 rpm for 36 h and then ultrasonicated (521, Branson, US) for 2 h until it appeared milky white. Afterwards, the emulsion was diluted to 6 L with a final oil concentration of 400 mg L⁻¹ for filtration experiments. Four different SDS concentrations (33, 66, 100, 133 mg L⁻¹) were respectively used in order to study the effect of SDS concentration on membrane fouling. NaCl (1, 10, 100 mM) and Ca²⁺ (1 mM) were added into the emulsion with 100 mg L⁻¹ SDS to study the effect of ionic strength and Ca²⁺ on membrane fouling, respectively. Each filtration run was finished on the same day to reduce the effect of oil droplet aggregates or coalescence. The pH of the emulsions was adjusted by HCl (0.1 M) and NaOH (0.1 M) and measured by a pH sensor (inoLab™ Multi 9420 - WTW). Electrical conductivity of the emulsion was measured by a multi-meter (inoLab™ Multi 9420 - WTW). The oil droplet size distribution and zeta potential were analyzed in triplicate with a particle size analyzer (Bluewave, Microtrac, USA) and a Malvern Zetasizer Nano ZS (Malvern Instruments Ltd., UK), respectively.

6.2.5. Fouling experiments with O/W emulsions

Constant flux crossflow fouling experiments

O/W emulsion filtration experiments were performed with a constant permeate flux crossflow fouling apparatus (Figure 6.1), which has been described in detail in Chen et al. (2020b). The effective filtration area of each membrane module was 0.003 m². The concentrate valve was closed during filtration and the feed pump (DDA12-10, Grundfos, Denmark) has a controlled flow (measured and adjusted by the pump). A constant crossflow velocity of 0.44 m/s was provided by a circulation pump (VerderGear, Verder B.V., the Netherlands). Because the pressure at the permeate side was equal to atmospheric, the TMP was thus determined by the average of the inlet and outlet pressures on the two sides of the membrane module, which were monitored by two pressure transducers (GS4200-USB, ESI, UK). The pressures were continuously logged with a time interval of 30 s to the computer. During the filtration, the membrane was fouled and the membrane resistance increased, resulting in an increase in TMP.

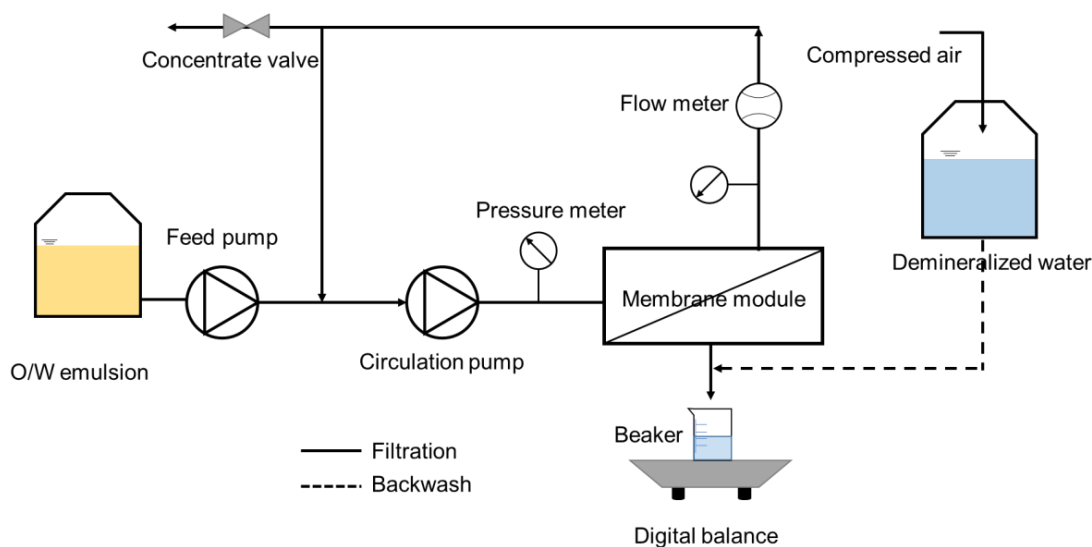


Figure 6.1. Schematic view of the constant flux crossflow filtration setup.

Filtration protocol

The filtration experiments were conducted at room temperature (22 ± 3 °C). Before each filtration experiment, the system was thoroughly cleaned with demineralized water to remove residual chemicals and air. Afterwards, the initial water permeance of each membrane was measured at the same permeate fluxes as used for O/W filtration with demineralized water. The fouling experiment for each membrane consisted of several cycles which were dependent on the filtration conditions (permeate flux and emulsion chemistry). The filtration cycle was applicable for all membranes. Each cycle consisted of three phases: 1) Filtration at a specified flux for a pre-set time (Table 6.2), 2) Backwashing the membrane module with demineralized water at a fixed pressure of 3 bar for 30 s to remove hydraulically reversible fouling, 3) Forward flush with feed emulsion for 15 s to remove the backwash remaining liquids and replace the solution in the loop with the fresh feed.

Three permeate fluxes ($90, 100, 110 \text{ L m}^{-2} \text{ h}^{-1}$) were respectively used to compare the membrane performance based on the threshold flux of the membranes, because then the effect of membrane surface properties on fouling can be well studied (Luo et al., 2012) and the filtration time for each flux was chosen based on the same volume of permeate production. The filtration time per cycle has an effect on membrane fouling; therefore, two different filtration times were selected at a flux of $110 \text{ L m}^{-2} \text{ h}^{-1}$ for comparison. When challenged with the oil emulsion with high salinity or Ca^{2+} concentration, the permeate flux and filtration time were reduced as severe

■ Chapter 6

membrane fouling was observed. Table 6.2 lists the characteristics of the O/W emulsion, the permeate flux and the corresponding filtration time per cycle. A short filtration time was used as a faster fouling was observed with extended filtration time, leading to a decrease in the permeate flux (Figure S6.1). In addition, in MF/UF, a filtration time of 15 min is common practice in full scale installations.

Table 6.2 Characteristics of the O/W emulsions, permeate flux and the corresponding filtration time per cycle for constant flux filtration experiments.

O/W emulsion					Permeate flux (L m ⁻² h ⁻¹)	Filtration time (min)
SDS (mg L ⁻¹)	pH	NaCl (mM)	Ca ²⁺ (mM)	Conductivity (μs cm ⁻¹)		
100	5.6	0	0	31	90	20
100	5.6	0	0	31	110	16
100	5.6	0	0	31	110	14
33	5.6	0	0	10	100	18
66	5.6	0	0	19	100	18
100	5.6	0	0	31	100	18
133	5.6	0	0	40	100	18
100	8	0	0	31	100	18
100	10	0	0	31	100	18
100	5.6	1	0	158	90	20
100	5.6	10	0	1305	60	12
100	5.6	100	0	11.58 ms cm ⁻¹	50	10
100	5.6	1	1	352	50	10

Between the various filtration runs, the membranes were first backwashed at 3 bar for 30 s and then they were chemically cleaned with a base solution by soaking them in a sodium hydroxide solution (0.01 M NaOH) for 1 h at 65 °C, followed by three times rinsing with demineralized water. Afterwards, the membranes were soaked in a citric acid solution (0.01M) for another 1 h at 65 °C, as recommended in literature (Fraga et al., 2017a; Zsirai et al., 2018). When the permeance of the membranes was not fully recovered after the chemical treatment, the membranes were heated at 200 °C for 2 h

in a muffle furnace (Nabertherm Controller P 300, Germany). In this way, the membrane performance was completely recovered for the next filtration experiment.

In addition to the filtration experiments, where a constant flux was used during each run, flux-stepping experiments were carried out with D0 and D90 to determine the membrane threshold flux, as recommended in literature (He et al., 2017a; Miller et al., 2014b). In this protocol, the permeate flux of the membrane was increased stepwise every 20 min from 40 to 80 L m⁻² h⁻¹ in an increment of 10 L m⁻² h⁻¹. Then the flux was further increased by 10 L m⁻² h⁻¹ until a flux of 110 L m⁻² h⁻¹ was reached with reduced filtration times (Table S6.1), as rapid fouling was observed at these high fluxes. TMP was continuously monitored during each filtration interval.

6.2.6. Data analysis

The initial pressure for each membrane varied due to the permeance differences. In order to better compare the membrane performance, the permeance (P) of the membranes during filtration were normalized to the initial P_0 , which was determined by the first value in the first cycle where the setting flux was reached.

The membrane resistance was calculated based on the resistance-in-series model, as shown in Eq. (1):

$$R_t = \frac{TMP}{\mu J} = R_m + R_r + R_{ir} \quad (1)$$

where J is the membrane flux (m/s), TMP is the applied trans-membrane pressure (Pa), μ is the dynamic viscosity of the permeate (Pa s), R_t (m⁻¹) represents the total resistance, which is consist of intrinsic membrane resistance (R_m), hydraulically reversible resistance (R_r), and irreversible unphysical removable resistance (R_{ir}). R_m was determined through the filtration of demineralized water and R_t was measured according to the final filtration pressure of each filtration cycle of O/W emulsion. The fouled membrane was backwashed with demineralized water under a pressure of 3 bar for 30s and then R_r was measured. Therefore, the R_{ir} could be calculated from $R_t - R_r - R_m$.

The permeance recovery (R_p) of the membrane was determined by the following equation:

$$R_p = P/P_0 \times 100\% \quad (2)$$

where P_0 is the initial permeance of the clean membrane, P is the initial permeance of the fouled membrane after backwashing with demineralized water or cleaning with chemicals.

The methods used to determine membrane rejection and the results were provided in the supplementary information (Figure S6.2, Figure S6.11 and Figure S6.13).

6.3. Results and discussion

6.3.1. Characteristics of oil emulsion and membranes

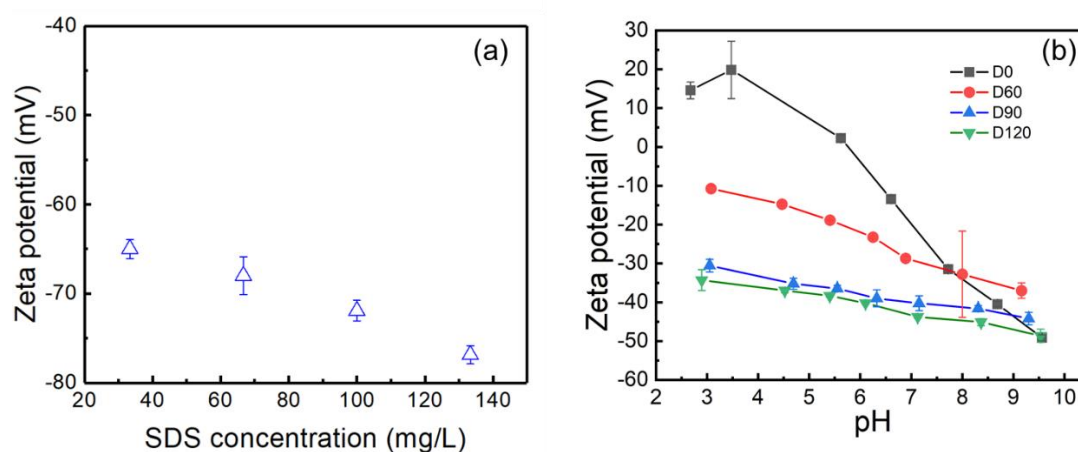


Figure 6.2. (a) Zeta potential of O/W emulsion (0 mM NaCl) stabilized by SDS at different surfactant concentrations, and (b) zeta potential of Al_2O_3 membrane (D0) and SiC-deposited membranes (D60, D90 and D120). The conductivity of the O/W emulsion was given in Table 2.

Characteristics of O/W emulsions, prepared at various SDS concentrations, were evaluated in terms of zeta potential (Figure 6.2a) and oil droplet size (Figure S6.3). The O/W emulsions, stabilized with SDS, were negatively charged with a zeta potential ranging from -65 to -77 mV. The majority of the oil droplet sizes were in the range of 1 to 10 μm and a small amount of even smaller oil droplets (70-100 nm) was observed when the concentration of SDS reached 133 mg L^{-1} (Figure S6.3). The zeta potential of the Al_2O_3 membrane was positive when the pH was lower than 6, while a negative surface charge was observed with a solution pH higher than 6 (Figure 6.2b). Similar results were also reported by Nagasawa et al. (2020), although in the studies by Atallah et al. (2017) and Kosmulski (2011), the IEP of Al_2O_3 membranes was determined to be around 8 or 9. All SiC-deposited membranes had a negative surface

charge in the investigated pH range (2-10). The zeta potentials of D90 and D120 were similar, but much lower than that of D0 and D60, possibly due to the thicker SiC layer on the sample surface with a longer deposition time (Yang et al., 2021). The results of other characteristics (pore size distribution, surface morphology, surface hydrophilicity and roughness) of the membranes are given in the supporting information (Figure S6.4, Figure S6.5, Figure S6.6 and Figure S6.7). Compared to the pristine Al_2O_3 membrane, the deposited membranes had a narrower pore size distribution and smaller average pore sizes.

6.3.2. Comparison of membrane fouling of the membranes

In chapter 5, we have systematically compared the fouling of pristine and SiC-deposited ceramic membranes for O/W emulsion filtration. It was concluded that D90 showed the best fouling control in SiC-deposited membranes. Therefore, D90 and D0 were used to study the effects of permeate flux, SDS concentration, pH, salinity, and Ca^{2+} concentration on membrane performance in the following sections.

6.3.3. Effect of permeate flux

The threshold fluxes of the membrane D0 and D90 were 93 and 87 $\text{L m}^{-2} \text{h}^{-1}$, respectively, as determined by the flux-stepping methods (Figure S6.8 and Figure S6.9). Therefore, three different permeate fluxes (90, 100, 110 $\text{L m}^{-2} \text{h}^{-1}$), were compared to study their effect on membrane fouling. At the flux of 90 $\text{L m}^{-2} \text{h}^{-1}$, close to the threshold flux, fouling of the membranes is mainly determined by the foulant-membrane interaction. When the flux is above the threshold flux (100 and 110 $\text{L m}^{-2} \text{h}^{-1}$), foulant-membrane and foulant-deposited-foulant interactions can be investigated under this condition (Luo et al., 2012).

The effect of permeate flux on the filtration of the O/W emulsion with the SiC-deposited membrane (D90) and Al_2O_3 membrane (D0) is shown in Figure 6.3. At a flux of 90 $\text{L m}^{-2} \text{h}^{-1}$, some fouling was observed in both membranes as permeance declined with time. The normalized permeance curves of the two membranes were parallel and overlapped in the first two cycles, indicating that reversible fouling was similar. With more filtration cycles, the permeance curves of D0 shifted down which was not observed in D90, suggesting that irreversible fouling happened in D0 (Figure 6.3a). When the permeate flux increased from 90 to 100 $\text{L m}^{-2} \text{h}^{-1}$, irreversible fouling became larger for both D0 and D90, as observed by lower initial normalized

Chapter 6

permeance of each cycle. The normalized permeance (84% recovery) of D90 was still higher than that (64% recovery) of D0 in the final cycle at the flux of $100 \text{ L m}^{-2} \text{ h}^{-1}$.

During fouling experiments, higher fluxes bring larger amounts of emulsified oil foulants per time unit to the membrane surface, increasing foulant accumulation on the membrane (Miller et al., 2014a; Miller et al., 2014b). On the other hand, higher fluxes cause a stronger drag force acting on oil droplets, which, consequently lead to the deformation and coalescence of attached droplets and squeezing of oil droplets across the membrane pores, resulting in irreversible fouling of the membrane (Chen et al., 2020c; Tummons et al., 2017). As shown in Figure 6.3c, with a further increase in the flux to $110 \text{ L m}^{-2} \text{ h}^{-1}$, a much higher irreversible fouling was observed in D90, compared to the lower fluxes, and close to that of D0. At this high flux, oil coalescence and internal fouling are more likely to occur, and therefore hydraulic cleaning became ineffective to remove the oil film (Figure 6.3d) (Zhu et al., 2017).

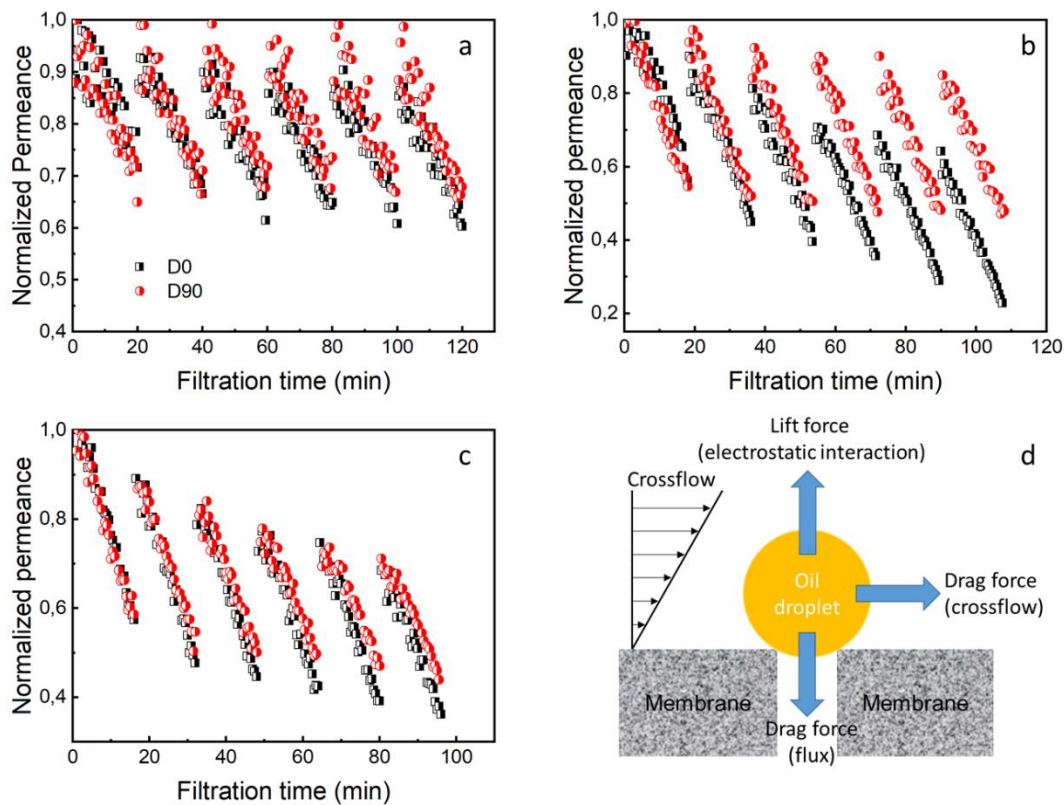


Figure 6.3. Normalized permeance of D0 (black) and D90 (red) compared at various fluxes: (a) $90 \text{ L m}^{-2} \text{ h}^{-1}$, (b) $100 \text{ L m}^{-2} \text{ h}^{-1}$, and (c) $110 \text{ L m}^{-2} \text{ h}^{-1}$. (d) Force balance on an oil droplet in crossflow filtration. The O/W emulsion has a pH of 5.6, oil concentration is 400 mg L^{-1} and the SDS is 100 mg L^{-1} .

When the water production during a filtration cycle was the same at the three studied fluxes, lower fouling was observed at a lower flux. However, further shortening the filtration time to 14 min per cycle at the highest flux ($110 \text{ L m}^{-2} \text{ h}^{-1}$) could control the fouling, especially for SiC-deposited membrane (Figure S6.10). In this case, permeance recovery of SiC-deposited membrane increased from 71% to 94%, which was higher than that (84%) of the Al_2O_3 membrane.

6.3.4. Effect of SDS concentration

The effect of SDS concentration on fouling of the Al_2O_3 membrane (D0) and SiC-deposited membrane (D90) is shown in Figure 6.4. At a low concentration of SDS (33 mg L^{-1}), the fouling of D90 was much less than that of D0, which can be observed by terminal normalized permeance and the recovery of the permeance of each cycle (Figure 6.4a). The higher (ir)reversible fouling of D0 was attributed to the lack of electrostatic repulsion between the membrane and oil droplets. Increasing the concentration of SDS in the feed had a positive effect on the fouling of both membranes, especially on the D0. As observed in Figure 6.4b, the permeance recovery in the final cycle of D0 and D90 increased from 61% to 70% and from 81% to 87%, when the concentration of SDS was increased from 33 to 100 mg L^{-1} , respectively. With a further increase in the SDS concentration in the feed to 133 mg L^{-1} , the fouling difference between D0 and D90 was further reduced, with a permeance recovery of 81% and 90% in the final cycle, respectively. Similar results were reported by Virga et al. (2020) (Virga et al., 2020), who found that less flux decline was observed for MF of an SDS stabilized O/W emulsion with a commercial SiC membrane, when SDS concentration increased from 0.1 to 1 times the critical micelle concentration (CMC). As SDS concentration was high (up to the CMC), O/W interfacial tension was considerably decreased, potentially leading to oil permeation through the membrane rather than accumulating on the membrane surface or in the pores. As a result, a higher permeate flux was observed. However, this mechanism cannot explain the results observed in our work, as the highest used SDS concentration (133 mg L^{-1}) was less than 0.06 times the CMC. In addition, no variations in oil rejection were observed for emulsions stabilized with different SDS concentrations (Figure S6.11).

The reversible and irreversible fouling of D0 and D90 was also evaluated by the fouling resistances (Figure S6.12). The R_r and R_{ir} of D0 were considerably decreased, from $46 \times 10^{12} \text{ m}^{-1}$ to $1.53 \times 10^{12} \text{ m}^{-1}$ and from $3.57 \times 10^{12} \text{ m}^{-1}$ to $0.7 \times 10^{12} \text{ m}^{-1}$, respectively, when the concentration of SDS was increased from 33 to 133 mg L^{-1} .

Chapter 6

However, the R_r and R_{ir} of D90 were only slightly decreased, from $3.1 \times 10^{12} \text{ m}^{-1}$ to $1.2 \times 10^{12} \text{ m}^{-1}$ and from $0.95 \times 10^{12} \text{ m}^{-1}$ to $0.4 \times 10^{12} \text{ m}^{-1}$, respectively.

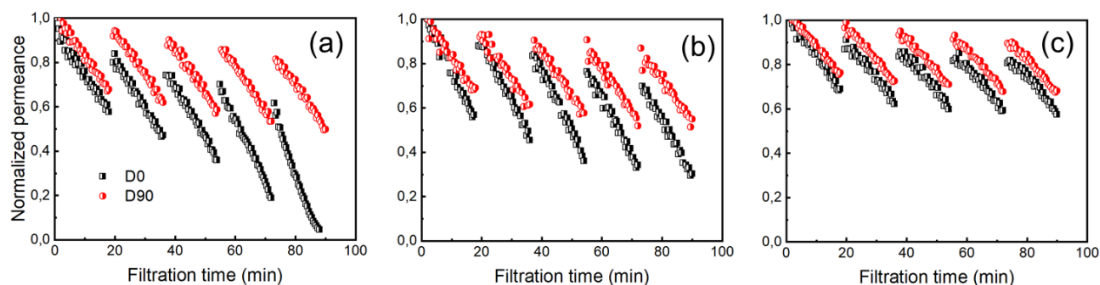


Figure 6.4. Normalized permeance of D0 and D90 compared at various SDS concentrations: (a) 33 mg L^{-1} , (b) 100 mg L^{-1} , and (c) 133 mg L^{-1} . The filtration experiments were conducted at the flux of $100 \text{ L m}^{-2} \text{ h}^{-1}$, O/W emulsion has a pH of 5.6, and the oil concentration is 400 mg L^{-1} .

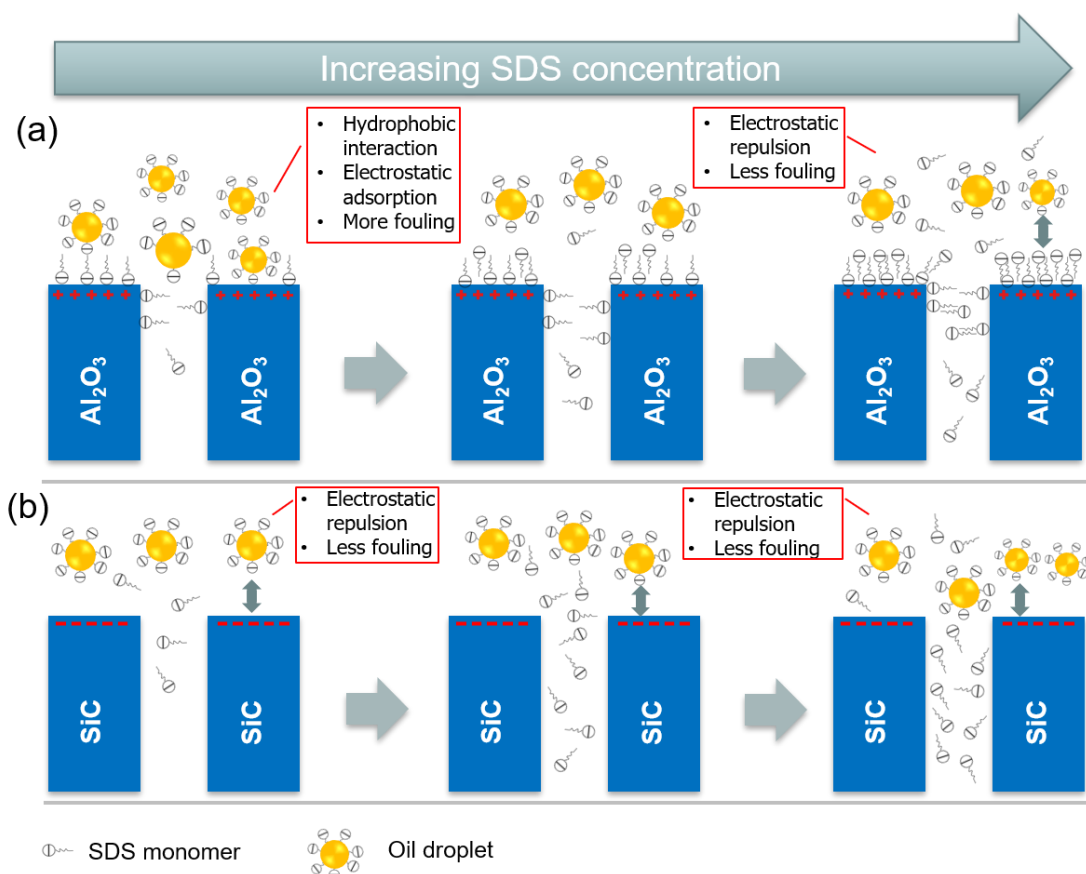


Figure 6.5. Proposed fouling mechanism of (a) Al_2O_3 and (b) SiC membranes during filtration of SDS stabilized O/W emulsions at various SDS concentrations.

The SiC-deposited membrane was negatively charged while the Al₂O₃ membrane had a positive surface charge at a pH of 5.6 (Figure 6.2b). A higher negative charge of the emulsion was observed with increasing SDS concentration, as determined with the zeta potential of the emulsions, prepared with various SDS concentrations (Figure 6.2a). According to the adsorption model proposed by Gu and Zhu (1990), the adsorption of surfactant at the liquid/solid surface takes place in two steps. In the first step, the head groups of surfactant monomers preferably adhere to the hydrophilic membrane surfaces to form the first layer. Subsequently, a second layer is adsorbed on the first one (Nguyen et al., 2015). In addition, a slight decline of permeance of the Al₂O₃ membrane was observed for SDS solution filtration, indicating that SDS was adsorbed on the Al₂O₃ membrane. However, no adsorption of SDS on the SiC-deposited ceramic membranes was observed as the permeance maintained constant (Figure S6.13). Therefore, the following fouling mechanism was proposed and is schematically shown in Figure 6.5. At a low SDS concentration (33 mg L⁻¹), most of the surfactants were used to stabilize the oil droplets, leaving a low concentration of free SDS monomers in the solution. The negatively charged head of the SDS (and hydrophilic) will be attached to the positively charged Al₂O₃ membrane surface due to electrostatic attraction, leaving the hydrophobic tails towards the bulk phase (Dobson et al., 2000). This forms a hydrophobic surfactant monolayer on the surface and therefore increases the fouling of D0 (Fernández et al., 2005; Matos et al., 2016). Increasing the SDS concentration, however, will result in a higher concentration of free surfactant monomers in the solution, and probably a new monolayer is formed on top of the pre-covered single monolayer on the membrane surface. In this case, the hydrophilic head (and negatively charged) of SDS is oriented towards the bulk phase as a result of hydrophobic interactions. Thus, the surface charge of the Al₂O₃ membrane is reversed from positive to negative (and again hydrophilic), which prevents the adsorption of oil droplets and alleviates the membrane fouling. The charge inversion of the membrane by surfactant has also been reported by Trinh et al. (2019), who found that surfactant-soaked membranes had the same charge as the surfactant-stabilized emulsion regardless of the surfactant type. However, surfactants and oil droplets can be hardly adsorbed on the membrane surface and in the membrane pores of the SiC-deposited membranes due to electrostatic repulsion (Lin and Rutledge, 2018; Zhang et al., 2009). The slightly improved fouling resistance of the SiC-deposited membranes can be ascribed to the enhanced electrostatic repulsion between the membrane and oil droplets with increased SDS concentration in the feed.

6.3.5. Effect of pH

To determine the effect of pH on membrane fouling, filtration experiments were conducted at three different pH values (Figure 6.6). We chose pH 5.6 as the starting point to study the fouling of the two membranes as it is the native pH of the fresh O/W emulsion. In addition, this pH is commonly observed in oily wastewater (Wenzlick and Siefert, 2020). In all cases, the fouling was less in the SiC-deposited membrane than in the Al₂O₃ membrane. In addition, both membranes experienced a decrease of fouling with an increase in pH. Specifically, the normalized initial permeance of D0 and D90 in the final filtration cycle increased from 64% to 89%, and 85% to 93%, when pH increased from 5.6 to 10, respectively. This pH dependency can be attributed to the fact that, as pH increases, the surface charge of the membrane becomes more negative (Zhang et al., 2009). As shown in Figure 6.2a, the zeta potential of the SiC-deposited membrane (D90) decreased from -37 mv to -44 mv with an increase in pH from 5.6 to 10, respectively. Consequently, the membrane surface was less prone to be fouled by the negatively charged oil droplets due to the stronger electrostatic repulsion. However, the surface charge of the Al₂O₃ membrane was positive at a pH of 5.6, and therefore more fouling was observed as it favourably interacted with the negatively charged solutes. The positively charged (+8 mv) surface was changed into negative (-49 mv) when filtering the feed with a pH of 10, and, therefore, electrostatic interaction became repulsive and contributed to decreased fouling (Abadikhah et al., 2018; Lee and Kim, 2014). Although the zeta potentials of Al₂O₃ and SiC-deposited membranes were similar at a pH of 10, the fouling of the SiC-deposited membrane was still lower than that of the Al₂O₃ membrane. This can possibly be ascribed to the stronger hydrophilic surface of the SiC-deposited membrane (water contact angle = 0°) than that of the Al₂O₃ membrane (water contact angle = 25°) (Figure S6.6). Xu et al. (2020) also compared the fouling of Al₂O₃ and SiC hollow fiber membranes for MF of O/W emulsions, a higher flux was observed for the more hydrophilic SiC membrane.

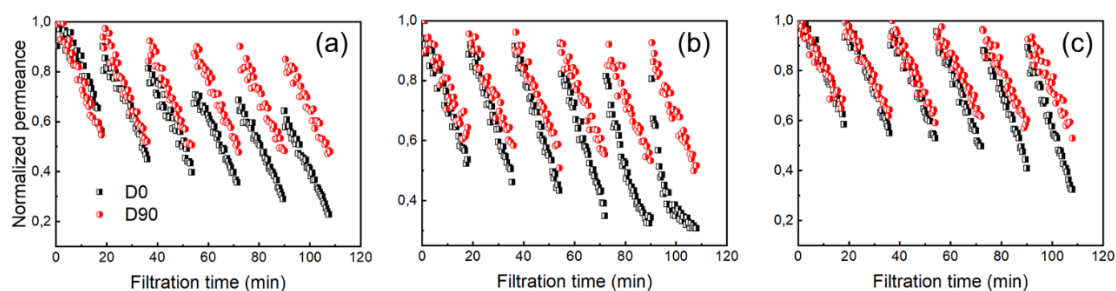


Figure 6.6. Normalized permeance of D0 and D90 compared at various pH: (a) pH = 5.6, (b) pH = 8, and (c) pH = 10. The filtration experiments were conducted at the constant flux of $100 \text{ L m}^{-2} \text{ h}^{-1}$, oil concentration is 400 mg L^{-1} and the SDS is 100 mg L^{-1} .

6.3.6. Effect of salinity and Ca^{2+}

It has been reported that the surface charge of oil emulsions and membranes decreases with the concentration of NaCl due to the compressed electrical double layer (He et al., 2017a; Tanudjaja et al., 2017). Although the droplet size of oil was not changed with the salinity (Figure S6.3), as shown in Figure 6.7, the fouling of both D0 and D90 became higher when NaCl concentration increased from 1 mM to 100 mM. However, the fouling of D90 was much lower than that of D0 when NaCl concentration was lower or equal to 10 mM. This indicates that the surface charge of the SiC-deposited membrane still had an effect on the fouling by oily wastewater with relatively low salinity, whereas, much more fouling was observed for both membranes when NaCl concentration reached 100 mM. At that salinity (100 mM NaCl), the flux recovery of D90 was close to that of D0, suggesting that irreversible fouling of the two membranes were similar. Probably, because, oil droplets were not easily lifted off the membrane with backwash, due to charge screening and an increase of cake layer density (Dickhout et al., 2019; He and Vidic, 2016).

Divalent cations such as Ca^{2+} and Mg^{2+} can also be present in oily wastewater. Their presence may accelerate membrane fouling due to more compression of the diffusion double layer compared to monovalent ions (Dickhout et al., 2017). As shown in Figure 6.7D, the membrane fouling was worse when 1 mM Ca^{2+} was added to the emulsions and the backwashing was not effective anymore to restore the permeance. Therefore, the irreversible fouling was considered to be the main contributor to the membrane fouling. This can be explained by two effects of Ca^{2+} in the emulsion: (1) lower electrostatic charge of oil droplets and membranes are to be expected due to a

compressed electrostatic layer when Ca^{2+} is present in the emulsion (Hong and Elimelech, 1997). Therefore, droplet coalescence on the membrane surface is promoted leading to a less permeable cake layer (Tummons et al., 2017); (2) SDS can interact with divalent Ca^{2+} , which may cause the formation of a complex between Ca^{2+} and the sulphate group of SDS (Panpanit et al., 2000; Sammalkorpi et al., 2009). As a result, less SDS molecules exist in the emulsion, as confirmed by permeate COD (Figure S6.14), leading to a higher irreversible fouling of the membranes (Virga et al., 2020). However, the irreversible fouling of D90 was still lower than that of D0, even though the electrostatic repulsion became weaker. Tummons et al. (2017) studied the effect of Mg^{2+} on the fouling of an Al_2O_3 UF membrane by SDS stabilized emulsions. The presence of Mg^{2+} (6.7 mM) in the emulsion was observed to promote the coalescence of oil droplets on the membrane surface, leading to a higher flux decline of the membrane due to the less porosity of the cake layer. When the Mg^{2+} concentration was sufficiently high (42.6 mM), attached oil droplets coalesced to reach a critical size, which can probably be removed by crossflow to minimize the fouling in the constant pressure filtration condition.

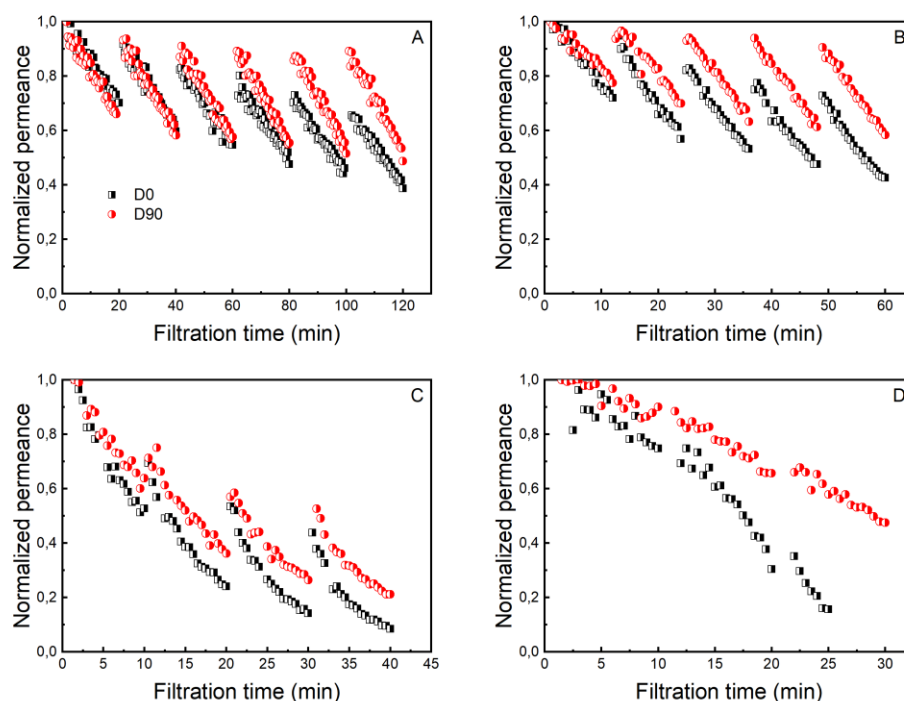


Figure 6.7. Normalized permeance of D0 and D90 compared at various concentrations of NaCl and 1 mM Ca^{2+} : (A) 1 mM NaCl, (B) 10 mM NaCl, (C) 100 mM NaCl and (D) 1 mM NaCl + 1 mM

Ca²⁺. The emulsion has an oil concentration of 400 mg L⁻¹, pH of 5.6 and the SDS of 100 mg L⁻¹.

6.3.7. Membrane cleaning efficacy

After filtration of O/W emulsions at high fluxes during multiple cycles, accumulation of irreversible fouling in membranes was inevitable. The permeance recovery of D0 and D90 were compared after backwashing, after NaOH (0.01 M) and after citric acid (0.01 M) cleaning (Figure 6.8). The efficacy of backwashing was investigated after six cycles of filtration at a flux of 110 L m⁻² h⁻¹, as was previously shown in Fig. 3c. The permeance recovery after backwashing of D90 (64%) was higher than that of D0 (45%), probably due to less sticky fouling in the membrane and to a more efficient backwashing. After soaking the membranes in NaOH (0.01 M) solution at 65 °C for 1 h, the permeance recovery of D0 and D90 reached up to 80% and 84%, respectively. The permeance of D90 could be further recovered to 98% after citric acid (0.01 M, 65 °C) treatment for 1h, while the permeance of D0 could only be recovered to 84%. A high permeance recovery (100%) was also observed by Fraga et al. (2017a) when using both acid and alkaline solutions to clean SiC membranes at 60 ± 5 °C after filtration of oily wastewater. However, the permeance recovery of D90 was lower, but still higher than that of D0, after filtration of O/W emulsions with either high salinity (100 mM NaCl) or the presence of Ca²⁺ (Figure S6.15).

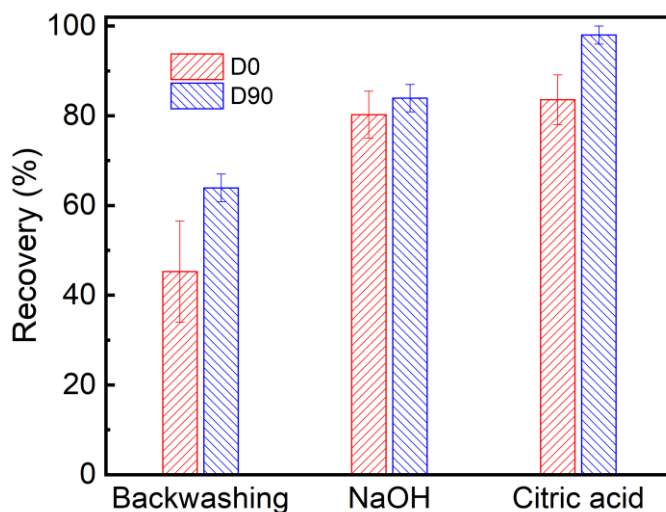


Figure 6.8. Permeance recovery of D0 and D90 with backwashing (3 bar/30s), NaOH (0.01 M, 65 °C) cleaning and citric acid (0.01 M, 65 °C) cleaning. The membranes were fouled after 6 cycles of O/W emulsion filtration at a constant flux of 110 L m⁻² h⁻¹, oil concentration of 400 mg L⁻¹ and pH of 5.6.

6.4. Conclusion

The performance of Al₂O₃ and SiC-deposited ceramic membranes was systematically compared during constant flux filtration of O/W emulsion with multiple filtration cycles. Both the operation and solution chemistry parameters affected the membrane fouling, while the extents varied, depending on the emulsion characteristics and operational parameters. The following conclusions were drawn:

- SiC-deposited membranes had a lower reversible and irreversible fouling than Al₂O₃ membranes, when, in multiple filtration cycles, the permeate flux was smaller or equal to 100 L m⁻² h⁻¹. The fouling of both membranes was similar when the flux reached to 110 L m⁻² h⁻¹.
- Increasing the concentration of SDS in the feed decreased fouling of both membranes, and a larger effect was observed for the Al₂O₃ membrane. The improved fouling resistance of the Al₂O₃ membrane can be ascribed to the effect of surfactant adsorption and charge inversion, while the enhanced

electrostatic repulsion between the membrane and oil droplets was responsible for the lower fouling of the SiC-deposited membrane.

- The fouling of both Al₂O₃ and SiC-deposited membranes was reduced with increased pH due to the more negative zeta potential of the membrane surface and thus a stronger electrostatic repulsion.
- The fouling of the SiC-deposited membrane was less with a low salinity emulsion (1 and 10 mM NaCl), while only a small difference in irreversible fouling was observed for Al₂O₃ and SiC-deposited membranes for high salinity emulsions (100 mM NaCl) due to charge screening effect.
- The presence of a low concentration of Ca²⁺ (1 mM) in the emulsion led to high irreversible fouling for both membranes.
- The chemical cleaning efficacy of the SiC-deposited membrane was higher than that of the Al₂O₃ membrane.

Acknowledgements

Mingliang Chen acknowledges the China Scholarship Council for his PhD scholarship under the State Scholarship Fund (No. 201704910894). We thank WaterLab at TU Delft for providing the help on the measurement of samples. We would like to thank Nadia van Pelt (TU Delft, The Netherlands) for her help on language and grammar issues of the manuscript. Bob Siemerink, and Iske Achterhuis from Twente University are acknowledged for the support concerning the zeta potential measurements. Guangze Qin is acknowledged for measuring the membrane water permeance.

Supplementary information

S6.1. Oil-in-water emulsion filtration with extended time

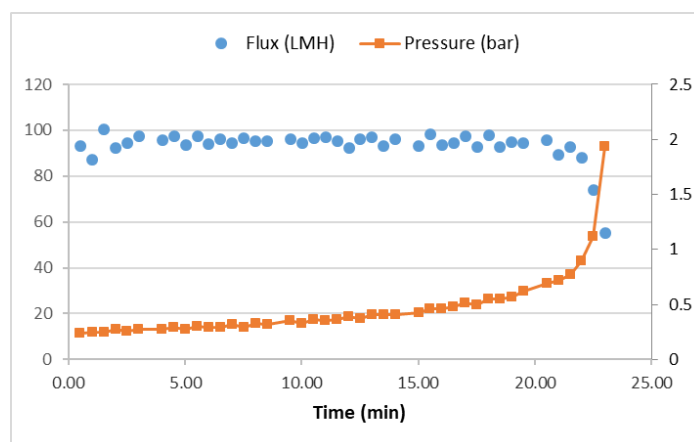


Figure S6.1. Oil-in-water emulsion filtration at a constant flux of 100 LMH by pristine alumina ceramic membrane with a crossflow velocity of 0.44 m/s. The emulsion had an oil concentration of 400 mg L⁻¹ and pH of 5.6.

S6.2. Calibration line of oil concentration

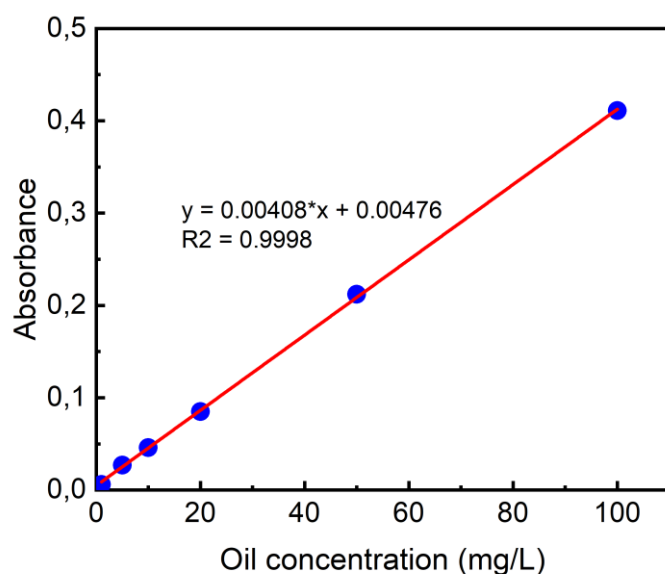


Figure S6.2. Linear relationship of oil concentration with UV-vis absorbance.

The oil concentration of the samples was measured by a UV/Vis spectrophotometer (GENESYS 10S UV-Vis, Thermo scientific, US) at 275 nm (Zhou et al., 2010), while chemical oxygen demand (COD) of the samples was measured by a Hach spectrophotometer (DR 3900, US) with COD cuvettes (LCK 514 and LCK 314, Hach)

(Marchese et al., 2000). The feed with various dilution times was used to make a calibration line (between oil concentration and absorbance) (Figure S6.2) with a regression coefficient higher than 0.999. Then the oil and COD rejection of the membranes were calculated by Eq. (S1):

$$R = \left(1 - \frac{C_p}{C_f}\right) \times 100\% \quad (S1)$$

where R is the rejection, C_p is the oil (mgL^{-1}) or COD concentration (mgL^{-1}) in the permeate, and C_f is the oil (mgL^{-1}) or COD concentration (mgL^{-1}) in the feed.

S6.3. Oil droplet size distribution

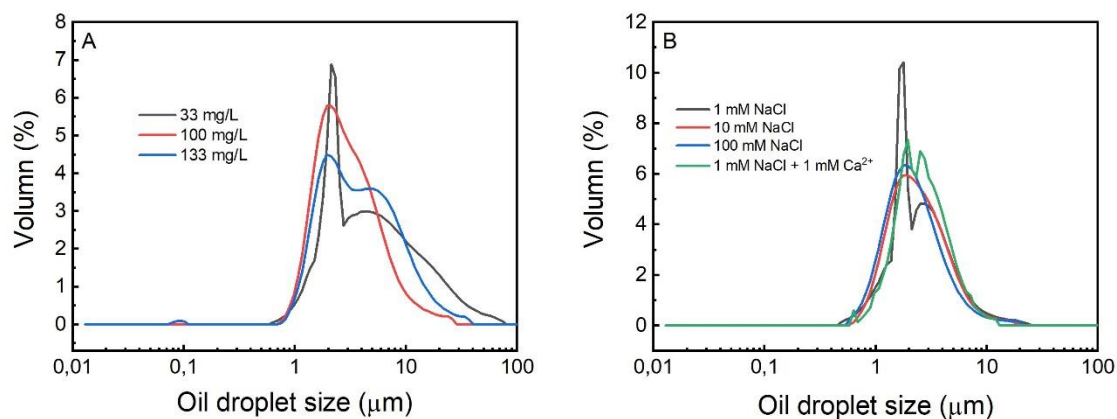


Figure S6.3. The droplet size distribution of oil in O/W emulsions at various concentrations of surfactant (A) and NaCl (B). No NaCl was added in the emulsion in (A) and the surfactant concentration is 100 mg/L in (B).

S6.4. Characterization results of the membranes

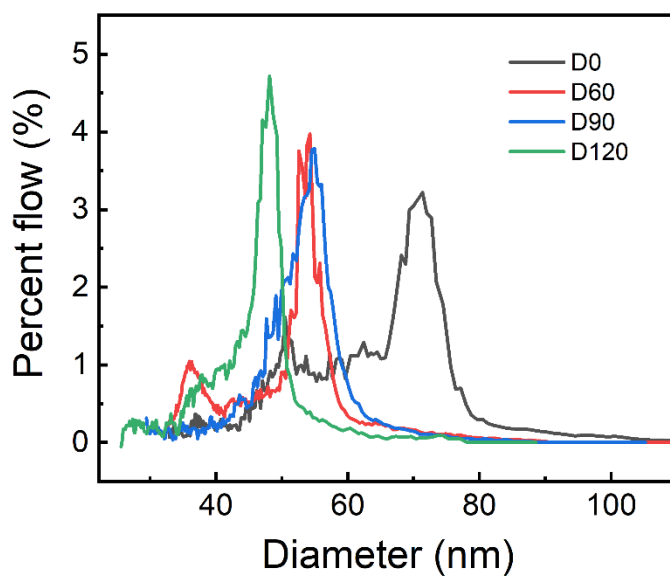


Figure S6.4. Pore size distribution of the membranes before and after SiC deposition.

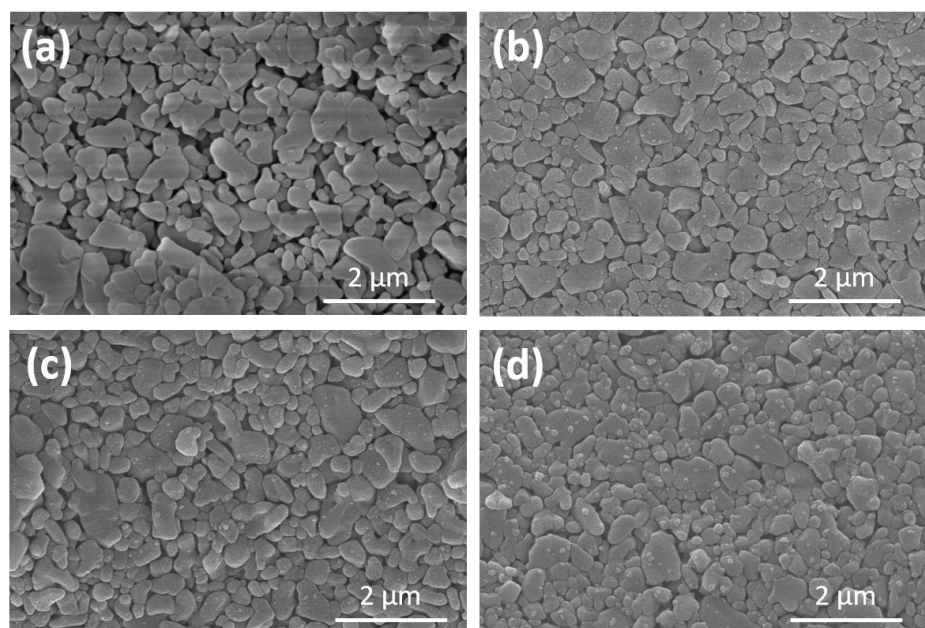


Figure S6.5. Surface SEM images of the alumina membrane and SiC-deposited ceramic membranes, (a) D0, (b) D60, (c) D90, and (d) D120.

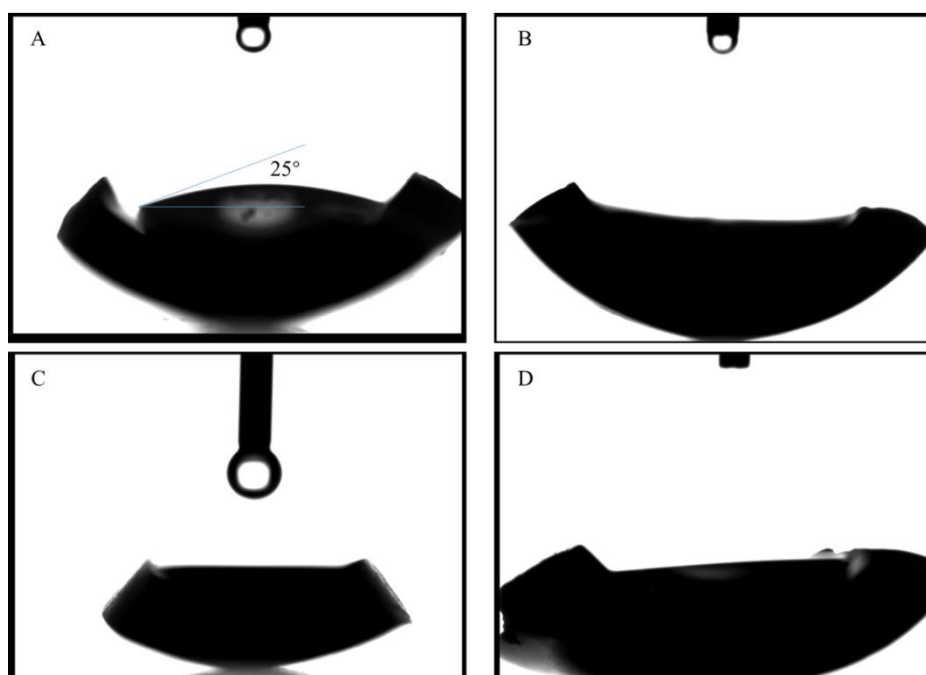


Figure S6.6. Water contact angle of the alumina membrane and SiC-deposited ceramic membranes, (A) D0, (B) D60, (C) D90, and (D) D120.

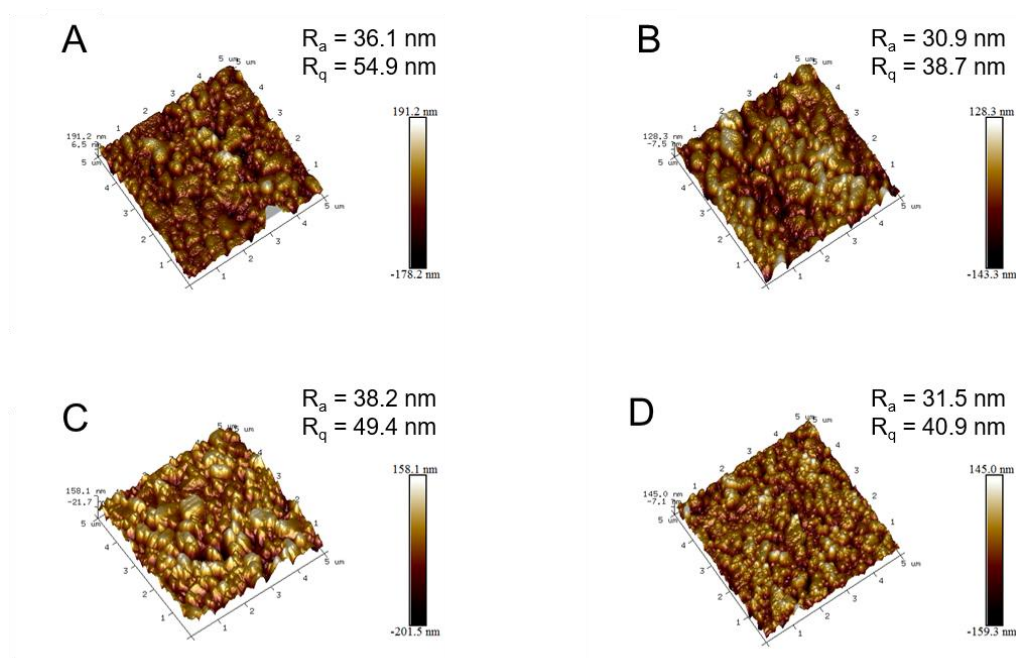


Figure S6.7. AFM micrographs and surface roughness of the alumina membrane and SiC-deposited ceramic membranes, (A) D0, (B) D60, (C) D90, and (D) D120.

S6.5. Flux stepping experiment

Table S6.1. The permeate flux and corresponding filtration time in flux stepping experiment.

Permeate flux (LMH)	40	50	60	70	80	90	100	110
Filtration time (min)	20	20	20	20	20	19	15	10

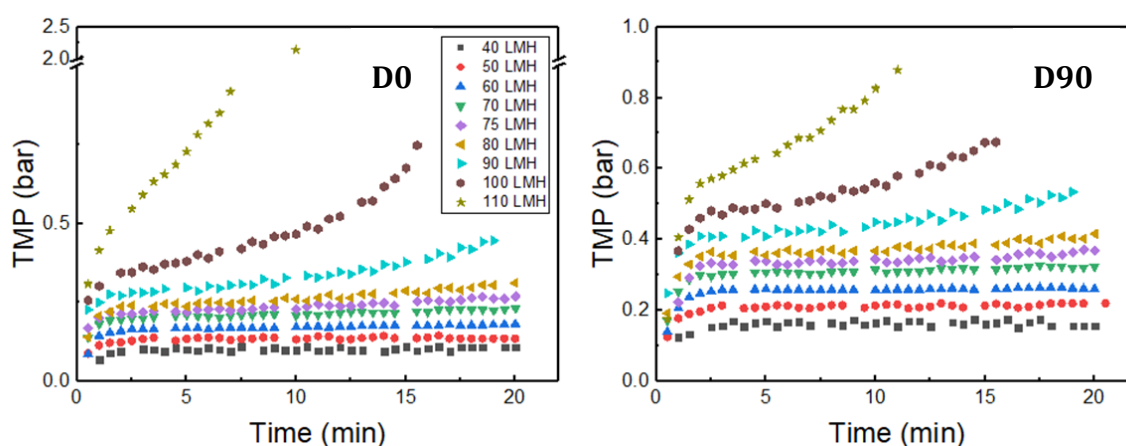


Figure S6.8. Flux stepping experiments with alumina (D0) and SiC-deposited (D90) membranes for 400 mg/L oil emulsion filtration (pH = 5.6, 66 mg/L SDS). The flux was gradually increased in 20-min, constant flux intervals from 40 to 110 LMH. The filtration time was reduced for fluxes of 90, 100, and 110 LMH as rapid fouling was observed at these high fluxes. TMP was continuously measured during each filtration interval.

S6.6. Threshold flux determination

In a laboratory study, threshold flux is typically estimated using a flux stepping technique. Three methods have been used to determine the threshold flux of the membrane based on the obtained data from flux stepping experiments (Kasemset et al., 2016; Miller et al., 2014b). The first method is to calculate the average fouling rate ($d(\text{TMP})/dt$) values at each flux step. In the second method, TMP_{avg} was first calculated from an average of TMP values recorded during each flux step. Then a linear regression of TMP_{avg} was drawn to estimate the threshold flux (Figure S6.9). This method was considered as most accurate one among the three methods (Kirschner et al., 2017). The third method used for threshold flux determination is ΔTMP , which is the TMP difference between the linear regressions of TMP data recorded over two adjacent flux steps at the time of flux increase. In this work, however, we only used the second method to determine the threshold flux of alumina (D0) and SiC-deposited (D90) membranes. The determined threshold flux of D90 (93 LMH) is higher than that of D0 (87 LMH), which indicates a better fouling resistance was obtained for SiC-deposited membrane.

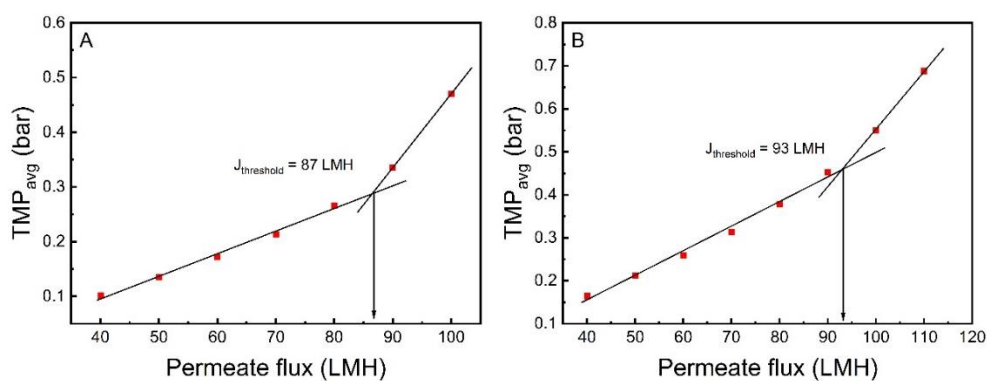


Figure S6.9. Threshold flux determination for alumina (D0) and SiC-deposited (D90) membranes challenged with 400 mg/L mineral oil emulsion feed (pH = 5.6, 66 mg/L SDS). The threshold flux is determined by TMP_{avg} method in (A) D0 and (B) D90, respectively. Values plotted as a function of flux are obtained from the experimental data in Fig. S6.8. The threshold flux values are denoted by the arrows pointing to the flux axis.

S6.7. Effect of filtration time on membrane fouling

At the permeate flux of $110 \text{ Lm}^{-2}\text{h}^{-1}$, serious fouling was observed in D0 and D90 at a filtration time of 16 min per cycle as oil droplets were easier to be dragged onto the

membrane surface as well as inside the pores at a higher flux (Fig. 3c). In order to reduce the irreversible fouling accumulated in each cycle at high flux, the filtration time can be shortened. As shown in Figure S6.10, both D0 and D90 experienced less fouling after reducing the filtration time per cycle to 14 min. The reversible and irreversible fouling of both membranes were much lower than the case filtered at a filtration time of 16 min per cycle. For example, the normalized permeance of D0 and D90 in the final filtration cycle was increased from 68% and 71% to 84% and 94% respectively. In addition, the reduced filtration time is more effective for D90 as less irreversible fouling was accumulated in the membrane. Despite the membrane fouling was well controlled with reduced filtration time, but less water was produced in this case as a higher percentage of permeate need to be used for backwashing.

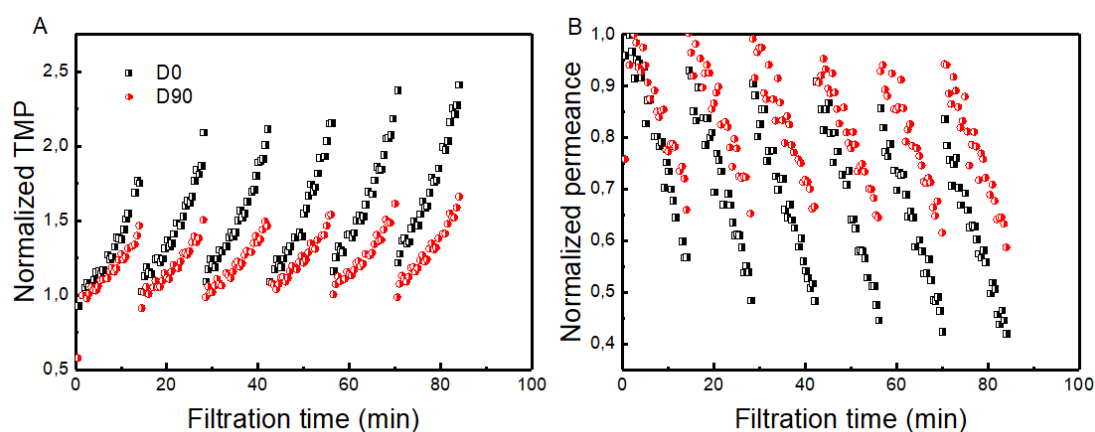


Figure S6.10. Normalized TMP (A) and permeance (B) of D0 and D90 compared at a filtration time of 14 min per cycle. The filtration experiments were conducted at the flux of $110 \text{ Lm}^{-2}\text{h}^{-1}$, O/W emulsion has a pH of 5.6, the oil concentration is 400 mgL^{-1} and the SDS is 100 mgL^{-1} .

S6.8. Effect of SDS concentration on fouling resistance and oil rejection of the membranes

Oil rejection of both membranes was not affected by the SDS concentrations in the feed, despite the oil rejection of D0 (99.5%) being a little lower than that of D90 (100%), as presented in Figure S6.11. The average sizes of oil droplets prepared at various SDS concentrations were similar and much larger than the membrane pore sizes (Figure S6.3), leading to the high rejection of oil for both membranes. The SiC-deposited membrane (D90) probably removed all oil droplets from the emulsions due to the combination of a smaller pore size, compared to D0, and electrostatic repulsion between the oil droplets and membrane surface. The observed oil rejection was much higher than those reported in literature (Virga et al., 2020; Xu et al., 2020) probably due to the smaller pore size of the membranes. Free SDS molecules gave the main contribution to COD in the permeate, since they can easily pass the membrane as they are much smaller as compared with the membrane pore sizes (71 and 54 nm). Therefore, a higher COD concentration was found in the permeate at a higher concentration of SDS in the feed (Figure S6.11).

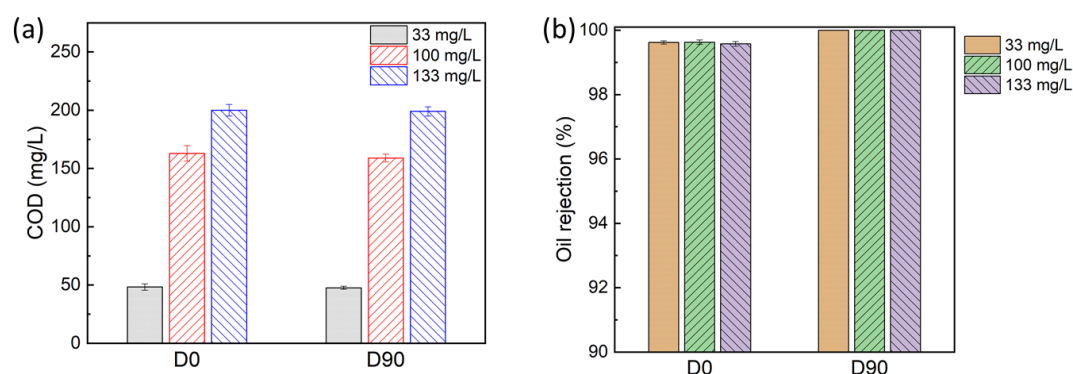


Figure S6.11. COD concentration (a) in the permeate and oil rejection (b) of D0 and D90 at various SDS concentrations. The O/W emulsion filtration experiments were conducted at the constant flux of $100 \text{ Lm}^{-2}\text{h}^{-1}$, oil concentration of 400 mgL^{-1} and pH of 5.6.

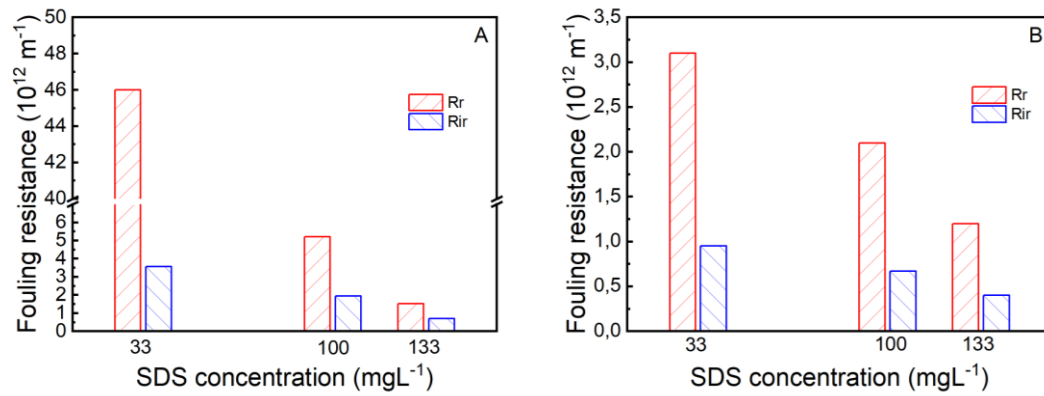


Figure S6.12. Fouling resistance of D0 (A) and D90 (B) challenged with oil emulsions at various SDS concentrations.

S6.9. Permeance of the ceramic membranes with and without SDS adsorption

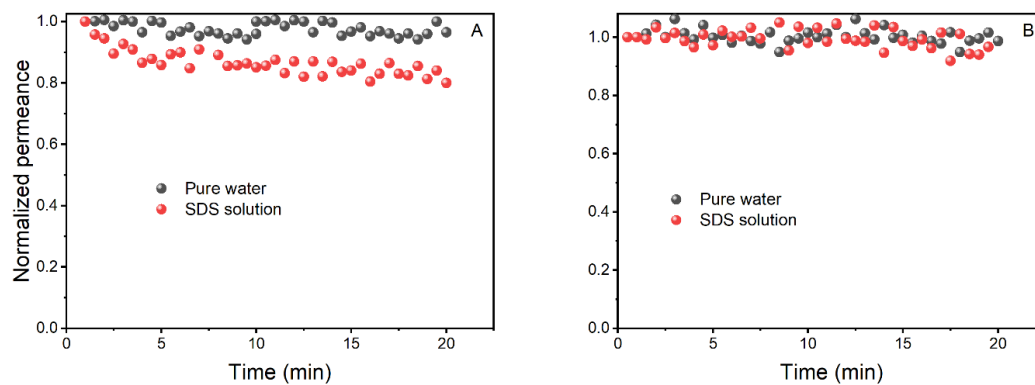


Figure S6.13. Normalized permeance of the ceramic membranes when filtering pure water and SDS solution (100 mg/L): (A) alumina (D0) and (B) SiC-deposited (D90) membranes.

S6.10. Effect of salinity and Ca^{2+} on oil and COD rejection of the membranes

A lower rejection of oil and COD was observed for high salinity emulsions (100 mM NaCl) (Figure S6.14). Due to the decreased oil-water interfacial tension with the increase in emulsion salinity, oil deformation is easier and penetration should occur (Virga et al., 2020).

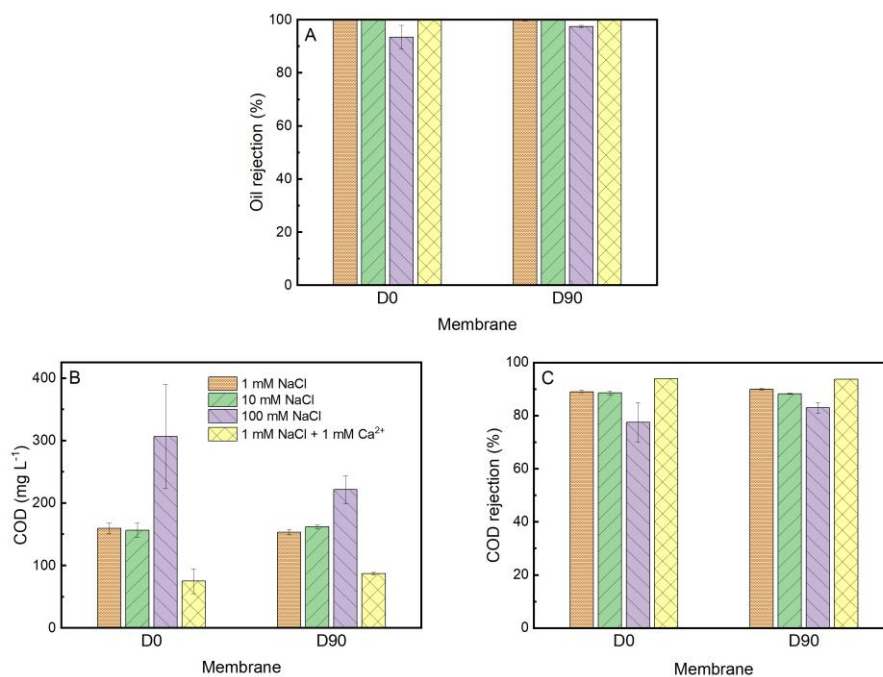


Figure S6.14. (a) Oil rejection, (b) COD and (c) COD rejection of alumina (D0) and SiC-deposited (D90) membranes for 400 mg/L oil emulsion filtration (pH = 5.6, 100 mg/L SDS) with 1 mM NaCl, 10 mM NaCl, 100 mM NaCl and 1 mM NaCl + 1 mM Ca^{2+} , respectively.

S6.11. Chemical cleaning

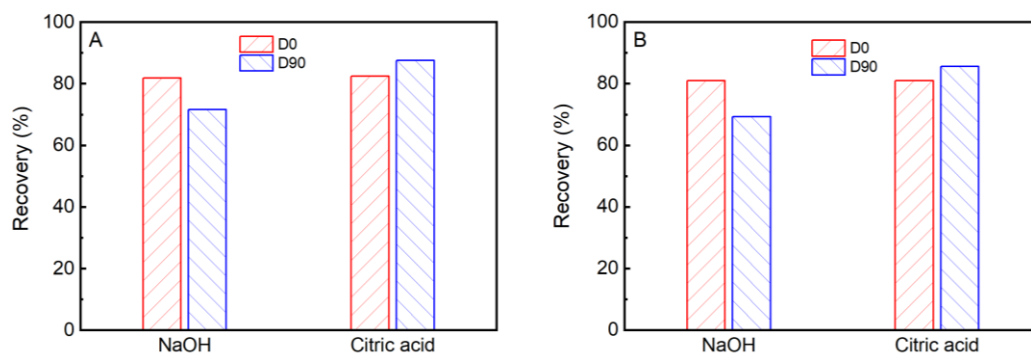


Figure S6.15. Chemical cleaning efficacy of alumina (D0) and SiC-deposited (D90) membranes for emulsion filtration with (A) 100 mM NaCl and (B) 1 mM NaCl + 1 mM Ca²⁺, respectively.

Chapter 7 |

Conclusion and outlook

7.1. General conclusions

Ceramic membrane filtration has been considered to be more effective for oily wastewater treatment, compared to their polymeric counterparts, due to high chemical and thermal stability, higher hydrophilic surface and lower fouling tendency.

In this thesis, we developed a composite SiC-deposited ceramic membrane for oil-in-water (O/W) emulsions separation. Such membranes were successfully deposited on Al₂O₃ supports by low pressure chemical vapor deposition (LPCVD) at low temperatures (750 °C). The fouling of these newly developed SiC-deposited ceramic membranes was closely related to their deposition parameters, filtration conditions (e.g., permeate flux, filtration mode) and feed (O/W emulsion) characteristics. On the one hand, depositing a SiC layer enhanced the repulsive forces between the membrane surface and oil droplets. On the other hand, it reduced the membrane permeance. Therefore, it is important to consider the trade-off between the decrease in permeance and the enhancement of repulsive force between the membrane surface and oil droplets in relation to membrane fouling. In addition, we found that constant flux filtration was more suitable for assessing the membrane fouling for O/W emulsions filtration, especially when membrane modification was involved. Compared to constant pressure filtration, this filtration mode made it easier to observe the effects of both permeance and surface properties on membrane fouling. Furthermore, we experimentally verified that the membrane fouling was strongly affected by the characteristics of O/W emulsions, including surfactant concentration, pH, salinity and concentration of divalent ions.

Overall, we successfully demonstrated that SiC-deposited ceramic membranes have lower fouling characteristics than that of the pristine Al₂O₃ membranes. Although there are still limitations, our SiC-deposited membranes showed the potential for further development.

7.2. Specific conclusions on the formulated research questions

In the following the specific conclusions, based on the formulated research questions of the thesis (see Chapter 1) are highlighted.

7.2.1. Highly permeable SiC-deposited Al₂O₃ ceramic membranes developed by LPCVD

Commercial SiC membranes are generally prepared via solid-state sintering at relatively high temperatures (up to 2000 °C). The production suffers from long production time and high costs. In Chapter 4, we demonstrated a more economical way to produce SiC-deposited ceramic membranes based on low-pressure chemical vapour deposition at a low temperature of 750 °C. The pure water permeance and pore sizes of the SiC-deposited ceramic membranes showed a linear relationship with the deposition time (0-120 min). In addition, the water permeance of the SiC-deposited ceramic membranes was much higher than those reported in literature with a similar pore size. This creates opportunities to develop low-fouling SiC membranes with tuned pore sizes on relatively cheap supports.

7.2.2. Fouling comparison at constant flux and constant transmembrane pressure conditions

Both constant pressure and constant flux filtrations can be applied to evaluate membrane fouling. Constant pressure filtration is more commonly used at laboratory scale as it is easier to build up. In practice, constant flux filtration is preferred to maintain a fixed water production. When it comes to compare membrane fouling before and after modification, it was found that the filtration mode has an influence on the performance.

In Chapter 5, we systematically compared the membrane fouling of a pristine alumina membrane and SiC-deposited membranes at the two filtration modes. In constant pressure filtration mode, membrane fouling was found to be only related to the permeance of the membranes, while the effect of surface properties was not observed. In contrast, in constant flux filtration, the improved surface hydrophilicity and charge of the modified membranes could improve membrane fouling resistance and it was even enhanced when backwash was incorporated. However, extensive modification had a negative impact on membrane fouling due to the huge loss of membrane permeance. Therefore, constant flux filtration with backwash is recommended to evaluate the membrane fouling before and after modification.

7.2.3. Fouling comparison of alumina membranes with and without a silicon carbide deposition in constant flux filtration mode

Membrane fouling is strongly affected by many factors such as feed characteristics, membrane properties and operational parameters (Chapter 2). In addition, oily wastewater normally has a complex composition, and each of them has been considered to have a contribution to membrane fouling.

In Chapter 6, the effects of emulsion chemistry (surfactant concentration, pH, salinity and Ca^{2+}) and operation parameters (permeate flux and filtration time) were comparatively evaluated for alumina and silicon carbide (SiC) deposited ceramic membranes. The SiC-deposited ceramic membranes showed a lower reversible and irreversible fouling when permeate flux was below or around the threshold flux. In addition, it exhibited a higher permeance recovery after physical and chemical cleaning, as compared to the alumina membranes. Increasing sodium dodecyl sulphate (SDS) concentration in the feed decreased the fouling of both membranes, but to a higher extent in the alumina membranes. The double layer adsorption of SDS on the alumina membrane surface was considered to be the main reason for the alleviation of membrane fouling. The fouling of both membranes could be reduced with increasing the pH of the emulsion, due to the enhanced electrostatic repulsion between oil droplets and membrane surface. Because of the screening of surface charge in a high salinity solution (100 mM NaCl), only a small difference in irreversible fouling was observed for alumina and SiC-deposited membranes under these conditions. The presence of Ca^{2+} in the emulsion led to high irreversible fouling of both membranes, because of the compression of diffusion double layer and the interactions between Ca^{2+} and SDS. The low fouling tendency and/or high cleaning efficacy of the SiC-deposited membranes indicated their potential for oily wastewater treatment.

7.3. Outlook

Although the successful deposition of SiC on Al_2O_3 membranes was demonstrated in this thesis, several challenges still remain:

7.3.1. Stability of SiC layer during chemical cleaning process

The fouling of ceramic membranes can be well controlled by regular backwashing in a short period. However, hydraulically irreversible fouling is gradually accumulated in membranes and must be removed by chemical cleaning to recover the membrane

performance and to reduce energy consumption. For this reason, the chemical stability and integrity of membranes is of importance to ensure their long-term filtration performance. For chemical cleaning, acid (e.g., HCl), base (e.g., NaOH) and hypochlorite (NaClO) are generally applied to remove organic and/or inorganic pollutants. Among them, NaClO is the most used reagents for ceramic membrane cleaning in water industry. The SiC layer, deposited by LPCVD, is amorphous, and the stability of such a layer was tested in acid and base solutions in a previous study by Morana (2015). Although the layer was confirmed to be stable in these aggressive solutions, the stability should be further verified, especially using a NaClO solution. If these amorphous SiC layers cannot withstand the NaClO solution, the deposition parameters should be optimized to obtain a crystalline layer at a higher temperature, which is supposedly more stable than their amorphous counterparts.

7.3.2. Developing SiC ultrafiltration and nanofiltration ceramic membranes

Currently, commercial SiC membranes are only made in the microfiltration (MF) range with pore sizes of 200 nm. SiC MF membranes are mainly used to remove large particles such as oil droplets, and they are not effective to reject organic solvents, small molecules and ions present in industrial waste streams. Considering the high hydrophilic and negatively charged surface of SiC, it can be expected that ceramic ultrafiltration (UF) and nanofiltration (NF) membranes, prepared with SiC, could provide a higher rejection and lower fouling property, compared to those currently prepared with ZrO₂ and TiO₂ at similar pore sizes. The technique of LPCVD has shown promising results on the linear tunability on pore sizes of supports in the UF range, which creates opportunities to produce low-fouling SiC UF membranes on various supports.

Atomic layer deposition (ALD), a technique to coat atomic-scale thin films based on self-limiting gas-phase growth mechanism, has also been considered as an potential route for the fabrication and modification of ceramic membranes (Weber et al., 2019; Yang et al., 2018a). In a study by Shang et al. (2017), tight ceramic NF was prepared by atmospheric pressure atomic layer deposition (APALD). This membrane ended up with a molecular weight cut-off (MWCO) of 300 Da, while maintaining a higher water permeability than commercially available ceramic NF membranes. This low MWCO of ceramic NF membranes could not be achieved by the most commonly applied sol-gel method (Kramer, 2019). The coating of SiC thin films with a few nanometer's thickness by ALD has been reported on silicon wafers with the same precursors as

used for LPCVD equipment (Nagasawa and Yamaguchi, 1993; 1994; Yagi and Nagasawa, 1997). Combined with other coating techniques, ALD may thus provide an opportunity to prepare SiC NF membranes for wastewater treatment, organic solvent separation and resource recovery from wastewater.

7.3.3. Ceramic membranes towards produced water treatment

Produced water, a by-product in oil & gas production, is one of the most complicated waste streams in industry. Besides the complex composition, one of the typical characteristic of produced water is the high salinity due to the abundance in ions and salts (Wenzlick and Siefert, 2020). The high salinity of produced water is supposed to negatively affect the electrostatic interactions between the charged foulants and charged membrane surfaces, because of the compressed double layer (Chapter 6). From this perspective, the focus of modifying ceramic membranes for produced water treatment should be on enhancing surface hydrophilicity (e.g., through the use of TiO_2 , ZrO_2 , graphene oxide or SiC) and designing regular surface patterns to induce fluid turbulence rather than surface charge. In addition, to reduce membrane fouling during produced water treatment, dynamic membranes, developed via pre-coating a protective layer on the membrane surface under pressure filtration, are a promising alternative (Anantharaman et al., 2020). This protective layer can effectively inhibit the direct contact of foulants from membrane surface, thereby decreasing membrane fouling. Once the protective layer is fouled, it can easily be removed with chemicals. Afterwards, a new protective layer can be formed in a same way for the next filtration cycle.

References

■ References

- Abadi, S.R.H., Sebzari, M.R., Hemati, M., Rekabdar, F. and Mohammadi, T., (2011). Ceramic membrane performance in microfiltration of oily wastewater. *Desalination* 265 (1-3), 222-228.
- Abadikhah, H., Wang, J.-W., Xu, X. and Agathopoulos, S., (2019). SiO₂ nanoparticles modified Si₃N₄ hollow fiber membrane for efficient oily wastewater microfiltration. *J. Water Process. Eng.* 29, 100799.
- Abadikhah, H., Zou, C.-N., Hao, Y.-Z., Wang, J.-W., Lin, L., Khan, S.A., Xu, X., Chen, C.-S. and Agathopoulos, S., (2018). Application of asymmetric Si₃N₄ hollow fiber membrane for cross-flow microfiltration of oily waste water. *J. Eur. Ceram. Soc.* 38 (13), 4384-4394.
- Abbasi, M., Mirfendereski, M., Nikbakht, M., Golshenas, M. and Mohammadi, T., (2010a). Performance study of mullite and mullite-alumina ceramic MF membranes for oily wastewaters treatment. *Desalination* 259 (1-3), 169-178.
- Abbasi, M., Reza Sebzari, M. and Mohammadi, T., (2011). Enhancement of Oily Wastewater Treatment by Ceramic Microfiltration Membranes using Powder Activated Carbon. *Chem. Eng. Technol.* 34 (8), 1252-1258.
- Abbasi, M., Salahi, A., Mirfendereski, M., Mohammadi, T. and Pak, A., (2010b). Dimensional analysis of permeation flux for microfiltration of oily wastewaters using mullite ceramic membranes. *Desalination* 252 (1-3), 113-119.
- Abbasi, M., Sebzari, M.R. and Mohammadi, T., (2012). Effect of metallic coagulant agents on oily wastewater treatment performance using mullite ceramic MF membranes. *Sep. Sci. Technol.* 47 (16), 2290-2298.
- Abdalla, M., Nasser, M., Kayvani Fard, A., Qiblawey, H., Benamor, A. and Judd, S., (2019). Impact of combined oil-in-water emulsions and particulate suspensions on ceramic membrane fouling and permeability recovery. *Sep. Purif. Technol.* 212, 215-222.
- Adham, S., Hussain, A., Minier-Matar, J., Janson, A. and Sharma, R., (2018). Membrane applications and opportunities for water management in the oil & gas industry. *Desalination* 440, 2-17.
- Aghaeinejad-Meybodi, A. and Ghasemzadeh, K. (2017) Current Trends and Future Developments on (Bio-) Membranes. Basile, A. and Ghasemzadeh, K. (eds), pp. 181-216, Elsevier.
- Ahmad, N.A., Goh, P.S., Abdul Karim, Z. and Ismail, A.F., (2018). Thin Film Composite Membrane for Oily Waste Water Treatment: Recent Advances and Challenges. *Membranes* 8 (4), 86.

■ References

- Al-Harbi, O.A., Khan, M.M. and Ozgur, C., (2017). Improving the performance of silica-based crossflow membranes by surface crystallization for treatment of oily wastewater. *J. Aust. Ceram. Soc.* 53 (2), 883-894.
- Alias, N.H., Jaafar, J., Samitsu, S., Matsuura, T., Ismail, A.F., Othman, M.H.D., Rahman, M.A., Othman, N.H., Abdullah, N., Paiman, S.H., Yusof, N. and Aziz, F., (2019). Photocatalytic nanofiber-coated alumina hollow fiber membranes for highly efficient oilfield produced water treatment. *Chem. Eng. J.* 360, 1437-1446.
- Amin, S.K., Abdallah, H., Roushdy, M. and El-Sherbiny, S., (2016). An overview of production and development of ceramic membranes. *Int. J. Appl. Eng. Res.* 11 (12), 7708-7721.
- Anantharaman, A., Chun, Y., Hua, T., Chew, J.W. and Wang, R., (2020). Pre-deposited dynamic membrane filtration – A review. *Water Res.* 173, 115558.
- Anis, S.F., Lalia, B.S., Lesimple, A., Hashaikeh, R. and Hilal, N., (2021). Superhydrophilic and underwater superoleophobic nano zeolite membranes for efficient oil-in-water nanoemulsion separation. *J. Water Process. Eng.* 40, 101802.
- Asif, M.B. and Zhang, Z., (2021). Ceramic membrane technology for water and wastewater treatment: A critical review of performance, full-scale applications, membrane fouling and prospects. *Chem. Eng. J.* 418, 129481.
- Atallah, C., Mortazavi, S., Tremblay, A.Y. and Doiron, A., (2019a). In-Process Steam Cleaning of Ceramic Membranes Used in the Treatment of Oil Sands Produced Water. *Ind. Eng. Chem. Res.* 58 (33), 15232-15243.
- Atallah, C., Mortazavi, S., Tremblay, A.Y. and Doiron, A., (2019b). Surface-Modified Multi-lumen Tubular Membranes for SAGD-Produced Water Treatment. *Energy Fuels* 33 (6), 5766-5776.
- Atallah, C., Tremblay, A.Y. and Mortazavi, S., (2017). Silane surface modified ceramic membranes for the treatment and recycling of SAGD produced water. *J. Petrol. Sci. Eng.* 157, 349-358.
- Azmi, N.F.A.N., Abdullah, N., Pauzi, M.Z.M., Rahman, M.A., Abas, K.H., Aziz, A.A., Othman, M.H.D., Jaafar, J. and Ismail, A.F., (2019). Highly permeable photo-catalytic mesoporous aluminum oxide membrane for oil emulsion separation. *J. Aust. Ceram. Soc.* 55 (2), 323-335.

■ References

- Barati, N., Husein, M.M. and Azaiez, J., (2020). Modifying ceramic membranes with in situ grown iron oxide nanoparticles and their use for oily water treatment. *J. Membr. Sci.*, 118641.
- Barbosa, A.d.S., Barbosa, A.d.S., Barbosa, T.L.A. and Rodrigues, M.G.F., (2018). Synthesis of zeolite membrane (NaY/alumina): Effect of precursor of ceramic support and its application in the process of oil–water separation. *Sep. Purif. Technol.* 200, 141-154.
- Bayat, A., Mahdavi, H.R., Kazemimoghaddam, M. and Mohammadi, T., (2016). Preparation and characterization of γ -alumina ceramic ultrafiltration membranes for pretreatment of oily wastewater. *Desalin. Water Treat.* 57 (51), 24322-24332.
- Bhave, R. and Fleming, H. (1988) Removal of oily contaminants in wastewater with microporous alumina membranes.
- Blankert, B., Van der Bruggen, B., Childress, A.E., Ghaffour, N. and Vrouwenvelder, J.S., (2021). Potential Pitfalls in Membrane Fouling Evaluation: Merits of Data Representation as Resistance Instead of Flux Decline in Membrane Filtration. *Membranes* 11 (7), 460.
- Bonekamp, B.C. (1996) *Membrane Science and Technology*. Burggraaf, A.J. and Cot, L. (eds), pp. 141-225, Elsevier.
- Cai, Y., Wang, Y., Chen, X., Qiu, M. and Fan, Y., (2015). Modified colloidal sol–gel process for fabrication of titania nanofiltration membranes with organic additives. *J. Membr. Sci.* 476, 432-441.
- Cakl, J., Bauer, I., Doleček, P. and Mikulášek, P., (2000). Effects of backflushing conditions on permeate flux in membrane crossflow microfiltration of oil emulsion. *Desalination* 127 (2), 189-198.
- Chang, H., Li, T., Liu, B., Vidic, R.D., Elimelech, M. and Crittenden, J.C., (2019). Potential and implemented membrane-based technologies for the treatment and reuse of flowback and produced water from shale gas and oil plays: A review. *Desalination* 455, 34-57.
- Chang, H., Liang, H., Qu, F., Liu, B., Yu, H., Du, X., Li, G. and Snyder, S.A., (2017). Hydraulic backwashing for low-pressure membranes in drinking water treatment: A review. *J. Membr. Sci.* 540, 362-380.
- Chang, H., Qu, F., Liu, B., Yu, H., Li, K., Shao, S., Li, G. and Liang, H., (2015). Hydraulic irreversibility of ultrafiltration membrane fouling by humic acid: Effects of membrane properties and backwash water composition. *J. Membr. Sci.* 493, 723-733.

■ References

- Chang, I.-S., Chung, C.-M. and Han, S.-H., (2001). Treatment of oily wastewater by ultrafiltration and ozone. *Desalination* 133 (3), 225-232.
- Chang, Q., Yang, B.W. and Wei, B.G., (2010a). Effects of Wettability and Zeta Potential of Filter Medium on Oil Removal. *Adv. Mat. Res.* 148-149, 58-70.
- Chang, Q., Zhou, J.-e., Wang, Y., Wang, J. and Meng, G., (2010b). Hydrophilic modification of Al₂O₃ microfiltration membrane with nano-sized γ -Al₂O₃ coating. *Desalination* 262 (1), 110-114.
- Chang, Q.B., Zhou, J.E., Wang, Y.Q., Liang, J., Zhang, X.Z., Cerneaux, S., Wang, X., Zhu, Z.W. and Dong, Y.C., (2014). Application of ceramic microfiltration membrane modified by nano-TiO₂ coating in separation of a stable oil-in-water emulsion. *J. Membr. Sci.* 456, 128-133.
- Changmai, M., Pasawan, M. and Purkait, M.K., (2019). Treatment of oily wastewater from drilling site using electrocoagulation followed by microfiltration. *Sep. Purif. Technol.* 210, 463-472.
- Chen, A.S.C., Flynn, J.T., Cook, R.G. and Casaday, A.L., (1991). Removal of Oil, Grease, and Suspended Solids From Produced Water With Ceramic Crossflow Microfiltration. *SPE-20291-PA 6* (02), 131-136.
- Chen, H., Jia, X., Wei, M. and Wang, Y., (2017). Ceramic tubular nanofiltration membranes with tunable performances by atomic layer deposition and calcination. *J. Membr. Sci.* 528, 95-102.
- Chen, L., Feng, Q., Huang, S., Lin, Z., Li, J. and Tian, X., (2020a). A grafted-liquid lubrication strategy to enhance membrane permeability in viscous liquid separation. *J. Membr. Sci.* 610, 118240.
- Chen, M., Heijman, S.G.J., Luiten-Olieman, M.W.J. and Rietveld, L.C., (2022). Oil-in-water emulsion separation: Fouling of alumina membranes with and without a silicon carbide deposition in constant flux filtration mode. *Water Res.* 216, 118267.
- Chen, M., Heijman, S.G.J. and Rietveld, L.C., (2021). State-of-the-Art Ceramic Membranes for Oily Wastewater Treatment: Modification and Application. *Membranes* 11 (11), 888.
- Chen, M., Shang, R., Sberna, P.M., Luiten-Olieman, M.W.J., Rietveld, L.C. and Heijman, S.G.J., (2020b). Highly permeable silicon carbide-alumina ultrafiltration membranes for oil-in-water filtration produced with low-pressure chemical vapor deposition. *Sep. Purif. Technol.* 253, 117496.

■ References

- Chen, M., Zhu, L., Chen, J., Yang, F., Tang, C.Y., Guiver, M.D. and Dong, Y., (2020c). Spinel-based ceramic membranes coupling solid sludge recycling with oily wastewater treatment. *Water Res.* 169, 115180.
- Chen, M.L., Zhu, L., Dong, Y.C., Li, L.L. and Liu, J., (2016a). Waste-to-Resource Strategy To Fabricate Highly Porous Whisker-Structured Mullite Ceramic Membrane for Simulated Oil-in-Water Emulsion Wastewater Treatment. *ACS Sustain. Chem. Eng.* 4 (4), 2098-2106.
- Chen, T., Duan, M. and Fang, S.W., (2016b). Fabrication of novel superhydrophilic and underwater superoleophobic hierarchically structured ceramic membrane and its separation performance of oily wastewater. *Ceram. Int.* 42 (7), 8604-8612.
- Chen, X.W., Hong, L., Xu, Y.F. and Ong, Z.W., (2012). Ceramic Pore Channels with Inducted Carbon Nanotubes for Removing Oil from Water. *ACS Appl. Mater. Interfaces* 4 (4), 1909-1918.
- Chen, Z., Zhang, D., Peng, E. and Ding, J., (2019). 3D-printed ceramic structures with in situ grown whiskers for effective oil/water separation. *Chem. Eng. J.* 373, 1223-1232.
- Ciora, R.J., Fayyaz, B., Liu, P.K.T., Suwanmethanond, V., Mallada, R., Sahimi, M. and Tsotsis, T.T., (2004). Preparation and reactive applications of nanoporous silicon carbide membranes. *Chem. Eng. Sci.* 59 (22), 4957-4965.
- Coca, J., Gutierrez, G. and Benito, J.M. (2011) *Water Purification and Management*. CocaPrados, J. and GutierrezCervello, G. (eds), pp. 1-+.
- Colombo, P., Mera, G., Riedel, R. and Soraru, G.D., (2010). Polymer-derived ceramics: 40 years of research and innovation in advanced ceramics. *J. Am. Ceram. Soc.* 93 (7), 1805-1837.
- Cui, J.Y., Zhang, X.F., Liu, H.O., Liu, S.Q. and Yeung, K.L., (2008). Preparation and application of zeolite/ceramic microfiltration membranes for treatment of oil contaminated water. *J. Membr. Sci.* 325 (1), 420-426.
- Cumming, I., Holdich, R. and Smith, I., (2000). The rejection of oil by microfiltration of a stabilised kerosene/water emulsion. *J. Membr. Sci.* 169 (1), 147-155.
- Dabir, S., Deng, W., Sahimi, M. and Tsotsis, T., (2017). Fabrication of silicon carbide membranes on highly permeable supports. *J. Membr. Sci.* 537, 239-247.
- Darvishzadeh, T. and Priezjev, N.V., (2012). Effects of crossflow velocity and transmembrane pressure on microfiltration of oil-in-water emulsions. *J. Membr. Sci.* 423, 468-476.

■ References

- Das, D., Baitalik, S., Haldar, B., Saha, R. and Kayal, N., (2018). Preparation and characterization of macroporous SiC ceramic membrane for treatment of waste water. *J. Porous Mater.* 25 (4), 1183-1193.
- Das, D., Kayal, N., Marsola, G.A., Damasceno, L.A. and Innocentini, M.D.d.M., (2020a). Permeability behavior of silicon carbide-based membrane and performance study for oily wastewater treatment. *Int. J. Appl. Ceram. Tec.* 17 (3), 893-906.
- Das, D., Nijhuma, K., Gabriel, A.M., Daniel, G.P.F. and Murilo, D.d.M.I., (2020b). Recycling of coal fly ash for fabrication of elongated mullite rod bonded porous SiC ceramic membrane and its application in filtration. *J. Eur. Ceram. Soc.* 40 (5), 2163-2172.
- Das, N. and Maiti, H.S., (2009). Ceramic membrane by tape casting and sol-gel coating for microfiltration and ultrafiltration application. *J. Phys. Chem. Solids* 70 (11), 1395-1400.
- De Lange, R., Hekkink, J., Keizer, K. and Burggraaf, A., (1995). Formation and characterization of supported microporous ceramic membranes prepared by sol-gel modification techniques. *J. Membr. Sci.* 99 (1), 57-75.
- de Leon, A. and Advincula, R.C., (2014). Reversible superhydrophilicity and superhydrophobicity on a lotus-leaf pattern. *ACS Appl. Mater. Interfaces* 6 (24), 22666-22672.
- de Wit, P., Kappert, E.J., Lohaus, T., Wessling, M., Nijmeijer, A. and Benes, N.E., (2015). Highly permeable and mechanically robust silicon carbide hollow fiber membranes. *J. Membr. Sci.* 475, 480-487.
- Dendooven, J., Deduytsche, D., Musschoot, J., Vanmeirhaeghe, R. and Detavernier, C., (2010). Conformality of Al₂O₃ and AlN deposited by plasma-enhanced atomic layer deposition. *J. Electrochem. Soc.* 157 (4), G111-G116.
- Deng, W., Yu, X., Sahimi, M. and Tsotsis, T.T., (2014). Highly permeable porous silicon carbide support tubes for the preparation of nanoporous inorganic membranes. *J. Membr. Sci.* 451, 192-204.
- Dickhout, J., Lammertink, R. and de Vos, W., (2019). Membrane Filtration of Anionic Surfactant Stabilized Emulsions: Effect of Ionic Strength on Fouling and Droplet Adhesion. *Colloids Interfaces* 3 (1), 9.
- Dickhout, J.M., Moreno, J., Biesheuvel, P.M., Boels, L., Lammertink, R.G.H. and de Vos, W.M., (2017). Produced water treatment by membranes: A review from a colloidal perspective. *J. Colloid Interface Sci.* 487, 523-534.

■ References

- Dobson, K.D., Roddick-Lanzilotta, A.D. and McQuillan, A.J., (2000). An in situ infrared spectroscopic investigation of adsorption of sodium dodecylsulfate and of cetyltrimethylammonium bromide surfactants to TiO₂, ZrO₂, Al₂O₃, and Ta₂O₅ particle films from aqueous solutions. *Vib. Spectrosc* 24 (2), 287-295.
- Dong, B.-B., Wang, F.-H., Yang, M.-Y., Yu, J.-L., Hao, L.-Y., Xu, X., Wang, G. and Agathopoulos, S., (2019). Polymer-derived porous SiOC ceramic membranes for efficient oil-water separation and membrane distillation. *J. Membr. Sci.* 579, 111-119.
- Duan, N., Zhang, X., Lu, C., Zhang, Y., Li, C. and Xiong, J., (2022). Effect of rheological properties of AlOOH sol on the preparation of Al₂O₃ nanofiltration membrane by sol-gel method. *Ceram. Int.* 48 (5), 6528-6538.
- Duraisamy, R.T., Beni, A.H. and Henni, A. (2013) *State of the Art Treatment of Produced Water*, InTech, Rijeka, Croatia
- Ebrahimi, M., Ashaghi, K.S., Engel, L., Willershausen, D., Mund, P., Bolduan, P. and Czermak, P., (2009). Characterization and application of different ceramic membranes for the oil-field produced water treatment. *Desalination* 245 (1), 533-540.
- Ebrahimi, M., Kerker, S., Schmitz, O., Schmidt, A.A. and Czermak, P., (2017). Evaluation of the fouling potential of ceramic membrane configurations designed for the treatment of oilfield produced water. *Sep. Sci. Technol.* 53 (2), 349-363.
- Ebrahimi, M., Willershausen, D., Ashaghi, K.S., Engel, L., Placido, L., Mund, P., Bolduan, P. and Czermak, P., (2010). Investigations on the use of different ceramic membranes for efficient oil-field produced water treatment. *Desalination* 250 (3), 991-996.
- Elyassi, B., Sahimi, M. and Tsotsis, T.T., (2007). Silicon carbide membranes for gas separation applications. *J. Membr. Sci.* 288 (1), 290-297.
- Eom, J.-H. and Kim, Y.-W., (2008). Effect of template size on microstructure and strength of porous silicon carbide ceramics. *J. Ceram. Soc. Jpn.* 116 (1358), 1159-1163.
- Eom, J.-H., Kim, Y.-W. and Song, I.-H., (2012). Effects of the initial α -SiC content on the microstructure, mechanical properties, and permeability of macroporous silicon carbide ceramics. *J. Eur. Ceram. Soc.* 32 (6), 1283-1290.
- Eom, J.H., Kim, Y.W., Yun, S.H. and Song, I.H., (2014). Low-cost clay-based membranes for oily wastewater treatment. *J. Ceram. Soc. Jpn.* 122 (1429), 788-794.
- Eray, E., Candelario, V.M., Boffa, V., Safafar, H., Østedgaard-Munck, D.N., Zahrtmann, N., Kadrispahic, H. and Jørgensen, M.K., (2021). A roadmap for the development and

■ References

applications of silicon carbide membranes for liquid filtration: Recent advancements, challenges, and perspectives. *Chem. Eng. J.* 414, 128826.

Facciotti, M., Boffa, V., Magnacca, G., Jørgensen, L.B., Kristensen, P.K., Farsi, A., König, K., Christensen, M.L. and Yue, Y., (2014). Deposition of thin ultrafiltration membranes on commercial SiC microfiltration tubes. *Ceram. Int.* 40 (2), 3277-3285.

Faibish, R.S. and Cohen, Y., (2001a). Fouling-resistant ceramic-supported polymer membranes for ultrafiltration of oil-in-water microemulsions. *J. Membr. Sci.* 185 (2), 129-143.

Faibish, R.S. and Cohen, Y., (2001b). Fouling and rejection behavior of ceramic and polymer-modified ceramic membranes for ultrafiltration of oil-in-water emulsions and microemulsions. *Colloid Surface A* 191 (1), 27-40.

Fakhru'l-Razi, A., Pendashteh, A., Abdullah, L.C., Biak, D.R., Madaeni, S.S. and Abidin, Z.Z., (2009). Review of technologies for oil and gas produced water treatment. *J. Hazard. Mater.* 170 (2-3), 530-551.

Fan, X., Zhao, H., Liu, Y., Quan, X., Yu, H. and Chen, S., (2015). Enhanced permeability, selectivity, and antifouling ability of CNTs/Al₂O₃ membrane under electrochemical assistance. *Environ. Sci. Technol.* 49 (4), 2293-2300.

Fernández, E., Benito, J.M., Pazos, C. and Coca, J., (2005). Ceramic membrane ultrafiltration of anionic and nonionic surfactant solutions. *J. Membr. Sci.* 246 (1), 1-6.

Field, R.W. and Pearce, G.K., (2011). Critical, sustainable and threshold fluxes for membrane filtration with water industry applications. *Adv. Colloid Interface Sci.* 164 (1), 38-44.

Fiksdal, L. and Leiknes, T., (2006). The effect of coagulation with MF/UF membrane filtration for the removal of virus in drinking water. *J. Membr. Sci.* 279 (1-2), 364-371.

Fraga, M.C., Sanches, S., Crespo, J.G. and Pereira, V.J., (2017a). Assessment of a New Silicon Carbide Tubular Honeycomb Membrane for Treatment of Olive Mill Wastewaters. *Membranes (Basel)* 7 (1).

Fraga, M.C., Sanches, S., Pereira, V.J., Crespo, J.G., Yuan, L., Marcher, J., de Yuso, M.V.M., Rodríguez-Castellón, E. and Benavente, J., (2017b). Morphological, chemical surface and filtration characterization of a new silicon carbide membrane. *J. Eur. Ceram. Soc.* 37 (3), 899-905.

■ References

- Fux, G. and Ramon, G.Z., (2017). Microscale Dynamics of Oil Droplets at a Membrane Surface: Deformation, Reversibility, and Implications for Fouling. *Environ. Sci. Technol.* 51 (23), 13842-13849.
- Gao, Y., Zhang, Y., Dudek, M., Qin, J., Øye, G. and Østerhus, S.W., (2020). A multivariate study of backpulsing for membrane fouling mitigation in produced water treatment. *J. Environ. Chem. Eng.*, 104839.
- Garmsiri, E., Rasouli, Y., Abbasi, M. and Izadpanah, A.A., (2017). Chemical cleaning of mullite ceramic microfiltration membranes which are fouled during oily wastewater treatment. *J. Water Process. Eng.* 19, 81-95.
- Ge, J., Jin, Q., Zong, D., Yu, J. and Ding, B., (2018). Biomimetic Multilayer Nanofibrous Membranes with Elaborated Superwettability for Effective Purification of Emulsified Oily Wastewater. *ACS Appl. Mater. Interfaces* 10 (18), 16183-16192.
- Geise, G.M., Lee, H.-S., Miller, D.J., Freeman, B.D., McGrath, J.E. and Paul, D.R., (2010). Water purification by membranes: The role of polymer science. *J. Polym. Sci., Part B: Polym. Phys.* 48 (15), 1685-1718.
- Geng, P. and Chen, G.H., (2016). Magneli Ti₄O₇ modified ceramic membrane for electrically-assisted filtration with antifouling property. *J. Membr. Sci.* 498, 302-314.
- George, S.M., (2010). Atomic Layer Deposition: An Overview. *Chem. Rev.* 110 (1), 111-131.
- Ghidossi, R., Veyret, D., Scotto, J.L., Jalabert, T. and Moulin, P., (2009). Ferry oily wastewater treatment. *Sep. Purif. Technol.* 64 (3), 296-303.
- Goh, P.S. and Ismail, A.F., (2018). A review on inorganic membranes for desalination and wastewater treatment. *Desalination* 434, 60-80.
- Golshenas, A., Sadeghian, Z. and Ashrafizadeh, S.N., (2020). Performance evaluation of a ceramic-based photocatalytic membrane reactor for treatment of oily wastewater. *J. Water Process. Eng.* 36, 101186.
- Gordon, R.G., Hausmann, D., Kim, E. and Shepard, J., (2003). A kinetic model for step coverage by atomic layer deposition in narrow holes or trenches. *Chem. Vapor Deposition* 9 (2), 73-78.
- Gu, Q., Chiang Albert Ng, T., Bao, Y., Yong Ng, H., Ching Tan, S. and Wang, J., (2021). Developing Better Ceramic Membranes for Water and Wastewater Treatment: Where Microstructure Integrates with Chemistry and Functionalities. *Chem. Eng. J.*, 130456.

■ References

- Gu, Q., Ng, T.C.A., Zhang, L., Lyu, Z., Zhang, Z., Ng, H.Y. and Wang, J., (2020). Interfacial diffusion assisted chemical deposition (ID-CD) for confined surface modification of alumina microfiltration membranes toward high-flux and anti-fouling. *Sep. Purif. Technol.* 235, 116177.
- Gu, T. and Zhu, B.-Y., (1990). The S-type isotherm equation for adsorption of nonionic surfactants at the silica gel—water interface. *Colloids Surf.* 44, 81-87.
- Guizard, C. (1996) *Membrane Science and Technology*, pp. 227-258, Elsevier.
- Gupta, R.K., Dunderdale, G.J., England, M.W. and Hozumi, A., (2017). Oil/water separation techniques: a review of recent progresses and future directions. *J. Mater. Chem. A* 5 (31), 16025-16058.
- Ha, H.Y., Nam, S.W., Lim, T.H., Oh, I.-H. and Hong, S.-A., (1996). Properties of the TiO₂ membranes prepared by CVD of titanium tetraisopropoxide. *J. Membr. Sci.* 111 (1), 81-92.
- He, C. and Vidic, R.D., (2016). Application of microfiltration for the treatment of Marcellus Shale flowback water: Influence of floc breakage on membrane fouling. *J. Membr. Sci.* 510, 348-354.
- He, Q., Hu, Y., Li, X., Liu, M., Yu, S. and Gao, C., (2022). Pore size regulation of polyamide composite membrane via a sol-gel process confined within the selective layer. *J. Membr. Sci.* 655, 120581.
- He, Z., Kasemset, S., Kirschner, A.Y., Cheng, Y.H., Paul, D.R. and Freeman, B.D., (2017a). The effects of salt concentration and foulant surface charge on hydrocarbon fouling of a poly(vinylidene fluoride) microfiltration membrane. *Water Res.* 117, 230-241.
- He, Z., Miller, D.J., Kasemset, S., Paul, D.R. and Freeman, B.D., (2017b). The effect of permeate flux on membrane fouling during microfiltration of oily water. *J. Membr. Sci.* 525, 25-34.
- He, Z., Miller, D.J., Kasemset, S., Wang, L., Paul, D.R. and Freeman, B.D., (2016). Fouling propensity of a poly(vinylidene fluoride) microfiltration membrane to several model oil/water emulsions. *J. Membr. Sci.* 514, 659-670.
- Hench, L.L. and West, J.K., (1990). The sol-gel process. *Chem. Rev.* 90 (1), 33-72.
- Hendren, Z.D., Brant, J. and Wiesner, M.R., (2009). Surface modification of nanostructured ceramic membranes for direct contact membrane distillation. *J. Membr. Sci.* 331 (1), 1-10.

■ References

- Heng, L., Yanling, Y., Weijia, G., Xing, L. and Guibai, L., (2008). Effect of pretreatment by permanganate/chlorine on algae fouling control for ultrafiltration (UF) membrane system. *Desalination* 222 (1), 74-80.
- Ho, C.-C. and Zydney, A.L., (2002). Transmembrane pressure profiles during constant flux microfiltration of bovine serum albumin. *J. Membr. Sci.* 209 (2), 363-377.
- Hofs, B., Ogier, J., Vries, D., Beerendonk, E.F. and Cornelissen, E.R., (2011). Comparison of ceramic and polymeric membrane permeability and fouling using surface water. *Sep. Purif. Technol.* 79 (3), 365-374.
- Hoinkis, J., Deowan, S.A., Panten, V., Figoli, A., Huang, R.R. and Drioli, E., (2012). Membrane bioreactor (MBR) technology—a promising approach for industrial water reuse. *Procedia Engineering* 33, 234-241.
- Hong, S. and Elimelech, M., (1997). Chemical and physical aspects of natural organic matter (NOM) fouling of nanofiltration membranes. *J. Membr. Sci.* 132 (2), 159-181.
- Hotza, D., Di Luccio, M., Wilhelm, M., Iwamoto, Y., Bernard, S. and Diniz da Costa, J.C., (2020). Silicon carbide filters and porous membranes: A review of processing, properties, performance and application. *J. Membr. Sci.* 610, 118193.
- Hu, X., Yu, Y., Zhou, J., Wang, Y., Liang, J., Zhang, X., Chang, Q. and Song, L., (2015). The improved oil/water separation performance of graphene oxide modified Al₂O₃ microfiltration membrane. *J. Membr. Sci.* 476, 200-204.
- Hua, F.L., Tsang, Y.F., Wang, Y.J., Chan, S.Y., Chua, H. and Sin, S.N., (2007). Performance study of ceramic microfiltration membrane for oily wastewater treatment. *Chem. Eng. J.* 128 (2-3), 169-175.
- Huang, A., Chen, L.H., Kan, C.C., Hsu, T.Y., Wu, S.E., Jana, K.K. and Tung, K.L., (2018a). Fabrication of zinc oxide nanostructure coated membranes for efficient oil/water separation. *J. Membr. Sci.* 566, 249-257.
- Huang, A. and Yang, W., (2007). Hydrothermal synthesis of uniform and dense NaA zeolite membrane in the electric field. *Microporous Mesoporous Mater.* 102 (1-3), 58-69.
- Huang, B.-C., Guan, Y.-F., Chen, W. and Yu, H.-Q., (2017). Membrane fouling characteristics and mitigation in a coagulation-assisted microfiltration process for municipal wastewater pretreatment. *Water Res.* 123, 216-223.

■ References

- Huang, S., Ras, R.H.A. and Tian, X., (2018b). Antifouling membranes for oily wastewater treatment: Interplay between wetting and membrane fouling. *Curr. Opin. Colloid Interface Sci.* 36, 90-109.
- Huang, Y., Li, H., Wang, L., Qiao, Y., Tang, C., Jung, C., Yoon, Y., Li, S. and Yu, M., (2015). Ultrafiltration Membranes with Structure-Optimized Graphene-Oxide Coatings for Antifouling Oil/Water Separation. *Adv. Mater. Interfaces* 2 (2), 1400433.
- Hube, S., Wang, J., Sim, L.N., Ólafsdóttir, D., Chong, T.H. and Wu, B., (2021). Fouling and mitigation mechanisms during direct microfiltration and ultrafiltration of primary wastewater. *J. Water Process. Eng.* 44, 102331.
- Hyun, S.H. and Kim, G.T., (1997). Synthesis of Ceramic Microfiltration Membranes for Oil/Water Separation. *Sep. Sci. Technol.* 32 (18), 2927-2943.
- Ibrahim, S., Ang, H.-M. and Wang, S., (2009). Removal of emulsified food and mineral oils from wastewater using surfactant modified barley straw. *Bioresour. Technol.* 100 (23), 5744-5749.
- Iliescu, C., Chen, B., Poenar, D.P. and Lee, Y.Y., (2008a). PECVD amorphous silicon carbide membranes for cell culturing. *Sensor. Actuat. B: Chem.* 129 (1), 404-411.
- Iliescu, C., Chen, B., Wei, J. and Pang, A.J., (2008b). Characterisation of silicon carbide films deposited by plasma-enhanced chemical vapour deposition. *Thin Solid Films* 516 (16), 5189-5193.
- Janknecht, P., Lopes, A.D. and Mendes, A.M., (2004). Removal of industrial cutting oil from oil emulsions by polymeric ultra- and microfiltration membranes. *Environ. Sci. Technol.* 38 (18), 4878-4883.
- Jarvis, P., Carra, I., Jafari, M. and Judd, S.J., (2022). Ceramic vs polymeric membrane implementation for potable water treatment. *Water Res.*, 118269.
- Jepsen, K., Bram, M., Pedersen, S. and Yang, Z., (2018). Membrane Fouling for Produced Water Treatment: A Review Study From a Process Control Perspective. *Water* 10 (7), 847.
- Jiang, Q., Rentschler, J., Perrone, R. and Liu, K., (2013). Application of ceramic membrane and ion-exchange for the treatment of the flowback water from Marcellus shale gas production. *J. Membr. Sci.* 431, 55-61.
- Jiang, Q., Wang, Y., Xie, Y., Zhou, M., Gu, Q., Zhong, Z. and Xing, W., (2022). Silicon carbide microfiltration membranes for oil-water separation: Pore structure-dependent wettability matters. *Water Res.*, 118270.

■ References

- Jiang, Q., Zhou, J., Miao, Y., Yang, S., Zhou, M., Zhong, Z. and Xing, W., (2020). Lower-temperature preparation of SiC ceramic membrane using zeolite residue as sintering aid for oil-in-water separation. *J. Membr. Sci.* 610, 118238.
- Jiao, K., Yu, X., Yuan, Z., Zhang, Y. and Liu, J., (2019). Enhanced filtration performance of Al₂O₃-SiC porous ceramic composite tube depending on microstructure and surface properties. *Desalin. Water Treat.* 150, 99-104.
- Jiménez, S., Micó, M.M., Arnaldos, M., Medina, F. and Contreras, S., (2018). State of the art of produced water treatment. *Chemosphere* 192, 186-208.
- Jin, Z., Shen, Y., Chen, X., Qiu, M. and Fan, Y., (2023). Construction of high-performance Ce-doped TiO₂ tight UF membranes for protein separation. *Appl. Surf. Sci.* 610, 155468.
- Jou, J.-D., Yoshida, W. and Cohen, Y., (1999). A novel ceramic-supported polymer membrane for pervaporation of dilute volatile organic compounds. *J. Membr. Sci.* 162 (1), 269-284.
- K. Shams Ashaghi, M.E., and P. Czermak, (2007). Ceramic Ultra- and Nanofiltration Membranes Water Treatment: A Mini Review. *Open Environ. Sci.* 1 (1).
- Kajitvichyanukul, P., Hung, Y.T. and Wang, L.K. (2011) *Membrane Technologies for Oil-Water Separation*, Humana Press, Totowa, NJ.
- Kang, H., Sun, Y., Li, Y., Qin, W. and Wu, X., (2020). Mechanically Robust Fish-Scale Microstructured TiO₂-Coated Stainless Steel Mesh by Atomic Layer Deposition for Oil-Water Separation. *Ind. Eng. Chem. Res.* 59 (48), 21088-21096.
- Kasemset, S., He, Z., Miller, D.J., Freeman, B.D. and Sharma, M.M., (2016). Effect of polydopamine deposition conditions on polysulfone ultrafiltration membrane properties and threshold flux during oil/water emulsion filtration. *Polymer* 97, 247-257.
- Kayvani Fard, A., Bukenhoudt, A., Jacobs, M., McKay, G. and Atieh, M.A., (2018a). Novel hybrid ceramic/carbon membrane for oil removal. *J. Membr. Sci.* 559, 42-53.
- Kayvani Fard, A., McKay, G., Buekenhoudt, A., Al Sulaiti, H., Motmans, F., Khraisheh, M. and Atieh, M., (2018b). *Inorganic Membranes: Preparation and Application for Water Treatment and Desalination*. *Materials (Basel)* 11 (1).
- Keramati, H., Saidi, M.H. and Zabetian, M., (2016). Stabilization of the Suspension of Zirconia Microparticle Using the Nanoparticle Halos Mechanism: Zeta Potential Effect. *J. Dispersion Sci. Technol.* 37 (1), 6-13.

■ References

- Khatib, S.J. and Oyama, S.T., (2013). Silica membranes for hydrogen separation prepared by chemical vapor deposition (CVD). *Sep. Purif. Technol.* 111, 20-42.
- Kim, E.-S., Hwang, G., Gamal El-Din, M. and Liu, Y., (2012). Development of nanosilver and multi-walled carbon nanotubes thin-film nanocomposite membrane for enhanced water treatment. *J. Membr. Sci.* 394-395, 37-48.
- Kim, J.J., Chinen, A. and Ohya, H., (1997). Membrane microfiltration oily water. *Macromolecular Symposia* 118, 413-418.
- Kim, S.C., Yeom, H.J., Kim, Y.W., Song, I.H. and Ha, J.H., (2017). Processing of alumina-coated glass-bonded silicon carbide membranes for oily wastewater treatment. *Int. J. Appl. Ceram. Tec.* 14 (4), 692-702.
- Kimura, K., Hane, Y., Watanabe, Y., Amy, G. and Ohkuma, N., (2004). Irreversible membrane fouling during ultrafiltration of surface water. *Water Res.* 38 (14), 3431-3441.
- Kimura, K., Tanaka, K. and Watanabe, Y., (2014). Microfiltration of different surface waters with/without coagulation: Clear correlations between membrane fouling and hydrophilic biopolymers. *Water Res.* 49, 434-443.
- Kirschner, A.Y., Chang, C.-C., Kasemset, S., Emrick, T. and Freeman, B.D., (2017). Fouling-resistant ultrafiltration membranes prepared via co-deposition of dopamine/zwitterion composite coatings. *J. Membr. Sci.* 541, 300-311.
- Kirschner, A.Y., Cheng, Y.-H., Paul, D.R., Field, R.W. and Freeman, B.D., (2019). Fouling mechanisms in constant flux crossflow ultrafiltration. *J. Membr. Sci.* 574, 65-75.
- Koltuniewicz, A.B. and Field, R.W., (1996). Process factors during removal of oil-in-water emulsions with cross-flow microfiltration. *Desalination* 105 (1-2), 79-89.
- König, K., Boffa, V., Buchbjerg, B., Farsi, A., Christensen, M.L., Magnacca, G. and Yue, Y., (2014). One-step deposition of ultrafiltration SiC membranes on macroporous SiC supports. *J. Membr. Sci.* 472, 232-240.
- Kosmulski, M., (2011). The pH-dependent surface charging and points of zero charge: V. Update. *J. Colloid Interface Sci.* 353 (1), 1-15.
- Kouchaki Shalmani, A., ElSherbiny, I.M.A. and Panglisch, S., (2020). Application-oriented mini-plant experiments using non-conventional model foulants to evaluate new hollow fiber membrane materials. *Sep. Purif. Technol.* 251, 117345.

■ References

- Krajewski, S.R., Kujawski, W., Bukowska, M., Picard, C. and Larbot, A., (2006). Application of fluoroalkylsilanes (FAS) grafted ceramic membranes in membrane distillation process of NaCl solutions. *J. Membr. Sci.* 281 (1-2), 253-259.
- Kramer, F. (2019) Ceramic nanofiltration for direct filtration of municipal sewage. Doctoral thesis, Delft University of Technology, Delft, The Netherlands.
- Kramer, F.C., Shang, R., Scherrenberg, S.M., Rietveld, L.C. and Heijman, S.J.G., (2019). Quantifying defects in ceramic tight ultra- and nanofiltration membranes and investigating their robustness. *Sep. Purif. Technol.* 219, 159-168.
- Kukli, K., Salmi, E., Jõgiaas, T., Zabels, R., Schuisky, M., Westlinder, J., Mizohata, K., Ritala, M. and Leskelä, M., (2016). Atomic layer deposition of aluminum oxide on modified steel substrates. *Surf. Coat. Technol.* 304 (Supplement C), 1-8.
- Kumar, K. and Chowdhury, A. (2020) Encyclopedia of Renewable and Sustainable Materials. Hashmi, S. and Choudhury, I.A. (eds), pp. 949-964, Elsevier, Oxford.
- Kumar, R.V., Ghoshal, A.K. and Pugazhenti, G., (2015). Elaboration of novel tubular ceramic membrane from inexpensive raw materials by extrusion method and its performance in microfiltration of synthetic oily wastewater treatment. *J. Membr. Sci.* 490, 92-102.
- Lee, J., Chae, H.-R., Won, Y.J., Lee, K., Lee, C.-H., Lee, H.H., Kim, I.-C. and Lee, J.-m., (2013). Graphene oxide nanoplatelets composite membrane with hydrophilic and antifouling properties for wastewater treatment. *J. Membr. Sci.* 448, 223-230.
- Lee, J., Kim, I.S., Hwang, M.-H. and Chae, K.-J., (2020). Atomic layer deposition and electrospinning as membrane surface engineering methods for water treatment: a short review. *Environ. Sci. Water Res. Technol.* 6 (7), 1765-1785.
- Lee, K. and Neff, J. (2011) Produced water: environmental risks and advances in mitigation technologies, Springer.
- Lee, L.L. and Tsai, D.S., (1998). Silicon carbide membranes modified by chemical vapor deposition using species of low sticking coefficients in a silane/acetylene reaction system. *J. Am. Ceram. Soc.* 81 (1), 159-165.
- Lee, M., Wu, Z. and Li, K. (2015) Advances in membrane technologies for water treatment, pp. 43-82, Elsevier.
- Lee, S.-J. and Kim, J.-H., (2014). Differential natural organic matter fouling of ceramic versus polymeric ultrafiltration membranes. *Water Res.* 48, 43-51.

■ References

- Lefebvre, O. and Moletta, R., (2006). Treatment of organic pollution in industrial saline wastewater: a literature review. *Water Res.* 40 (20), 3671-3682.
- Lehman, S.G. and Liu, L., (2009). Application of ceramic membranes with pre-ozonation for treatment of secondary wastewater effluent. *Water Res.* 43 (7), 2020-2028.
- Leskelä, M. and Ritala, M., (2003). Atomic Layer Deposition Chemistry: Recent Developments and Future Challenges. *Angew. Chem. Int. Ed.* 42 (45), 5548-5554.
- Li, C., Sun, W., Lu, Z., Ao, X. and Li, S., (2020). Ceramic nanocomposite membranes and membrane fouling: A review. *Water Res.* 175, 115674.
- Li, F., Li, L., Liao, X. and Wang, Y., (2011). Precise pore size tuning and surface modifications of polymeric membranes using the atomic layer deposition technique. *J. Membr. Sci.* 385-386, 1-9.
- Li, F., Yang, Y., Fan, Y., Xing, W. and Wang, Y., (2012). Modification of ceramic membranes for pore structure tailoring: The atomic layer deposition route. *J. Membr. Sci.* 397, 17-23.
- Li, L., Gao, E.-Z., Abadikhah, H., Wang, J.-W., Hao, L.-Y., Xu, X. and Agathopoulos, S., (2018). Preparation of a Porous, Sintered and Reaction-Bonded Si₃N₄ (SRBSN) Planar Membrane for Filtration of an Oil-in-Water Emulsion with High Flux Performance. *Materials* 11 (6), 990.
- Li, L., Liu, N., McPherson, B. and Lee, R., (2008). Influence of counter ions on the reverse osmosis through MFI zeolite membranes: implications for produced water desalination. *Desalination* 228 (1-3), 217-225.
- Li, R., Li, N., Hou, J., Yu, Y., Liang, L., Yan, B. and Chen, G., (2021). Aquatic environment remediation by atomic layer deposition-based multi-functional materials: A review. *J. Hazard. Mater.* 402, 123513.
- Lin, T., Pan, S., Chen, W. and Bin, S., (2013). Role of pre-oxidation, using potassium permanganate, for mitigating membrane fouling by natural organic matter in an ultrafiltration system. *Chem. Eng. J.* 223, 487-496.
- Lin, Y.-M. and Rutledge, G.C., (2018). Separation of oil-in-water emulsions stabilized by different types of surfactants using electrospun fiber membranes. *J. Membr. Sci.* 563, 247-258.
- Lin, Y. and Burggraaf, A., (1993). Experimental studies on pore size change of porous ceramic membranes after modification. *J. Membr. Sci.* 79 (1), 65-82.

■ References

- Lin, Y.M., Song, C. and Rutledge, G.C., (2019). Functionalization of Electrospun Membranes with Polyelectrolytes for Separation of Oil-In-Water Emulsions. *Adv. Mater. Interfaces* 6 (23), 1901285.
- Liu, M., Wang, S., Wei, Z., Song, Y. and Jiang, L., (2009). Bioinspired design of a superoleophobic and low adhesive water/solid interface. *Adv. Mater.* 21 (6), 665-669.
- Liu, N., Li, L., McPherson, B. and Lee, R., (2008). Removal of organics from produced water by reverse osmosis using MFI-type zeolite membranes. *J. Membr. Sci.* 325 (1), 357-361.
- Liu, R., Raman, A.K.Y., Shaik, I., Aichele, C. and Kim, S.-J., (2018). Inorganic microfiltration membranes incorporated with hydrophilic silica nanoparticles for oil-in-water emulsion separation. *J. Water Process. Eng.* 26, 124-130.
- Lobo, A., Cambiella, Á., Benito, J.M., Pazos, C. and Coca, J., (2006). Ultrafiltration of oil-in-water emulsions with ceramic membranes: Influence of pH and crossflow velocity. *J. Membr. Sci.* 278 (1-2), 328-334.
- Loganathan, K., Chelme-Ayala, P. and El-Din, M.G., (2015). Effects of different pretreatments on the performance of ceramic ultrafiltration membrane during the treatment of oil sands tailings pond recycle water: a pilot-scale study. *J. Environ. Manage.* 151, 540-549.
- Lou, Y., Liu, G., Liu, S., Shen, J. and Jin, W., (2014). A facile way to prepare ceramic-supported graphene oxide composite membrane via silane-graft modification. *Appl. Surf. Sci.* 307, 631-637.
- Lu, D., Zhang, T., Gutierrez, L., Ma, J. and Croué, J.-P., (2016a). Influence of Surface Properties of Filtration-Layer Metal Oxide on Ceramic Membrane Fouling during Ultrafiltration of Oil/Water Emulsion. *Environ. Sci. Technol.* 50 (9), 4668-4674.
- Lu, D., Zhang, T. and Ma, J., (2015a). Ceramic membrane fouling during ultrafiltration of oil/water emulsions: roles played by stabilization surfactants of oil droplets. *Environ. Sci. Technol.* 49 (7), 4235-4244.
- Lu, D.W., Cheng, W., Zhang, T., Lu, X.L., Liu, Q.L., Jiang, J. and Ma, J., (2016b). Hydrophilic Fe₂O₃ dynamic membrane mitigating fouling of support ceramic membrane in ultrafiltration of oil/water emulsion. *Sep. Purif. Technol.* 165, 1-9.
- Lu, D.W., Zhang, T. and Ma, J., (2015b). Ceramic Membrane Fouling during Ultrafiltration of Oil/Water Emulsions: Roles Played by Stabilization Surfactants of Oil Droplets. *Environ. Sci. Technol.* 49 (7), 4235-4244.

■ References

- Lu, Y., Ganguli, R., Drewien, C.A., Anderson, M.T., Brinker, C.J., Gong, W., Guo, Y., Soyez, H., Dunn, B. and Huang, M.H., (1997). Continuous formation of supported cubic and hexagonal mesoporous films by sol-gel dip-coating. *Nature* 389 (6649), 364.
- Luo, J., Ding, L., Wan, Y. and Jaffrin, M.Y., (2012). Threshold flux for shear-enhanced nanofiltration: Experimental observation in dairy wastewater treatment. *J. Membr. Sci.* 409-410, 276-284.
- Lyu, Z., Ng, T.C.A., Tran-Duc, T., Lim, G.J.H., Gu, Q., Zhang, L., Zhang, Z., Ding, J., Phan-Thien, N., Wang, J. and Ng, H.Y., (2020). 3D-printed surface-patterned ceramic membrane with enhanced performance in crossflow filtration. *J. Membr. Sci.* 606, 118138.
- Ma, H., Bowman, C.N. and Davis, R.H., (2000). Membrane fouling reduction by backpulsing and surface modification. *J. Membr. Sci.* 173 (2), 191-200.
- Ma, H., Hakim, L.F., Bowman, C.N. and Davis, R.H., (2001). Factors affecting membrane fouling reduction by surface modification and backpulsing. *J. Membr. Sci.* 189 (2), 255-270.
- Maguire-Boyle, S.J., Huseman, J.E., Ainscough, T.J., Oatley-Radcliffe, D.L., Alabdulkarem, A.A., Al-Mojil, S.F. and Barron, A.R., (2017). Superhydrophilic Functionalization of Microfiltration Ceramic Membranes Enables Separation of Hydrocarbons from Frac and Produced Water. *Sci. Rep.* 7 (1), 12267.
- Mahmodi, G., Ronte, A., Dangwal, S., Wagle, P., Echeverria, E., Sengupta, B., Vatanpour, V., Mclroy, D.N., Ramsey, J.D. and Kim, S.-J., (2022). Improving antifouling property of alumina microfiltration membranes by using atomic layer deposition technique for produced water treatment. *Desalination* 523, 115400.
- Mantel, T., Jacki, E. and Ernst, M., (2021). Electrosorptive removal of organic water constituents by positively charged electrically conductive UF membranes. *Water Res.* 201, 117318.
- Mao, H., Bu, J., Da, X., Chen, X., Qiu, M., Verweij, H. and Fan, Y., (2020). High-performance self-cleaning piezoelectric membrane integrated with in-situ ultrasound for wastewater treatment. *J. Eur. Ceram. Soc.* 40 (10), 3632-3641.
- Mao, H., Bu, J., Qiu, M., Ding, D., Chen, X., Verweij, H. and Fan, Y., (2019). PZT/Ti composite piezoceramic membranes for liquid filtration: Fabrication and self-cleaning properties. *J. Membr. Sci.* 581, 28-37.

■ References

- Mao, H., Qiu, M., Bu, J., Chen, X., Verweij, H. and Fan, Y., (2018). Self-Cleaning Piezoelectric Membrane for Oil-in-Water Separation. *ACS Appl. Mater. Interfaces* 10 (21), 18093-18103.
- Marchese, J., Ochoa, N.A., Pagliero, C. and Almandoz, C., (2000). Pilot-Scale Ultrafiltration of an Emulsified Oil Wastewater. *Environ. Sci. Technol.* 34 (14), 2990-2996.
- Martin, C.J. and Cherry, T.M., (1898). The nature of the antagonism between toxins and antitoxins. *Proc. R. Soc. Lond.* 63 (389-400), 420-432.
- Marzouk, S.S., Naddeo, V., Banat, F. and Hasan, S.W., (2021). Preparation of TiO₂/SiO₂ ceramic membranes via dip coating for the treatment of produced water. *Chemosphere* 273, 129684.
- Matos, M., Gutiérrez, G., Lobo, A., Coca, J., Pazos, C. and Benito, J.M., (2016). Surfactant effect on the ultrafiltration of oil-in-water emulsions using ceramic membranes. *J. Membr. Sci.* 520, 749-759.
- Mavrov, V., Chmiel, H., Kluth, J., Meier, J., Heinrich, F., Ames, P., Backes, K. and Usner, P., (1998). Comparative study of different MF and UF membranes for drinking water production. *Desalination* 117 (1-3), 189-196.
- Mavukkandy, M.O., McBride, S.A., Warsinger, D.M., Dizge, N., Hasan, S.W. and Arafat, H.A., (2020). Thin film deposition techniques for polymeric membranes– A review. *J. Membr. Sci.* 610, 118258.
- Mekonnen, M.M. and Hoekstra, A.Y., (2016). Four billion people facing severe water scarcity. *Sci. Adv.* 2 (2), e1500323.
- Meng, G., Ma, G., Ma, Q., Peng, R. and Liu, X., (2007). Ceramic membrane fuel cells based on solid proton electrolytes. *Solid State Ion.* 178 (7), 697-703.
- Mestre, S., Gozalbo, A., Lorente-Ayza, M.M. and Sánchez, E., (2019). Low-cost ceramic membranes: A research opportunity for industrial application. *J. Eur. Ceram. Soc.* 39 (12), 3392-3407.
- Miller, D.J., Dreyer, D.R., Bielawski, C.W., Paul, D.R. and Freeman, B.D., (2017). Surface Modification of Water Purification Membranes. *Angew. Chem. Int. Ed.* 56 (17), 4662-4711.
- Miller, D.J., Kasemset, S., Paul, D.R. and Freeman, B.D., (2014a). Comparison of membrane fouling at constant flux and constant transmembrane pressure conditions. *J. Membr. Sci.* 454, 505-515.

■ References

- Miller, D.J., Kasemset, S., Wang, L., Paul, D.R. and Freeman, B.D., (2014b). Constant flux crossflow filtration evaluation of surface-modified fouling-resistant membranes. *J. Membr. Sci.* 452, 171-183.
- Mohammadi, T., Pak, A., Karbassian, M. and Golshan, M., (2004). Effect of operating conditions on microfiltration of an oil-water emulsion by a kaolin membrane. *Desalination* 168, 201-205.
- Molinari, R., Grande, C., Drioli, E., Palmisano, L. and Schiavello, M., (2001). Photocatalytic membrane reactors for degradation of organic pollutants in water. *Catal. Today* 67 (1), 273-279.
- Monash, P. and Pugazhenthii, G., (2011). Effect of TiO₂ addition on the fabrication of ceramic membrane supports: A study on the separation of oil droplets and bovine serum albumin (BSA) from its solution. *Desalination* 279 (1-3), 104-114.
- Morana, B. (2015) Silicon carbide thin films for MEMS nanoreactors for in-situ transmission electron microscopy. Doctoral thesis, Delft University of Technology, Delft, The Netherlands.
- Morana, B., Pandraud, G., Creemer, J.F. and Sarro, P.M., (2013). Characterization of LPCVD amorphous silicon carbide (a-SiC) as material for electron transparent windows. *Mater. Chem. Phys.* 139 (2), 654-662.
- Motta Cabrera, S., Winnubst, L., Richter, H., Voigt, I. and Nijmeijer, A., (2021). Industrial application of ceramic nanofiltration membranes for water treatment in oil sands mines. *Sep. Purif. Technol.* 256, 117821.
- Mozia, S., (2010). Photocatalytic membrane reactors (PMRs) in water and wastewater treatment. A review. *Sep. Purif. Technol.* 73 (2), 71-91.
- Mueller, J., Cen, Y. and Davis, R.H., (1997). Crossflow microfiltration of oily water. *J. Membr. Sci.* 129 (2), 221-235.
- Munirasu, S., Haija, M.A. and Banat, F., (2016). Use of membrane technology for oil field and refinery produced water treatment—A review. *Process Saf. Environ.* 100, 183-202.
- Murić, A., Petrinić, I. and Christensen, M.L., (2014). Comparison of ceramic and polymeric ultrafiltration membranes for treating wastewater from metalworking industry. *Chem. Eng. J.* 255, 403-410.
- Nady, N., Franssen, M.C.R., Zuilhof, H., Eldin, M.S.M., Boom, R. and Schroën, K., (2011). Modification methods for poly(arylsulfone) membranes: A mini-review focusing on surface modification. *Desalination* 275 (1-3), 1-9.

■ References

- Nagasawa, H., Omura, T., Asai, T., Kanezashi, M. and Tsuru, T., (2020). Filtration of surfactant-stabilized oil-in-water emulsions with porous ceramic membranes: Effects of membrane pore size and surface charge on fouling behavior. *J. Membr. Sci.* 610, 118210.
- Nagasawa, H. and Yamaguchi, Y.-i., (1993). Atomic level epitaxy of 3C-SiC by low pressure vapour deposition with alternating gas supply. *Thin Solid Films* 225 (1), 230-234.
- Nagasawa, H. and Yamaguchi, Y.-i., (1994). Mechanisms of SiC growth by alternate supply of SiH₂Cl₂ and C₂H₂. *Appl. Surf. Sci.* 82-83, 405-409.
- Nair, B.N., Yamaguchi, T., Okubo, T., Suematsu, H., Keizer, K. and Nakao, S.-I., (1997). Sol-gel synthesis of molecular sieving silica membranes. *J. Membr. Sci.* 135 (2), 237-243.
- Nandi, B., Uppaluri, R. and Purkait, M., (2009). Treatment of oily waste water using low-cost ceramic membrane: Flux decline mechanism and economic feasibility. *Sep. Sci. Technol.* 44 (12), 2840-2869.
- Nandi, B.K., Moparthi, A., Uppaluri, R. and Purkait, M.K., (2010). Treatment of oily wastewater using low cost ceramic membrane: Comparative assessment of pore blocking and artificial neural network models. *Chem. Eng. Res. Des.* 88 (7A), 881-892.
- Nazzal, F.F. and Wiesner, M.R., (1996). Microfiltration of oil-in-water emulsions. *Water Environ. Res* 68 (7), 1187-1191.
- Nguyen, L.A.T., Schwarze, M. and Schomäcker, R., (2015). Adsorption of non-ionic surfactant from aqueous solution onto various ultrafiltration membranes. *J. Membr. Sci.* 493, 120-133.
- Nguyen, T.-K., Phan, H.-P., Kamble, H., Vadivelu, R., Dinh, T., Iacopi, A., Walker, G., Hold, L., Nguyen, N.-T. and Dao, D.V., (2017). Superior Robust Ultrathin Single-Crystalline Silicon Carbide Membrane as a Versatile Platform for Biological Applications. *ACS Appl. Mater. Interfaces* 9 (48), 41641-41647.
- Nomura, M., Seshimo, M., Aida, H., Nakatani, K., Gopalakrishnan, S., Sugawara, T., Ishikawa, T., Kawamura, M. and Nakao, S.-i., (2006). Preparation of a catalyst composite silica membrane reactor for steam reforming reaction by using a counterdiffusion CVD method. *Ind. Eng. Chem. Res.* 45 (11), 3950-3954.
- Nyamutswa, L.T., Zhu, B., Collins, S.F., Navaratna, D. and Duke, M.C., (2020). Light conducting photocatalytic membrane for chemical-free fouling control in water treatment. *J. Membr. Sci.* 604, 118018.

■ References

- Obaid, M., Mohamed, H.O., Yasin, A.S., Yassin, M.A., Fadali, O.A., Kim, H. and Barakat, N.A.M., (2017). Under-oil superhydrophilic wetted PVDF electrospun modified membrane for continuous gravitational oil/water separation with outstanding flux. *Water Res.* 123, 524-535.
- Ognier, S., Wisniewski, C. and Grasmick, A., (2004). Membrane bioreactor fouling in sub-critical filtration conditions: a local critical flux concept. *J. Membr. Sci.* 229 (1-2), 171-177.
- Ordóñez, R., Hermosilla, D., San Pío, I. and Blanco, Á., (2011). Evaluation of MF and UF as pretreatments prior to RO applied to reclaim municipal wastewater for freshwater substitution in a paper mill: A practical experience. *Chem. Eng. J.* 166 (1), 88-98.
- Padaki, M., Murali, R.S., Abdullah, M.S., Misdan, N., Moslehyani, A., Kassim, M.A., Hilal, N. and Ismail, A.F., (2015). Membrane technology enhancement in oil-water separation. A review. *Desalination* 357, 197-207.
- Paiman, S.H., Rahman, M.A., Uchikoshi, T., Nordin, N.A.H.M., Alias, N.H., Abdullah, N., Abas, K.H., Othman, M.H.D., Jaafar, J. and Ismail, A.F., (2020). In situ growth of α -Fe₂O₃ on Al₂O₃/YSZ hollow fiber membrane for oily wastewater. *Sep. Purif. Technol.* 236, 116250.
- Panpanit, S., Visvanathan, C. and Muttamara, S., (2000). Separation of oil-water emulsion from car washes. *Water Sci. Technol.* 41 (10-11), 109-116.
- Park, H., Kim, Y., An, B. and Choi, H., (2012). Characterization of natural organic matter treated by iron oxide nanoparticle incorporated ceramic membrane-ozonation process. *Water Res.* 46 (18), 5861-5870.
- Park, H.B., Kamcev, J., Robeson, L.M., Elimelech, M. and Freeman, B.D., (2017). Maximizing the right stuff: The trade-off between membrane permeability and selectivity. *Science* 356 (6343).
- Pearce, G.K., (2008). UF/MF pre-treatment to RO in seawater and wastewater reuse applications: a comparison of energy costs. *Desalination* 222 (1-3), 66-73.
- Pedenaud, P., Wayne, E., Samuel, H. and Didier, B. (2011) Ceramic Membrane And Core Pilot Results For Produced Water Management, p. 16, Offshore Technology Conference, Rio de Janeiro, Brazil.
- Pedersen, H., (2016). Time as the Fourth Dimension: Opening up New Possibilities in Chemical Vapor Deposition. *Chem. Mater.* 28 (3), 691-699.

■ References

- Pendergast, M.M. and Hoek, E.M.V., (2011). A review of water treatment membrane nanotechnologies. *Energy Environ. Sci.* 4 (6), 1946-1971.
- Porcelli, N. and Judd, S., (2010). Chemical cleaning of potable water membranes: A review. *Sep. Purif. Technol.* 71 (2), 137-143.
- Prado-Rubio, O., Cardona, D., Svendsen, T. and Yuan, L., (2012). SiC Membrane Pilot Plant Ultrafiltration Test for Produced Water Treatment, Ocelote Field–Hocol (COLOMBIA). Company Report, Liqtech.
- Qiu, M., Chen, X., Fan, Y. and Xing, W. (2017) *Comprehensive Membrane Science and Engineering (Second Edition)*. Drioli, E., Giorno, L. and Fontananova, E. (eds), pp. 270-297, Elsevier, Oxford.
- Raffin, M., Germain, E. and Judd, S., (2013). Wastewater polishing using membrane technology: a review of existing installations. *Environ. Technol.* 34 (5), 617-627.
- Ramirez, J.A. and Davis, R.H., (1998). Application of cross-flow microfiltration with rapid backpulsing to wastewater treatment. *J. Hazard. Mater.* 63 (2), 179-197.
- Rana, D. and Matsuura, T., (2010). Surface Modifications for Antifouling Membranes. *Chem. Rev.* 110 (4), 2448-2471.
- Rashad, M., Logesh, G., Sabu, U. and Balasubramanian, M., (2021). A novel monolithic mullite microfiltration membrane for oil-in-water emulsion separation. *J. Membr. Sci.* 620, 118857.
- Rasouli, Y., Abbasi, M. and Hashemifard, S.A., (2017a). Investigation of in-line coagulation-MF hybrid process for oily wastewater treatment by using novel ceramic membranes. *J. Clean. Prod.* 161, 545-559.
- Rasouli, Y., Abbasi, M. and Hashemifard, S.A., (2017b). Oily wastewater treatment by adsorption-membrane filtration hybrid process using powdered activated carbon, natural zeolite powder and low cost ceramic membranes. *Water Sci. Technol.* 76 (4), 895-908.
- Rezakazemi, M., Dashti, A., Riasat Harami, H., Hajilari, N. and Inamuddin, (2018). Fouling-resistant membranes for water reuse. *Environ. Chem. Lett.* 16 (3), 715-763.
- Sakka, S. (2013) *Handbook of Advanced Ceramics (Second Edition)*. Somiya, S. (ed), pp. 883-910, Academic Press, Oxford.
- Salahi, A., Noshadi, I., Badrnezhad, R., Kanjilal, B. and Mohammadi, T., (2013). Nanoporous membrane process for oily wastewater treatment: optimization using response surface methodology. *J. Environ. Chem. Eng.* 1 (3), 218-225.

■ References

- Sammalkorpi, M., Karttunen, M. and Haataja, M., (2009). Ionic Surfactant Aggregates in Saline Solutions: Sodium Dodecyl Sulfate (SDS) in the Presence of Excess Sodium Chloride (NaCl) or Calcium Chloride (CaCl₂). *J. Phys. Chem. B* 113 (17), 5863-5870.
- Saththasivam, J., Loganathan, K. and Sarp, S., (2016). An overview of oil–water separation using gas flotation systems. *Chemosphere* 144, 671-680.
- Sea, B.-K., Ando, K., Kusakabe, K. and Morooka, S., (1998). Separation of hydrogen from steam using a SiC-based membrane formed by chemical vapor deposition of triisopropylsilane. *J. Membr. Sci.* 146 (1), 73-82.
- Senapati, S. and Maiti, P. (2020) 2D Nanoscale Heterostructured Materials. Jit, S. and Das, S. (eds), pp. 243-255, Elsevier.
- Shams Ashaghi, K., Ebrahimi, M. and Czermak, P., (2007). Ceramic ultra-and nanofiltration membranes for oilfield produced water treatment: a mini review. *Open Environ. Sci.* 1 (1).
- Shang, R., Goulas, A., Tang, C.Y., de Frias Serra, X., Rietveld, L.C. and Heijman, S.G.J., (2017). Atmospheric pressure atomic layer deposition for tight ceramic nanofiltration membranes: Synthesis and application in water purification. *J. Membr. Sci.* 528, 163-170.
- Shang, R., Vuong, F., Hu, J., Li, S., Kemperman, A.J.B., Nijmeijer, K., Cornelissen, E.R., Heijman, S.G.J. and Rietveld, L.C., (2015). Hydraulically irreversible fouling on ceramic MF/UF membranes: Comparison of fouling indices, foulant composition and irreversible pore narrowing. *Sep. Purif. Technol.* 147, 303-310.
- Shi, H., He, Y., Pan, Y., Di, H.H., Zeng, G.Y., Zhang, L. and Zhang, C.L., (2016). A modified mussel-inspired method to fabricate TiO₂ decorated superhydrophilic PVDF membrane for oil/water separation. *J. Membr. Sci.* 506, 60-70.
- Shi, L., Lei, Y., Huang, J., Shi, Y., Yi, K. and Zhou, H., (2019). Ultrafiltration of oil-in-water emulsions using ceramic membrane: Roles played by stabilized surfactants. *Colloid Surface A* 583, 123948.
- Shi, Y., Meng, Y., Chen, D., Cheng, S., Chen, P., Yang, H., Wan, Y. and Zhao, D., (2006). Highly Ordered Mesoporous Silicon Carbide Ceramics with Large Surface Areas and High Stability. *Adv. Funct. Mater.* 16 (4), 561-567.
- Shi, Y., Zheng, Q., Ding, L., Yang, F., Jin, W., Tang, C.Y. and Dong, Y., (2022). Electro-Enhanced Separation of Microsized Oil-in-Water Emulsions via Metallic Membranes: Performance and Mechanistic Insights. *Environ. Sci. Technol.* 56 (7), 4518-4530.

■ References

- Shirzadi, M., Ueda, M., Hada, K., Fukasawa, T., Fukui, K., Mino, Y., Tsuru, T. and Ishigami, T., (2022). High-Resolution Numerical Simulation of Microfiltration of Oil-in-Water Emulsion Permeating through a Realistic Membrane Microporous Structure Generated by Focused Ion Beam Scanning Electron Microscopy Images. *Langmuir* 38 (6), 2094-2108.
- Shu, L., Xing, W. and Xu, N., (2007). Effect of Ultrasound on the Treatment of Emulsification Wastewater by Ceramic Membranes. *Chin. J. Chem. Eng.* 15 (6), 855-860.
- Silalahi, S.H.D. and Leiknes, T., (2009). Cleaning strategies in ceramic microfiltration membranes fouled by oil and particulate matter in produced water. *Desalination* 236 (1), 160-169.
- Silalahi, S.H.D., Leiknes, T., Ali, J. and Sanderson, R., (2009). Ultrasonic time domain reflectometry for investigation of particle size effect in oil emulsion separation with crossflow microfiltration. *Desalination* 236 (1-3), 143-151.
- Simonič, M., (2019). Membrane surface properties and their effects on real waste oil-in-water emulsion ultrafiltration. *Water SA* 45 (3), 367-373.
- Singh, P., Manikandan, N.A., Purnima, M., Pakshirajan, K. and Pugazhenthii, G., (2020). Recovery of lignin from water and methanol using low-cost kaolin based tubular ceramic membrane. *J. Water Process. Eng.* 38, 101615.
- Skibinski, B., Müller, P. and Uhl, W., (2016). Rejection of submicron sized particles from swimming pool water by a monolithic SiC microfiltration membrane: Relevance of steric and electrostatic interactions. *J. Membr. Sci.* 499, 92-104.
- Song, C.W., Wang, T.H., Pan, Y.Q. and Qiu, J.S., (2006). Preparation of coal-based microfiltration carbon membrane and application in oily wastewater treatment. *Sep. Purif. Technol.* 51 (1), 80-84.
- Srijaroonrat, P., Julien, E. and Aurelle, Y., (1999). Unstable secondary oil/water emulsion treatment using ultrafiltration: fouling control by backflushing. *J. Membr. Sci.* 159 (1), 11-20.
- Starr, B.J., Tarabara, V.V., Herrera-Robledo, M., Zhou, M., Roualdès, S. and Ayral, A., (2016). Coating porous membranes with a photocatalyst: Comparison of LbL self-assembly and plasma-enhanced CVD techniques. *J. Membr. Sci.* 514, 340-349.

■ References

- Suresh, K., Srinu, T., Ghoshal, A.K. and Pugazhenth, G., (2016). Preparation and characterization of TiO₂ and gamma-Al₂O₃ composite membranes for the separation of oil-in-water emulsions. *RSC Adv.* 6 (6), 4877-4888.
- Tang, C.Y., Chong, T. and Fane, A.G., (2011). Colloidal interactions and fouling of NF and RO membranes: a review. *Adv. Colloid Interface Sci.* 164 (1-2), 126-143.
- Tanudjaja, H.J., Hejase, C.A., Tarabara, V.V., Fane, A.G. and Chew, J.W., (2019). Membrane-Based Separation for Oily Wastewater: A Practical Perspective. *Water Res.* 156, 347-365.
- Tanudjaja, H.J., Tarabara, V.V., Fane, A.G. and Chew, J.W., (2017). Effect of cross-flow velocity, oil concentration and salinity on the critical flux of an oil-in-water emulsion in microfiltration. *J. Membr. Sci.* 530, 11-19.
- Tetteh, E.K., Rathilal, S., Asante-Sackey, D. and Chollom, M.N., (2021). Prospects of synthesized magnetic TiO₂-based membranes for wastewater treatment: A review. *Materials* 14 (13), 3524.
- Thibault, Y., McEvoy, J.G., Mortazavi, S., Smith, D. and Doiron, A., (2017). Characterization of fouling processes in ceramic membranes used for the recovery and recycle of oil sands produced water. *J. Membr. Sci.* 540, 307-320.
- Tian, J., Trinh, T.A., Kalyan, M.N., Ho, J.S. and Chew, J.W., (2020). In-situ monitoring of oil emulsion fouling in ultrafiltration via electrical impedance spectroscopy (EIS): Influence of surfactant. *J. Membr. Sci.*, 118527.
- Tomczak, W. and Gryta, M., (2020). Application of ultrafiltration ceramic membrane for separation of oily wastewater generated by maritime transportation. *Sep. Purif. Technol.*, 118259.
- Trinh, T.A., Han, Q., Ma, Y. and Chew, J.W., (2019). Microfiltration of oil emulsions stabilized by different surfactants. *J. Membr. Sci.* 579, 199-209.
- Tsai, H.-Y., Huang, A., Soesanto, J.F., Luo, Y.-L., Hsu, T.-Y., Chen, C.-H., Hwang, K.-J., Ho, C.-D. and Tung, K.-L., (2019). 3D printing design of turbulence promoters in a cross-flow microfiltration system for fine particles removal. *J. Membr. Sci.* 573, 647-656.
- Tsuru, T., Hironaka, D., Yoshioka, T. and Asaeda, M., (2001). Titania membranes for liquid phase separation: effect of surface charge on flux. *Sep. Purif. Technol.* 25 (1-3), 307-314.
- Tummons, E., Han, Q., Tanudjaja, H.J., Hejase, C.A., Chew, J.W. and Tarabara, V.V., (2020). Membrane fouling by emulsified oil: A review. *Sep. Purif. Technol.* 248, 116919.

■ References

- Tummons, E.N., Chew, J.W., Fane, A.G. and Tarabara, V.V., (2017). Ultrafiltration of saline oil-in-water emulsions stabilized by an anionic surfactant: Effect of surfactant concentration and divalent counterions. *J. Membr. Sci.* 537, 384-395.
- Tummons, E.N., Tarabara, V.V., Chew, Jia W. and Fane, A.G., (2016). Behavior of oil droplets at the membrane surface during crossflow microfiltration of oil-water emulsions. *J. Membr. Sci.* 500, 211-224.
- Vacassy, R., Guizard, C., Thoraval, V. and Cot, L., (1997). Synthesis and characterization of microporous zirconia powders: application in nanofilters and nanofiltration characteristics. *J. Membr. Sci.* 132 (1), 109-118.
- Vasanth, D., Pugazhenth, G. and Uppaluri, R., (2011). Fabrication and properties of low cost ceramic microfiltration membranes for separation of oil and bacteria from its solution. *J. Membr. Sci.* 379 (1-2), 154-163.
- Virga, E., Bos, B., Biesheuvel, P.M., Nijmeijer, A. and de Vos, W.M., (2020). Surfactant-dependent Critical Interfacial Tension in Silicon Carbide Membranes for Produced Water Treatment. *J. Colloid Interface Sci.* 571, 222-231.
- Voigt, I., Richter, H., Stahn, M., Weyd, M., Puhlfürß, P., Prehn, V. and Günther, C., (2019). Scale-up of ceramic nanofiltration membranes to meet large scale applications. *Sep. Purif. Technol.* 215, 329-334.
- Vrijenhoek, E.M., Hong, S. and Elimelech, M., (2001). Influence of membrane surface properties on initial rate of colloidal fouling of reverse osmosis and nanofiltration membranes. *J. Membr. Sci.* 188 (1), 115-128.
- Vroman, T., Beaume, F., Armanges, V., Gout, E. and Remigy, J.-C., (2020). Critical backwash flux for high backwash efficiency: Case of ultrafiltration of bentonite suspensions. *J. Membr. Sci.*, 118836.
- Wang, C.-F. and Tsai, D.-S., (2000). Low pressure chemical vapor deposition of silicon carbide from dichlorosilane and acetylene. *Mater. Chem. Phys.* 63 (3), 196-201.
- Wang, H., Lundin, S.-T.B., Takanabe, K. and Oyama, S.T., (2022a). Synthesis of size-controlled boehmite sols: Application in high-performance hydrogen-selective ceramic membranes. *J. Mater. Chem. A* 10 (24), 12869-12881.
- Wang, P., Xu, N. and Shi, J., (2000). A pilot study of the treatment of waste rolling emulsion using zirconia microfiltration membranes. *J. Membr. Sci.* 173 (2), 159-166.

■ References

- Wang, Q., Wang, X., Wang, Z., Huang, J. and Wang, Y., (2013). PVDF membranes with simultaneously enhanced permeability and selectivity by breaking the tradeoff effect via atomic layer deposition of TiO₂. *J. Membr. Sci.* 442, 57-64.
- Wang, X., Sun, K., Zhang, G., Yang, F., Lin, S. and Dong, Y., (2022b). Robust zirconia ceramic membrane with exceptional performance for purifying nano-emulsion oily wastewater. *Water Res.* 208, 117859.
- Wang, Z., Ma, J., Tang, C.Y., Kimura, K., Wang, Q. and Han, X., (2014). Membrane cleaning in membrane bioreactors: A review. *J. Membr. Sci.* 468, 276-307.
- Weber, M., Julbe, A., Kim, S.S. and Bechelany, M., (2019). Atomic layer deposition (ALD) on inorganic or polymeric membranes. *J. Appl. Phys.* 126 (4), 041101.
- Wei, C.C. and Li, K., (2009). Preparation and Characterization of a Robust and Hydrophobic Ceramic Membrane via an Improved Surface Grafting Technique. *Ind. Eng. Chem. Res.* 48 (7), 3446-3452.
- Wei, W., Zhang, W., Jiang, Q., Xu, P., Zhong, Z., Zhang, F. and Xing, W., (2017). Preparation of non-oxide SiC membrane for gas purification by spray coating. *J. Membr. Sci.* 540, 381-390.
- Wei, Y., Qi, H., Gong, X. and Zhao, S., (2018). Specially Wetttable Membranes for Oil-Water Separation. *Adv. Mater. Interfaces* 5 (23), 1800576.
- Wenzlick, M. and Siefert, N., (2020). Techno-economic analysis of converting oil & gas produced water into valuable resources. *Desalination* 481, 114381.
- Werber, J.R., Osuji, C.O. and Elimelech, M., (2016). Materials for next-generation desalination and water purification membranes. *Nat. Rev. Mater.* 1 (5).
- Weschenfelder, S., Fonseca, M., Costa, B. and Borges, C., (2019). Influence of the use of surfactants in the treatment of produced water by ceramic membranes. *J. Water Process. Eng.* 32, 100955.
- Weschenfelder, S.E., Borges, C.P. and Campos, J.C., (2015a). Oilfield produced water treatment by ceramic membranes: Bench and pilot scale evaluation. *J. Membr. Sci.* 495, 242-251.
- Weschenfelder, S.E., Fonseca, M.J.C. and Borges, C.P., (2021). Treatment of produced water from polymer flooding in oil production by ceramic membranes. *J. Petrol. Sci. Eng.* 196, 108021.

■ References

- Weschenfelder, S.E., Louvise, A.M.T., Borges, C.P., Meabe, E., Izquierdo, J. and Campos, J.C., (2015b). Evaluation of ceramic membranes for oilfield produced water treatment aiming reinjection in offshore units. *J. Petrol. Sci. Eng.* 131, 51-57.
- Willet, J., Wetser, K., Vreeburg, J. and Rijnaarts, H.H.M., (2019). Review of methods to assess sustainability of industrial water use. *Water Resour. Ind.* 21, 100110.
- Wu, H., Sun, C., Huang, Y., Zheng, X., Zhao, M., Gray, S. and Dong, Y., (2022). Treatment of oily wastewaters by highly porous whisker-constructed ceramic membranes: Separation performance and fouling models. *Water Res.* 211, 118042.
- Wu, J., Chen, F., Huang, X., Geng, W. and Wen, X., (2006). Using inorganic coagulants to control membrane fouling in a submerged membrane bioreactor. *Desalination* 197 (1), 124-136.
- Wu, W., Huang, R., Qi, W., Su, R. and He, Z., (2018). Bioinspired Peptide-Coated Superhydrophilic Poly(vinylidene fluoride) Membrane for Oil/Water Emulsion Separation. *Langmuir* 34 (22), 6621-6627.
- Xia, C., Zha, S., Yang, W., Peng, R., Peng, D. and Meng, G., (2000). Preparation of yttria stabilized zirconia membranes on porous substrates by a dip-coating process. *Solid State Ion.* 133 (3), 287-294.
- Xing, J., Liang, H., Chuah, C.J., Bao, Y., Luo, X., Wang, T., Wang, J., Li, G. and Snyder, S.A., (2019). Insight into Fe (II)/UV/chlorine pretreatment for reducing ultrafiltration (UF) membrane fouling: Effects of different natural organic fractions and comparison with coagulation. *Water Res.* 167, 115112.
- Xu, M., Xu, C., Rakesh, K.P., Cui, Y., Yin, J., Chen, C., Wang, S., Chen, B. and Zhu, L., (2020). Hydrophilic SiC hollow fiber membranes for low fouling separation of oil-in-water emulsions with high flux. *RSC Adv.* 10 (8), 4832-4839.
- Xu, X., Bao, Y., Song, C., Yang, W., Liu, J. and Lin, L., (2004). Microwave-assisted hydrothermal synthesis of hydroxy-sodalite zeolite membrane. *Microporous Mesoporous Mater.* 75 (3), 173-181.
- Yagi, K. and Nagasawa, H., (1997). 3C-SiC growth by alternate supply of SiH₂Cl₂ and C₂H₂. *J. Cryst. Growth* 174 (1-4), 653-657.
- Yang, B., Geng, P. and Chen, G., (2015). One-dimensional structured IrO₂ nanorods modified membrane for electrochemical anti-fouling in filtration of oily wastewater. *Sep. Purif. Technol.* 156, 931-941.

■ References

- Yang, C., Zhang, G., Xu, N. and Shi, J., (1998). Preparation and application in oil–water separation of $ZrO_2/\alpha-Al_2O_3$ MF membrane. *J. Membr. Sci.* 142 (2), 235-243.
- Yang, G. and Park, S.-J., (2019). Conventional and Microwave Hydrothermal Synthesis and Application of Functional Materials: A Review. *Materials* 12 (7), 1177.
- Yang, H.-C., Waldman, R., Chen, Z. and Darling, S., (2018a). Atomic layer deposition for membrane interface engineering. *Nanoscale* 10, 20505-20513.
- Yang, H.-C., Xie, Y., Chan, H., Narayanan, B., Chen, L., Waldman, R.Z., Sankaranarayanan, S.K.R.S., Elam, J.W. and Darling, S.B., (2018b). Crude-Oil-Repellent Membranes by Atomic Layer Deposition: Oxide Interface Engineering. *ACS Nano* 12 (8), 8678-8685.
- Yang, M., Hadi, P., Yin, X., Yu, J., Huang, X., Ma, H., Walker, H. and Hsiao, B.S., (2021). Antifouling nanocellulose membranes: How subtle adjustment of surface charge lead to self-cleaning property. *J. Membr. Sci.* 618, 118739.
- Yang, Q., Luo, J., Guo, S., Hang, X., Chen, X. and Wan, Y., (2019). Threshold flux in concentration mode: Fouling control during clarification of molasses by ultrafiltration. *J. Membr. Sci.* 586, 130-139.
- Yang, W. and Li, L., (2017). Efficiency Evaluation and Policy Analysis of Industrial Wastewater Control in China. *Energies* 10 (8), 1201.
- Yang, Y., Chen, R. and Xing, W., (2011a). Integration of ceramic membrane microfiltration with powdered activated carbon for advanced treatment of oil-in-water emulsion. *Sep. Purif. Technol.* 76 (3), 373-377.
- Yang, Y., Li, J., Wang, H., Song, X., Wang, T., He, B., Liang, X. and Ngo, H.H., (2011b). An Electrocatalytic Membrane Reactor with Self-Cleaning Function for Industrial Wastewater Treatment. *Angew. Chem. Int. Ed.* 50 (9), 2148-2150.
- Yao, Y., Zhang, B., Jiang, M., Hong, X., Wu, Y., Wang, T. and Qiu, J., (2022). Ultra-selective microfiltration SiO_2 /carbon membranes for emulsified oil-water separation. *J. Environ. Chem. Eng.* 10 (3), 107848.
- Yeo, Z.Y., Chew, T.L., Zhu, P.W., Mohamed, A.R. and Chai, S.-P., (2013). Synthesis and performance of microporous inorganic membranes for CO_2 separation: a review. *J. Porous Mater.* 20 (6), 1457-1475.
- Yu, L., Han, M. and He, F., (2017). A review of treating oily wastewater. *Arab. J. Chem.* 10, S1913-S1922.
- Zaidi, A., Simms, K. and Kok, S., (1992). The use of micro/ultrafiltration for the removal of oil and suspended solids from oilfield brines. *Water Sci. Technol.* 25 (10), 163-176.

■ References

- Zhang, B., Yang, C., Zheng, Y., Wu, Y., Song, C., Liu, Q. and Wang, Z., (2021). Modification of CO₂-selective mixed matrix membranes by a binary composition of poly (ethylene glycol)/NaY zeolite. *J. Membr. Sci.* 627, 119239.
- Zhang, D.-S., Abadikhah, H., Wang, J.-W., Hao, L.-Y., Xu, X. and Agathopoulos, S., (2019). β -SiAlON ceramic membranes modified with SiO₂ nanoparticles with high rejection rate in oil-water emulsion separation. *Ceram. Int.* 45 (4), 4237-4242.
- Zhang, D., Wang, G., Zhi, S., Xu, K., Zhu, L., Li, W., Zeng, Z. and Xue, Q., (2018a). Superhydrophilicity and underwater superoleophobicity TiO₂/Al₂O₃ composite membrane with ultra low oil adhesion for highly efficient oil-in-water emulsions separation. *Appl. Surf. Sci.* 458, 157-165.
- Zhang, F., Shi, Z.W., Chen, L.S., Jiang, Y.J., Xu, C.Y., Wu, Z.H., Wang, Y.Y. and Peng, C.S., (2017). Porous superhydrophobic and superoleophilic surfaces prepared by template assisted chemical vapor deposition. *Surf. Coat. Technol.* 315, 385-390.
- Zhang, H., Zhong, Z. and Xing, W., (2013). Application of ceramic membranes in the treatment of oilfield-produced water: Effects of polyacrylamide and inorganic salts. *Desalination* 309, 84-90.
- Zhang, Q., Fan, Y. and Xu, N., (2009). Effect of the surface properties on filtration performance of Al₂O₃-TiO₂ composite membrane. *Sep. Purif. Technol.* 66 (2), 306-312.
- Zhang, R., Liu, Y., He, M., Su, Y., Zhao, X., Elimelech, M. and Jiang, Z., (2016a). Antifouling membranes for sustainable water purification: strategies and mechanisms. *Chem. Soc. Rev.* 45 (21), 5888-5924.
- Zhang, S., Jiang, G., Gao, S., Jin, H., Zhu, Y., Zhang, F. and Jin, J., (2018b). Cupric Phosphate Nanosheets-Wrapped Inorganic Membranes with Superhydrophilic and Outstanding Anticrude Oil-Fouling Property for Oil/Water Separation. *ACS Nano* 12 (1), 795-803.
- Zhang, W., Luo, J., Ding, L. and Jaffrin, M.Y., (2015). A Review on Flux Decline Control Strategies in Pressure-Driven Membrane Processes. *Ind. Eng. Chem. Res.* 54 (11), 2843-2861.
- Zhang, X.-L., Yamada, H., Saito, T., Kai, T., Murakami, K., Nakashima, M., Ohshita, J., Akamatsu, K. and Nakao, S.-i., (2016b). Development of hydrogen-selective triphenylmethoxysilane-derived silica membranes with tailored pore size by chemical vapor deposition. *J. Membr. Sci.* 499, 28-35.

■ References

- Zhao, Y., Tan, Y., Wong, F.-S., Fane, A.G. and Xu, N., (2005). Formation of dynamic membranes for oily water separation by crossflow filtration. *Sep. Purif. Technol.* 44 (3), 212-220.
- Zhong, J., Sun, X.J. and Wang, C.L., (2003). Treatment of oily wastewater produced from refinery processes using flocculation and ceramic membrane filtration. *Sep. Purif. Technol.* 32 (1-3), 93-98.
- Zhong, Z.X., Xing, W.H. and Zhang, B.B., (2013). Fabrication of ceramic membranes with controllable surface roughness and their applications in oil/water separation. *Ceram. Int.* 39 (4), 4355-4361.
- Zhou, J.-e., Chang, Q., Wang, Y., Wang, J. and Meng, G., (2010). Separation of stable oil-water emulsion by the hydrophilic nano-sized ZrO_2 modified Al_2O_3 microfiltration membrane. *Sep. Purif. Technol.* 75 (3), 243-248.
- Zhou, Y., Fukushima, M., Miyazaki, H., Yoshizawa, Y.-i., Hirao, K., Iwamoto, Y. and Sato, K., (2011). Preparation and characterization of tubular porous silicon carbide membrane supports. *J. Membr. Sci.* 369 (1), 112-118.
- Zhu, L., Chen, M.L., Dong, Y.C., Tang, C.Y., Huang, A.S. and Li, L.L., (2016). A low-cost mullite-titania composite ceramic hollow fiber microfiltration membrane for highly efficient separation of oil-in-water emulsion. *Water Res.* 90, 277-285.
- Zhu, L., Dong, X., Xu, M., Yang, F., Guiver, M.D. and Dong, Y., (2019). Fabrication of mullite ceramic-supported carbon nanotube composite membranes with enhanced performance in direct separation of high-temperature emulsified oil droplets. *J. Membr. Sci.* 582, 140-150.
- Zhu, X. and Jassby, D., (2019). Electroactive Membranes for Water Treatment: Enhanced Treatment Functionalities, Energy Considerations, and Future Challenges. *Acc. Chem. Res.* 52 (5), 1177-1186.
- Zhu, X., Loo, H.-E. and Bai, R., (2013). A novel membrane showing both hydrophilic and oleophobic surface properties and its non-fouling performances for potential water treatment applications. *J. Membr. Sci.* 436, 47-56.
- Zhu, X.B., Dudchenko, A., Gu, X.T. and Jassby, D., (2017). Surfactant-stabilized oil separation from water using ultrafiltration and nanofiltration. *J. Membr. Sci.* 529, 159-169.
- Zhu, Y.Z., Wang, D., Jiang, L. and Jin, J., (2014). Recent progress in developing advanced membranes for emulsified oil/water separation. *NPG Asia Mater.* 6, e101.

■ References

Zou, D., Chen, X., Drioli, E., Qiu, M. and Fan, Y., (2019a). Facile Mixing Process To Fabricate Fly-Ash-Enhanced Alumina-Based Membrane Supports for Industrial Microfiltration Applications. *Ind. Eng. Chem. Res.* 58 (20), 8712-8723.

Zou, D., Fan, W., Xu, J., Drioli, E., Chen, X., Qiu, M. and Fan, Y., (2021). One-step engineering of low-cost kaolin/fly ash ceramic membranes for efficient separation of oil-water emulsions. *J. Membr. Sci.* 621, 118954.

Zou, D., Qiu, M., Chen, X., Drioli, E. and Fan, Y., (2019b). One step co-sintering process for low-cost fly ash based ceramic microfiltration membrane in oil-in-water emulsion treatment. *Sep. Purif. Technol.* 210, 511-520.

Zou, D., Xu, J., Chen, X., Drioli, E., Qiu, M. and Fan, Y., (2019c). A novel thermal spraying technique to fabricate fly ash/alumina composite membranes for oily emulsion and spent tin wastewater treatment. *Sep. Purif. Technol.* 219, 127-136.

Zsirai, T., Al-Jaml, A.K., Qiblawey, H., Al-Marri, M., Ahmed, A., Bach, S., Watson, S. and Judd, S., (2016). Ceramic membrane filtration of produced water: Impact of membrane module. *Sep. Purif. Technol.* 165, 214-221.

Zsirai, T., Qiblawey, H., Buzatu, P., Al-Marri, M. and Judd, S.J., (2018). Cleaning of ceramic membranes for produced water filtration. *J. Petrol. Sci. Eng.* 166, 283-289.

Summary

Water scarcity, population growth, and climate change are causing a shortage of water resources globally. Industries are turning to the reclamation and reuse of wastewater, including oily wastewater, which is a major byproduct of oil and gas extraction. The small droplet size of oil-in-water emulsions, however, makes them difficult to remove using traditional methods like coagulation and flocculation, gravitational settling, dissolved air flotation, hydrocyclone, and adsorption.

Membrane separation has emerged as one of the most promising techniques to deal with oil-in-water emulsions due to its high removal efficiency and small footprint. The main challenge for the wider adoption of membrane technology for oily wastewater treatment is membrane fouling. Membrane fouling is a pervasive problem in water purification membranes. It could cause serious negative effects, such as a decline in water production, higher operational pressure and associated higher energy consumption.

Ceramic membranes, particularly SiC membranes, are a promising method for removing small oil droplets from water. They are physically and chemically stable and have high fouling resistance to oil droplets. SiC membranes have better permeability and lower fouling tendency compared to other ceramic membranes. However, their high cost limits their widespread application in the market.

In this research, extensive literature reviews were first performed (Chapters 2 and 3) and then we proposed a new method, low-pressure chemical vapor deposition (LPCVD), to prepare SiC-deposited ceramic membranes for oily wastewater treatment. With LPCVD, a layer of SiC was deposited on alumina supports at a lower temperature (750 °C), compared to 2000 °C for commercial SiC preparations. Due to the low water contact angle ($< 5^\circ$) and negatively charged surface, these SiC-deposited alumina ceramic membranes are expected to be more fouling resistant to oil emulsions than the pristine alumina membranes. The performance of deposited membranes is influenced not only by the coated SiC layer but also by the filtration modes used for evaluation. As a result, we respectively used constant pressure and constant flux filtration to assess the fouling of ceramic membranes with and without SiC deposition. Additionally, the emulsion chemistry, such as surfactant concentration, pH, salinity, and Ca^{2+} , plays a crucial role in the interactions between oil droplets and the membrane surface, which can cause membrane fouling. Understanding these mechanisms can be a crucial step towards the feasibility of using LPCVD to prepare SiC membranes for treating oily wastewater with lower fouling.

First, novel SiC-deposited ceramic membranes were developed by LPCVD at a relatively low temperature (750 °C) (Chapter 4). Different deposition times varying from 0 to 150

■ Summary

min were used to tune membrane pore size. The pure water permeance of the membranes only decreased from $350 \text{ L m}^{-2} \text{ h}^{-1} \text{ bar}^{-1}$ to $157 \text{ L m}^{-2} \text{ h}^{-1} \text{ bar}^{-1}$ when the deposition time was increased from 0 to 120 min. Correspondingly, the membrane pore size was narrowed down from 71 to 47 nm. Increasing the deposition time from 120 to 150 min mainly resulted in the formation of a thin, dense layer on top of the support instead of in the pores. Notably, the SiC layer rendered the pristine membrane surface more hydrophilic and negatively charged, effectively reducing membrane fouling during oil emulsion filtration.

Next, the fouling of SiC-deposited ceramic membranes and the pristine alumina membrane was respectively compared at constant pressure and constant flux filtration conditions (Chapter 5). The threshold flux of the membranes was first determined by flux-stepping experiments. Afterwards, membrane filtration was respectively conducted at below and above the threshold flux. In single cycle constant flux filtration experiment, the fouling tendency of the membranes was consistent with the results of threshold flux experiments. However, the inclusion of backwash in constant flux experiments led to a change in the fouling tendency, which was also dependent on the permeate flux. The improved surface hydrophilicity and charge made backwash more efficient for the modified membranes while extensive modification has a negative effect on membrane fouling resistance due to the huge loss in membrane permeance. In contrast, constant transmembrane pressure experiments showed that the order of membrane fouling was only related to membrane permeance, and no effect of surface properties was observed. Therefore, constant flux filtration experiments with backwash are recommended to be applied to evaluate the performance of the membranes with and without modification.

Finally, the impact of emulsion chemistry and operational parameters on the fouling of alumina membranes with and without a SiC deposition was systematically studied under constant flux filtration mode with backwash (Chapter 6). The results showed that the SiC-deposited membrane had a lower reversible and irreversible fouling when permeate flux was below $110 \text{ L m}^{-2} \text{ h}^{-1}$. In addition, a higher permeance recovery after physical and chemical cleaning was observed, as compared to the alumina membranes. The fouling of both membranes was decreased with the increase of sodium dodecyl sulphate (SDS) concentration in the feed, but to a higher extent in the alumina membranes. Increasing the pH of the emulsion could reduce the fouling of both membranes due to the enhanced electrostatic repulsion between oil droplets and membrane surface. Under high salinity conditions (100 mM NaCl), the screening of surface charge resulted in only a small difference in irreversible fouling between the alumina and SiC-deposited membranes. The presence of Ca^{2+} in the emulsion led to high irreversible fouling of both membranes, because of the compression of diffusion double layer and the interactions between Ca^{2+}

■ Summary

and SDS. The low fouling tendency and/or high cleaning efficiency of the SiC-deposited membranes indicated their potential for oily wastewater treatment.

Overall, this dissertation shows that the fouling of SiC-deposited ceramic membranes is lower than that of the pristine alumina membranes towards oil-in-water emulsion treatment. Although there are still limitations, these SiC-deposited membranes show the potential for further development.

■ Summary

Acknowledgements

Life is full of ups and downs, and unfortunately, my PhD journey has been no exception. Looking back on the past 5 years and 9 months, I realize how much I've learned and grown during this challenging journey. However, I'm also grateful for the countless people who have supported me along the way. Without their help, I wouldn't have been able to complete any of the important milestones in this journey.

First and foremost, I would like to express my sincere gratitude to my promotors, Luuk Rietveld and Bas Heijman. They have been my guiding light, my source of inspiration and my pillars of support throughout my entire research project. Their immense knowledge and plentiful experience have encouraged me in all the time of my academic research and daily life.

I would like to extend a special thank you to Dr. Ran Shang, my daily supervisor during the first year of my PhD. I will always remember our first meeting with Bas and you, where I struggled to express my ideas and thoughts clearly due to my limited oral English skills. However, Dr. Shang quickly became the bridge of communication between me and Bas, helping to clarify my ideas and ensuring that my voice was heard.

I want to express my heartfelt gratitude to Prof. Yingchao Dong, my former supervisor during my master's studies in China. The knowledge and experience that I gained from you and your research group have been invaluable in shaping my PhD research. Your mentorship not only inspired me to pursue my PhD but also provided a strong foundation for my academic journey. Thanks to your guidance, I had the privilege of meeting Prof. Louis Winnubst and Dr. Mieke Luiten-Olieman from the University of Twente at the end of my first year of PhD. Their expertise and support have been instrumental in helping me to overcome various challenges and obstacles in my research.

Prof. Louis, thanks for inviting me to give a presentation in your group and giving me valuable advice on my first paper. Mieke, I'm so glad to have you as a member of my research project in the second year of my PhD. You are always professional on inorganic membranes and thanks for arranging everything to measure the samples in the membrane clusters, at the University of Twente. In addition, thanks for offering me an opportunity to continue the research in your group.

Paolo and Bruno, you two are the cornerstones of my thesis. I'm so honoured to meet your guys at the EKL lab. Without your generous help and support, I would have been stuck and unable to continue my research with LPCVD. Your kindness and willingness to help have been invaluable to me throughout my journey. Whenever I needed assistance, you were always there with a helping hand.

■ Acknowledgements

I am grateful for my wonderful colleagues in Sanitary Engineering, who have made my time here such a positive experience. In particular, I want to express my thanks to my officemates from the first year in Room 4.54: Carina, Anto, Anna, Sara, Emile, Lenno, Bruno, Javier, Daniel, ... Despite coming from different corners of the world, we all found ourselves here together, and I feel so lucky to have met you all. I want to thank Irene and Franca for their help and discussions during our lab experiments. Your insights and guidance were invaluable.

Also, I would like to thank the Water Lab and our secretaries at Sanitary Engineering: Armand, Patricia, Jane, Mariska, Tamara, and Rielle. Your warm and patient support made my work in the lab and my life on campus so much easier. Thank you for being there for me, and for making my time here such a memorable one.

Furthermore, I want to extend my heartfelt appreciation to my Chinese friends and colleagues in Delft: Gang, Hongxiao, Liangfu, Feifei, Xiaochen, Peng, Guoshuai, Hongbo, Cuijie, Jenny, Nan, Bin, Max, Lihua, Zhe, Shuo, Tianlong, Guangze, Jiamin, Dengxiao, Coco, Qi, Yuke, and many more. Your presence has brought so much color and joy to my life here.

I would also like to take a moment to express my deep appreciation for Yang. In both the ups and downs of life and work, you have been my unwavering source of support and comfort. When I have felt frustrated or overwhelmed, your listening ear and encouraging words have lifted me up and given me the strength to carry on. Our journey together has been a true learning experience. Even though I may not understand all the intricacies of your work with qubits and quantum computers, I am in awe of your brilliance and dedication. You inspire me to reach for the stars and to never give up on my dreams.

I gratefully acknowledge the China Scholarship Council (CSC) and the Lamminga fund for the financial supports throughout my Ph.D. research. Also, I would like to thank all the committee members for their time and comments on my thesis.

Last but not the least, I would like to extend my deepest gratitude to my family: my parents and to my brother and sister in law and their lovely daughter and son for supporting me spiritually throughout writing this thesis. Without their support and love, I would not have achieved any of this. I love all of you!

Mingliang Chen

July, 2023, in Delft

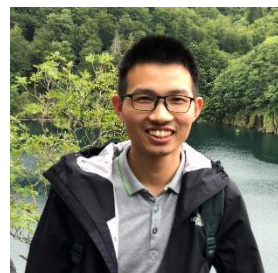
CURRICULUM VITAE

Family name: Chen 陈

Given name: Mingliang 明亮

Date of birth: 20 June 1990

Place of birth: Taihu County, Anhui Province, China



Education

2017-2023 PhD candidate - Delft University of Technology
Sanitary Engineering

2013-2016 Master - University of Chinese Academy of Sciences
Environmental Engineering

2009-2013 Bachelor - Anhui University of Science and Technology
Environmental Engineering

Experience

2023-2024 Postdoc researcher - Delft University of Technology
Product & Process Engineering

2022-2023 Postdoc researcher - University of Twente
Inorganic Membranes Group

2016-2017 Research assistant - Institute of Urban Environment, CAS
Produced water treatment with electrochemical oxidation

List of Publications

Chen, M., Heijman, S.G., Luiten-Olieman, M.W. and Rietveld, L.C., 2022. Oil-in-water emulsion separation: Fouling of alumina membranes with and without a silicon carbide deposition in constant flux filtration mode. *Water Research*, 216, 118267.

Chen, M., Heijman, S.G. and Rietveld, L.C., 2021. State-of-the-art ceramic membranes for oily wastewater treatment: Modification and application. *Membranes*, 11(11), 888 (Editor's Choice).

Chen, M., Shang, R., Sberna, P.M., Luiten-Olieman, M.W., Rietveld, L.C. and Heijman, S.G., 2020. Highly permeable silicon carbide-alumina ultrafiltration membranes for oil-in-water filtration produced with low-pressure chemical vapor deposition. *Separation and Purification Technology*, 253, 117496.

Chen, M., Zhu, L., Chen, J., Yang, F., Tang, C.Y., Guiver, M.D. and Dong, Y., 2020. Spinel-based ceramic membranes coupling solid sludge recycling with oily wastewater treatment. *Water Research*, 169, 115180.

Chen, M., Zhu, L., Dong, Y., Li, L. and Liu, J., 2016. Waste-to-resource strategy to fabricate highly porous whisker-structured mullite ceramic membrane for simulated oil-in-water emulsion wastewater treatment. *ACS Sustainable Chemistry & Engineering*, 4(4), 2098-2106.

Chen, M., Heijman, S. G., & Rietveld, L. C. (2023). Ceramic membrane filtration for oily wastewater treatment: basics, membrane fouling and fouling control. To be submitted for publication.

Chen, M., Heijman, S. G., & Rietveld, L. C. (2023). Evaluation of fouling by oil-in-water emulsion at constant flux and constant transmembrane pressure: Implications for modification of ceramic membranes. To be submitted for publication.

Chen, M., Nijboer, M.P., Kovalgin, A.Y., Nijmeijer A., Roozeboom, F., & Luiten-Olieman, M.W.J. (2023). Atmospheric-Pressure Atomic Layer Deposition: recent applications and new emerging applications in high-porosity/3D materials. Submitted to *Dalton Transactions*.

Ma, L., Dong, X., **Chen, M.**, Zhu, L., Wang, C., Yang, F., & Dong, Y. (2017). Fabrication and water treatment application of carbon nanotubes (CNTs)-based composite membranes: a review. *Membranes*, 7(1), 16.

Zhu, L., **Chen, M.**, Dong, Y., Tang, C. Y., Huang, A., & Li, L. (2016). A low-cost mullite-titania composite ceramic hollow fiber microfiltration membrane for highly efficient separation of oil-in-water emulsion. *Water Research*, 90, 277-285.

Li, L., **Chen, M.**, Dong, Y., Dong, X., Cerneaux, S., Hampshire, S., Cao, J., Zhu, L., Zhu, Z. & Liu, J. (2016). A low-cost alumina-mullite composite hollow fiber ceramic membrane fabricated via phase-inversion and sintering method. *Journal of the European Ceramic Society*, 36(8), 2057-2066.